Erasmus+ Programme Key Action 2 Cooperation Partnerships
for Higher Education (KA220-HED)
Agreement number 2023-1-RO01-KA220-HED-000155412
European Network for Additive Manufacturing in Industrial Design for Ukrainian Context

AMAZE

E-TOOLKIT MANUAL FOR DIGITAL LEARNING IN PRODUCING COMPLEX DESIGN INDUSTRIAL PARTS

Diana BĂILĂ, Cătălin ZAHARIA, Ionuț RADU, Andrei DUMITRESCU, Nicolae IONESCU

Adam PATALAS, Paweł ZAWADZKI, Natalia WIERZBICKA, Remigiusz ŁABUDZKI

Igor FODCHUK, Mariana BORCHA, Volodymyr ROMANKEVYCH, Yuriy SOBKO, Nataliia VATAMANIUK

Beatriz Gloria BONILLA GARCÍA, César Arcadio BONILLA GARCÍA, Sergio VIZCAINO

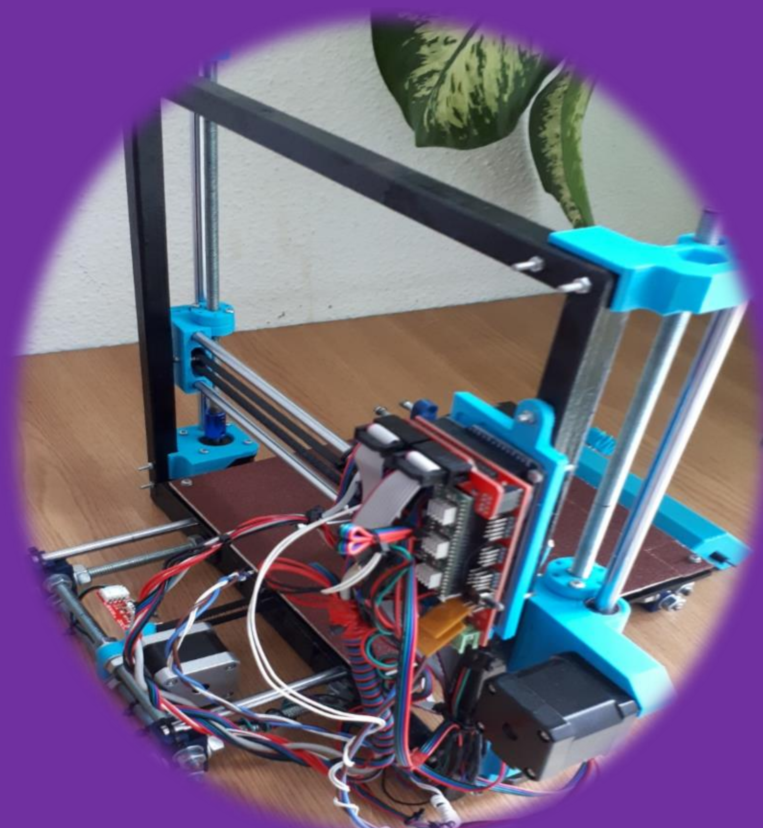

2024

Co-funded by the European Union

Erasmus+ Programme Key Action 2 Cooperation Partnerships for Higher Education (KA220-HED)
Agreement number 2023-1-RO01-KA220-HED-000155412
European Network for Additive Manufacturing in Industrial Design for Ukrainian Context

Diana BĂILĂ • Cătălin ZAHARIA • Ionuț RADU • Andrei DUMITRESCU
Nicolae IONESCU • Adam PATALAS • Paweł ZAWADZKI • Natalia WIERZBICKA
Remigiusz ŁABUDZKI • Igor FODCHUK • Mariana BORCHA
Volodymyr ROMANKEVYCH • Yuriy SOBKO • Nataliia VATAMANIUK
Beatriz Gloria BONILLA GARCÍA • César Arcadio BONILLA GARCÍA • Sergio VIZCAINO

AMAZE

E-TOOLKIT MANUAL FOR DIGITAL LEARNING IN PRODUCING COMPLEX DESIGN INDUSTRIAL PARTS

Editura PRINTECH

E-ISBN 978-606-23-1595-5

Co-funded by the European Union

Erasmus+ Programme Key Action 2 Cooperation Partnerships for Higher Education (KA220-HED)
Agreement number 2023-1-RO01-KA220-HED-000155412
European Network for Additive Manufacturing in Industrial Design for Ukrainian Context

e-Toolkit
Additive Manufacturing

Project Title	**European Network for Additive Manufacturing in Industrial Design for Ukrainian Context** **2023-1-RO01-KA220-HED-000155412**
Output	**IO2 - AMAZE e-toolkit manual for digital learning in producing complex design industrial parts**
Module	**Module 1** **Additive Manufacturing**
Date of Delivery	**June 2024**
Authors	**Diana BĂILĂ, Cătălin ZAHARIA, Ionuț-Cristian RADU**
Version	**FINAL VARIANT, *14.06.2024***

Contents

1 Additive Manufacturing toolkit for industrial parts

Product 1: Hydraulic pump body – SLDPRT. file Politehnica Bucharest Partner

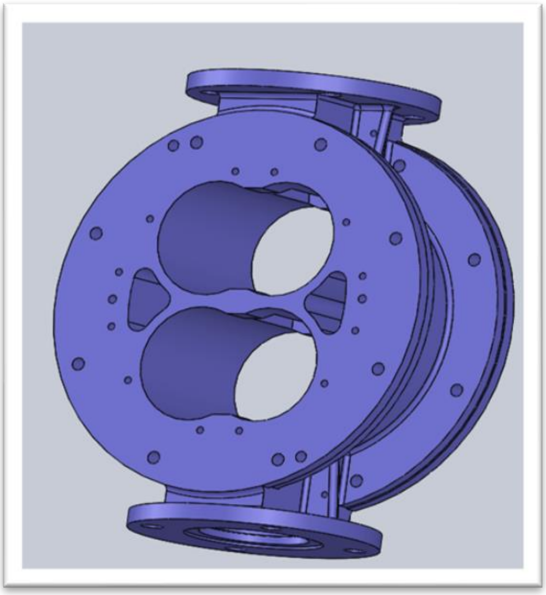

Fig.1. Hydraulic pump body

1.1. CAD Modeling

CAD modeling is used by many designers to create elaborated computerized models of objects before they are physically produced. CAD stands for computer-aided design. Engineers, architects, and even artists use computers to assist with their design projects. Computers allow them to visualize their designs and confront problems before they have expended any of the resources necessary to put them into physical form [1-58].

CAD modeling varies depending on the type of project. Some models are simple two-dimensional representations of different views of an object, while others are intricate three-dimensional cross-sections that display every detail in great depth. Some CAD models are even animated, demonstrating how all the components work together to fulfill the design's function.

Many different professions make use of computer-aided design. It is an important industrial art involved in automotive, aerospace, prosthetic, and artistic designs. The use of CAD modeling is extremely widespread; anything from chairs to rockets can be designed with the aid of computer programs. Among other titles, CAD modelers are referred to as CAD monkeys, designers, and digital information engineers. A single CAD file, 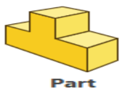

can be made, edited and continually tweaked until the object is ready for production.

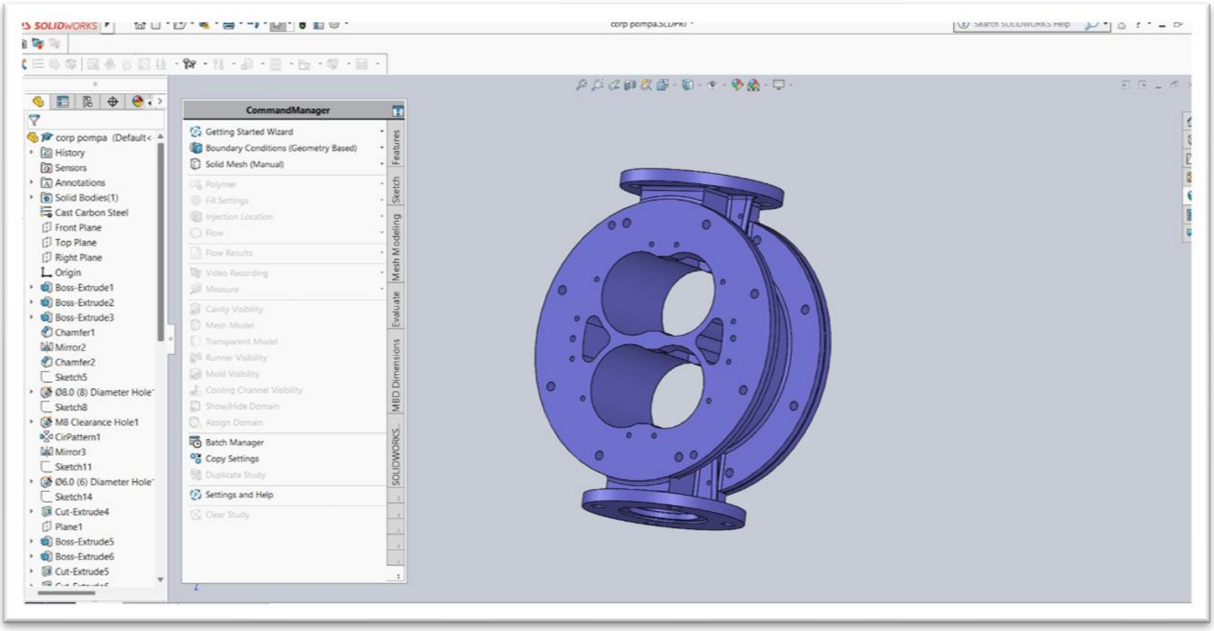

Fig.2. SolidWorks – SLDPRT. file

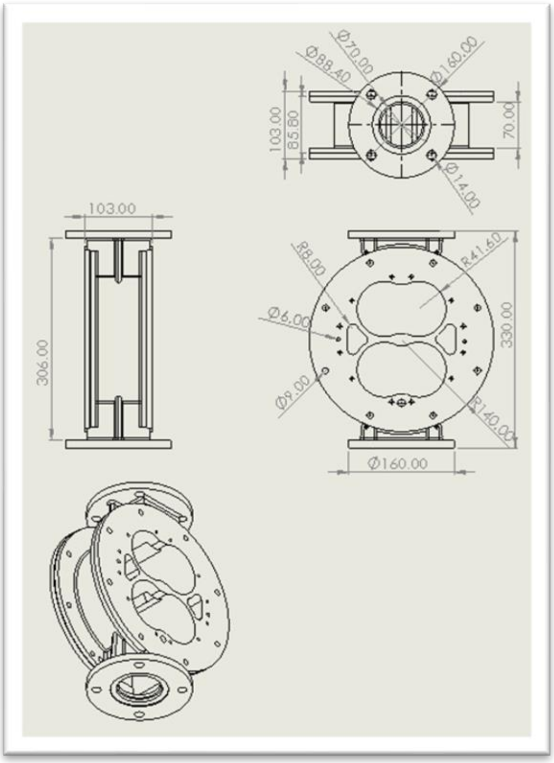

SolidWorks is a solid modeling computer-aided design (CAD) and computer-aided engineering (CAE) application published by Dassault Systèmes, as in figure 2 [1].

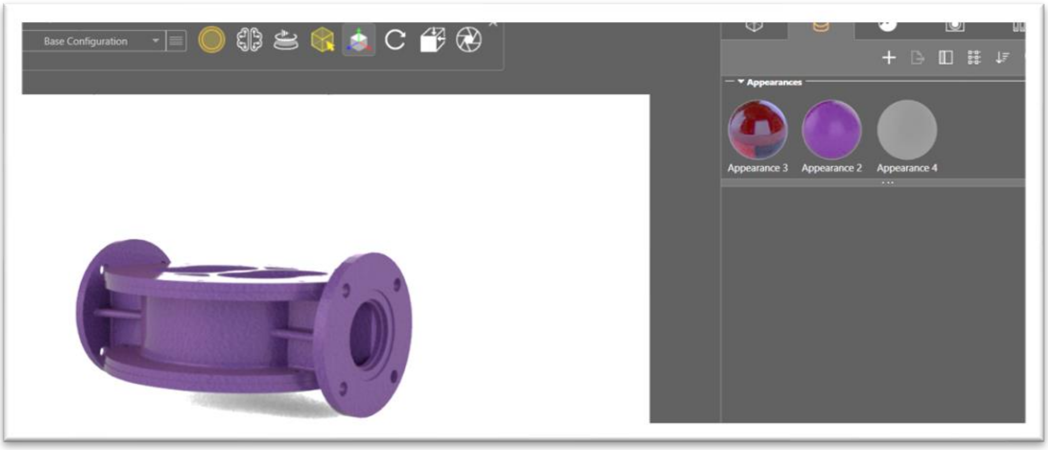

Fig.3. SolidWorks Visualize 2019 – hydraulic pomp body with different texture mapping

The CAD software allows the creation of three-dimensional models using various geometric entities, such as lines, rectangles, curved surfaces, and interconnected points in 3D space.

The 3D models can be realized by algorithms, using CAD software or by Reverse Engineering using a 3D scanner that collects information's concerning the dimensions and the 3D shape of the object. SolidWorks Visualize 2019 permits their surfaces to be further defined with texture mapping, as in figure 3 [1].

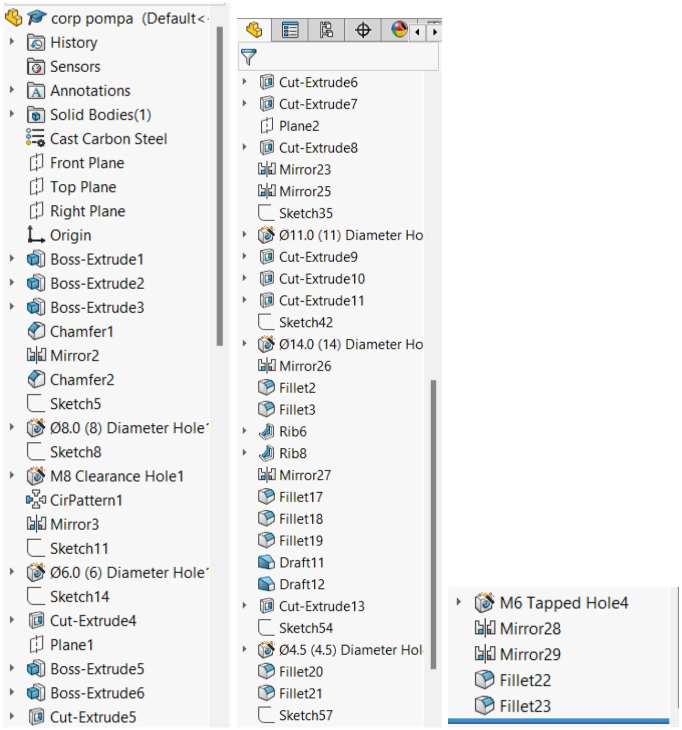

1.2. STL file

To design the hydraulic pump body, a new work session was started in SolidWorks by selecting "Part" as it is a single design component. After designing the hydraulic pump body, the file was saved as "Hydraulic pump body" in SLDPRT format. For manufacturing using additive manufacturing technology, the solid part was converted to an STL file. The file was saved with a .stl extension, and the resolution (coarse, fine, or custom) was selected from the properties menu. Fine quality was chosen for meshing the product, as shown in Figure 4. A total of 22,478 triangles were used for the meshing process [1-58].

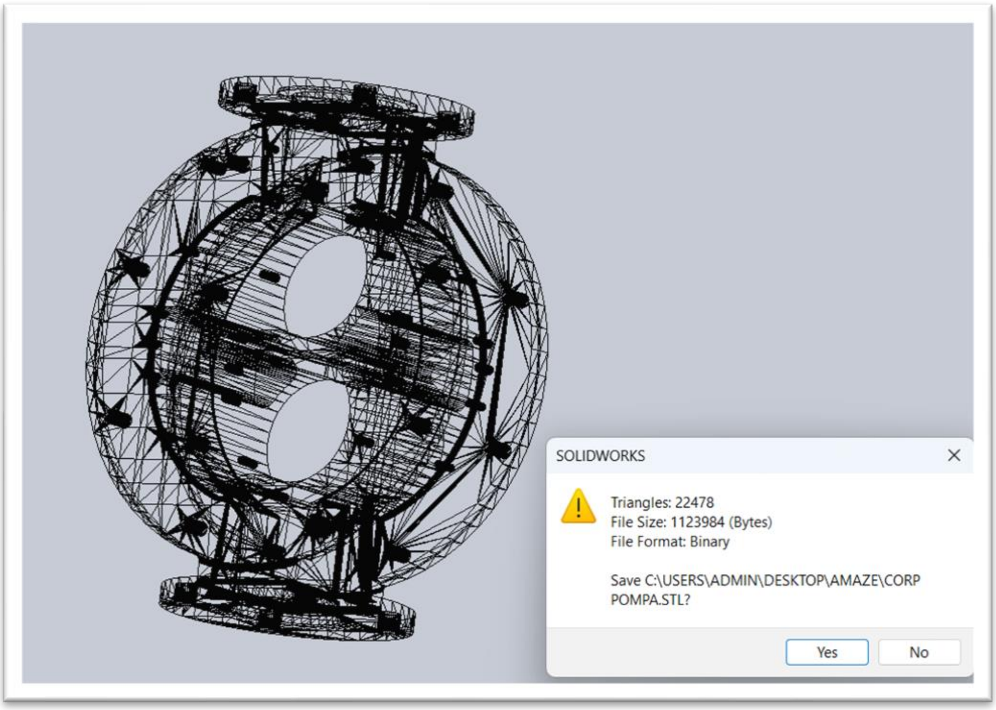

Fig.4. Hydraulic pomp body meshing – STL. file

1.3. 3D Printing software's

Additive Manufacturing (AM) technologies fundamentally differ from material removal processes (such as cutting, EDM, and laser processing) and material redistribution processes (like casting, injection molding, forging, and stamping) in that parts are created by adding material layer by layer, guided by a CAD file.

These technologies have emerged as a result of achievements and advancements in fine mechanics, numerical control, laser technology, computing, software, and the development of new materials.

The specificity of these additive manufacturing processes is their ability to make parts and complex three-dimensional objects, starting from a CAD file, without the need for it use of machine tools or certain tools. The basic element of prototype additive manufacturing technologies is "the section" [1-58].

The pieces are quantified in sections and made using a repetitive process of construction, section by section, reducing a three-dimensional problem to one flat. This dimensional reduction leads to a decrease in accuracy and quality surfaces due to the scale effect.

The steps required for the additive manufacturing of a part are as follows:

- designing the three-dimensional (3D) model of the part, using a design program computer aided (CAD).
- transferring the CAD model to the sectioning processor. The best-known method of sectioning is the approximation of the model with flat triangular elements.
- sectioning the 3D virtual model with parallel planes to the working plane of the rapid manufacturing machine of prototypes and generation of orders for control equipment of the machine.
- the construction of the part (material, supports required during the model, how will be added a new layer, marking the contours for each section, marking the area between the exterior and interior contour of a section.
- cleaning and finishing of the part (operations in which the supports used at construction and excess material are eliminated) [1-58].

Regarding solid CAD modeling, Additive Manufacturing systems are becoming an important and motivating factor for companies that produce solid modelling systems, such as: Solidworks, Unigraphics, I-DEAS, Catia, Inventor, Onshape, AutoCAD, Pro / Engineer, etc.

The top software for FDM (Fused Deposition Modeling) printers includes Ultimaker Cura, BCN3D Cura, Voxelizer, and Z-Suite, while for SLA (Stereolithography) and DLP (Digital Light Processing) printers, popular options include FormLabs and Photocentric.

By visiting Ultimaker's resources page and downloading the free Ultimaker Cura software, you can then generate the necessary G-code file to print the part. The first step is to open Ultimaker Cura software and drag the part, in. stl format, into the workspace, as shown in Figure 5. The software allows you to select the 3D printer required for the job; in this case, the Ultimaker S5 is used. To start printing, you need to connect the 3D printer to the laptop using a cable, memory card, or via a wireless connection [1-58].

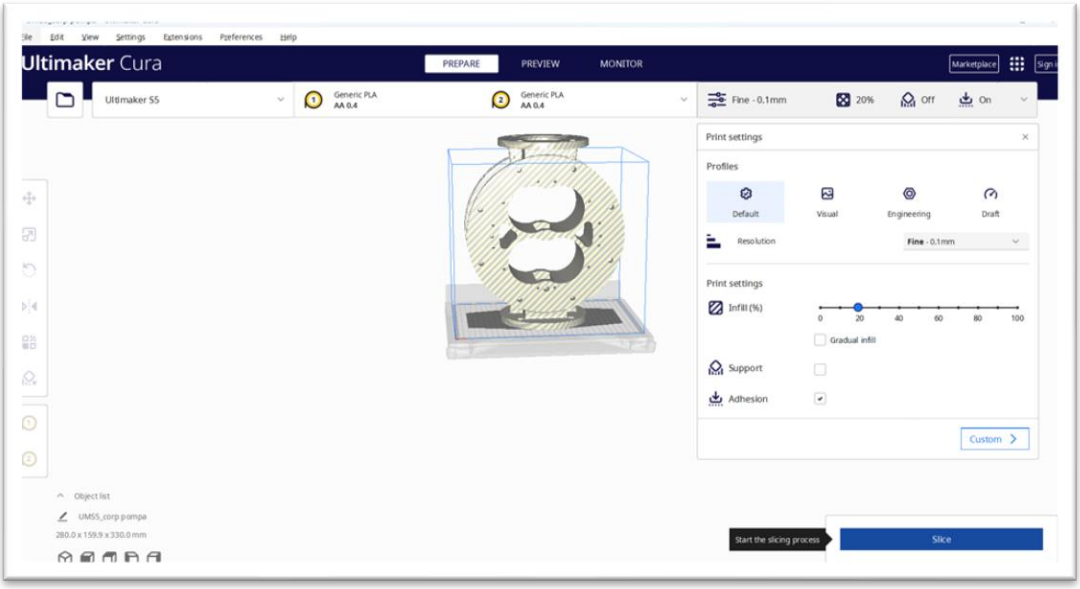

Fig.5. Open Ultimaker Cura software and introduce the STL. file of part

The software allows you to move the part on the work platform along the X, Y, and Z axes and adjust the scale of the part along these axes, as shown in Figure 6. The software allows you to rotate the part along the X, Y, and Z axes, duplicate parts on the work platform, and print mirrored versions of the parts.

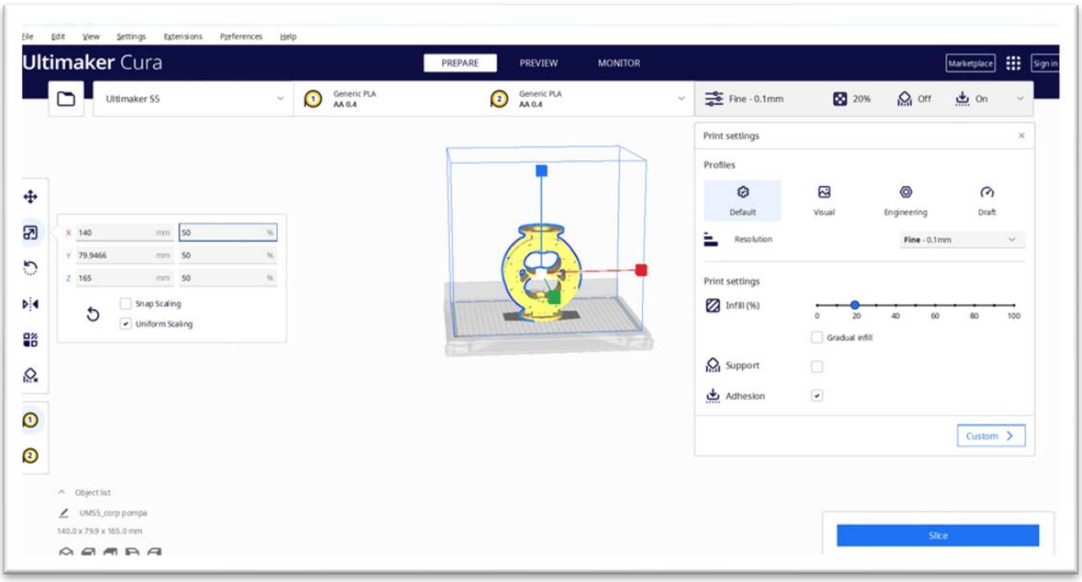

Fig.6. Change the part scale, after X, Y, Z axis

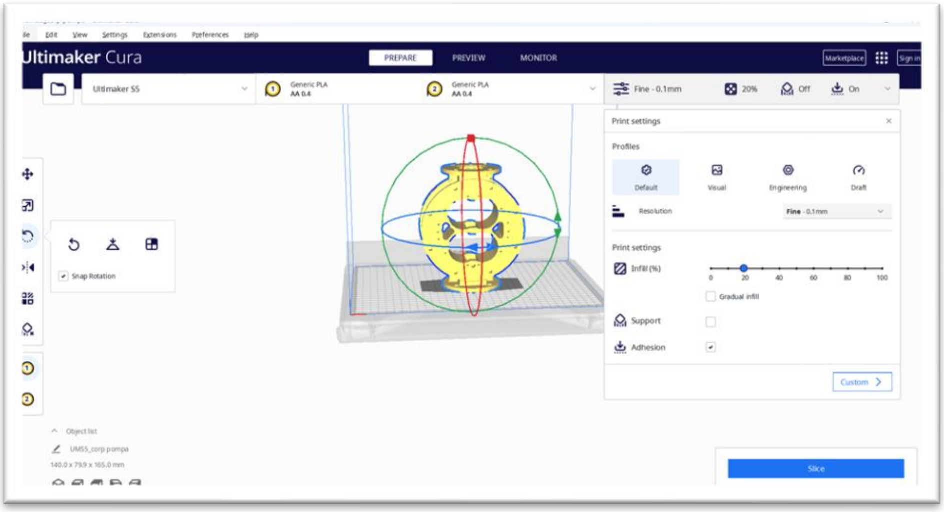

Fig.7. Rotation of the part after X, Y, Z axis

The software allows you to select different materials for printing, such as polylactic acid (PLA), acrylonitrile butadiene styrene (ABS), polyethylene terephthalate (PET), and others. For the hydraulic pump body, PLA material was chosen, with the mechanical properties listed in Table 1 [1-58]. ABS and PLA are the most common materials used in FDM printing and are generally similar in cost. ABS has superior mechanical properties but is harder to print compared to PLA. Material properties can be chosen using the free site https://www.totalmateria.com/page.aspx?ID=Home&LN=RO

Table 1. The mechanical properties of polylactic acid

Properties	Values	Units
Density	1.25	g/cm3
Poisson's Ratio	0.36	-
Shear Modulus G	2.4	GPa
Melting Temperature	173	ºC
Glass transition temperature	60	ºC
Thermal Conductivity	0.13	W/m-K
Extruded Temperature	160-220	ºC
Heat Resistance	110	ºC
Young's Modulus	3.5	GPa
Tensile Strength	61.5	MPa
Compressive Strength	93.8	MPa
Elongation at Break	6	%
Flexural Strength	88.8	MPa
Hardness Shore D	85	A
Impact Strength	30.8	kJ/m2
Yield Strength	60	MPa
Standard Tolerance	+/-0.05	mm
Biodegradable	yes	-

Due to its lower printing temperature, PLA is easier to print with and is better suited for parts with fine details. It is ideal for applications where strength, ductility, machinability, and thermal stability are required. However, PLA is more prone to warping. The mechanical properties of PLA are presented in Table 1.

For the 3D printing process, only a single extruder, Extruder 1 (Fig. 8), was used. However, generally, two extruders can be employed - one for supports and the other for part manufacturing, as shown in Fig. 9.

The software allows customization of the 3D printing process, as shown in Figure 10 (a and b), or the use of recommended parameters for part manufacturing, as illustrated in Figure 11 [1-58].

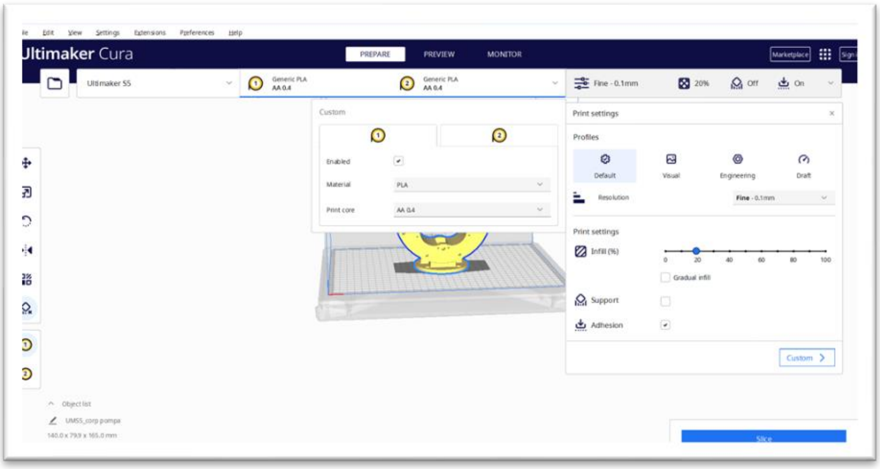

Fig 8. 3D Printing Extruder

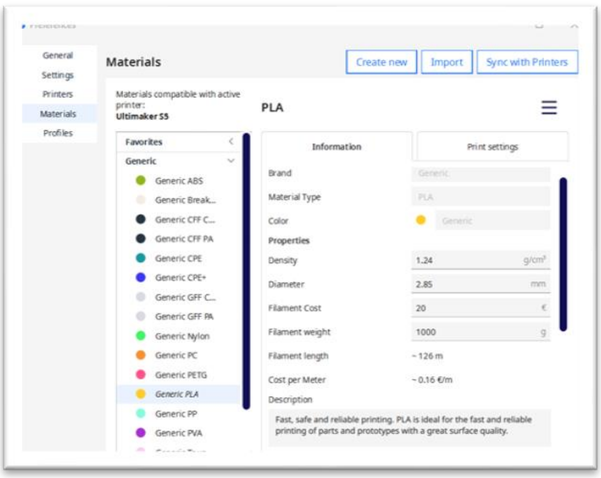

Fig.9. Choosing the PLA filament for Additive Manufacturing

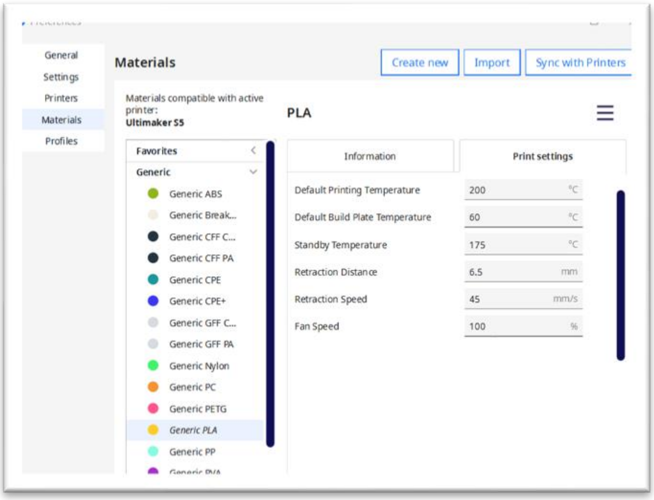

Fig.10a. Printing settings for PLA material

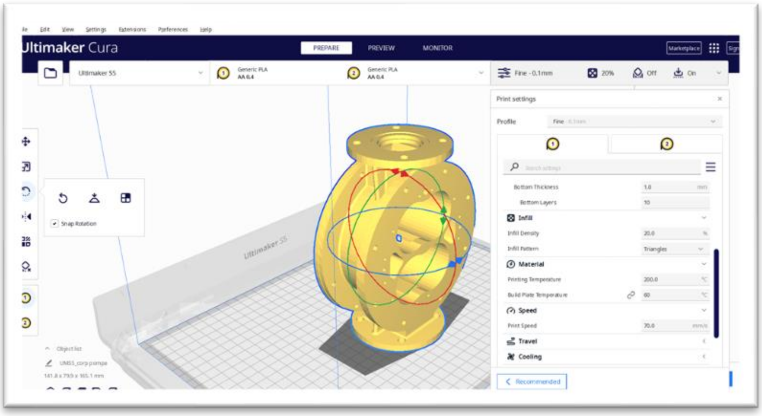

Fig.10b. Manufacturing parameters for custom Additive Manufacturing without supports

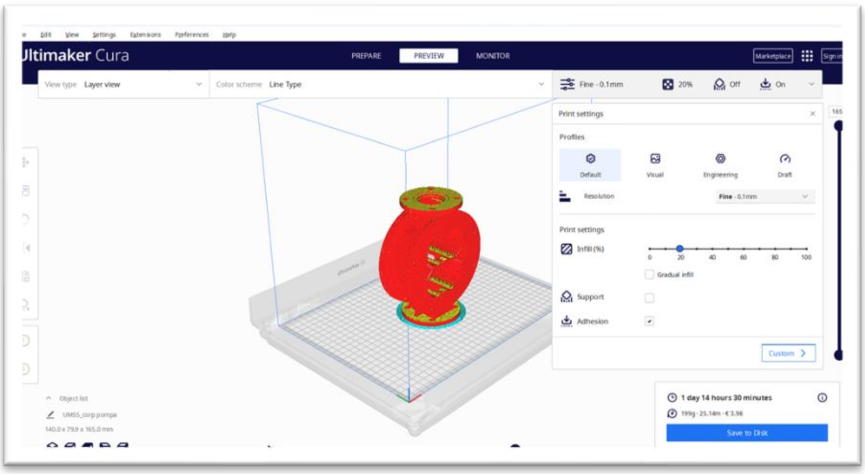

Fig.11. Recommended manufacturing parameters for the part by the software

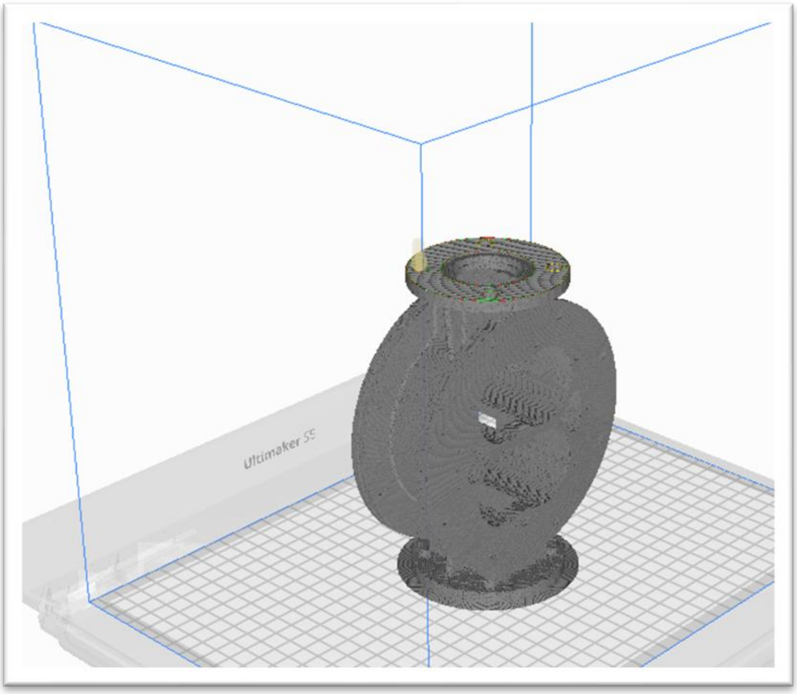

Fig.12. Preview the manufacturing 3D Printing process

To slice the parts, click the blue 'Slice' button. The software will then provide information about the manufacturing time (1 day, 14 hours, and 30 minutes), the cost of the part (3.98 euros, assuming a 1kg PLA filament costs 20 euros), and the material consumption (199 g, with a filament length of 25.14 meters. The software allows the use of supports when high accuracy is required or the omission of supports for faster printing. Additionally, the software provides a preview of the 3D printing process through a short simulation video, as shown in Figure 12 [1-58].

To save the part file in Ultimaker Cura, click on 'Save Project,' as shown in Figure 13. This will generate a 'Summary - Cura Project' (Figure 14), which can then be saved as a .3mf file, as illustrated in Figure 15. 

The software allows you to export the file in various formats, as shown in Figure 16. The G-code file format, which is necessary for 3D printing, was selected, as depicted in Figure 17.

Figure 18 shows the G-code for the hydraulic pump body part. The printing time is estimated at 1 day, 14 hours, and 30 minutes, with a filament consumption of 199 g and a length of 25.14 meters. The cost of the part is 3.98 euros, assuming a filament cost of 20 euros per kilogram.

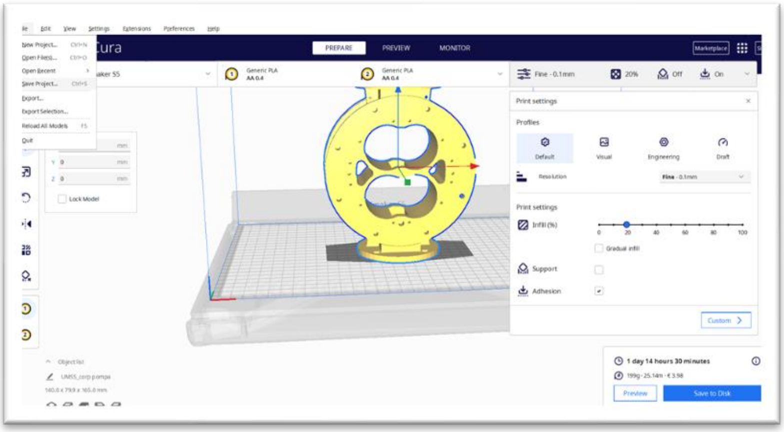

Fig.13. Save Project

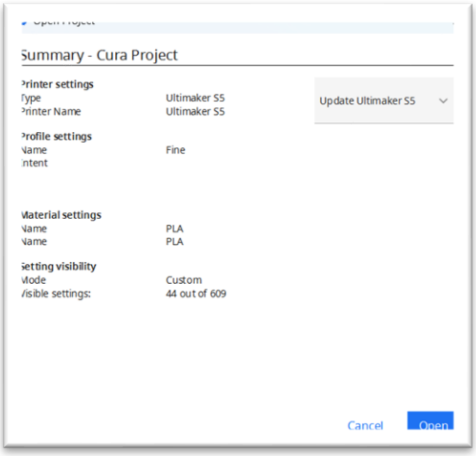

Fig.14. Summary - Cura Project

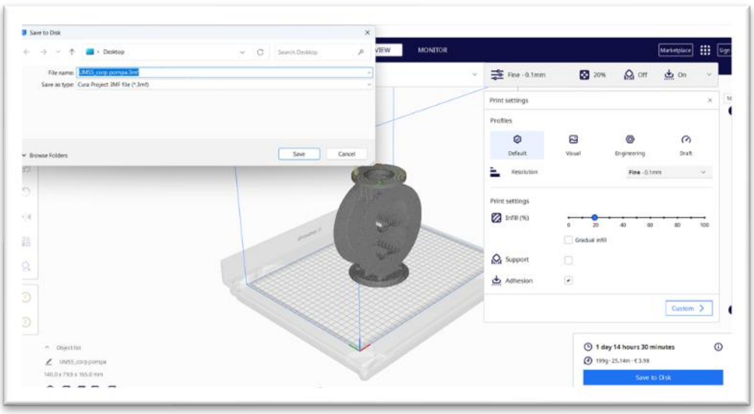

Fig.15. Save project as 3mf. file

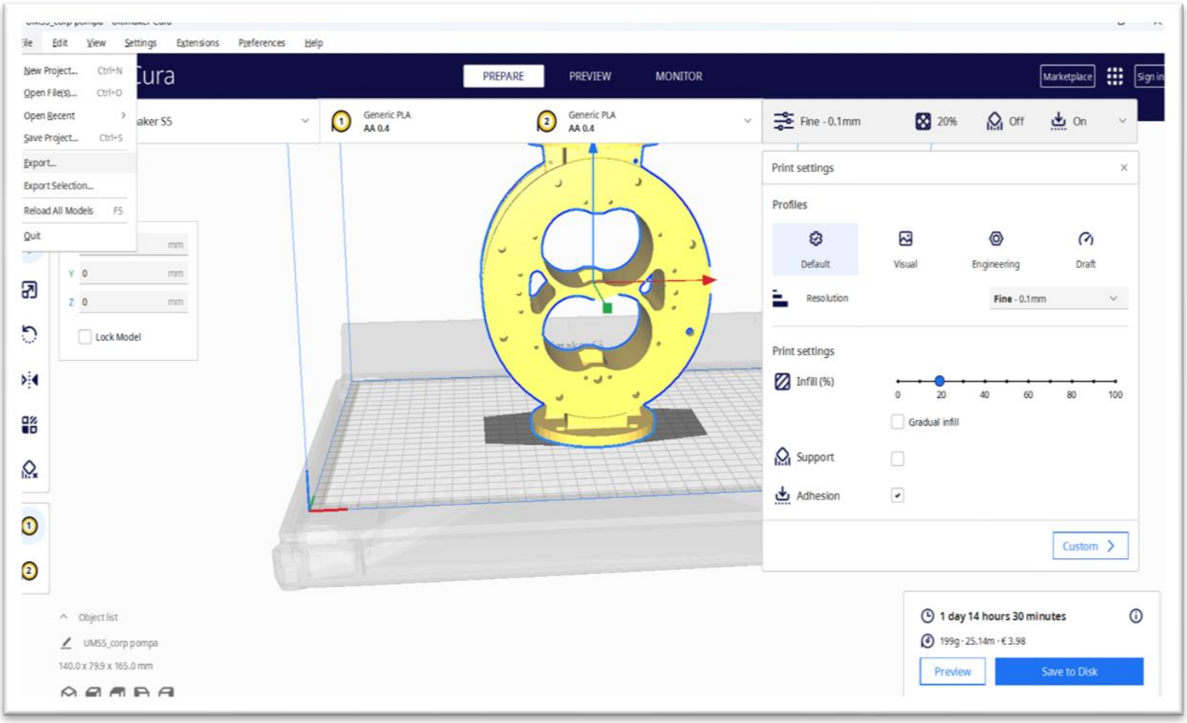

Fig.16. Export file

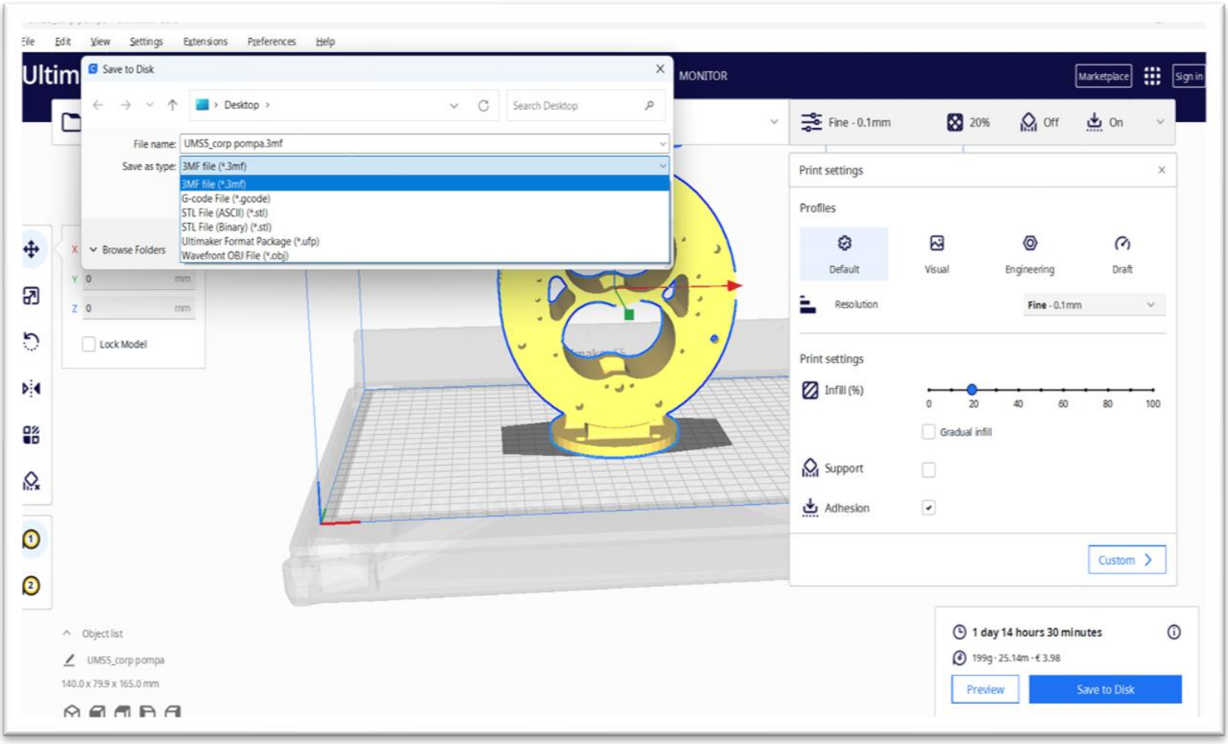

Fig.17. Different extension for file export

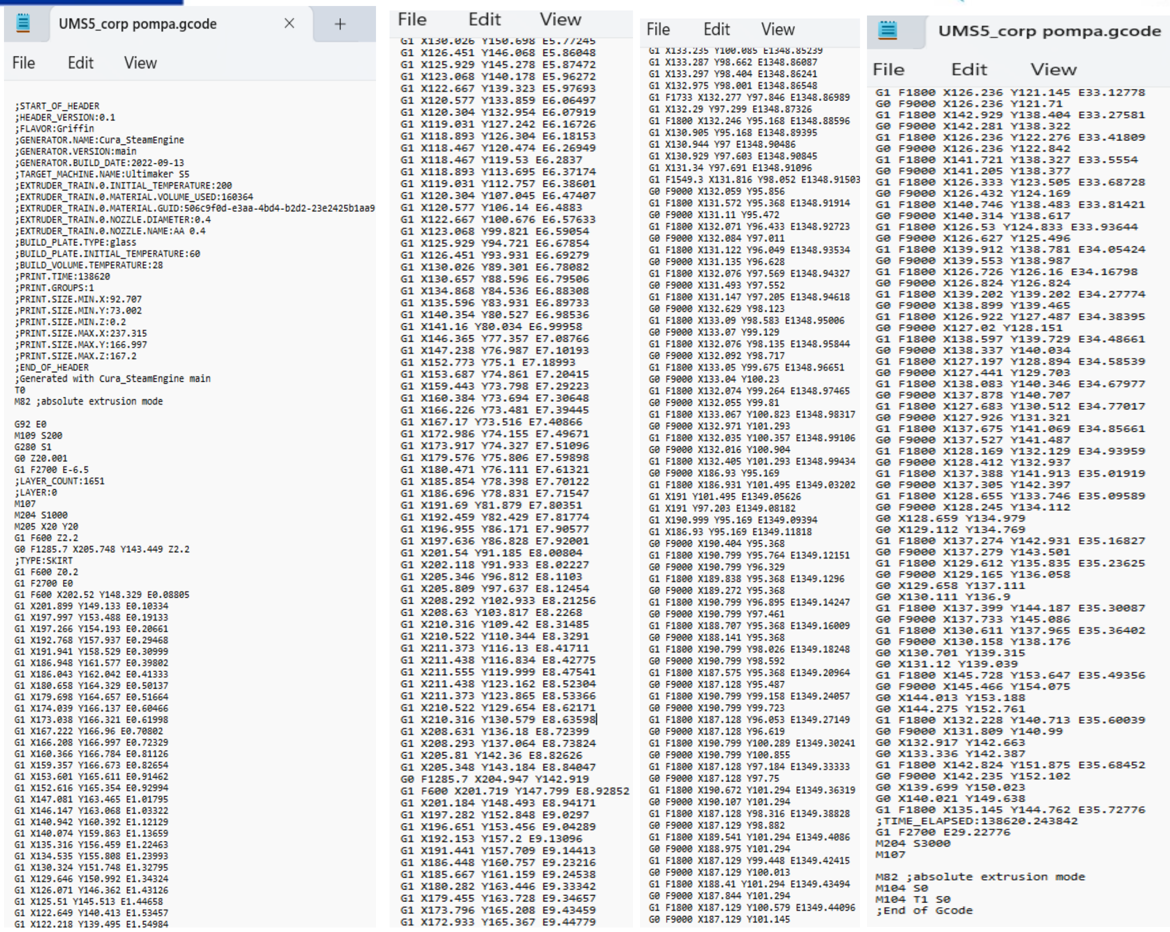

UMS5_corp pompa.gcode

File Edit View

```
;START_OF_HEADER
;HEADER_VERSION:0.1
;FLAVOR:Griffin
;GENERATOR.NAME:Cura_SteamEngine
;GENERATOR.VERSION:main
;GENERATOR.BUILD_DATE:2022-09-13
;TARGET_MACHINE.NAME:Ultimaker S5
;EXTRUDER_TRAIN.0.INITIAL_TEMPERATURE:200
;EXTRUDER_TRAIN.0.MATERIAL.VOLUME_USED:160364
;EXTRUDER_TRAIN.0.MATERIAL.GUID:506c9f0d-e3aa-4bd4-b2d2-23e2425b1aa9
;EXTRUDER_TRAIN.0.NOZZLE.DIAMETER:0.4
;EXTRUDER_TRAIN.0.NOZZLE.NAME:AA 0.4
;BUILD_PLATE.TYPE:glass
;BUILD_PLATE.INITIAL_TEMPERATURE:60
;BUILD_VOLUME.TEMPERATURE:28
;PRINT.TIME:138620
;PRINT.GROUPS:1
;PRINT.SIZE.MIN.X:92.707
;PRINT.SIZE.MIN.Y:73.002
;PRINT.SIZE.MIN.Z:0.2
;PRINT.SIZE.MAX.X:237.315
;PRINT.SIZE.MAX.Y:166.997
;PRINT.SIZE.MAX.Z:167.2
;END_OF_HEADER
;Generated with Cura_SteamEngine main
T0
M82 ;absolute extrusion mode

G92 E0
M109 S200
G280 S1
G0 Z20.001
G1 F2700 E-6.5
;LAYER_COUNT:1651
;LAYER:0
M107
M204 S1000
M205 X20 Y20
G1 F600 Z2.2
G0 F1285.7 X205.748 Y143.449 Z2.2
;TYPE:SKIRT
G1 F600 Z0.2
G1 F2700 E0
G1 F600 X202.52 Y148.329 E0.08805
G1 X201.899 Y149.133 E0.10334
G1 X197.997 Y153.488 E0.19133
G1 X197.266 Y154.193 E0.20661
G1 X192.768 Y157.937 E0.29468
G1 X191.941 Y158.529 E0.30999
G1 X186.948 Y161.577 E0.39802
G1 X186.043 Y162.042 E0.41333
G1 X180.658 Y164.329 E0.50137
G1 X179.698 Y164.657 E0.51664
G1 X174.039 Y166.137 E0.60466
G1 X173.038 Y166.321 E0.61998
G1 X167.222 Y166.96 E0.70802
G1 X166.208 Y166.997 E0.72329
G1 X160.366 Y166.784 E0.81126
G1 X159.357 Y166.673 E0.82654
G1 X153.601 Y165.611 E0.91462
G1 X152.616 Y165.354 E0.92994
G1 X147.081 Y163.465 E1.01795
G1 X146.147 Y163.068 E1.03322
G1 X140.942 Y160.392 E1.12129
G1 X140.074 Y159.863 E1.13659
G1 X135.316 Y156.459 E1.22463
G1 X134.535 Y155.808 E1.23993
G1 X130.324 Y151.748 E1.32795
G1 X129.646 Y150.992 E1.34324
G1 X126.071 Y146.362 E1.43126
G1 X125.51 Y145.513 E1.44658
G1 X122.649 Y140.413 E1.53457
G1 X122.218 Y139.495 E1.54984
```

File Edit View

```
G1 X130.026 Y150.698 E5.77245
G1 X126.451 Y146.068 E5.86048
G1 X125.929 Y145.278 E5.87472
G1 X123.068 Y140.178 E5.96272
G1 X122.667 Y139.323 E5.97693
G1 X120.577 Y133.859 E6.06497
G1 X120.304 Y132.954 E6.07919
G1 X119.031 Y127.242 E6.16726
G1 X118.893 Y126.304 E6.18153
G1 X118.467 Y120.474 E6.26949
G1 X118.467 Y119.53 E6.2837
G1 X118.893 Y113.695 E6.37174
G1 X119.031 Y112.757 E6.38601
G1 X120.304 Y107.045 E6.47407
G1 X120.577 Y106.14 E6.4883
G1 X122.667 Y100.676 E6.57633
G1 X123.068 Y99.821 E6.59054
G1 X125.929 Y94.721 E6.67854
G1 X126.451 Y93.931 E6.69279
G1 X130.026 Y89.301 E6.78082
G1 X130.657 Y88.596 E6.79506
G1 X134.868 Y84.536 E6.88308
G1 X135.596 Y83.931 E6.89733
G1 X140.354 Y80.527 E6.98536
G1 X141.16 Y80.034 E6.99958
G1 X146.365 Y77.357 E7.08766
G1 X147.238 Y76.987 E7.10193
G1 X152.773 Y75.1 E7.18993
G1 X153.687 Y74.861 E7.20415
G1 X159.443 Y73.798 E7.29223
G1 X160.384 Y73.694 E7.30648
G1 X166.226 Y73.481 E7.39445
G1 X167.17 Y73.516 E7.40866
G1 X172.986 Y74.155 E7.49671
G1 X173.917 Y74.327 E7.51096
G1 X179.576 Y75.806 E7.59898
G1 X180.471 Y76.111 E7.61321
G1 X185.854 Y78.398 E7.70122
G1 X186.696 Y78.831 E7.71547
G1 X191.69 Y81.879 E7.80351
G1 X192.459 Y82.429 E7.81774
G1 X196.955 Y86.171 E7.90577
G1 X197.636 Y86.828 E7.92001
G1 X201.54 Y91.185 E8.00804
G1 X202.118 Y91.933 E8.02227
G1 X205.346 Y96.812 E8.1103
G1 X205.809 Y97.637 E8.12454
G1 X208.292 Y102.933 E8.21256
G1 X208.63 Y103.817 E8.2268
G1 X210.316 Y109.42 E8.31485
G1 X210.522 Y110.344 E8.3291
G1 X211.373 Y116.13 E8.41711
G1 X211.438 Y116.834 E8.42775
G1 X211.555 Y119.999 E8.47541
G1 X211.438 Y123.162 E8.52304
G1 X211.373 Y123.865 E8.53366
G1 X210.522 Y129.654 E8.62171
G1 X210.316 Y130.579 E8.63598
G1 X208.631 Y136.18 E8.72399
G1 X208.293 Y137.064 E8.73824
G1 X205.81 Y142.36 E8.82626
G1 X205.348 Y143.184 E8.84047
G0 F1285.7 X204.947 Y142.919
G1 F600 X201.719 Y147.799 E8.92852
G1 X201.184 Y148.493 E8.94171
G1 X197.282 Y152.848 E9.0297
G1 X196.651 Y153.456 E9.04289
G1 X192.153 Y157.2 E9.13096
G1 X191.441 Y157.709 E9.14413
G1 X186.448 Y160.757 E9.23216
G1 X185.667 Y161.159 E9.24538
G1 X180.282 Y163.446 E9.33342
G1 X179.455 Y163.728 E9.34657
G1 X173.796 Y165.208 E9.43459
G1 X172.933 Y165.367 E9.44779
```

File Edit View

```
G1 X133.235 Y100.085 E1348.85239
G1 X133.287 Y98.662 E1348.86087
G1 X133.297 Y98.404 E1348.86241
G1 X132.975 Y98.001 E1348.86548
G1 F1733 X132.277 Y97.846 E1348.86989
G1 X132.29 Y97.299 E1348.87326
G1 F1800 X132.246 Y95.168 E1348.88596
G1 X130.905 Y95.168 E1348.89395
G1 X130.944 Y97 E1348.90486
G1 X130.929 Y97.603 E1348.90845
G1 X131.34 Y97.691 E1348.91096
G1 F1549.3 X131.816 Y98.052 E1348.91503
G0 F9000 X132.059 Y95.856
G1 F1800 X131.572 Y95.368 E1348.91914
G0 F9000 X131.11 Y95.472
G1 F1800 X132.071 Y96.433 E1348.92723
G0 F9000 X132.084 Y97.011
G1 F1800 X131.122 Y96.049 E1348.93534
G0 F9000 X131.135 Y96.628
G1 F1800 X132.076 Y97.569 E1348.94327
G0 F9000 X131.493 Y97.552
G1 F1800 X131.147 Y97.205 E1348.94618
G0 F9000 X132.629 Y98.123
G1 F1800 X133.09 Y98.583 E1348.95006
G0 F9000 X133.07 Y99.129
G1 F1800 X132.076 Y98.135 E1348.95844
G0 F9000 X132.092 Y98.717
G1 F1800 X133.05 Y99.675 E1348.96651
G0 F9000 X133.04 Y100.23
G1 F1800 X132.074 Y99.264 E1348.97465
G0 F9000 X132.055 Y99.81
G1 F1800 X133.067 Y100.823 E1348.98317
G0 F9000 X132.971 Y101.293
G1 F1800 X132.035 Y100.357 E1348.99106
G0 F9000 X132.016 Y100.904
G1 F1800 X132.405 Y101.293 E1348.99434
G0 F9000 X186.93 Y95.169
G1 F1800 X186.931 Y101.495 E1349.03202
G1 X191 Y101.495 E1349.05626
G1 X191 Y97.203 E1349.08182
G1 X190.999 Y95.169 E1349.09394
G1 X186.93 Y95.169 E1349.11818
G0 F9000 X190.404 Y95.368
G1 F1800 X190.799 Y95.764 E1349.12151
G0 F9000 X190.799 Y96.329
G1 F1800 X189.838 Y95.368 E1349.1296
G0 F9000 X189.272 Y95.368
G1 F1800 X190.799 Y96.895 E1349.14247
G0 F9000 X190.799 Y97.461
G1 F1800 X188.707 Y95.368 E1349.16009
G0 F9000 X188.141 Y95.368
G1 F1800 X190.799 Y98.026 E1349.18248
G0 F9000 X190.799 Y98.592
G1 F1800 X187.575 Y95.368 E1349.20964
G0 F9000 X187.128 Y95.487
G1 F1800 X190.799 Y99.158 E1349.24057
G0 F9000 X190.799 Y99.723
G1 F1800 X187.128 Y96.053 E1349.27149
G0 F9000 X187.128 Y96.619
G1 F1800 X190.799 Y100.289 E1349.30241
G0 F9000 X190.799 Y100.855
G1 F1800 X187.128 Y97.184 E1349.33333
G0 F9000 X187.128 Y97.75
G1 F1800 X190.672 Y101.294 E1349.36319
G0 F9000 X190.107 Y101.294
G1 F1800 X187.128 Y98.316 E1349.38828
G0 F9000 X187.129 Y98.882
G1 F1800 X189.541 Y101.294 E1349.4086
G0 F9000 X188.975 Y101.294
G1 F1800 X187.129 Y99.448 E1349.42415
G0 F9000 X187.129 Y100.013
G1 F1800 X188.41 Y101.294 E1349.43494
G0 F9000 X187.844 Y101.294
G1 F1800 X187.129 Y100.579 E1349.44096
G0 F9000 X187.129 Y101.145
```

UMS5_corp pompa.gcode

File Edit View

```
G1 F1800 X126.236 Y121.145 E33.12778
G0 F9000 X126.236 Y121.71
G1 F1800 X142.929 Y138.404 E33.27581
G0 F9000 X142.281 Y138.322
G1 F1800 X126.236 Y122.276 E33.41809
G0 F9000 X126.236 Y122.842
G1 F1800 X141.721 Y138.327 E33.5554
G0 F9000 X141.205 Y138.377
G1 F1800 X126.333 Y123.505 E33.68728
G0 F9000 X126.432 Y124.169
G1 F1800 X140.746 Y138.483 E33.81421
G0 F9000 X140.314 Y138.617
G1 F1800 X126.53 Y124.833 E33.93644
G0 F9000 X126.627 Y125.496
G1 F1800 X139.912 Y138.781 E34.05424
G0 F9000 X139.553 Y138.987
G1 F1800 X126.726 Y126.16 E34.16798
G0 F9000 X126.824 Y126.824
G1 F1800 X139.202 Y139.202 E34.27774
G0 F9000 X138.899 Y139.465
G1 F1800 X126.922 Y127.487 E34.38395
G0 F9000 X127.02 Y128.151
G1 F1800 X138.597 Y139.729 E34.48661
G0 F9000 X138.337 Y140.034
G1 F1800 X127.197 Y128.894 E34.58539
G0 F9000 X127.441 Y129.703
G1 F1800 X138.083 Y140.346 E34.67977
G0 F9000 X137.878 Y140.707
G1 F1800 X127.683 Y130.512 E34.77017
G0 F9000 X127.926 Y131.321
G1 F1800 X137.675 Y141.069 E34.85661
G0 F9000 X137.527 Y141.487
G1 F1800 X128.169 Y132.129 E34.93959
G0 F9000 X128.412 Y132.937
G1 F1800 X137.388 Y141.913 E35.01919
G0 F9000 X137.305 Y142.397
G1 F1800 X128.655 Y133.746 E35.09589
G0 F9000 X128.245 Y134.112
G0 X128.659 Y134.979
G0 X129.112 Y134.769
G1 F1800 X137.274 Y142.931 E35.16827
G0 F9000 X137.279 Y143.501
G1 F1800 X129.612 Y135.835 E35.23625
G0 F9000 X129.165 Y136.058
G0 X129.658 Y137.111
G0 X130.111 Y136.9
G1 F1800 X137.399 Y144.187 E35.30087
G0 F9000 X137.733 Y145.086
G1 F1800 X130.611 Y137.965 E35.36402
G0 F9000 X130.158 Y138.176
G0 X130.701 Y139.315
G0 X131.12 Y139.039
G1 F1800 X145.728 Y153.647 E35.49356
G0 F9000 X145.466 Y154.075
G0 X144.013 Y153.188
G0 X144.275 Y152.761
G1 F1800 X132.228 Y140.713 E35.60039
G0 F9000 X131.809 Y140.99
G0 X132.917 Y142.663
G0 X133.336 Y142.387
G1 F1800 X142.824 Y151.875 E35.68452
G0 F9000 X142.235 Y152.102
G0 X139.699 Y150.023
G0 X140.021 Y149.638
G1 F1800 X135.145 Y144.762 E35.72776
;TIME_ELAPSED:138620.243842
G1 F2700 E29.22776
M204 S3000
M107

M82 ;absolute extrusion mode
M104 S0
M104 T1 S0
;End of Gcode
```

Fig.18. G-code file for hydraulic pomp body

Fig.19. Hydraulic pump body printed by FDM

Product 2: Cable fixing clamp. Files - Politehnica Bucharest

2.1.Design of cable fixing clamp

The purpose of this research was to compare three 3D printing technologies—SLA, DLP, and FDM - in order to determine the optimal processing option based on factors such as processing precision, manufacturing time, software, costs, materials used, and post-processing treatment [1-5].

Additive Manufacturing (AM) technologies for prototypes are fundamentally different from material removal processes (such as cutting, EDM, and laser processing) and material redistribution processes (such as casting, injection molding, forging, and stamping) because parts are created by adding material only where and as much as necessary.

The specificity of these additive manufacturing processes is their ability to make complex three-dimensional parts and objects, starting from a CAD file, without the need to use machine tools or certain SDVs.

The basic element of additive prototyping technologies is the "section".

The parts are quantified in sections and made using a repetitive construction process, section by section, reducing a three-dimensional problem to a flat one. This dimensional reduction leads to a decrease in the accuracy and quality of the surfaces due to the scale effect.

The FDM rapid prototyping system, also known as Thermoplastic Extrusion Modeling, was patented by Stratasys Inc. in 1993. Thermoplastic extrusion/melt deposition modeling is the most widely used additive manufacturing technology due to its simplicity and affordability. It is used in modeling, prototyping but also in production applications.

FDM printing technology consists of passing a filament of plastic material through an extruder that heats it up to its melting point, then applying it uniformly (by extruding) layer upon layer with high accuracy to physically print the 3D model according to the CAD file.

The thermoplastic material is heated to molten state, then it is extruded through a small-diameter nozzle and deposited in layers with a thickness of several tenths of a millimeter.

The deposition is carried out by a modeling head equipped with one or two extrusion nozzles. The raw material, in the form of a filament with a diameter of 1.75, 2.85, or 3 mm, is used. A crucial element of the FDM process is maintaining a temperature within the heating-extrusion head that keeps the material in a pasty state.

The advantages of FDM technology include its user-friendly nature, quiet operation, and safety for office environments.

Usable objects and parts can be produced, with a wide range of materials available. The price of 3D printers (kits and assembled models) as well as consumables (rolls with plastic filaments) is extremely affordable. FDM manufacturing technology features ease of use. The disadvantages of this process are the slow construction speed in the case of complex geometries, the possibility of the existence of non-uniformly printed areas (non-glued layers), low impermeability, poor resolution and accuracy for small parts and fine details (microns).

Applications of the FDM process consist of making durable parts and subassemblies for functional testing, conceptual design, presentation and marketing models, detail parts for food or medical applications, plastic subassemblies for high temperature applications, very small series productions.

Stereolithography (SLA) is an additive manufacturing technology known for solidifying liquid raw material through photopolymerization. SLA was the first process to enable the direct generation of a physical model from computer-generated data. The parts solidify under the influence of a low-power laser (5-10 W).

This technology enables the creation and manufacture of models, prototypes, and parts layer by layer, using selective photopolymerization for solidification. This process is activated by a light beam, which forms bonds between unsaturated molecules, creating polymer chains.

The desired 3D model is initially sliced into cross sections. For each layer, the laser beam traces a cross-section of the partial pattern on the surface of the liquid resin. Exposure to ultraviolet laser light solidifies the model drawn on liquid resin resulting in a solid built (3D printed) layer that is added to the previously built layer. After the pattern has been drawn, the platform descends a distance equal to the thickness of a single layer, typically between 0.05 mm and 0.15 mm.

The accuracy of the printed parts is excellent, with a high-quality surface finish and good to very good printing speed. The materials used include photosensitive liquid resins and newly developed ceramic materials.

SLA technological advantages are the prototyping of parts with complex and highly detailed geometries, very fine and precise printed surfaces, large part construction sizes, the printed parts can be used as a master mold for the industries of injection molding (injection molding), thermoforming, casting metals and parts resistant to high temperatures.

SLA technological disadvantages consist of average resistance to mechanical processing, unsustainability over time, long exposure to the sun damages parts that become brittle and brittle, requires troublesome post-processing operations (with potentially dangerous chemicals).

DLP (Digital Light Processing) printing technology is an additive manufacturing process that uses UV light to solidify liquid photopolymer resins. The DLP process is a type of stereolithography commonly used in rapid prototyping services.

The main difference between DLP and SLA is the use of a light projector that solidifies the resin of a photosensitive polymer, versus a laser as used in the stereolithography process. A DLP printer projects the 3D cross-sectional image of the object onto the surface of the resin. The resin exposed to the light source hardens as the car's build platform lowers, allowing a new layer of fresh resin to be deposited to be solidified by the light. Once the part is fully fabricated, additional post-processing such as backing material removal, chemical bath and UV drying can be performed. Since the entire cross-section is designed in a single exposure, the construction speed of a layer (section) is constant regardless of the complexity of the geometry. Regardless of whether a simple part is printed or 10 complex parts simultaneously, the printing speed remains constant. DLP technology costs are superior to FDM.

In DLP, the accuracy of the printed parts is very high, with an excellent surface finish. The print speed is also good, especially for multiple objects and complex geometries.

The materials used by DLP technology are different types of resins, photopolymers, transparent resins, wax-based polymers.

The advantages of DLP technology include finely detailed and precise printed surfaces, making it ideal for use in the jewelry industry, dental technology, and electronics. It also produces durable prototypes suitable for processing and offers a diverse range of resins, including biomedical materials certified for medical use and transparent resins for packaging prototypes. Additionally, DLP printers are stable with few moving parts.

2.2. Comparison of the processing accuracy of FDM, DLP and SLA technologies in Industrial Design and Architecture

As part of the experimental research, various functional prototypes of 3D parts were created. The 3D printers used in the research were Formlabs (SLA technology), Photocentric Crystal (DLP technology), and Zortrax (FDM technology).

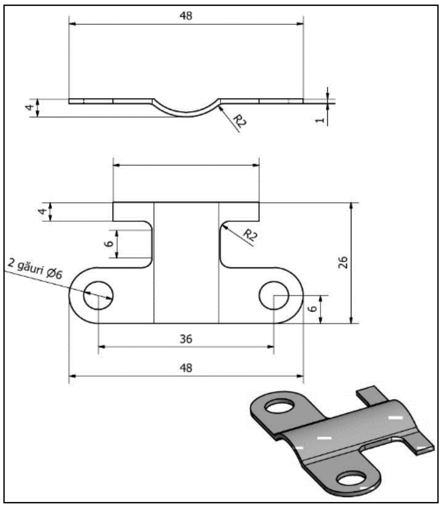

Fig.1. Design of cable fixing clamp

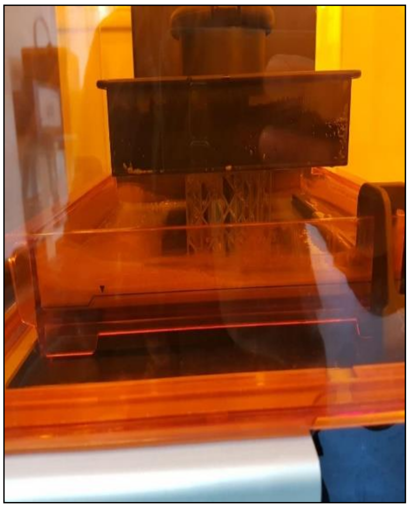

Fig.2. The SLA process for the Cable Fixing Clamp

The Formlabs Form2 3D printer (fig. 1) is a modern, state-of-the-art printer that produces parts with an accuracy of 25-300 microns. It is equipped with a low power laser (P=250 mW and λ=405 nm). The software used is Preform. The file types used are STL, OBJ or FORM.

A 3D model of the cable fixing clip was designed using SolidWorks software as part of the TDPR project. The PreForm software was used to prepare the 3D printing of the landmark, as shown in Figure 3. The landmark will consist of 1,030 layers, with a printing duration of 4 hours and 18 minutes, consuming approximately 20.97 ml of photopolymerizable resin.

The material used was a gray photopolymerizable resin with exceptional mechanical strength, specifically designed for manufacturing prototypes and models in mechanical engineering that require high rigidity. The mechanical properties of this material are listed in Table 1, and the chemical properties are detailed in Table 2. The cost of this resin is $149.

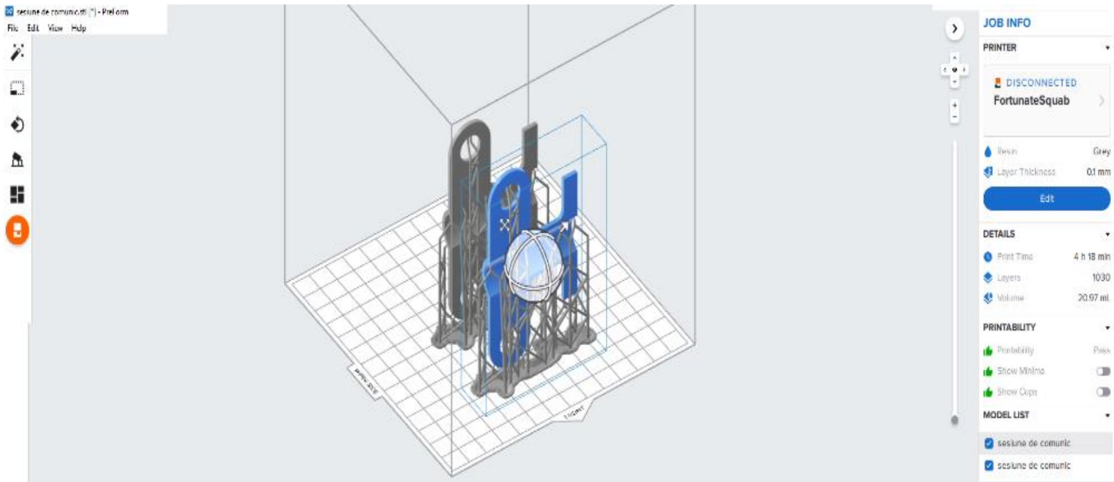

Fig.3. The STL file of the Cable Fixing Clamp, using the PreForm software

Table 1. The mechanical properties of the grey photopolymerizable resin used in SLA technology

	METRIC[1]		IMPERIAL[1]		METHOD
	Green[2]	Post-Cured[3]	Green[2]	Post-Cured[3]	
Tensile Properties					
Ultimate Tensile Strength	35 MPa	61 MPa	5076 psi	8876 psi	ASTM D 638-14
Tensile Modulus	1.4 GPa	2.6 GPa	203 ksi	377 ksi	ASTM D 638-14
Elongation	32.5 %	13 %	32.5 %	13 %	ASTM D 638-14
Flexural Properties					
Flexural Stress at 5% Strain	39 MPa	86 MPa	5598 psi	12400 psi	ASTM D 790-15
Flexural Modulus	0.94 GPa	2.2 GPa	136 ksi	319 ksi	ASTM D 790-15
Impact Properties					
Notched IZOD	not tested	18.7 J/m	not tested	0.351 ft-lbf/in	ASTM D256-10
Temperature Properties					
Head Deflection Temp. @ 1.8 MPa	not tested	62.4 C	not tested	144.3 °F	ASTM D 648-16
Heat Deflection Temp. @ 0.45 MPa	not tested	77.5 C	not tested	171.5 °F	ASTM D 648-16
Thermal Expansion (-30 to 30° C)	not tested	78.5 um/m/C	not tested	43.4 µin/in/°F	ASTM E 831-13

Table 2. The chemical properties of the photopolymerizable resin used in SLA technology

Mechanical Properties	24 hr weight gain (%)	Mechanical Properties	24 hr weight gain (%)
Acetic Acid, 5 %	0.75	Hydrogen Peroxide (3 %)	0.75
Acetone	10.77	Isooctane	0.02
Isopropyl Alcohol	1.56	Mineral Oil, light	0.35
Bleach, ~5 % NaOCl	0.65	Mineral Oil, heavy	0.27
Butyl Acetate	0.84	Salt Water (3.5 % NaCl)	0.64
Diesel	0.08	Sodium hydroxide (0.025 %, pH = 10)	0.72
Diethyl glycol monomethyl ether	2.38	Water	0.83
Hydrolic Oil	0.16	Xylene	0.42
Skydrol 5	0.54	Strong Acid (HCl Conc)	8.21

Table 3. The mechanical properties of the different types of resins used by the Formlab Form2 3D printer

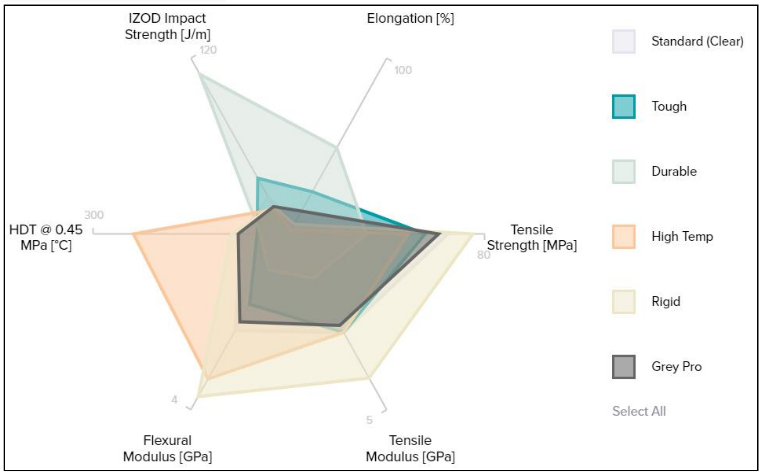

The mechanical properties of the different types of resins used by the Formlab Form2 3D printer are presented in table 3. The resins used by SLA technology are used in the aeronautical industry, the automobile industry, medicine (dentistry, orthodontics), in the jewelry industry, architecture, etc.

An attempt was made to manufacture the same part on a 3D printer, Zortrax from fig.5, uses FDM technology, the software used being the ZSuite software from fig.6. The thickness of the deposited layer is 0.09 mm, the material used is ABS, and the melting temperature of the filament in the extruder is between 200-220°C. The table is heated up to 60°C during manufacturing. For efficient cooling of the deposited layer, 1 cooler is used. G-code generation for 3D printing is performed. In this case, the piece will have 980 layers, the layer thickness is 0.09 mm, 7.34 m of ABS filament will be used, and the 3D printing time will be approximately 5 hours and 22 minutes. The 3D printed part by FDM technology is shown in fig.8. The cost of a roll of ABS filament is $20.

Fig.5. 3D printer Zortrax M200

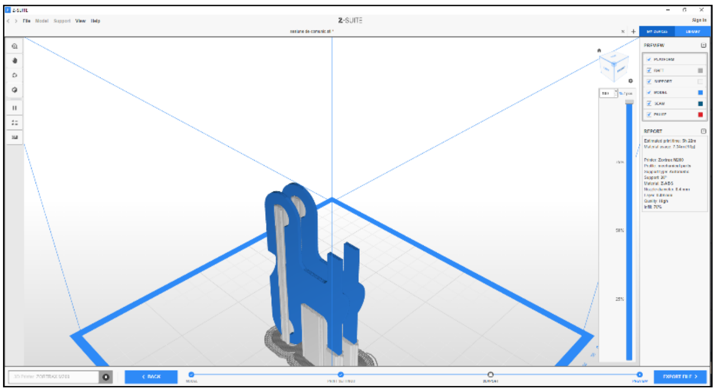

Fig.6. The ZSuite software used for the preparation of 3D printing through FDM

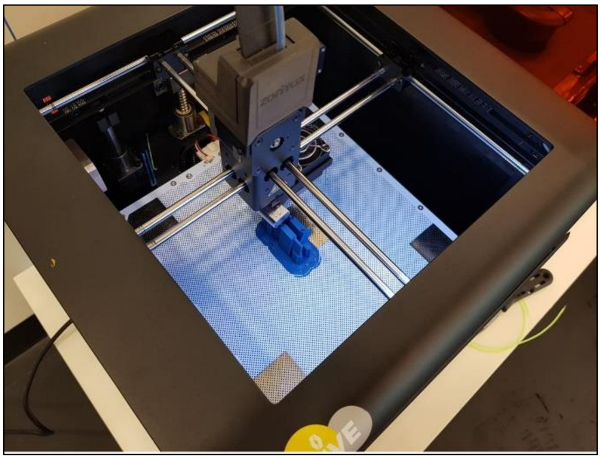

Fig. 7. The machining process using FDM technology for the Cable Fixing Clamp

Fig. 8. 3D printed piece through FDM technology

For the DLP (Digital Light Processing) technology, a Photocentric Crystal 3D printer (as shown in Fig. 9) was used, with bisphenol A ethoxylate diacrylate (Ebecryl 150) as the material. The mechanical and chemical properties of this material are presented in Table 4. The printer's software, Photocentric Studio, was used to prepare the print. The piece was sectioned into approximately 24 layers, as shown in Fig. 10. The 3D printing process took 20 minutes and consumed 0.20 ml of photopolymerizable resin. Figure 11 shows the part printed using DLP technology.

Fig.9. 3D printer Photocentric Crystal Fig.11. 3D part manufactured by DLP

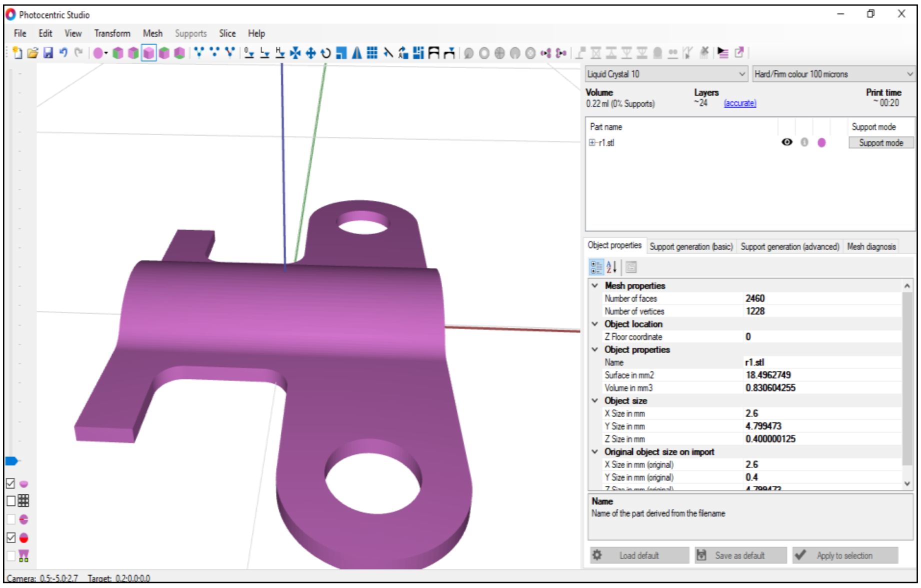

Fig. 10. The Photocentric Studio software used to prepare 3D printing through DLP technology

Table 4. The mechanical and chemical properties of the resin photopolymerizable Ebecryl 150

SPECIFICATIONS[1]	VALUE
Acid value, mg KOH/g, max.	5
Appearance	Clear liquid
Color, Gardner scale, max.	2
Viscosity, 25°C, cP/mPa·s	1150-1650
TYPICAL PHYSICAL PROPERTIES	
Density, g/ml at 25°C	1.14
Flash point, Setaflash, °C	>100
Functionality, theoretical	2
Refractive index (n_D at 20°C)	1.5294
Vapor pressure, mm Hg at 20°C	<0.01
TYPICAL CURED PROPERTIES[2]	
Tensile strength, psi (MPa)	6300 (43)
Elongation at break, %	9
Young's modulus, psi (MPa)	180000 (1241)
Glass transition temperature, °C[3]	41

After comparing the three 3D printing technologies for manufacturing the Cable Fixing Clamp, it was determined that SLA technology is the optimal choice. Although it is more expensive, it provides the necessary precision for part production. In terms of time, all three technologies offer approximately equal durations, but the costs vary significantly, with FDM technology clearly offering the lowest manufacturing price. The Photocentric Studio software is quite complex. Parts manufactured using SLA and DLP technologies require post-processing in a UV oven at 200°C for half an hour to enhance their mechanical properties.

It is recommended to use FDM technology for creating more robust functional prototypes that do not require high precision or fine details, such as those in TFP projects. On the other hand, SLA and DLP technologies are better suited for manufacturing smaller parts, such as landmarks in TDPR projects.

All three technologies typically use traditional plastic materials, sometimes reinforced with metal, wood, or glass particles, and are employed to manufacture functional prototypes with complex surfaces, depending on the desired mechanical properties.

Product 3: Flange.stl file – Politehnica Bucharest

3.1. CAD file

For the industrial parts, we can use the technology SLA and DLP, that are most simple to used and can permit the 3D Printing with a great accuracy the complex parts, as flange model from Fig.1.

SLA (Stereolithography) and DLP (Digital Light Processing) technologies use photocurable vinyl- or epoxy-functional oligomers for photopolymerization [1-58].

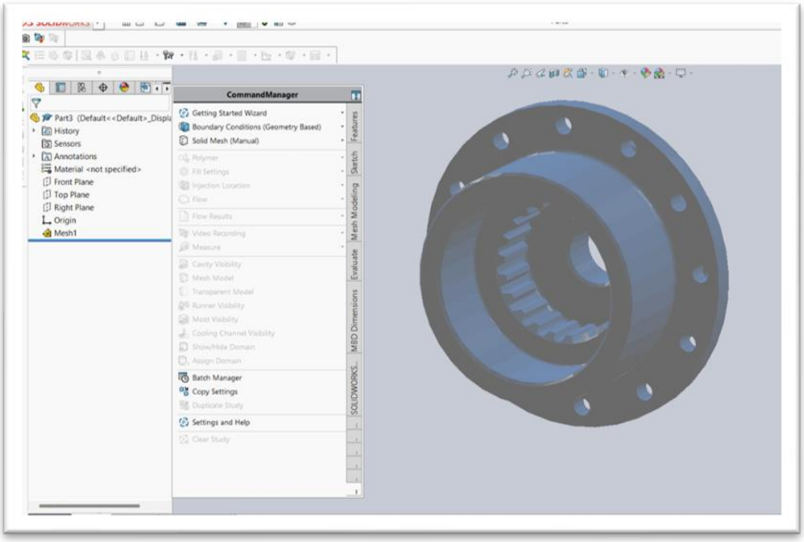

Fig.1. flange stl. file for printing

Table 1 presents the mechanical properties of Bisphenol A Ethoxylate Diacrylate resin. Other resins used in SLA manufacturing include polyurethane resins.

Table 1. The mechanical properties of Bisphenol A Ethoxylate Diacrylate

Bisphenol A Ethoxylate Diacrylate

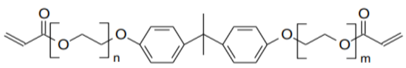

n + m ~ 4

INTRODUCTION

EBECRYL 150 is an ethoxylated bisphenol A diacrylate commonly used as reactive diluent in UV/EB cure applications. EBECRYL 150 can improve the cure response, hardness, and chemical resistance of UV/EB curable coatings and inks while maintaining good adhesion, and without imparting brittleness.

PERFORMANCE HIGHLIGHTS

EBECRYL 150 is characterized by:

- High reactivity
- Moderate viscosity
- High refractive index

UV/EB curable formulated products containing EBECRYL 150 are characterized by:

- Hardness
- Chemical resistance
- Good adhesion
- Improved wetting

The actual properties of UV/EB cured products also depend on the selection of other formulation components such as oligomers, additives and photoinitiators.

SPECIFICATIONS(1)	VALUE
Acid value, mg KOH/g, max.	5
Appearance	Clear liquid
Color, Gardner scale, max.	2
Viscosity, 25°C, cP/mPa·s	1150-1650
TYPICAL PHYSICAL PROPERTIES	
Density, g/ml at 25°C	1.14
Flash point, Setaflash, °C	>100
Functionality, theoretical	2
Refractive index (n_D at 20°C)	1.5294
Vapor pressure, mm Hg at 20°C	<0.01
TYPICAL CURED PROPERTIES(2)	
Tensile strength, psi (MPa)	6300 (43)
Elongation at break, %	9
Young's modulus, psi (MPa)	180000 (1241)
Glass transition temperature, °C(3)	41

3.2. STL file

The file formats that 3D printers can accept are limited to several special 3D dataset files, mainly the Standard Tessellation Language (STL) format and some newer formats called Additive Manufacturing File Format (AMF) or 3D Manufacturing Format (3MF). The model data must be converted into files in these formats before it can be 3D printed.

There are several software that can meet the demands of image processing, ranging from interactive medical image processing software like Mimics (Materialise), D2P (3D Systems), and CAD model processing software like Magics (Materialise), Geomagic Studio (3D

Systems) and SolidWorks (Dassault Systems). In many cases, using multiple software together can integrate different functions [1-58].

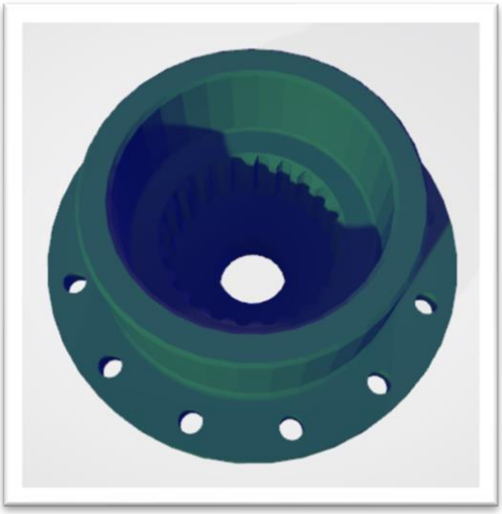

Fig.2. SolidWorks Visualize 2019 – flange with different texture mapping

Figure 2 shows the various texture mappings selected using SolidWorks Visualize 2019.

3.3. 3D Printing software

For printing it used a SLA printer, FormLabs Form 3B+ (Fig.3) and the free software PreForm PreForm and the resin chosen was Flexible and the layer thickness was 0.1 mm, such in Fig.4.

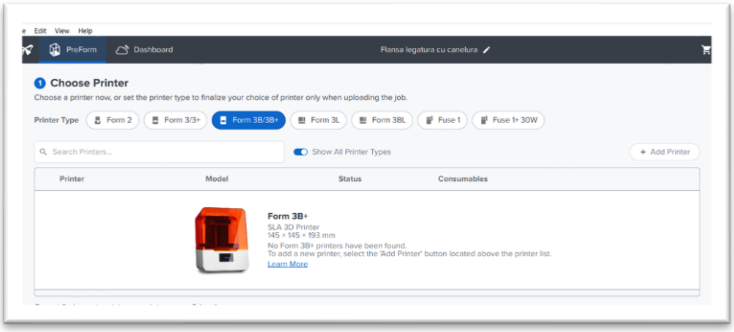

Fig. 3. Software PreForm, Form 3B+ printer chosen

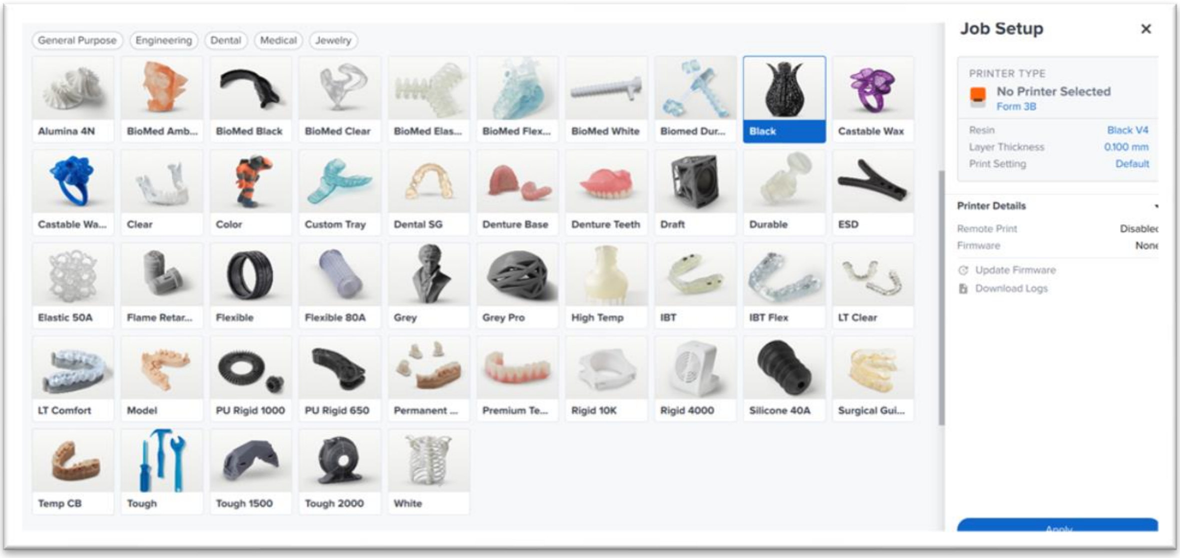

Fig.4. Photopolymerisable resin and layer thickness chosen

In Figure 5, the orientation tool can be used to move the part on the worktable. In Figure 6, supports can be selected to sustain the part during the 3D printing process. The chosen layout is presented in Figure 7, and to start the 3D print, click the orange button labeled 'Start a Print,' as shown in Figure 8 [1-58].

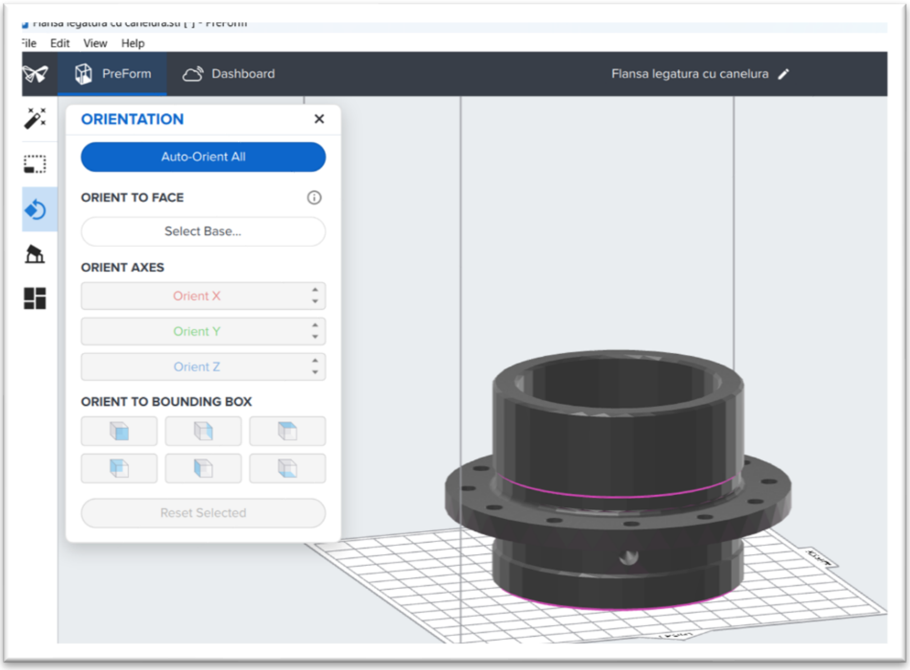

Fig.5. Orientation X,Y,Z on the worktable of the part

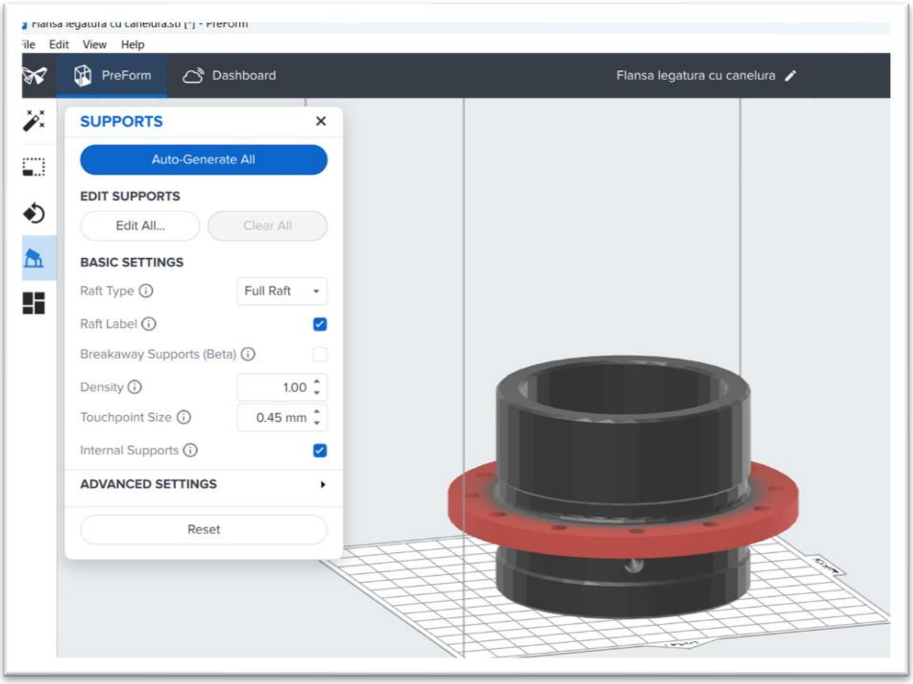

Fig.6. Supports chosen to sustain the part during the 3D Printing process

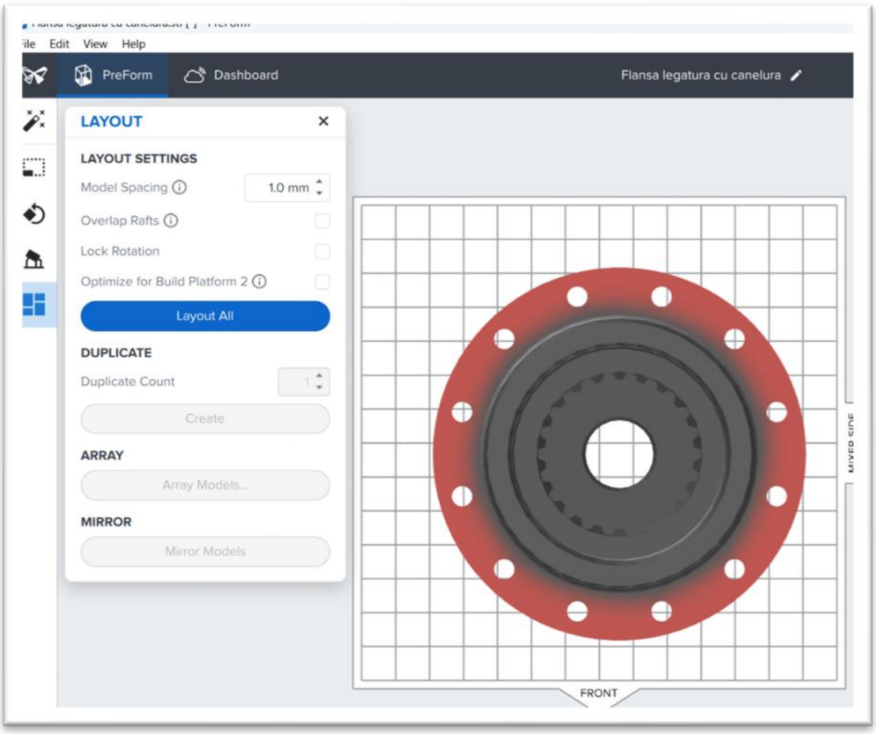

Fig.7. The layout chosen

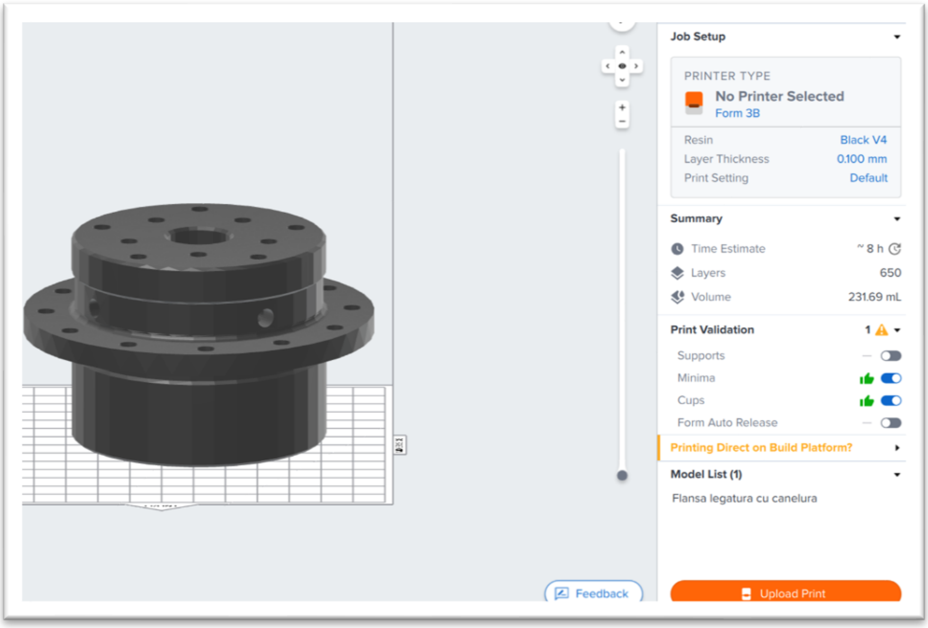

Fig.8. The orange button – Start a print

In Figure 9, the flange STL file was dragged onto the 3D printer's worktable. However, the part is too large for the available worktable space, causing it to appear red.

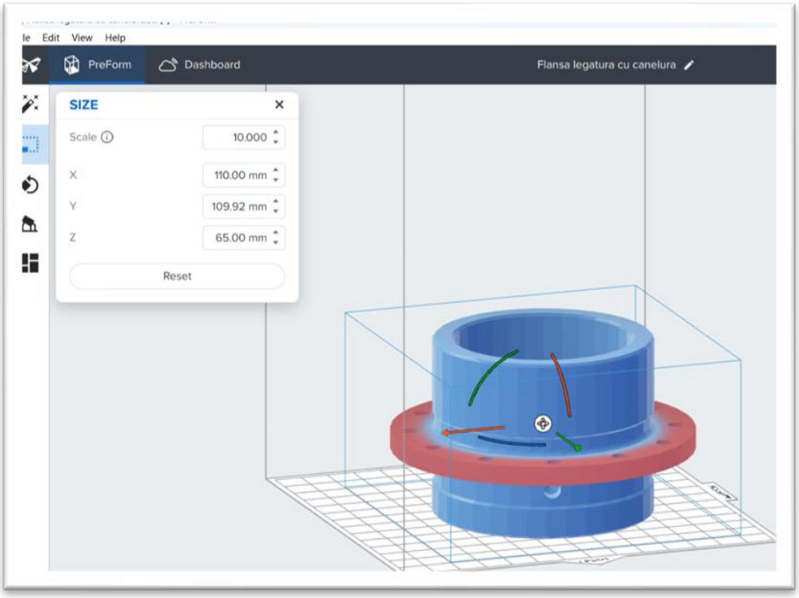

Fig.9. The scale of flange STL. file on the worktable

In this case, it was changed the scale at 10:1 and was calculating orientation and generating the supports as in figure 10 [1-58].

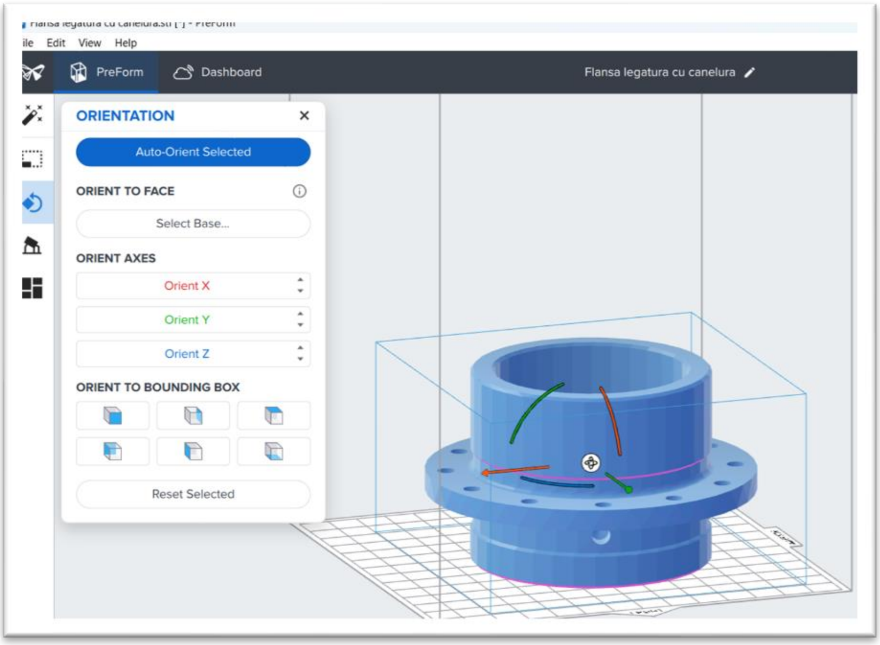

Fig.10. Change the scale at 10:1 and was calculating orientation and generating the supports

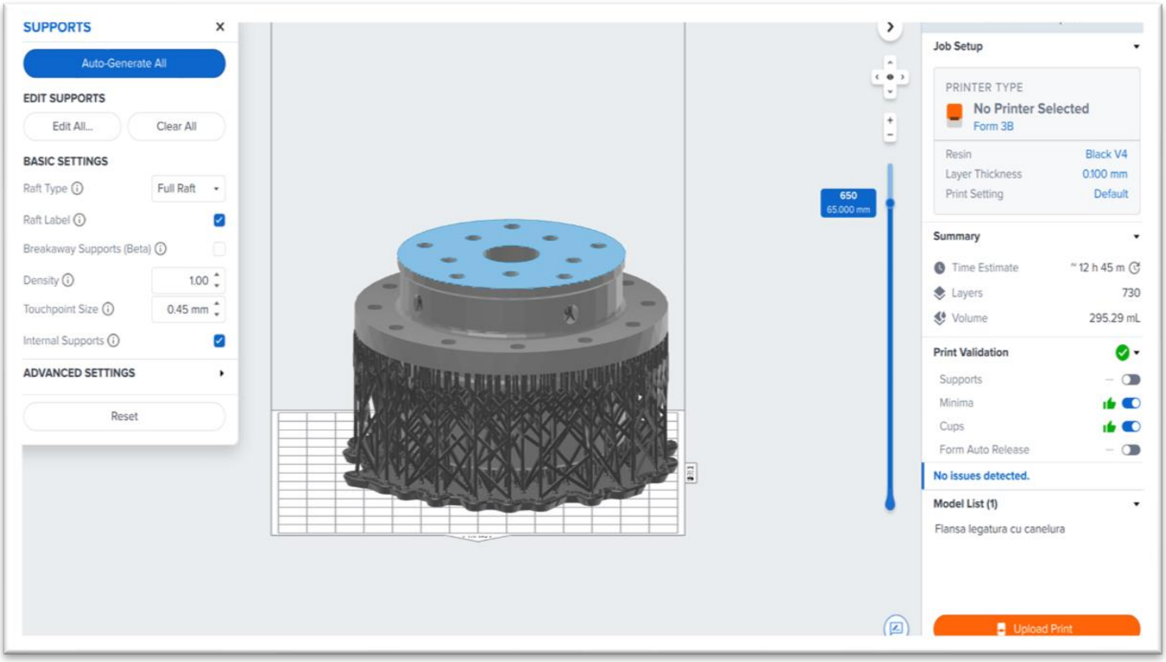

Fig.11. Calculating orientation and generating supports

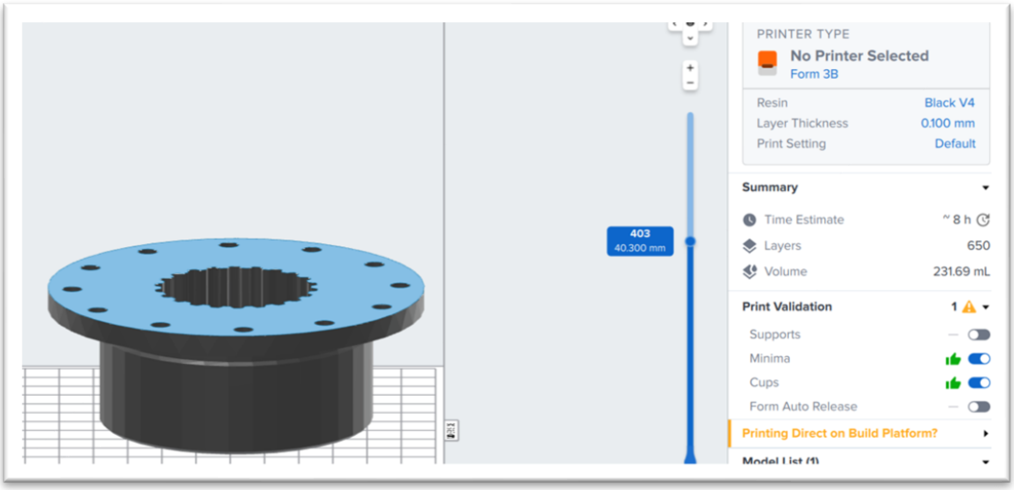

Fig.12. Surface printed at the layer 403

For orientation and supports, you can click on the respective buttons, and the program will generate them automatically, or you can adjust them manually, as shown in Figure 11. The program also allows you to view the slicing of the part layer by layer, specifying the layer number and highlighting in blue the area being printed at layer 403, as shown in Figure 12. Additionally, the program provides details such as the resin volume used (231.69 mL), the number of layers (650), and the approximate print time (8 hours).

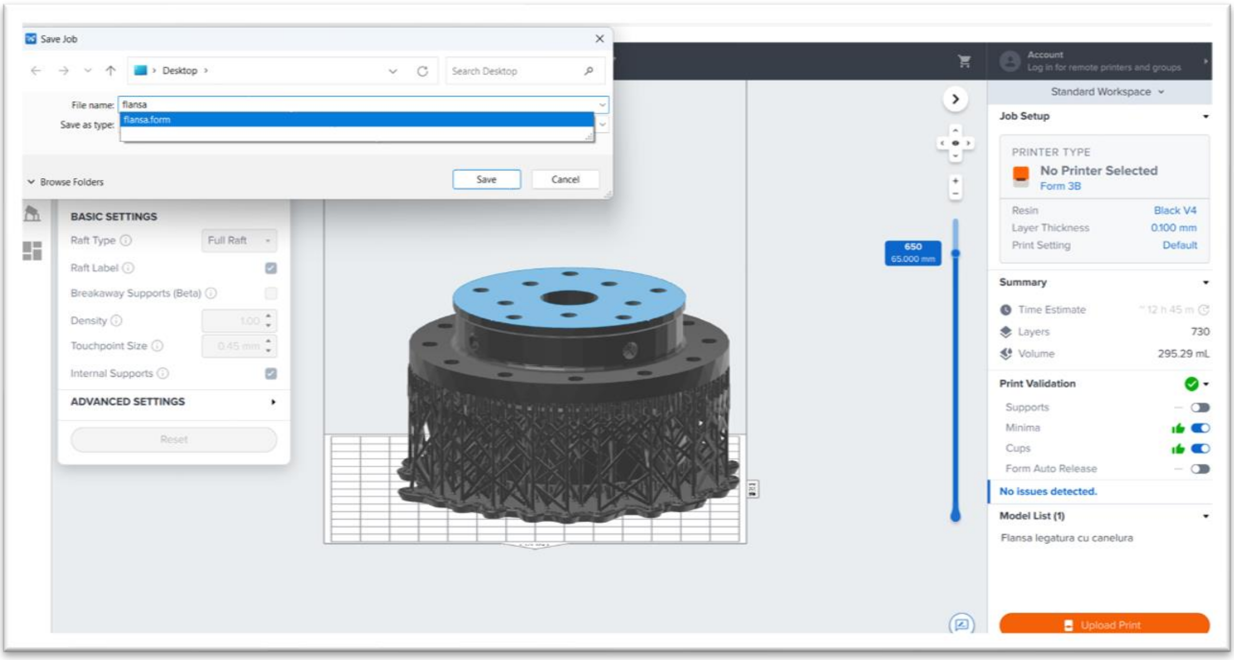

Fig.13. Save the file as Flange with the extension .FORM

In figure 13, the printing setting of the flange with supports is saved such as Flange.FORM , using the software PreForm. Concerning the resin, it was used Black V4, print time 12h 47 minutes, 730 layers, 295.29mL. To start the 3D printing of the part, click the orange "Print" button, as shown in Figure 14, after connecting the printer online or via a cable to the laptop.

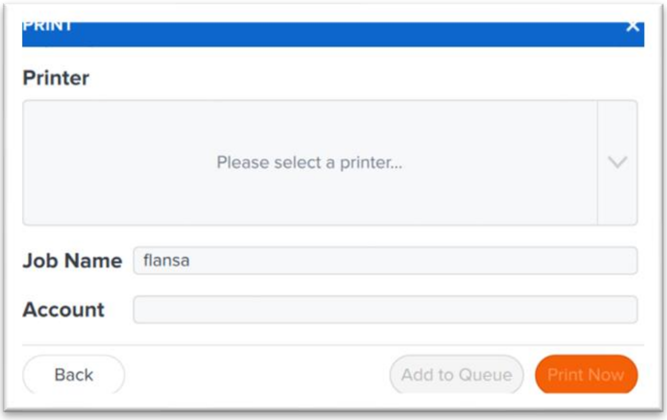

Fig.14. Click on the orange button to print

Figure 15 shows the flange printed using SLA technology. After printing, the supports are removed, and the parts are cleaned in isopropyl alcohol. They are then placed in a UV furnace for 30 minutes at a temperature of 210°C to enhance their mechanical properties [1-58].

Fig.15. Flange printed by SLA

4. Conclusions

In the future, further research could focus on developing multi-material and multi-color prototypes using additive manufacturing technologies. This research would explore the use of various silicones and colored plastic materials, which are essential for producing diverse industrial parts and devices.

The use of various silicones would be particularly interesting for manufacturing more complex industrial parts, as it would enable the production of components with excellent chemical, physical, and mechanical properties [1-58].

The implications of this research are significant for the manufacturing of industrially designed parts with complex forms, which could be applied in fields such as automotive, aerospace, tooling, architecture, and industrial design, among others.

5. References

1. Ratner Buddy D., Hoffman Allan S., Schoen Frederick J., Lemons Jack E.- Biomaterials Science, An introduction to materials in medicine –Academic Press, 2013;
2. https://en.wikipedia.org/wiki/3D_printing
3. https://3dscentral.3dsystems.com/?option=com_content&view=category&id=312&itemid=734
4. http://www.bibus.hu/fileadmin/editors/countries/bihun/product_data/zcorp/documents/zcorp_series_zprinter_310_plus_manual_en.pdf
5. http://sldtech.com/wp-content/uploads/2008/10/consumables_catalog_.pdf
6. http://www.star-prototype.com/blog/top-7-methods-for-making-3d-rapid-prototypes/
7. https://en.wikipedia.org/wiki/Fused_deposition_modeling
8. http://www.erpro.fr/ABS-deposition?lang=fr
9. https://en.wikipedia.org/wiki/Stereolithography
10. http://intech-ind.com/sla-machines-in-rapid-prototyping/
11. MacDonald D. – Applying Stereolithography to produce usable prototypes and tooling, Proceedings of the 2nd European Conference on Rapid Prototyping and Manufacturing, Nottingham (UK), 1993, pp113- 118, ISBN 0951975919;
12. Earle J. – Graphics for engineers, 5th edition, Pretince-Hall, 1999, ISBN 0130160075;
13. Hague R., Dickens P.M. – Finite element analysis calculated stresses in investment casting shells using stereolithography models as patterns, Proceedings of 5th European Conference on Rapid Prototyping and Manufacturing, Helsinki (Finland) 14th – 16th june 1996, pp31-46, ISBN 0951975951;
14. http://envisiontec.com/3d-printers/ultra-3sp-family/
15. https://en.wikipedia.org/wiki/Digital_Light_Processing

16. The Best Industrial Metal and Plastic 3D Printers I 3D Systems
17. Berce P. & others - Tehnologii de fabricație prin adăugare de material și aplicațiile lor – Romanian Academy Edition, Bucharest 2014;
18. https://www.3dsystems.com/3d-printers/prox-dmp-320
19. https://www.3dsystems.com/3d-printers/prox-dmp-300
20. https://www.3dsystems.com/3d-printers/prox-dmp-200
21. https://www.3dsystems.com/3d-printers/prox-dmp-100
22. https://www.optomec.com/wp-content/uploads/2014/04/LENS_450_Datasheet-WEB.pdf
23. https://www.optomec.com/wp-content/uploads/2014/04/LENS_MR-7_WEB.pdf
24. https://www.optomec.com/wp-content/uploads/2014/04/LENS_850-R_Web_0716.pdf
25. http://iopscience.iop.org/article/10.1088/0022-3727/48/3/035303
26. https://www.rtejournal.de/ausgabe2/103
27. http://lycees.ac-rouen.fr/maupassant/Melec/co/Communication/FTTH/web/res/image_14.png
28. http://www.myshared.ru/slide/1324038/
29. http://deuns.chez.com/sciences/cristallo/cristallo44.html
30. http://shopmetaltech.com/fabricating-technology/fabricating/nd-yag-or-fiber-laser-for-micro
31. https://en.wikipedia.org/wiki/Transverse_mode
32. https://extrudehone.com/enhanced-finishing-solution-metal-3d-printing
33. http://www.scielo.br/scielo.php?script=sci_arttext&pid=S1516-14392007000200019 [156] https://www.eos.info/additive_manufacturing/for_technology_interested
34. http://www.mdpi.com/2073-4352/3/4/517/htm
35. http://www.sciencedirect.com/science/article/pii/S0141635916300721#bib0225
36. http://www.mdpi.com/2075-4701/6/11/286/htm
37. http://www.nae.fr/wp-content/uploads/2015/07/FabAdditiveMetallique_TechnoOpportunites-NAE.pdf
38. http://www.scielo.br/scielo.php?script=sci_arttext&pid=S1516-14392015000700024
39. http://www.sciencedirect.com/science/article/pii/S0264127516313296
40. https://www.youtube.com/watch?v=KbXJb4wcxnw
41. http://www.mdpi.com/1996-1944/9/12/975#
42. http://www.mdpi.com/1996-1944/10/9/1055
43. http://www.sciencedirect.com/science/article/pii/S0030399214000632
44. http://www.insidemetaladditivemanufacturing.com/blog/visual-guide-to-the-most-common-defects
45. http://slideplayer.com/slide/4731730/
46. http://www.sciencedirect.com/science/article/pii/S1359645417308170

47. https://www.researchgate.net/publication/277020783_Surface_texture_measurement_for_additive
48. http://www.sciencedirect.com/science/article/pii/S135964541630088X
49. https://www.assemblymag.com/articles/93176-additive-manufacturing-takes-off-in-aerospace-industry
50. https://alopexoninnovation.com/category/systems-engineering/
51. https://www.researchgate.net/publication/294109314
52. https://www.sciencedirect.com/science/article/pii/S0264127519305751#fig0005
53. https://www.sciencedirect.com/science/article/pii/S0264127518300303?casa_token=NqqBRt_j0u4AAAAA:ypnAxH32t1hY5JaawJelewifiQYZUg0PskVYkAnWymwxaWc2RhSCkOn8R0uvV6etCNX2eY1RQd6G#f0020
54. https://www.metal-am.com/articles/material-selection-for-the-3d-printing-of-injection-moulding-tooling/
55. ISO/ASTM 52900:2021(en), Additive manufacturing
56. Ultimaker Cura: Ultimaker Cura: Powerful, easy-to-use 3D printing software
57. PreForm software
58. Voxelizer software

Co-funded by the European Union

AMAZE

Erasmus+ Programme Key Action 2 Cooperation Partnerships for Higher Education (KA220-HED)
Agreement number 2023-1-RO01-KA220-HED-000155412
European Network for Additive Manufacturing in Industrial Design for Ukrainian Context- Acronym: AMAZE

e-Toolkit
Smart (Intelligent) Materials

Project Title	**European Network for Additive Manufacturing in Industrial Design for Ukrainian Context 2023-1-RO01-KA220-HED-000155412**
Output	**IO2 - AMAZE e-toolkit manual for digital learning in producing complex design industrial parts**
Module	**Module 2.1.** **Smart (Intelligent) Materials used in industry**
Date of Delivery	**June 2024**
Authors	**Adam PATALAS, Paweł ZAWADZKI Natalia WIERZBICKA, Remigiusz ŁABUDZKI**
Version	**FINAL VARIANT, *14.06.2024***

Contents

Introduction

Smart materials characteristic

Smart materials, also known as intelligent or responsive materials, represent a significant advancement in engineering applications due to their ability to dynamically respond to environmental stimuli such as temperature, pressure, electric fields, and magnetic fields. These materials are characterized by their ability to alter their properties in real-time, offering enhanced mechanical performance, efficiency, and adaptability compared to traditional materials [1], [2].The versatility of smart materials is evident in their wide range of applications across various fields. In mechanical engineering, they are used to improve the performance and adaptability of systems, allowing for real-time adjustments to environmental changes[1]. In the realm of digital technology and sensors, smart materials enhance detection sensitivity and accuracy, making them invaluable in biomedical applications where biocompatibility and precise response to stimuli are crucial[3], [4]. One of the most notable classes of smart materials includes shape memory alloys (SMAs) and shape memory polymers (SMPs), which exhibit the shape memory effect (SME).

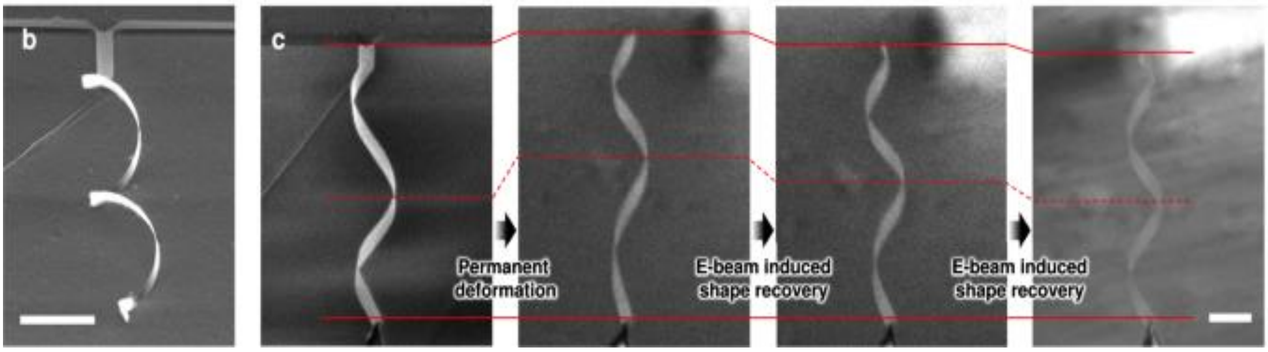

Figure 1. Schape memory effect in ferroic nanocomposites [5]

This property allows them to return to a pre-defined shape upon exposure to specific stimuli, making them suitable for challenging applications in medical devices, robotics, and aerospace designs [2], [3]. These materials are also integral to the development of smart clothing, where they enable the integration of chemical sensors into textiles. In sustainable energy applications, smart materials play a crucial role in enhancing energy efficiency and conservation. They are used in smart rooftops, thermoelectrics, photovoltaics, and other innovations to conserve renewable energy sustainably. For instance, shape memory materials like Nitinol are embedded in wind turbine blades to improve aerodynamic efficiency, while piezoelectric nanogenerators convert mechanical energy into electrical energy, offering sustainable energy solutions[6]. The biomedical field has also seen transformative applications of smart materials. These materials can mimic natural biological processes, providing innovative solutions in drug delivery, tissue engineering, and diagnostics. They enable precise targeting and controlled release of therapeutic agents, reducing side effects and improving therapeutic outcomes [4], [7].

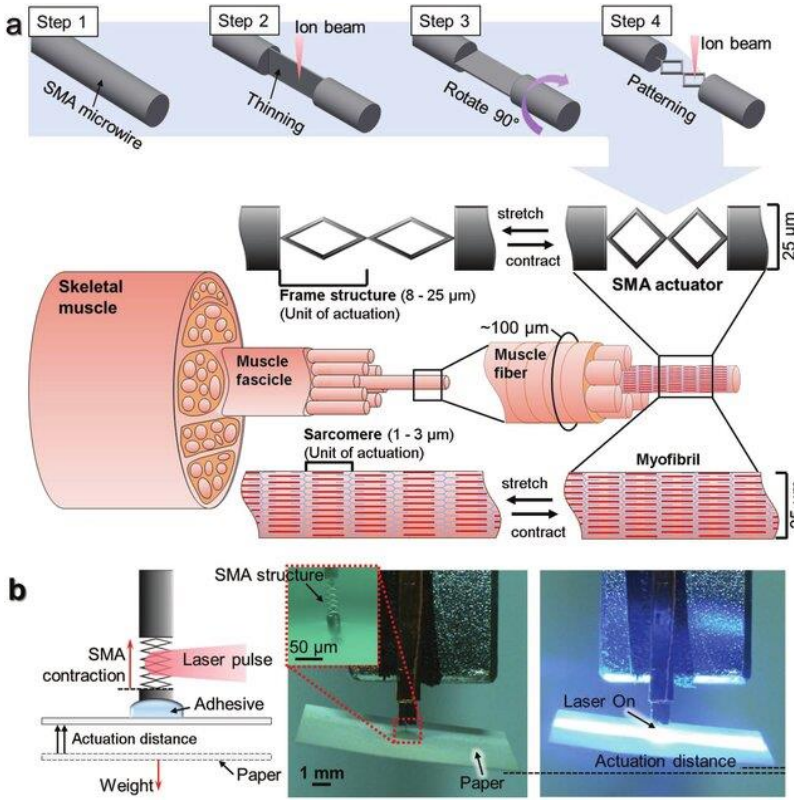

Figure 2. The process involves creating a diamond-shaped SMA structure and designing artificial muscle fibers. First, an SMA wire is selected and milled into a thin plate using focused ion beam technology. The sample is then rotated, and the desired pattern is fabricated. The laser-activated SMA actuator successfully lifted a small piece of paper [8]

Smart materials in biomedicine include metal-based nanomedicines and nanomaterials designed for specific tumor conditions, enhancing the efficacy of cancer therapies [6]. Despite their promising applications, the development and integration of smart materials pose challenges, such as the need for further research to optimize their properties and expand their applications. The interdisciplinary nature of smart materials research necessitates collaboration across various scientific and engineering fields to overcome these challenges and fully realize their potential [6], [9]. In conclusion, smart materials are revolutionizing engineering applications by offering adaptive, efficient, and sustainable solutions across multiple industries. Their ability to respond to environmental stimuli and their integration into diverse applications underscore their importance in advancing technology and addressing contemporary challenges in energy, healthcare, and beyond[10], [11].

Smart materials in mechanical engineering

Smart materials are increasingly integrated into various engineering fields due to their unique properties and ability to respond to external stimuli. They are applied across different engineering disciplines in several innovative ways.

In aerospace engineering, smart materials are used to enhance aircraft wings and fuselages through adaptive structures and materials, improving aerodynamic performance. They also play a role in vibration damping and control systems and are utilized in shape memory alloys for actuators and deployable structures. Mechanical engineering benefits from smart materials through their contribution to precision actuators and sensors in robotics. These materials are critical for vibration and shock absorption systems and are employed in self-healing materials to boost durability and longevity. [12]

In automotive engineering, smart materials are applied in active suspension systems using magnetorheological and electrorheological fluids. Shape memory alloys are employed for adaptive control systems, while energy-absorbing materials enhance safety and crashworthiness.

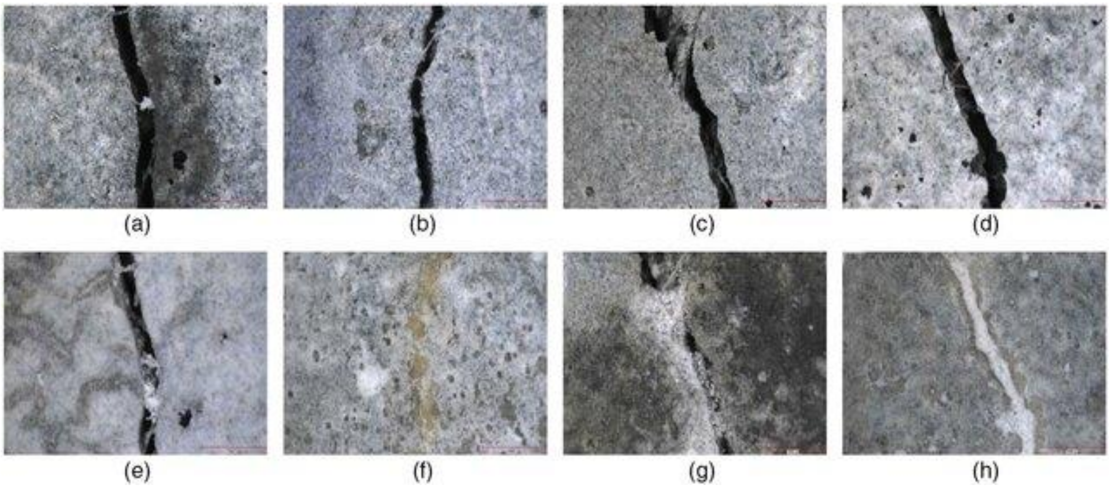

Figure 3. Example of self-healing concrete [13]

Civil engineering utilizes smart materials for structural health monitoring, adaptive building facades, and self-healing concrete. They also play a role in vibration control for bridges and high-rise buildings.[13] Biomedical engineering leverages smart materials in the development of artificial muscles and flexible actuators for prosthetics and orthotics. They are used in responsive drug delivery systems, implants, tissue engineering, and regenerative medicine. In electronics engineering, smart materials are incorporated into sensors and actuators for consumer electronics. They are used in energy harvesting systems, such as those with piezoelectric materials, and in flexible and stretchable electronic devices.[12] Nanotechnology employs nano-engineered smart materials for advanced coatings and surfaces. Responsive nanomaterials are utilized in drug delivery and diagnostic applications, while nano-actuators and sensors are integrated into micro-electromechanical systems (MEMS).

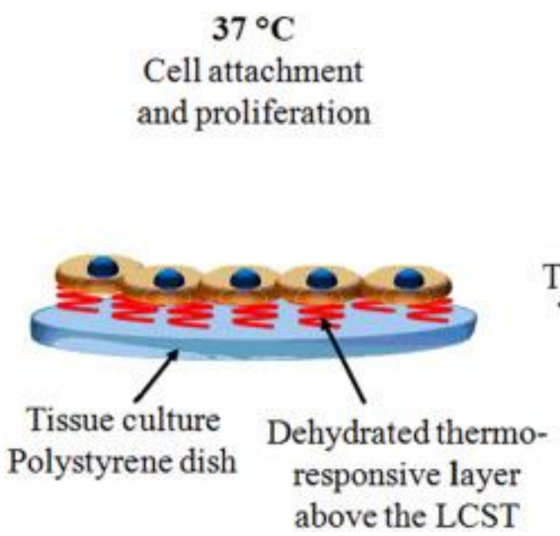

Figure 4. Mechanism of cell attachment to and detachment from thermo-responsive modified tissue culture polystyrene (TCPS) surfaces in response to a temperature modification

Energy engineering benefits from smart materials through the use of phase change materials for thermal energy storage. They contribute to energy-efficient buildings and systems, including photovoltaic and thermoelectric devices. Structural engineering sees applications of smart materials in adaptive structural components for load-bearing purposes, self-healing materials for maintenance and repair, and systems designed for vibration control and noise reduction. In environmental engineering, smart materials are used for water purification, environmental monitoring, and responsive materials for pollution control and waste management. They also support adaptive systems for climate control and energy efficiency in buildings. [14], [15]

Smart Materials Applications in Mechanical Engineering [12], [13], [14], [15]:

1. Shape Memory Alloys (SMA):
   - Actuators in robotics and aerospace systems.
   - Vibration dampers in mechanical structures.
   - Self-healing materials for structural components.
2. Piezoelectric Materials:
   - Sensors in precision engineering.
   - Actuators for micro-positioning systems.
   - Energy harvesting devices in automotive systems.

3. Magnetostrictive Materials:
    - Actuators in hydraulic systems.
    - Torque sensors in automotive applications.
    - Vibration control in mechanical systems.
4. Electroactive Polymers (EAP):
    - Artificial muscles for robotics.
    - Flexible actuators in biomedical devices.
    - Tunable lenses in optical systems.
5. Thermochromic and Photochromic Materials:
    - Smart windows for energy-efficient buildings.
    - Temperature indicators in mechanical systems.
    - Wearable sensors for health monitoring.
6. Magnetorheological and Electrorheological Fluids:
    - Adaptive shock absorbers in automotive suspension.
    - Clutches and brakes in mechanical systems.
    - Tunable vibration isolators.
7. Self-Healing Materials:
    - Automotive coatings with scratch resistance.
    - Composite materials in aerospace applications.
    - Polymers in structural health monitoring.
8. Phase Change Materials (PCM):
    - Thermal management in electronics.
    - Heat storage systems in HVAC.
    - Passive cooling in buildings and vehicles.
9. Photomechanical Materials:
    - Light-driven actuators in micro-mechanical systems.
    - Optical switches and displays.
    - Energy-efficient light-driven devices.
10. Magnetic Shape Memory Alloys (MSMA):
    - High-precision actuators in robotics.
    - Sensors in industrial automation.

- Micro-actuators in medical devices.

Nitinol
Nitinol characteristics

Nitinol, a nickel-titanium alloy, is a prominent smart material known for its unique characteristics, including shape memory effect and superelasticity, which have led to its widespread application across various industries. These properties allow Nitinol to return to its original shape after deformation when exposed to a specific thermal stimulus, making it highly valuable in applications requiring actuation and sensing capabilities [16], [17].

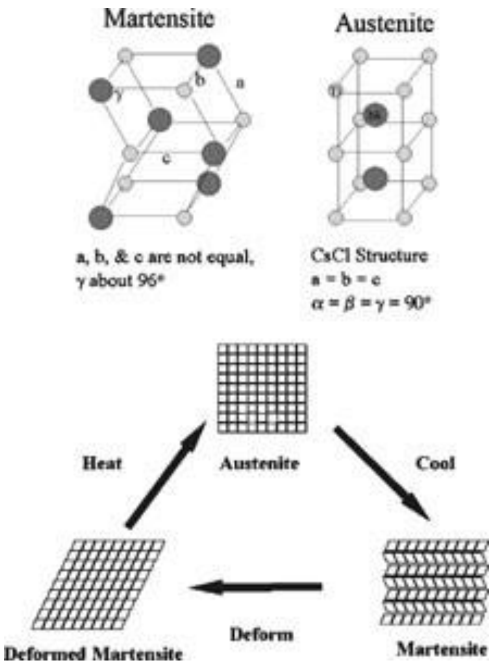

Figure 5. The atomic structure of the nitinol alloy [18]

One of the defining features of Nitinol is its shape memory effect, which is the ability to undergo deformation at one temperature and recover its original, undeformed shape upon heating. This property is particularly useful in creating actuators and sensors, as it allows for the design of systems that can respond dynamically to environmental changes without the need for additional mechanical components [19], [20]. The superelasticity of Nitinol, which allows it to undergo significant strain and recover without permanent deformation, further enhances its utility in applications requiring flexibility and resilience [21]. In the biomedical field, Nitinol's biocompatibility and mechanical properties make it an ideal material for medical devices such as stents, orthodontic devices, and surgical instruments. Its ability to mimic the behavior of human muscles by contracting upon heating and returning to its original shape upon cooling is particularly advantageous in minimally invasive surgeries and other medical applications [19], [21], [22]. Nitinol's application extends beyond the biomedical industry. In architecture, it is used in kinetic facade systems that adapt to environmental conditions, leveraging its shape memory properties to create responsive building elements without additional energy consumption [22]. In the automotive and aerospace industries, Nitinol is used in smart composites and actuators, where its high strength-to-weight ratio and corrosion resistance are beneficial [23], [24].

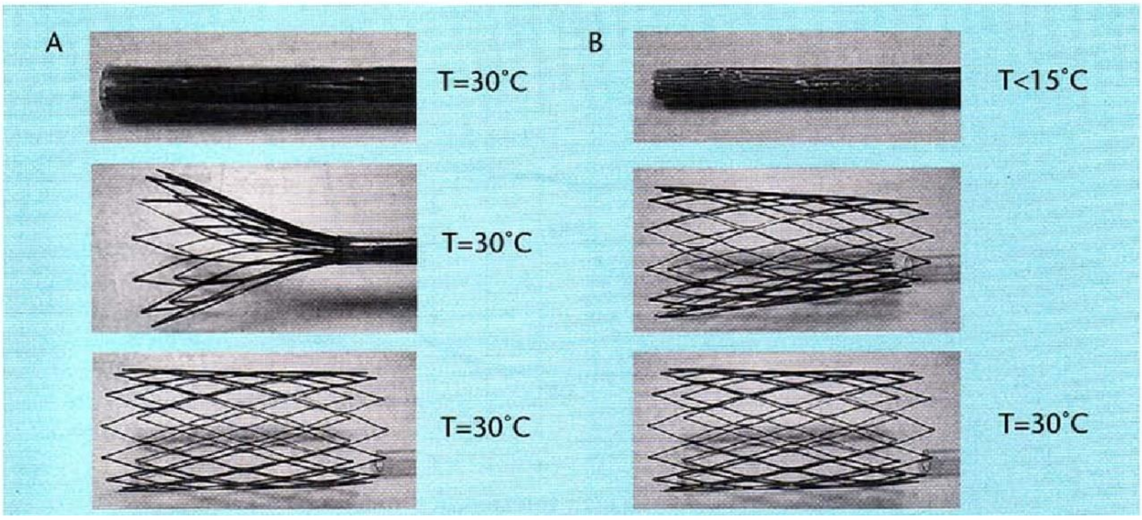

Figure. 6. (A) Elastic deployment of a “slotted-tube” type nitinol stent. (B) Cold deployment and thermal recovery of the stent (demonstration device) [25]

The integration of Nitinol in smart composites, such as those reinforced with fibrillated cellulose, has shown significant improvements in mechanical properties, including yield strength, modulus of elasticity, and impact energy, while also enhancing corrosion resistance. These composites demonstrate self-healing capabilities, further showcasing Nitinol's potential in advanced material applications [23]. Moreover, advancements in 4D printing technology have expanded the applicability of Nitinol by enabling the creation of structures that change shape over time in response to environmental stimuli. This technology is particularly promising in the development of robotic systems and automated guided vehicles, where Nitinol's properties can be harnessed for path tracking and interaction with dynamic environments [26]. In summary, Nitinol's unique characteristics, including its shape memory effect, superelasticity, and biocompatibility, make it a versatile smart material with applications across various fields, from biomedical devices to architectural systems and advanced composites. Its ability to respond to thermal stimuli and recover its original shape without additional mechanical input underscores its potential in innovative design and engineering solutions[17], [24], [27].

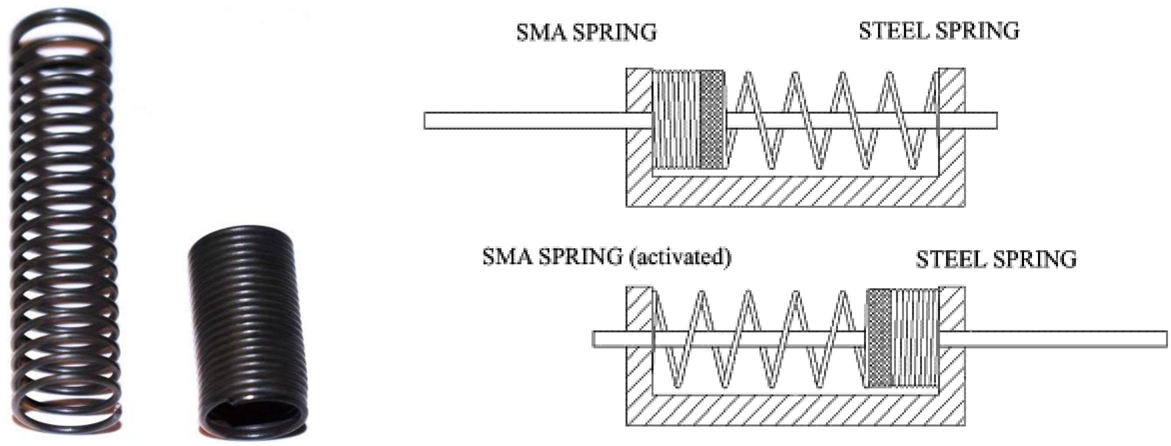

Figure 7. An example of a spring made of NiTi alloy and examples of the operating principle [28]

Compared to other SMAs, Nitinol stands out due to its large recoverable strain limit of approximately 8%, which is significantly higher than many other SMAs. This property is crucial for applications requiring substantial deformation and recovery, such as self-deploying actuators and folding structures in aerospace[29]. Additionally, Nitinol's biocompatibility and superelasticity make it a preferred choice for biomedical implants and devices, where it can endure the dynamic environment of the human body without losing functionality[30].

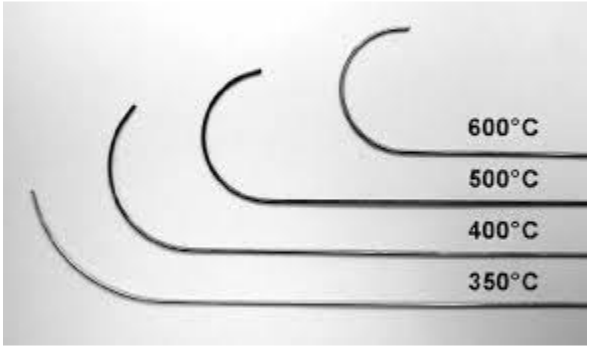

Figure 8. Nitinol wire shaped into hooks and heat treated at 350, 400, 500, and 600 °C for five minutes.

However, Nitinol also presents challenges, particularly in manufacturing and joining processes. Traditional welding methods can lead to brittle intermetallic phases, reducing the strength and functional performance of the joints. This limitation is a significant hurdle in expanding Nitinol's applications, especially when joining it with other materials[29]. Modern additive manufacturing techniques, such as Powder Bed Fusion and Directed Energy Deposition, are being explored to overcome these challenges by enabling the production of complex Nitinol components with improved precision and reduced material sensitivity[30]. Furthermore, the phase transformation characteristics of Nitinol can be influenced by heat treatment conditions, affecting its transition temperatures and hysteresis. This sensitivity necessitates precise control during manufacturing to ensure desired performance, particularly in medical applications where superelasticity at body temperature is critical[31]. In summary, while Nitinol offers superior mechanical properties and biocompatibility compared to other SMAs, its application is limited by manufacturing and joining challenges. Advances in additive manufacturing and joining technologies are essential to fully exploit Nitinol's potential across various industries[29], [30].

Experimental research

Nitinol spring

In this experiment, we will create a spring using Nitinol—a remarkable material known for its shape memory properties. Nitinol is an alloy of nickel and titanium that can "remember" a specific shape and return to it when heated. Through this process, we will carry out a fascinating programming procedure that allows us to create a spring that returns to its original form after being deformed. This experiment not only demonstrates the unique characteristics of Nitinol but also helps to understand how phase transformations can influence the mechanical properties of the material.

Materials

- Nitinol Wire: Wire with a diameter of about 0.5-1 mm. Ensure it's a shape memory alloy.
- Mandrel for winding the wire: A metal rod, pencil, pen, or other cylindrical objects to serve as the spring form.
- Pliers: For shaping and holding the wire.
- Gas torch or oven: For heating the Nitinol wire to program the shape memory.
- Container with cold water: For rapidly cooling (quenching) the wire after heating.
- Protective gloves and goggles: For safety while working with hot materials.

Procedure

a. Step 1: Preparing the Nitinol Wire
   - Cutting the wire: Cut a piece of Nitinol wire about 10-20 cm long (the length can be adjusted according to the desired spring size).

Figure 9. Fragments of Nitinol wire prepared to experiment [32]

- Forming: Using pliers, begin winding the wire around the chosen cylindrical object (e.g., rod or pen), creating a tight coil. Ensure the coils are even and closely wound around the form.

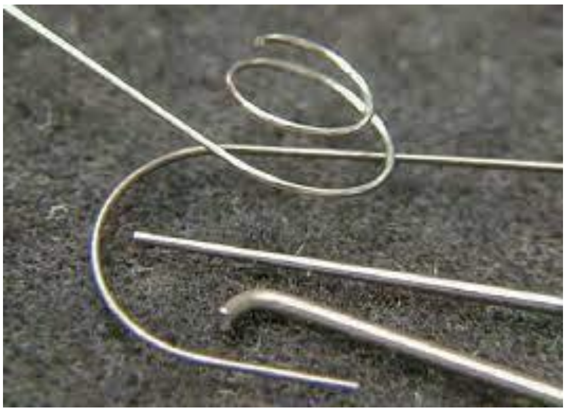

Figure 10. Sample of Nitinol wire formed into spring [33]

If you want even spacing between coils, you can use thin spacers or evenly shift the wire while winding.

b. Step 2: Programming the Shape Memory

- Heating: Place the wound wire on the form in the gas torch or oven heated to around 500-550°C. Heating should last from a few minutes to about 10 minutes to ensure the entire wire reaches the required temperature. The wire should glow red but not melt. If using an oven, place the wire on a metal tray and try not to exceed the maximum temperature recommended for your oven.
-

Figure 11. Heating a Nitinol wire in gas torch [34]

- Cooling: After heating, quickly transfer the wire (still on the form) to the container with cold water. Rapid cooling will quench the wire, setting its shape.

Figure 12. Cooling a Nitinol wire in cold water [35]

c. Step 3: Testing the Spring

- Removing from the form: After the wire has completely cooled, carefully remove the spring from the form.

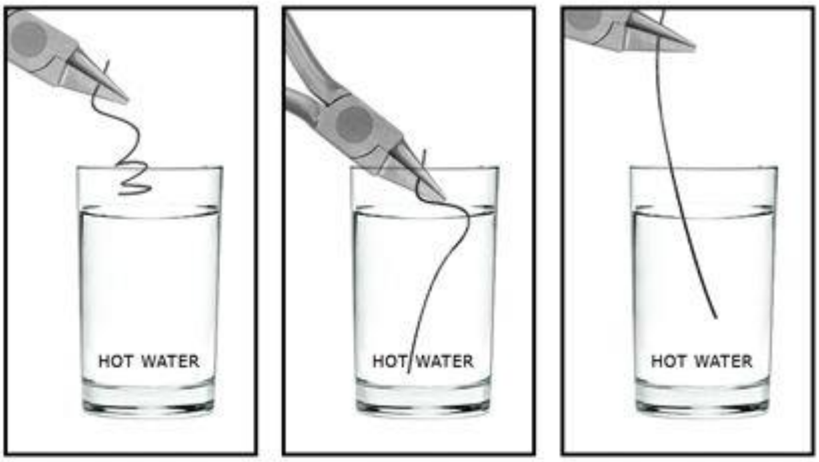

Figure 13. Testing a shape memory of a Nitinol wire [36]

- Testing the shape memory: Try stretching or deforming the spring by hand. Then place the spring in hot water (around 60-80°C) and observe how it returns to its original shape.You can also experiment with different temperatures to see how heat affects shape recovery speed.

d. Step 4: Modifications and Further Experiments

Varying the number of coils: You can change the number of coils and the diameter of the form to create different types of springs and see how their properties differ.
Load testing: Test the spring by applying various loads to see how shape memory affects the spring's ability to return to its original shape.
Experimenting with different temperatures: Test how the spring reacts to various temperature ranges to determine the optimal temperature for returning to the programmed shape.

Nitinol actuator

Nitinol, due to its shape memory properties, is widely used in various fields, including engineering, where it functions as an actuator. A Nitinol actuator is a device that can perform movement or induce a shape change in response to a change in temperature or electrical current. In this experiment, we will create a simple Nitinol actuator that contracts when an electric current is passed through it and then returns to its original length when the current is turned off.

Materials

- Nitinol Wire: Wire with a diameter of 0.5-1 mm suitable for electrical applications.
- Power Source: Battery, adjustable power supply, or laboratory power supply (recommended voltage: 3-5 V).
- Voltmeter: To measure voltage.
- Ammeter: To measure current.
- Spring or Weight: To apply force to the wire.
- Pliers and Scissors: For manipulating the wire.
- Alligator Clips or Electrical Clamps: To connect the wire to the electrical circuit.
- Thermometer: To monitor the wire's temperature.

Procedure

a. Step 1: Preparing the Nitinol Wire
   - Cutting the Wire: Cut a piece of Nitinol wire about 10-15 cm long (length can be adjusted according to the desired actuator size).
   - Securing the Wire: Attach one end of the wire to a fixed point, such as a clamp or holder. Attach the other end of the wire to a spring or weight that will apply stretching force to the wire.

b. Step 2: Setting Up the Electrical Circuit
   - Connecting Power: Connect the Nitinol wire to the electrical circuit. Use alligator clips or electrical clamps to connect the wire ends to the positive and negative terminals of the power source.
   - Monitoring Parameters: Connect the voltmeter and ammeter at appropriate points in the circuit to monitor voltage and current flowing through the wire during the experiment.

Figure 14. Example of Nitinol actuator connected to power supply [37]

c. Step 3: Operating the Actuator

- Turning on the Power: Turn on the power source and gradually increase the voltage, while observing how the wire begins to contract. This contraction is due to the shape memory effect, as the wire returns to its originally programmed shape (shortened) when its temperature rises.

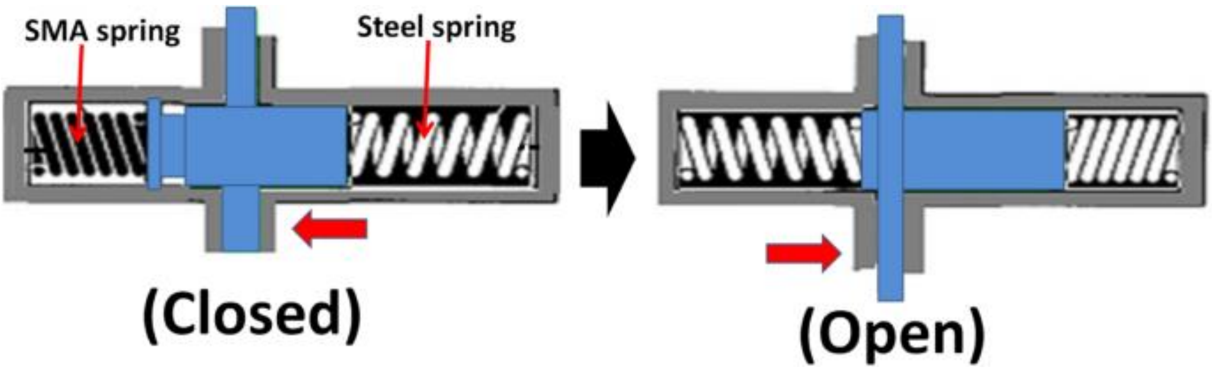

Figure 15. Sample of a SMA actuator configuration [38]

- Measuring Current and Voltage: Monitor the voltage and current in the circuit. Increasing the voltage will increase the current through the wire, causing it to heat up and contract.

- Note: Do not exceed the recommended voltage and current values for your wire to avoid damaging the material.

d. Step 4: Testing the Actuator
   - Observing Movement: Observe how the weight or spring changes its position in response to the wire's contraction. When you turn off the power, the wire will cool down and gradually return to its original length.
   - Repeating Cycles: You can repeat the process multiple times to observe the actuator's durability and its ability to cycle repeatedly.

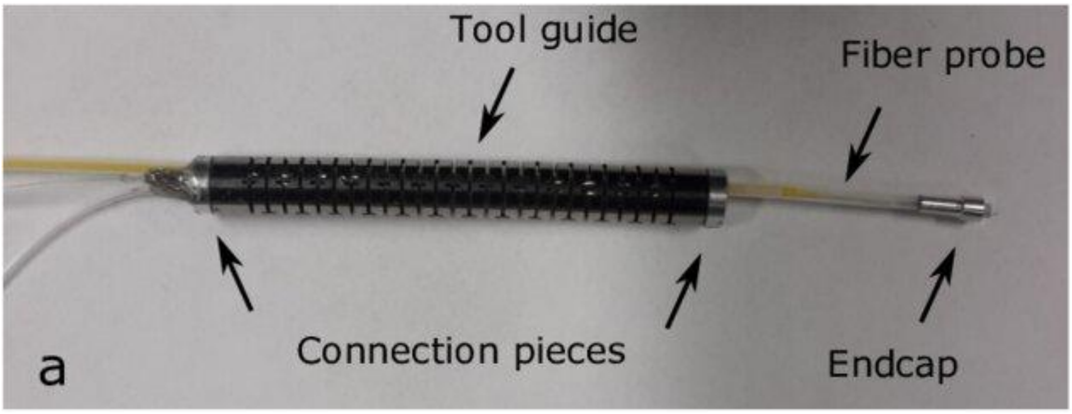

Figure 16. Example of actuator with probe inserted through it and fitted inside a conical endcap [39]

e. Step 5: Analyzing Results
   - Measuring Length Changes: Measure the length of the wire before, during, and after actuator operation to determine how much the wire contracts in response to current.
   - Studying Response Time: Record the time it takes for the wire to fully contract and return to its original length after the current is turned off.
   - Testing Different Loads: Test the actuator with various weights or springs to see how the load affects the actuator's performance.
   - Further Experiments:
   - Adjusting Voltage: Experiment with different voltage levels to see how they affect the speed and force of the wire's contraction.

- Using Different Wire Lengths: Test how changing the length of the Nitinol wire affects its properties as an actuator.
- Combining Wires: Try using multiple Nitinol wires simultaneously to create a more complex or stronger actuator.

Summary

Creating a Nitinol actuator is an excellent way to understand how Nitinol can be used to convert electrical energy into mechanical movement. This experiment demonstrates how effectively Nitinol functions as an actuator material and opens possibilities for further research into its applications in modern engineering.

Magnetorheological fluid

Magnetorheological fluid characteristic

Magnetorheological fluids (MRFs) are smart materials whose rheological properties can be dynamically altered by an external magnetic field, making them highly versatile for various applications. These fluids consist of micron-sized ferromagnetic particles suspended in a non-magnetic carrier fluid, often with additives to prevent particle agglomeration and sedimentation[40], [41].

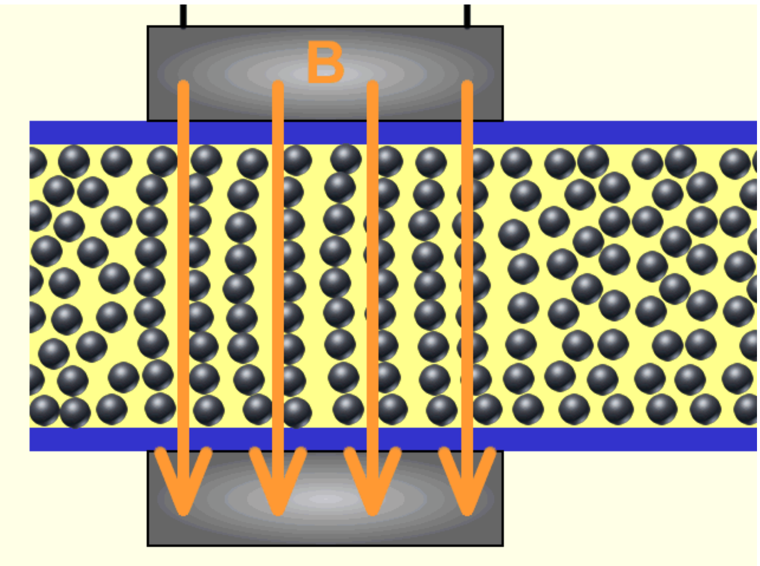

Figure 17. Schematic of a magnetorheological fluid solidifying and blocking a pipe in response to an external magnetic field [42]

One of the primary applications of MRFs is in the field of vibration control and adaptive devices. Their ability to change viscosity and shear strength under a magnetic field allows them to be used in systems such as vibration dampers, shock absorbers, and mounts. These applications benefit from the rapid, continuous, and reversible changes in the state of the system that MRFs can provide [43]. In the automotive industry, MRFs are employed in suspension systems to improve ride comfort and handling by adjusting the damping characteristics in real-time[41]. MRFs are also utilized in mechanical systems such as brakes, clutches, and valves. These applications leverage the fluid's ability to transition from a liquid to a semi-solid state, providing a controllable resistance to motion. This property is particularly useful in anti-lock braking systems and magnetic clutches, where precise control over mechanical forces is required. In the medical field, MRFs are gaining traction for their ability to meet specific force and torque requirements. They are used in lower limb prostheses, exoskeletons, orthoses, and rehabilitation devices to provide natural and stable limb motions.

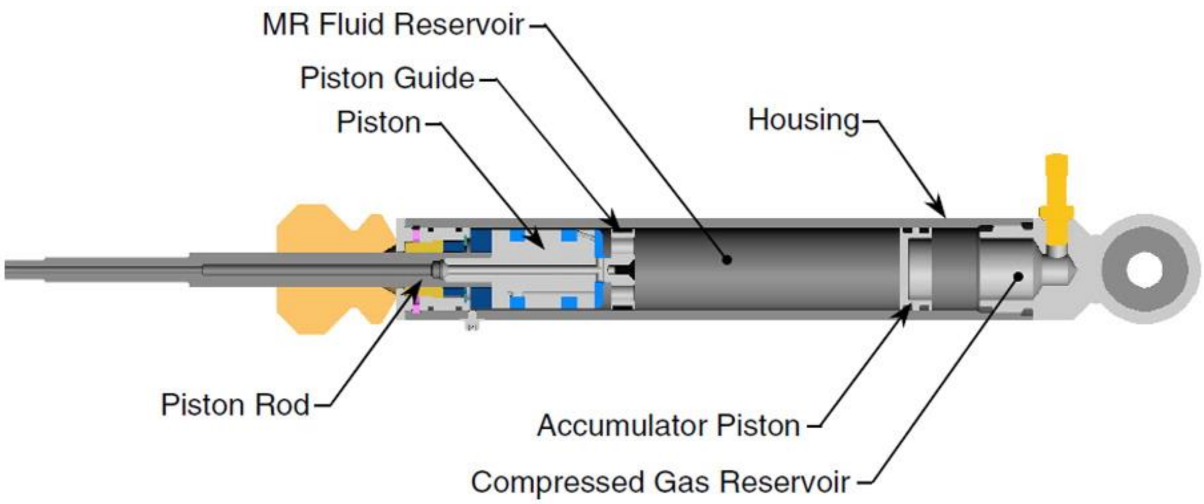

Figure 18. Example of MRFs damper

Additionally, MRFs are employed in haptic devices and tactile displays to offer high-resolution feedback, enhancing user interaction and training experiences [44], [45]. The oil and gas industry also explores the potential of MRFs in drilling and completion operations. Their tunable rheological properties can help control fluid losses, provide a set-on-demand slurry, and act as a sealing mechanism in challenging drilling environments. This adaptability is crucial for operations within narrow pressure windows, where traditional fluids may fail [45].

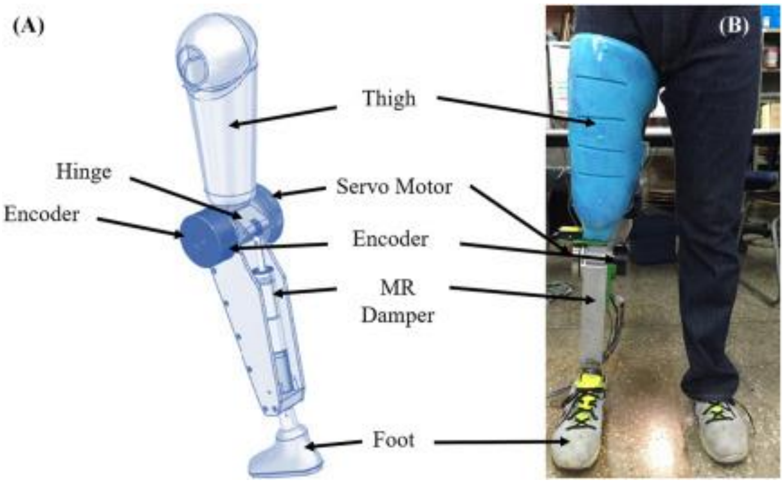

Figure 19. Medical application of magnetorheological fluid [46]

Furthermore, MRFs have been developed for high-temperature applications, expanding their utility in environments where conventional fluids might degrade. These novel MRFs maintain their rheological properties even at elevated temperatures, making them suitable for use in high-temperature industrial processes [45]. Despite their numerous applications, challenges such as stability and sedimentation remain. The development of MRFs with improved stability and reduced sedimentation rates is ongoing, aiming to enhance their performance and broaden their applicability in modern industries[45]. In summary, MRFs are employed across a wide range of applications due to their unique ability to change properties under a magnetic field. From automotive and medical devices to industrial and drilling operations, MRFs offer innovative solutions that enhance performance and adaptability in various systems. Continued research and development are expected to further expand their applications and address existing limitations.

Experimental research of MRF’s

Experiment Description:

Magnetorheological (MR) fluid is a unique material that changes its mechanical properties in response to a magnetic field. This is due to the presence of microscopic ferromagnetic particles suspended in a carrier liquid, such as oil or water. When exposed to a magnetic field, these ferromagnetic particles align, causing a significant increase in the fluid's viscosity and mechanical properties.

Figure 20. MR Fluid: (a) Liquid Phase. (b) Solid Phase. [47]

This experiment aims to investigate how the viscosity of MR fluid changes in response to a magnetic field and to explore its practical applications, such as in shock absorbers and actuators.

Materials:

- Magnetorheological Fluid (MR): Sufficient quantity for the experiment.
- Permanent Magnet or Electromagnet: Source of magnetic field with adjustable strength.
- Viscosity Measurement Equipment: Such as a viscometer or rheometer.
- Containers: For storing and testing the MR fluid.
- Measurement Tube: For introducing MR fluid into the device.
- Power Supply: Needed if using an electromagnet.
- Thermometer: For monitoring the fluid temperature.

Co-funded by the
European Union

Figure 21. Devices for experiment: viscometer and electromagnet

Procedure:

Step 1: Preparation of Magnetorheological Fluid

1. Fill Containers: Pour the MR fluid into several containers to have samples for testing.
2. Initial Viscosity Measurement: Measure the viscosity of the MR fluid using a viscometer or rheometer to obtain a baseline value before applying the magnetic field. Record these values.

Step 2: Application of Magnetic Field

1. Position Magnet: Place the permanent magnet or electromagnet close to the first container with MR fluid to create a magnetic field. Ensure that the field is uniformly applied to the MR fluid.
2. Adjust Field: If using an electromagnet, adjust the current to control the strength of the magnetic field. Start with low values and gradually increase to observe the fluid's response.

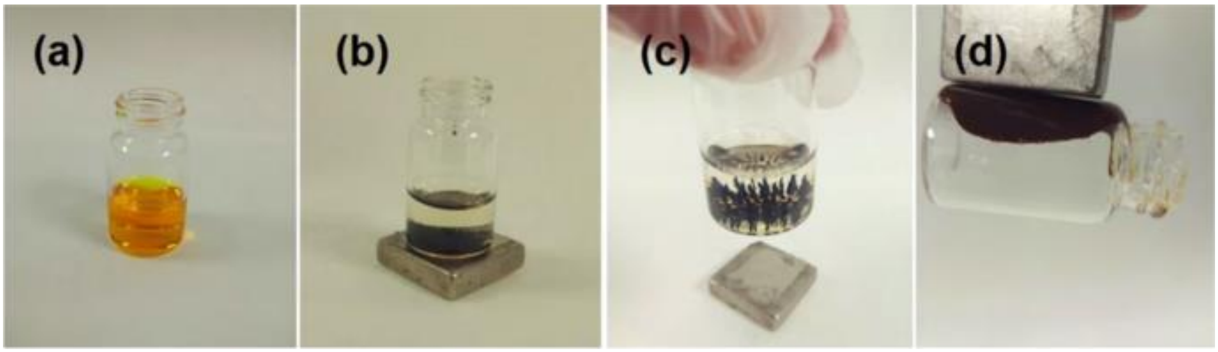

Figure 22. Example of MRF experiment [48]

Step 3: Measurement of Viscosity and Observation of Changes

1. Viscosity Measurement: After applying the magnetic field, measure the viscosity of the MR fluid again using the viscometer. Compare the new values with the initial ones to determine changes in viscosity.
2. Observe Changes: Note any changes in the consistency of the MR fluid and any internal structures that may form in response to the magnetic field. Observe how the fluid reacts to different magnetic field strengths and how quickly it returns to its original state after the field is turned off.

Step 4: Analysis of Practical Applications

1. Testing Vibration Damping: Place the MR fluid in a vibration damping system, such as a damper or shock absorber. Examine how the damping properties change in response to varying intensities of the magnetic field. Measure the effectiveness of damping at different field settings.
2. Actuator Simulation: If you have access to an MR actuator, conduct tests to assess how the actuator's force changes in response to different levels of the magnetic field. Measure the force and analyze how the magnetic field affects the actuator's performance.

Summary

This experiment provides practical insight into the behavior of magnetorheological fluid and its ability to alter viscosity in response to a magnetic field. Analyzing these changes and their impact on applications such as vibration damping and actuators demonstrates how MR fluid can be utilized in advanced technologies. The results can help in designing systems that use MR fluid properties for precise control of forces and movements.

Conclusions

The toolkit provides a comprehensive overview of smart materials and their diverse applications. Smart materials, including shape memory alloys (SMAs), shape memory polymers (SMPs), piezoelectric materials, and magnetorheological fluids, exhibit unique properties that allow them to respond dynamically to environmental stimuli. These materials are used in various fields such as mechanical engineering, aerospace, automotive, biomedical engineering, and energy systems, enhancing performance and adaptability.

Shape Memory Alloys (SMAs), like Nitinol, are notable for their shape memory effect and superelasticity. They return to their original shape when exposed to specific stimuli, making them valuable for medical devices, robotics, and adaptive structures. Piezoelectric materials generate electrical charge in response to mechanical stress, used in sensors and energy harvesting. Magnetorheological fluids change their viscosity in response to magnetic fields, useful in vibration damping and adaptive devices. Experimental research includes creating Nitinol springs and actuators, demonstrating their shape memory and actuation capabilities. Magnetorheological fluids are tested to observe changes in viscosity under magnetic fields, showing their potential in applications like shock absorbers and actuators.

Overall, smart materials are revolutionizing engineering and technology by providing adaptive, efficient, and sustainable solutions across various industries. Challenges in their development, such as manufacturing constraints and property optimization, are being addressed through ongoing research and interdisciplinary collaboration.

References

[1] Abhyuday Mangla, “Smart Materials and their Applications in Mechanical Engineering,” *Darpan International Research Analysis*, vol. 12, no. 3, pp. 38–49, Jul. 2024, doi: 10.36676/dira.v12.i3.55.

[2] M. Yildirim and Z. Candan, “Smart materials: The next generation in science and engineering,” *Mater Today Proc*, Oct. 2023, doi: 10.1016/j.matpr.2023.10.116.

[3] S. Kashyap and S. Sarkar, “SMART MATERIALS: APPLICATION IN FUTURISTIC TECHNOLOGY,” in *Futuristic Trends in Chemical Material Sciences & Nano Technology Volume 3 Book 11*, Iterative International Publishers, Selfypage Developers Pvt Ltd, 2024, pp. 82–96. doi: 10.58532/V3BECS11P1CH8.

[4] F. Chen, J. Dong, W. Sun, D. Di Iorio, S. V. Wegner, and W. Zeng, “Editorial: Construction of smart materials for biomedical application,” *Front Bioeng Biotechnol*, vol. 11, Aug. 2023, doi: 10.3389/fbioe.2023.1278243.

[5] D. Kim *et al.*, “Shape-memory effect in twisted ferroic nanocomposites,” *Nat Commun*, vol. 14, no. 1, p. 750, Feb. 2023, doi: 10.1038/s41467-023-36274-w.

[6] J. Bhattacharjee and S. Roy, “Smart materials for sustainable energy,” *Natural Resources Conservation and Research*, vol. 7, no. 1, p. 5536, May 2024, doi: 10.24294/nrcr.v7i1.5536.

[7] M. A. Savi, “An Overview of Smart Material Systems and Structures,” 2024, pp. 1–21. doi: 10.1007/978-3-031-59804-3_1.

[8] H. Lee, M. Kim, G. Lee, C. Kim, and S. Ahn, “Shape Memory Alloy (SMA)-Based Microscale Actuators with 60% Deformation Rate and 1.6 kHz Actuation Speed,” *Small*, vol. 14, no. 23, Jun. 2018, doi: 10.1002/smll.201801023.

[9] P. S. Bahadur, R. Srivastava, and V. Srivastava, “Review on the Development of Smart Materials, Including Shape Memory Alloys, Characterization, and Recent Applications,” 2023, pp. 107–139. doi: 10.4018/978-1-6684-9224-6.ch005.

[10] R. Roy, D. Bhakta, and S. Roy, “Applications and Types of Smart Materials,” 2023, pp. 266–296. doi: 10.4018/978-1-6684-9224-6.ch013.

[11] M. J. and S. R. J., “Smart Materials in Biomedicine,” 2023, pp. 31–55. doi: 10.4018/978-1-6684-9224-6.ch002.

[12] Y. Yang and P. Jiao, “Nanomaterials and nanotechnology for biomedical soft robots,” *Mater Today Adv*, vol. 17, 2023, doi: 10.1016/j.mtadv.2022.100338.

[13] A. Sellitto and A. Riccio, “Overview and future advanced engineering applications for morphing surfaces by Shape Memory Alloy Materials,” *Materials*, vol. 12, no. 5, 2019, doi: 10.3390/ma12050708.

[14] E. J. Barbero, *Introduction to composite materials design, third edition*. 2017. doi: 10.1201/9781315296494.

[15] S. Kamila, “Introduction, classification and applications of smart materials: An overview,” *Am J Appl Sci*, vol. 10, no. 8, 2013, doi: 10.3844/ajassp.2013.876.880.

[16] S. Sławski, J. Hartwich, R. Bartusiak, and S. Duda, “Assessment of the Bonding Force between the Thin NiTi Wire and 3D Printed Polymeric Matrix,” in *2024 11th International Workshop on Metrology for AeroSpace (MetroAeroSpace)*, IEEE, Jun. 2024, pp. 73–77. doi: 10.1109/MetroAeroSpace61015.2024.10591552.

[17] R. Dutta, L. Chen, D. Renshaw, and D. Liang, “Artificial intelligence automates the characterization of reversibly actuating planar-flow-casted NiTi shape memory alloy foil,” *PLoS One*, vol. 17, no. 10, p. e0275485, Oct. 2022, doi: 10.1371/journal.pone.0275485.

[18] A. Szold, “Nitinol: shape-memory and super-elastic materials in surgery,” *Surg Endosc*, vol. 20, no. 9, pp. 1493–1496, Sep. 2006, doi: 10.1007/s00464-005-0867-1.

[19] I. Y. Paez-Pidiache, N. B. Lozada-Castillo, and A. Luviano-Juárez, “Caracterización de las SMAs y sus aplicaciones: Una revisión,” *Pädi Boletín Científico de Ciencias Básicas e Ingenierías del ICBI*, vol. 8, no. 16, pp. 1–10, Jan. 2021, doi: 10.29057/icbi.v8i16.5713.

[20] A. Battal and S. Yazıcı, “The Use of Smart Materials in Architecture: Nitinol-based Foldable Façade Systems,” *Journal of Technology in Architecture Design and Planning*, vol. 1, no. 1, pp. 1–9, May 2023, doi: 10.26650/JTADP.01.001.

[21] R. Chaudhari, J. J. Vora, and D. M. Parikh, “A Review on Applications of Nitinol Shape Memory Alloy,” 2021, pp. 123–132. doi: 10.1007/978-981-33-4176-0_10.

[22] A. Behera, “Smart applications of NiTi shape memory alloy in biomedical industries,” in *Nickel-Titanium Smart Hybrid Materials*, Elsevier, 2022, pp. 327–354. doi: 10.1016/B978-0-323-91173-3.00007-9.

[23] M. Yildirim, I. Mutlu, and Z. Candan, “Development and characterization of smart composites reinforced with fibrillated cellulose and nickel-titanium alloy,” *Int J Biol Macromol*, vol. 267, p. 131189, May 2024, doi: 10.1016/j.ijbiomac.2024.131189.

[24] A. Ghosh, A. Sharma, and N. Gupta, “Smart materials advancements, applications and challenges in the shift to Industry 4.0,” in *Industry 4.0 and Climate Change*, London: CRC Press, 2022, pp. 177–188. doi: 10.1201/9781003293576-15.

[25] D. Stockel, “Nitinol - A material with unusual properties,” *Endovascular Update*, no. 1, 1998.

[26] K. K. Shree Kant, "Emerging Field of Soft Tactile Sensors in 4D Printing Stimulus with Smart Material Nitinol Using Piezo Resistive Technique," *Tuijin Jishu/Journal of Propulsion Technology*, vol. 44, no. 3, 2023, doi: 10.52783/tjjpt.v44.i3.720.

[27] S. Mishra, M. Kumar, and Y. Kishor Sharma, "Fabrication and characterization of nitinol reinforced metal matrix smart composite: A review," *Mater Today Proc*, Jan. 2023, doi: 10.1016/j.matpr.2022.12.256.

[28] G. Costanza, M. E. Tata, and C. Calisti, "Nitinol one-way shape memory springs: Thermomechanical characterization and actuator design," *Sens Actuators A Phys*, vol. 157, no. 1, pp. 113–117, Jan. 2010, doi: 10.1016/j.sna.2009.11.008.

[29] Z. Cao, S. G. Price, and I. McCue, "Similar and Dissimilar Joining of Nitinol through Transient Liquid Phase Bonding," May 2024, pp. 113–114. doi: 10.31399/asm.cp.smst2024p0113.

[30] M. Sathishkumar *et al.*, "Possibilities, performance and challenges of nitinol alloy fabricated by Directed Energy Deposition and Powder Bed Fusion for biomedical implants," *J Manuf Process*, vol. 102, pp. 885–909, Sep. 2023, doi: 10.1016/j.jmapro.2023.08.024.

[31] L. Öncel and M. Açma, "Effect of heat treatment conditions on the phase transformation characteristics of nitinol," *Journal of Innovative Engineering and Natural Science*, vol. 4, no. 2, pp. 621–630, Jul. 2024, doi: 10.61112/jiens.1484623.

[32] "https://cisglobal.en.made-in-china.com/product/vwdTlEKACrfX/China-Nitinol-Shape-Memory-Super-Elastic-Wire-1-0-mm-0-039-5-Feet-.html."

[33] L. M. D. Schetky and M. H. Wu, "Issues in the further development of nitinol properties and processing for medical device applications," in *Medical Device Materials - Proceedings of the Materials and Processes for Medical Devices Conference 2003*, 2003.

[34] "https://www.google.com/imgres?q=heating%20nitinol%20wire%20in%20torch&imgurl=https%3A%2F%2Fi.ytimg.com%2Fvi%2F_CiErseFED8%2Fmaxresdefault.jpg&imgrefurl=https%3A%2F%2Fwww.youtube.com%2Fwatch%3Fv%3D_CiErseFED8&docid=fmRTRaXdFbecSM&tbnid=RU_iFTijbw3x9M&vet=12ahUKEwjosOKFjoaIAxU9SPEDHaazC90QM3oECBwQAA..i&w=1280&h=720&hcb=2&ved=2ahUKEwjosOKFjoaIAxU9SPEDHaazC90QM3oECBwQAA."

[35] "https://www.teachersource.com/product/nitinol-spring."

[36] "https://www.haines.com.au/memory-wire-nitinol-90cm.html."

[37] "https://i.ytimg.com/vi/PxBPpPRkv6A/maxresdefault.jpg."

[38] S. Ahmed, C.-H. Goh, J. K. Allen, F. Mistree, P. Zagade, and B. P. Gautham, “Hot Forging of Automobile Steel Gear Blanks: An Exploration of the Solution Space,” in *Volume 2B: 40th Design Automation Conference*, American Society of Mechanical Engineers, Aug. 2014. doi: 10.1115/DETC2014-34197.

[39] A. Devreker *et al.*, “Fluidic actuation for intra-operative in situ imaging,” in *IEEE International Conference on Intelligent Robots and Systems*, 2015. doi: 10.1109/IROS.2015.7353553.

[40] X. Yin, J. Yan, S. Wen, and J. Zhang, “Magnetorheological Fluid-Based Bending Actuator for Magnetic Sensing,” *IEEE Robot Autom Lett*, vol. 7, no. 4, 2022, doi: 10.1109/LRA.2022.3214082.

[41] H. Eshgarf, A. Ahmadi Nadooshan, and A. Raisi, “An overview on properties and applications of magnetorheological fluids: Dampers, batteries, valves and brakes,” *J Energy Storage*, vol. 50, 2022, doi: 10.1016/j.est.2022.104648.

[42] “https://commons.wikimedia.org/wiki/File:MRF-Effekt-static-crop.png.”

[43] S. Bagg, P. Shetye, A. Wala, P. Sarfare, and R. Shah, “DESIGN AND ANALYSIS OF SUSPENSION SYSTEM USING MR FLUID,” *International Journal Of Trendy Research In Engineering And Technology*, vol. 07, no. 02, 2023, doi: 10.54473/ijtret.2023.7205.

[44] P. Skalski and K. Kalita, “Role of magnetorheological fluids and elastomers in today’s world,” 2017. doi: 10.1515/ama-2017-0041.

[45] M. Dassisti and G. Brunetti, “Introduction to Magnetorheological Fluids,” in *Encyclopedia of Smart Materials*, 2021. doi: 10.1016/B978-0-12-803581-8.11744-8.

[46] J.-S. Oh and S.-B. Choi, “Medical applications of magnetorheological fluids—a review,” in *Magnetic Materials and Technologies for Medical Applications*, Elsevier, 2022, pp. 485–500. doi: 10.1016/B978-0-12-822532-5.00008-X.

[47] C.-H. Lee and M.-G. Jang, “Virtual Surface Characteristics of a Tactile Display Using Magneto-Rheological Fluids,” *Sensors*, vol. 11, no. 3, pp. 2845–2856, Mar. 2011, doi: 10.3390/s110302845.

[48] M. Osial, M. Nowicki, E. Klejman, and L. Frąś, “Investigation of the well-dispersed magnetorheological oil-based suspension with superparamagnetic nanoparticles using modified split Hopkinson pressure bar,” *Rheol Acta*, vol. 61, no. 2, pp. 111–122, Feb. 2022, doi: 10.1007/s00397-021-01318-9.

Co-funded by the European Union

AMAZE

Erasmus+ Programme Key Action 2 Cooperation Partnerships for Higher Education (KA220-HED)
Agreement number 2023-1-RO01-KA220-HED-000155412
European Network for Additive Manufacturing in Industrial Design for Ukrainian Context- Acronym: AMAZE

e-Toolkit
Smart (Intelligent) Materials

Project Title	**European Network for Additive Manufacturing in Industrial Design for Ukrainian Context 2023-1-RO01-KA220-HED-000155412**
Output	**IO2 - AMAZE e-toolkit manual for digital learning in producing complex design industrial parts**
Module	**Module 2.2. Smart (Intelligent) Materials used in industrial and architectural design**
Date of Delivery	**June 2024**
Authors	**Igor FODCHUK, Mariana BORCHA, Volodymyr ROMANKEVYCH, Yuriy SOBKO**
Version	**FINAL VARIANT, *14.06.2024***

Co-funded by the European Union

AMAZE

Content

Introduction

The development of high-strength concrete mixtures is usually based on the targeted modification of the phase composition by fine aggregates. Among the technological aggregates that exhibit high chemical activity with cements, special attention is paid to amorphous condensed microsilica (MS) with a microsphere size in the range of 100-300 nm. The presence of MS helps to accelerate the hydration of the alite and belite phases of the cement and optimises the density of the grain packing. This leads to a higher density of the cement matrix, as well as the generation of a large amount of calcium silicate hydrate (CSH).

Metakaolin, a product of dehydration of kaolin clay (a natural hydroalumina), is also an effective modifier, which compacts the microstructure of the concrete matrix during the hardening of hydrate formations. Its other quality is pozzolanic activity, which is of a mixed aluminate-silica nature. According to the data, in the system of interaction of «aluminium, calcium and water oxides» «Al_2O_3-CaO-H_2O» at an early stage, the formation of alumina hydrate gel $Al(OH)_3$ is possible, which in the future depending on the hydrogen content of the medium and other factors, crystallises into high-base calcium hydroaluminates 4CaO-Al_2O_3-nH_2O, hydrogranates, hydrohelenite C_2ASN_8 and low-base calcium hydrosilicates CSH-I.

New approaches to the chemical modification of the cement matrix set the task of substantiating the cause-and-effect relationships between the processes of structure formation and quality control of the starting material, which is a necessary condition for obtaining high-strength concrete.

The introduction of a complex of X-ray, correlation-optical and electron-array methods for diagnosing the state of polycrystalline materials, as well as establishing the features of phase transformations at the microstructural level, is an urgent task today. That is why the development of ways to reduce the defectiveness of the structure and limit the deformation properties of high-strength composites is becoming an important task for both research and engineering practice.

Currently, active experimental research is being conducted to determine the physical and mechanical characteristics of high-strength concrete. However, the problem of full-scale testing and research into their use in the construction industry is still relevant. This requires a detailed analysis and creation of models of physical and chemical processes of microstructure development depending on changes in the phase composition of the cement composite.

To this day, pilot projects for the use of ultra-high-strength composites in structures have already been implemented, which show the prospects for the use of ultra-high-strength composites in special construction. These structures include foundations of power plants, hydropower facilities, bridge supports and structures operating under extreme compression and in aggressive environments.

In order to achieve the goals of high-strength concrete production, a number of studies of the input materials and the finished concrete composite are required. This guideline provides a list of laboratory studies required for the preparation of ultra-high-strength concrete.

Laboratory work №1

Production and storage of cement prisms

Introduction:

Laboratory work on the production and storage of cement prisms is a key part of the study of cement properties and its uses in the construction industry. This process requires precision, consistency and compliance with regulatory requirements to obtain reliable results.

The purpose of this laboratory work is to study the methods of production and storage of cement prisms, as well as to determine their strength in accordance with established standards.

To achieve this goal, the work involves:

preparation of equipment and materials: includes familiarisation with the necessary equipment and tools, as well as preparation of the premises in accordance with the requirements;

production of cement prisms: the process of creating cement prisms follows a certain sequence of actions, which is reflected in regulatory documents and instructions;

storage and handling of prisms: after production, cement prisms are stored and prepared for future testing. This stage is also important to ensure the reliability of the results;

prism strength testing: after the required storage period, the cement prisms are tested to determine their strength in accordance with standardised procedures.

The results of this laboratory work can be used to assess the quality of cement, as well as to compare different types of cement or formulations. This approach is important in the construction industry to ensure the safety and reliability of building structures.

1.1. Regulatory documents:

EN 196-1:2005-05 Cement testing methods. Part 1: strength determination [1].

1.2. Equipment and support devices

1. Mixer with two speeds (EN 196-1:2005-05) [1];

Fig 1.1. Mixer for cement mixture.

2. Triprism mould 40 × 40 × 160 mm (EN 196-1:2005-05) ;

Fig. 1.2. Triprism mould 40 × 40 × 160 mm (EN 196-1:2005-05) [2].

3. Vibrating table (EN 196-1:2005-05), the amplitude of the vibrating table should be 0.75 ± 0.10 mm when working with an empty mould;

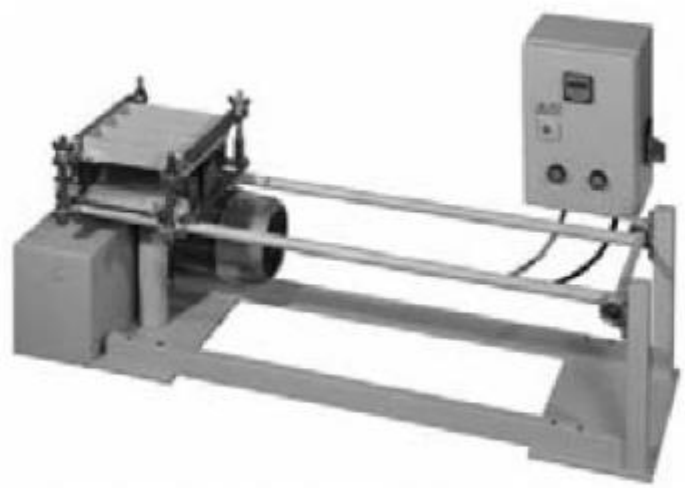

Fig. 1.3. Vibrating table (EN 196-1:2005-05) [2].

4. Precision scales, weighing range 2 kg, reading accuracy 0.1 g;
5. Laboratory spoons;
6. Scales with an accuracy of ±1 g;

Fig. 1.4. Laboratory scales

7. Thermometer;
8. Humidity tester;
9. Laboratory clock with a second hand (or electronic one);
10. Steel ruler, 300 × 30 × 2 mm;
11. Glass, steel or plastic cover, 210 × 185 × 6 mm;
12. Wet box or cabinet for storing samples;
13. Sample storage box with tap water and plastic mesh;

Fig. 1.5. Box for storing samples [2].

14. Thermostat;
15. CEN sand in bags (supplier: Normensand GmbH, 59269 Beckum);
16. Cement (EN 197-1:2011, IDT);
17. Cleaning tools (made of material softer than mould);
18. Rubber scraper;
19. Plastic or rubber hammer.

1.3. Composition of the cement solution:

The solution shall consist (by weight) of one part of cement, three parts of CEN standard sand and a half part of water. Water-cement ratio should be 0.50.

Each batch for three specimens shall contain (450 ± 2) g of cement, (1350 ± 5) g of sand and (225 ± 1) g of water.

1.4. Requirements for the premises:

The temperature of 20 ± 2 °C and relative humidity of at least 50 % should be maintained in the laboratory where the samples are prepared.

The temperature in the climatic chamber or cabinet for storing specimens in moulds should be maintained at 20.0 ± 1.0 °C, the relative humidity – at least 90 %.

Tanks for curing specimens in water, as well as the grids with which they are equipped, should be made of a material that does not react with cement. The water temperature should be 20.0 ± 1.0 °C. The temperature and relative humidity of the air in the laboratory and the temperature of the water in the sample storage box should be recorded at least once during the working day. The temperature and relative humidity in the climatic chamber or cabinet, as appropriate, should be recorded every four hours.

1.5. Procedure steps:

1. Cement, CEN standard sand, water and equipment for manufacturing and testing specimens shall be stored at a temperature of 20 ± 2 °C. In order to comply with the temperature regime, the nominal value according to which the control is carried out should be the average temperature value within the specified range of its fluctuations.

2. After assembling the mould, grease it inside a little. Weigh the mould if you need to determine the density of the fresh mixture and lable it.

3. Weigh out 450 ± 2 g of the cement to be tested; pour out 225 ± 1 g of water.

4. Pour the water into the mixer and add the required amount of cement. Record date and time of the test.

5. Lift the mixer tray with the hand lever, switch on speed I and mix for 30 seconds at 140 ± 1 rpm.

6. During the next 30 seconds (from 31 to 60 seconds), continue to add the standard CEN sand from the packaged bag and mix at speed I.

7. Switch the mortar mixer to the second speed (285 ± 10 rpm) and continue mixing (from 61 s to 90 s).

8. Turn off the mixer (91s to 180s). During the first 15 s, use a rubber scraper to remove the solution from the walls of the bowl to the mixing zone, continue mixing (181s to 240s).

9. Switch on the mixer at speed II (285 ± 10 rpm).

10. Firmly fix the prism mould to the vibrating table.

11. Switch on the vibrating table and within 15 seconds fill the three compartments of the mould with spoon approximately halfway, always starting from the right.

12. Allow the vibrating table to run for 15 seconds (16 to 30 seconds).

13. During the next 15 seconds, pour the remaining solution into the mould, starting from the right side, until the mould is filled to the brim (31 to 45 s).

14. Allow the vibrator to run for 75 seconds (46 to 120 seconds).

15. Switch off the vibrating table.

16. Disconnect the mould, remove the fixing frame and use a steel ruler to remove any excess solutiuon, then smooth the surface.

17. Clean the top surfaces of the bars.

18. Cover the mould with lightly oiled plates.

19. Place the moulds in the storage box and store for 20-24 hours (if the strength is too low, store for another 24 hours).

20. Carefully remove the prisms from the mould (use a plastic or rubber hammer). It should be done in 24 hours 20 minutes before the test.

21. Cover the prisms with a damp cloth for testing after 24 or 48 hours (if it is not possible to remove them from the mould after 24 hours).

22. Label samples.

23. Store them in a container filled with water for testing after 2, 7, or 28 days. The water should be at least 5 mm above samples [1].

Laboratory work №2

Bending and compressive strength testing of cement prisms

Introduction:

The aim of this laboratory work is to determine the bending and compressive strength of cement prisms. Strength testing is an important step in determining the quality of building materials, as they are subjected to various types of mechanical loads during operation.

The test methodology involves the use of standardised bending and compressive strength testing equipment. These include the TMC-3224 press, a bending strength tester, and a compression strength insert. In bending, a cement prism is placed on two supports with certain distances between them and subjected to a load until it breaks. The results are measured in MPa.

In this work, experiments will be carried out to test the strength of cement prisms using the specified methods and devices. The results of these tests will help to obtain important data on the quality and reliability of cement materials under certain mechanical loading conditions.

2.1 Essence of the method:

Using a standardised bending strength tester prism,, lockated on two supports with defined distances between the supports and a central load, is subjected to bending tension until it breaks. The result is given in MPa (equivalent to N/mm²).

2.2. Regulatory references:

EN 196-1:2007 Methods of testing cement. Part 1: Determination of strength (EN 196-1:2005) [3].

2.2. Tools and accessories:

1. TMC-3224 automatic compression testing machinein accordance with EN 196-1:2005-05, load up to 10 kN with a load increase accuracy of ± 1% (50 ± 10) N/s [4];

Fig. 2.1. TMC-3224 automatic compression testing machine

2. Caliper;
3. Wet wipes;

4. Rag;
5. Scales with an accuracy of ±1 g.

2.3. Instruments for testing samples for strength and bending:

Notice. The use of this device is voluntary. If it is necessary to determine only the compressive strength, the prism specimens can be broken in another way that does not cause additional stresses in the prism halves.

The bending strength can be determined using a specialised device or by attaching it to a compression test press. In both cases, the equipment must meet the following requirements.

The bending strength test device shall be capable of applying a load of up to 10 kN with an accuracy of ±1.0% of the applied load in the upper part (4/5) of its measuring range, and shall be capable of increasing the load at a rate of 50 ± 10 N/s. The test press shall be equipped with a bending device consisting of two supports made of steel rollers with a diameter of 10.0 ± 0.5 mm, spaced at a distance of 100.0 ± 0.5 mm from each other, and a third steel roller of the same diameter, placed midway between the other two, to transfer the load. The length of these rollers should be between 45 and 50 mm. The loading diagram is shown in Fig. 2.2.

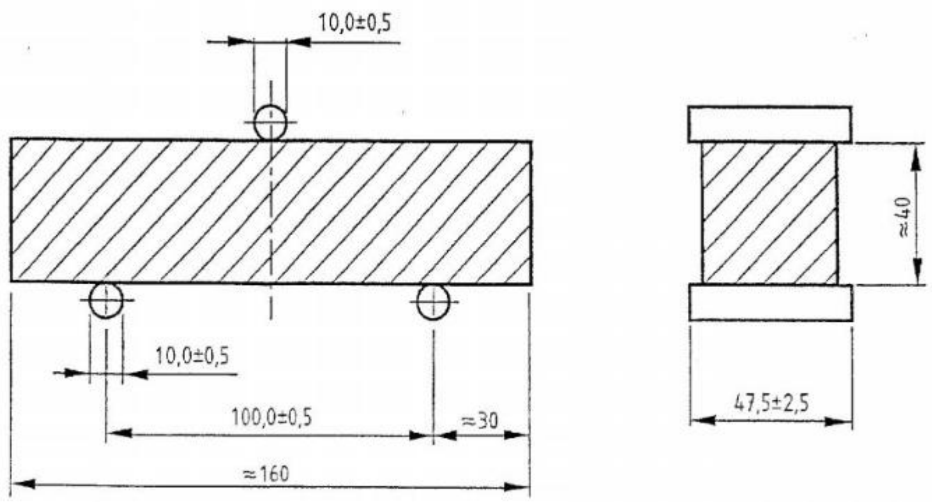

Fig. 2.2. Loading diagram for determining bending strength

The axes of the steel rollers shall be in three vertical parallel planes and shall remain parallel, equidistant and perpendicular to the longitudinal axis of the clamped specimen during the test. One of the supports and the load transfer roller shall be slightly deflected to ensure that the load is distributed evenly along the width of the specimen without the occurrence of torsional stresses.

2.4. Testing compressive strength

The compression testing machineshall have a suitable load range (note 1). When controlled in accordance with EN ISO 75001, the machineshall, in the upper part (4/5) of the measuring range, provide an accuracy of ±1.0 % with respect to the recorded load and the possibility of an adjustable increase in load at a rate of up to 2400 ±200 N/s. The indicator device shall show the load value obtained when the test specimen is broken and after the load is removed. If a pressure gauge is used, this can be achieved by means of a towing arrow, and if a digital display is used, by means of a flash drive. Manually operated test presses shall be equipped with a stepping mechanism for gradually increasing the load.

The vertical axis of the piston must be aligned with the vertical axis of compression testing machineand the piston must move along the vertical axis of the machine when loaded. The equal-acting line of the applied loads shall pass through the centre of the specimen prism. The surface of the bottom pressure plate shall be perpendicular to the axis of the test press and remain perpendicular when loaded.

The centre of the spherical support of the upper plate must coincide with the intersection of the vertical axis of the test press with the plane of the lower surface of the upper pressure plate to within ±1 mm. The upper pressure plate must be sufficiently movable to allow for force contact, but the relative position of the upper and lower plates must remain rigid when loaded.

Compression testing machineshall be equipped with tungsten carbide plates or alternatively hardened steel plates by Vickers hardness of at least 600 kgf/mm². These plates shall have a thickness of at least 10 mm, a width of 40.0 ± 0.1 mm and a length of 40.0 ± 0.1 mm. The flatness tolerance of the pressure plates in accordance with ISO 1101 for the entire surface in contact with the sample shall be no more than 0.01 mm. The surface roughness according to ISO 1302 of the new plates shall not be smoother than № 3 and not coarser than № 6.

Alternatively, two backing plates made of tungsten carbide or hardened steel by Vickers hardness of at least 600 kgf/mm² and a minimum thickness of 10 mm that meet the requirements for plates may be used. A device that centres the auxiliary plates to within ±0.5 mm of the axis of the loading system and a device that centres the auxiliary plates to within ±0.5 mm of the centre of the second plate is also required. If testing machineis not equipped with a spherical support or if the spherical support is blocked or its diameter exceeds 120 mm, an insert must be used.

Note 1: Testing machinemay have two or more load ranges. The maximum load of the lower range can be approximately 1/5 of the maximum load of the next range.

Note 2. Testing machine shall be equipped with an automatic load increase control and a device for recording the results.

Note 3. The spherical support of the machine may be lubricated to facilitate adhesion to the prism test specimen so that the pressure plate cannot move under the test load. High pressure lubricants are not suitable for this purpose.

Note 4. The designations «vertical», «bottom», «top» refer to conventional testing machines, which are usually arranged as vertical machines. However, machines with non-vertical axes are also acceptable.

2.5. Testing machine **insert for compressive strength testing**

If an insert is required (Fig. 2.2), it is positioned between the machine plates to transfer the load to the pressure planes of the prism specimen. This insert has a lower pressure plate that can be inserted into the lower pressure plate of the press. The upper pressure plate receives the load from the upper press platen via a spherical insert support located between them. This support is an integral part of the device, which is able to slide vertically in the insert, which guides its movement, without significant friction. The insert shall be kept clean at all times and the spherical support shall be so easily rotated that the pressure plate is initially adherent to the prism specimen under test and then remains stationary during the test.

Note 1. The spherical support of the insert may be oiled to facilitate adhesion to the specimen, but in such a way that the pressure plate cannot move under the test load.

Note 2. It is desirable that the pressure punch 2 (Fig. 2.3) automatically returns to its original position after crushing the test specimen [4].

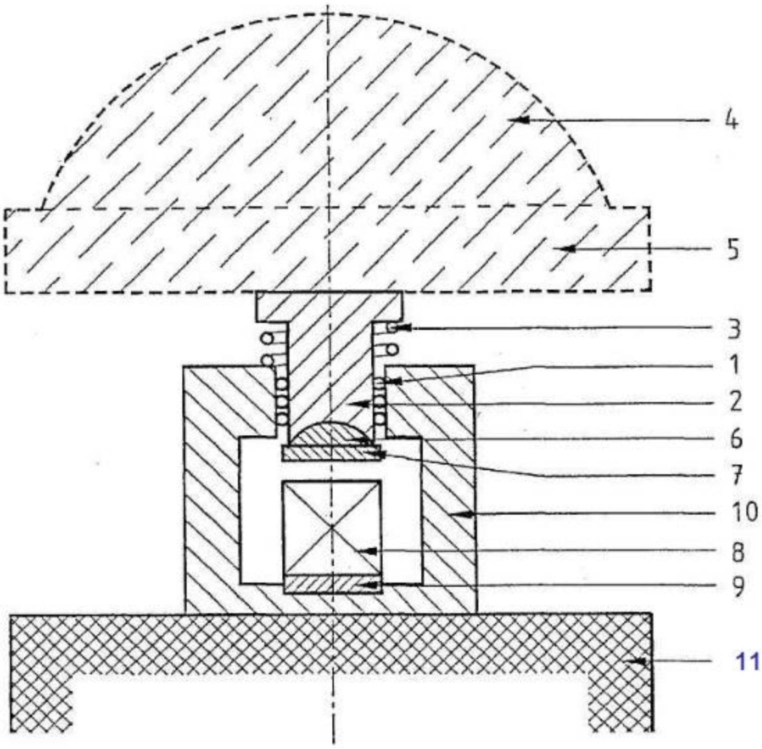

Fig. 2.3. Typical insert for compressive strength testing [3]**:**

1 - ball bearing; 2 - pressure punch; 3 - return spring; 4 - spherical support of the testing machine; 5 - upper pressure plate of the testing machine; 6 - spherical support of the insert; 7 - upper pressure spring of the insert; 8 - test specimen; 9 - lower pressure spring of the insert; 10 - insert; 11 - lower pressure plate of the testing machine.

2.6. Procedure steps:

Bending tension tests in an automatic compression testing machine.

1. Take the test sample from the storage water container. The age of the test samples must be calculated from the very begining. Tests for different age groups should be carried out with the following time tolerances:

   24 h ± 15 min

   48 h ± 30 min

   72 h ± 45 min

   7 days ± 2 hours

   ≥ 28 days ± 8 hours

2. Cover with a damp cloth before testing (for 15 minutes) and wipe with a clean cloth before testing.
3. Insert the prism into the standard press insert for the compression test. Insert the prism with the side surfaces resting on the support rollers.
4. Load the prism evenly with an increasing load of 50 ± 10 N/s until it breaks.
5. The tensile strength in bending R_f is calculated in MPa according to equation 2.1:

$$R_f = \frac{1.5 \times F_f \times L}{b^3} \ [\text{MPa}], \qquad 2.1$$

where:

R_f - bending tensile strength in MPa or N/mm²;

b - length of the side of the prism cross-section in mm;

F_f - central applied breaking load in N;

L is the distance between the supports in mm [4]

Laboratory work №3

Preparation of the concrete sample

Introduction:

Laboratory work №3 is devoted to the preparation of a concrete sample for further physical and mechanical tests. In this work, an experimental fibre-concrete mixture is used, which is modified with a complex of fine modifiers based on microsilica and metakaolin. This mixture was created taking into account the regulatory requirements specified in patent UA 150717 [5].

The composition of the fibre-reinforced concrete mix includes various components, such as cement, sand, crushed stone, microsilica, metakaolin, superplasticiser, and others, each of which plays a role in shaping the structure and properties of concrete. The expected compressive strength is 120 MPa, which meets the project requirements.

This paper describes in detail the process of preparing the fibre-reinforced concrete mix, which includes a three-stage mixing of the components using an electric mixer. The peculiarities of sample formation in accordance with the established standards EN 206-1:2001-07 [6] are also described.

The laboratory work is aimed at studying the properties and quality of concrete that can be used in the construction industry and is an important step in the study and improvement of building materials.

For physical and mechanical tests, an experimental fibre-reinforced concrete mixture modified with a complex of fine modifiers based on microsilica and metakaolin is being prepared.

3.1. Regulatory references:

Patent UA 150717

https://base.uipv.org/searchINV/search.php?action=viewdetails&IdClaim=281059 [5]б

3.2. Composition of fibre-reinforced concrete mix:

Table 3.1.

Ratio of components for concrete by weight in %:

Name of components	Weight, %:
Cement CEMI 42.5	21,5
Quartz sand, fr. 0,4-0,63 mm	24,5
Granite crushed stone, fr. – 2-5 mm	7,98
Granite crushed stone, fr.- 5-10 mm	9,59
Granite crushed stone, fr. – 10-20 mm	20,39
Microsilica, fr. - 0.1-0.3 µm	6,75
Metakaolin, fr. - 140 microns	1,12
Superplasticiser based on polycarboxylate esters	1,12
Plastic fibre	1,12
Water	the rest
Expected compressive strength in kN	**1205**

Table 3.2.

Composition of fibre-reinforced concrete mix

Name of components	Composition kg/m^3
PCI 500 cement (DSTU B V.2.746:2010)	600
Quartz powder 50 microns	30
Quartz sand, fraction 0,4-0,63 mm	520
Diorite crushed stone, fraction 2/5 mm	315
Diorite crushed stone, fraction 5/10 mm	315

Crushed stone diorite fraction 10/20 mm	660
Microsilica 0.1-0.3 microns.	60
Metakaolin 140 microns	30
Distilled water	160
Fibre	1%
Superplasticiser based on polycarboxylate esters	5%
Expected compressive strength in kN	1205

3.3. Preparation of fibre-reinforced concrete mix:

The fibre-reinforced concrete mix is prepared by a three-stage mixing process using an electric mixer.

First, mix portland cement with sand, crushed stone, mineral aggregate and polypropylene fibre, and then prepare the liquid phase by mixing latex, water and superplasticiser. At the final stage, add the liquid phase to the mixture of dry components while mixing [5].

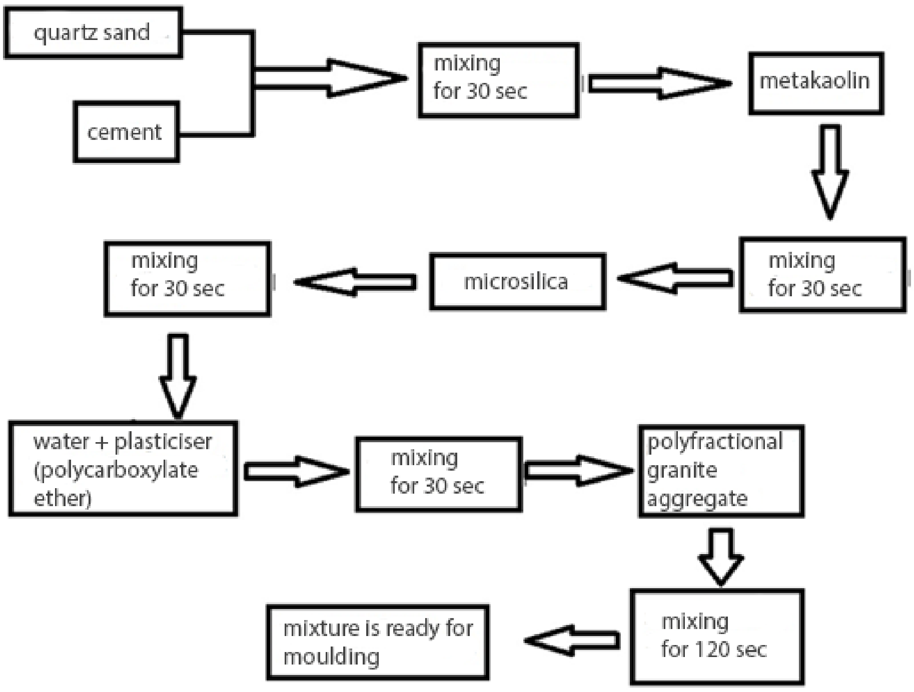

Fig. 3.1. Mixing technology

Samples are formed in accordance with EN 206-1:2001-07.

Laboratory work №4.

Concrete strength class

Introduction:

The compressive strength of concrete is a key parameter that determines its ability to withstand loads and provide stability to building structures. In this paper, we review two methods for measuring this characteristic: the compressive strength of concrete cubes and cylinders. Both methods are based on compressive testing of specimens in accordance with relevant standards, such as EN 12390-12:2020 [7].

In the first stage of the work, we consider the procedure for testing concrete cubes for compressive strength. This method involves subjecting cube-shaped specimens to compression until they fracture. After the test, the compressive strength is calculated using the appropriate formula, which allows us to assess the quality and suitability of concrete for construction purposes.

At the second stage of our work, we are investigating the testing of concrete cylindrical specimens for strength using an automatic compression testing machine. This method involves applying a compressive load to the circular surfaces of a cylindrical specimen until it breaks. After the test is completed, the compressive strength is calculated, which allows us to assess the quality and suitability of concrete for building structures.

4.1. Compressive strength of concrete cubes

The strength of concrete is its strength, experimentally obtained on several samples, taking into account the standard deviation.

The strength class of concrete is its standard compressive strength at a confidence level of 95%, i.e. the average deviation of the strength values of standard samples with a coefficient of variation V of 0.135.

4.2. Type of test:

In a compression testing machine, a cube-shaped test specimen is subjected to compression until it collapses. The determined maximum load is divided by the pressure area, and the result is given in N/mm² (equivalent to MPa).

4.3. Regulatory references:

EN 12390-12:2020 Testing of hardened concrete. Part 3. Compressive strength of test samples [7].

4.4. Tools and equipment

1. TMC-3224 automatic compression testing machine for compression testing according to EN 206-1:2001-07 load speed controller or load speed indicator or stopwatch [6];

Fig. 4.1. TMC-3224 automatic compression testing machine

2. Caliper;
3. Square;
4. Scales, weighing range 30 kg. Weighing accuracy 10 g;
5. Wet cloth;
6. Hand brush.

4.5. Procedure steps:

Preparation of the samples.

1. The test samples shall comply with the requirements of DIN EN 123901 [8] and DIN EN 12390-2 [9]. Damaged samples or samples with a large number of cavities shall not be tested. Nominal dimensions *d* for cubes – 100, 150, 200, 250 and 300 mm. The basic size of the sample should be at least 3.5 times the maximum fraction size.
2. Determine the dimensions of the test samples (Fig. 4.2) and specify them with an accuracy of 1 mm.

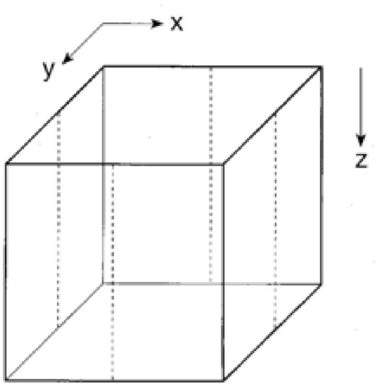

Fig. 4.2. Measurement points for clean surfaces (dotted lines) [2]

If the dimensions or shape of the test samples do not meet the requirements of EN 12390-1 due to exceeding the relevant tolerances, the test samples shall be rejected, corrected or tested in accordance with EN 12390-3, Annex B [10].

3. Calculate the average surface area A_c of the pressure region using Equation 4.1:

$$A_c = x_m \times y_m \ [mm^2], \qquad 4.1$$

where:

A_c – the average surface area of the load application, mm^2;

x – average width of the cube (*x* direction), mm;

y – average length of the cube (*y* direction), mm.

Compressive strength test

4. If the test is performed after storage in water, wipe off excess moisture from the sample with a cloth.
5. Wipe the contact surfaces of the cubes and the test press with a damp cloth.

6. Centre the cube on the pressure plate of the testing machine. The maximum deviation from the centre is 1.5 mm for an edge length of 150 mm (corresponding to + 1 % of the edge length).
7. Adjust the testing machineto the required measurement range.
8. Advance the piston slightly, check the zero point on the pressure gauge scale, set the resistance pointer to the load pointer if the load rate specifications are used. Otherwise, pre-select the download speed using the digital program.
9. Select the loading speed 0.6 ± 0.2 N/(mm^2·s) (MPa/s).
10. Move the pressure plates to the cube plane-parallel, centered and with effort.
11. Start loading. After applying the initial load, which should not exceed approximately 30% of the breaking load, the load is applied to the sample without impact and continuously increased at a previously set loading rate (±10%) until the maximum load (breaking load).
12. Depending on the technical equipment, check the set download speed using a stopwatch or download speed sensor. In manually operated presses, any tendency to decrease the selected loading speed in the limit load range should be corrected by readjustment. This check is not necessary for machines with electronic control, since automatic control is used.
13. Load the cube to failure at the selected load level, read and record the maximum load in kN. Draw any unusual or unsatisfactory failure pattern or relate it to the failure pattern specified in the standard.
14. Calculate the compressive strength limit according to equation 4.2:

$$f_{\mathrm{c,cube}} = \frac{1000 \times F}{A_c} \ \ [\mathrm{N/mm^2}], \qquad 4.2$$

where:

$f_{\mathrm{c,cube}}$ - compressive strength of the cube, N/mm² (MPa);

F - maximum load, KN;

A_c - the area of load application, mm² (Equation 4.1)

15. The value should be rounded to 0.1 N/mm² (corresponds to 0.1 MPa).

16. If the type of fracture is unusual (Fig. 4.4.), specify the number of the fracture type.

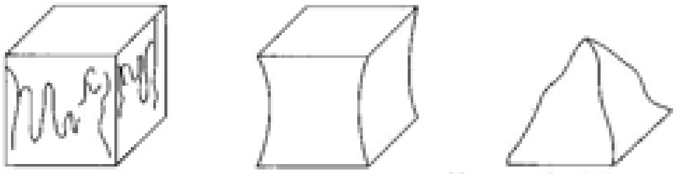

Fig. 4.3. Normal types of destruction of cubic samples [2]

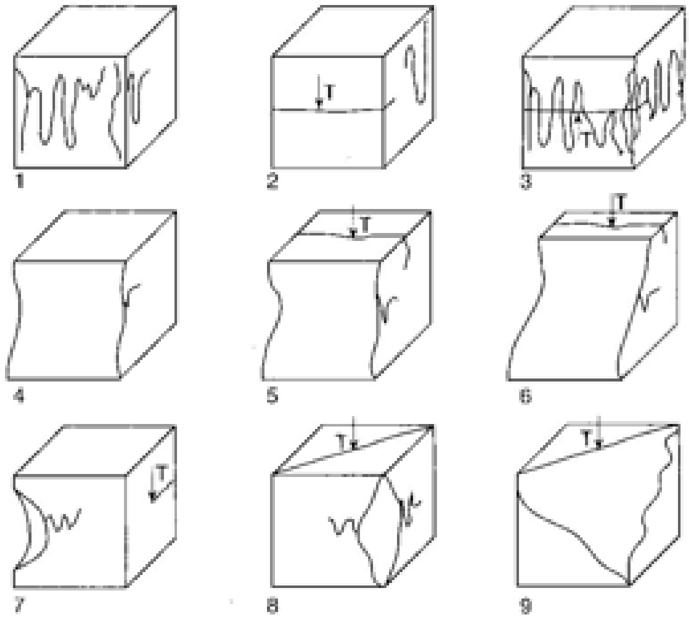

Fig. 4.4. Examples of unusual types of fractures on cubes [2]

4.6. Rating

Unless otherwise agreed, the compressive strength is determined on test cubes with a rib length of 150 mm and under storage conditions according to DIN EN 12390-2:2001-06, Annex NA. Compressive strength limit during storage according to the reference method according to DIN EN 12390 -2:2009-08 (f) can be calculated based on the storage compressive strength according to DIN EN 12390-2:2001-06, Annex NA, (fy) according to equation 4.3 or 4.4 [9]:

Ordinary concrete up to and including C50/60:

$$f_{c,cube} = 0{,}92 \times f_{c,dry} \qquad 4.3$$

High strength ordinary concrete class C55/67:

$$f_{c,cube} = 0{,}95 \times f_{c,dry} \qquad 4.4$$

This dependence is used only to calculate the compressive strength of the cube and only takes into account different storage conditions.

If cubes with an edge length of 150 mm are used instead of cubes with an edge length of 100 mm, the value can be calculated by the equation 4.5.

$$f_{c,cube(150mm)} = 0{,}97 \times f_{c,dry\,(100mm)} \qquad 4.5$$

4.7. Compressive strength of concrete cylinders

A compression testing machine is used to apply a compressive load to the circular surfaces of a cylindrical sample until it breaks. The determined maximum load, divided by the compression area of the cylinder, gives the limit of compressive strength, which is expressed in N/mm² (equivalent to MPa).

4.8. Regulatory references:

DIN EN 12390-3 Testing of hardened concrete Part 3: Compressive strength of samples [10].

4.9. Tools and equipment

1. Compression testing machine (Fig. 4.1.);
2. Load speed controller or load speed indicator or stopwatch;
3. Calipers;
4. Rectangle;
5. Scales, weighing range 30 kg. Weighing accuracy 10 g;
6. Wet cloth;
7. Hand brush.

4.10. Procedure steps:

Preparation of cylinders

1. Check the evenness of the contact surfaces using a square.

2. Measure the dimensions of the test samples as shown in Fig. 4.5, and specify them with an accuracy of 1 mm.

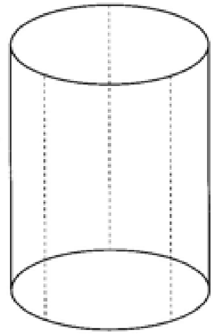

Fig. 4.5. Points for measuring the height of the cylinder [2]

Compressive strength test

3. If the test is performed after storage in water, wipe excess moisture from the sample with a cloth.

4. Wipe the contact surfaces of the cylinders with a damp cloth.

5. Place the cylinder in the center of the pressure plate of the test press. The deviation from the center should not exceed 1.5 mm for a diameter of 150 mm (corresponding to + 1% of the diameter).

6. Adjust the testing machine to the required measurement range.

7. Move the pressure plates against the cylinder with force and apply an initial load that is a maximum of 30% of the expected breaking load.

8. Check the set load speed using a stopwatch or speed sensor load speed controller.

9. Load the cylinder to the maximum load with the selected load level. If manual control is used in the break phase, adjust as necessary.

10. Read the maximum load.

11. Convert the maximum load to the compressive strength using the equation 4.6:

$$f_{\mathrm{c,cyl}} = \frac{1000 \times F}{A_c} \quad [\mathrm{N/mm^2}], \qquad 4.6$$

where:

$f_{\mathrm{c,cyl}}$ – compressive strength under cylindrical load, N/mm² (MPa);

F – maximum load, kN;

A_c – load application area, mm².

12. Round the value to the nearest 0.1 N/mm² (equivalent to 0.1 MPa).

13. If the fracture type is unusual (see Fig. 4.6 and 4.7), specify the fracture type number.

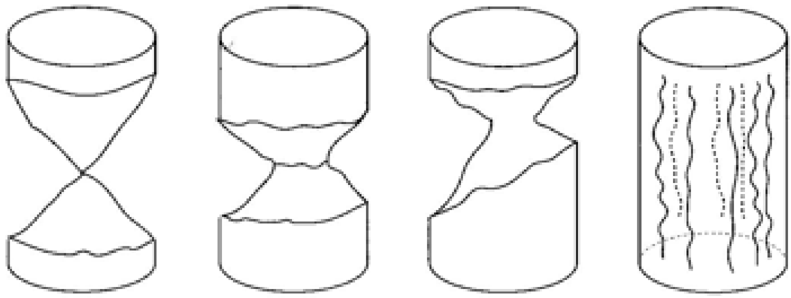

Fig. 4.6. Normal destruction of cylindrical samples [2]

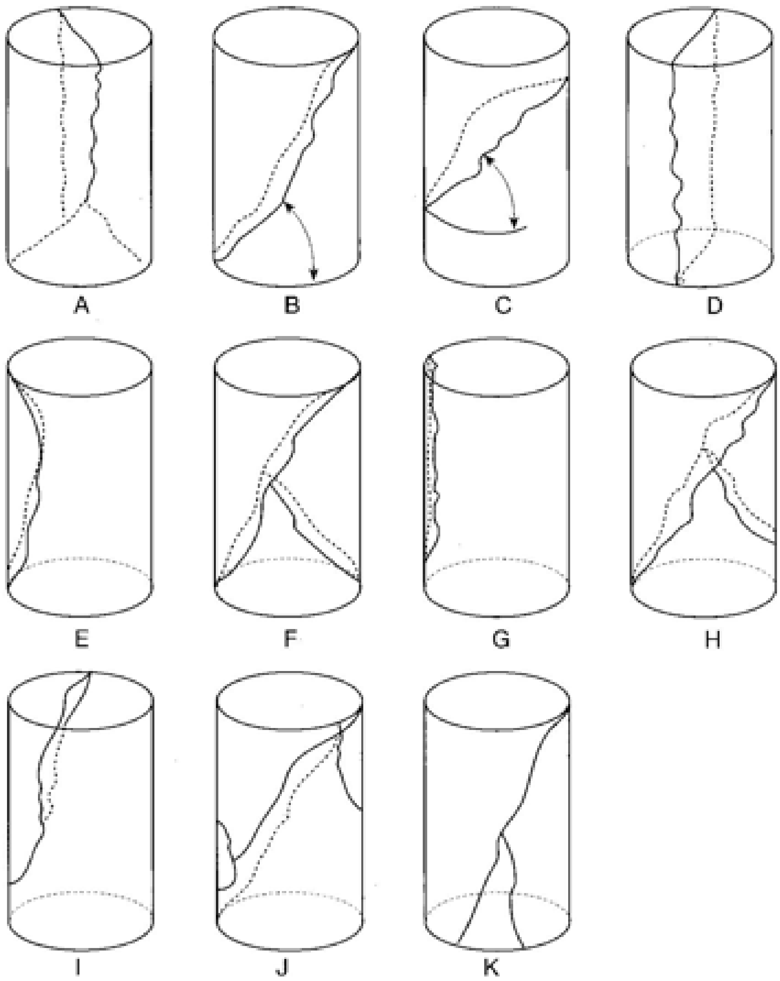

Fig. 4.7. Examples of unusual patterns of cylinder destruction [2]

4.11. Rating

The assignment of the compressive strength class of concrete cylinders with a diameter of 150 mm after storage in water is performed according to DIN EN 206-1 [6], Table 4.1.

Table 4.1.

Strength class for cylinder and cube samples

Class of compressive strength	Characteristics of strength in cylinder samples	Characteristics of strength in cube samples
C8/10	8	10
C12/15	12	15
C16/20	16	20
C20/25	20	25
C25/30	25	30
C30/37	30	37
C35/45	35	45
C50/60	50	60
C55/67	55	67
C60/75	60	75
C100/115	100	115

The formation of the structure of the ultra-high-strength composite occurs during physicochemical reactions, which are accompanied by the binding of free water with clinker minerals of cement, the formation of a saturated solution of crystal hydrates and their subsequent crystallization. Considering the complexity and insufficient study of these physico-chemical processes, there are different theoretical interpretations about their nature and sequence. The first work on the development of ultra-high-strength composite began in the seventies in the United States of America [15]. High-strength concrete was used for the first time in 1997 in the expansion (completion - reconstruction) of the Katten nuclear power plant in France [16].

Laboratory work №5

X-ray studies of cement

Introduction

Cement is the main building material used throughout the world to create concrete, mortar and other construction materials. The quality of cement significantly affects the durability and reliability of construction objects. Since cement has a complex mineralogical composition, it is important to carefully control its properties at all stages of production and use. One of the most effective methods of analysis is X-ray research.

X-ray examination of cement includes several methods, among which X-ray fluorescence analysis and X-ray structural analysis are the most widespread and important. These methods make it possible to determine the chemical composition and phase structure of cement, which are critically important for its quality and compliance with standards.

X-ray fluorescence analysis is used to quickly and accurately determine the elemental composition of cement. It allows to identify the main components, such as oxides of calcium, silicon, aluminum, iron and other elements that affect the properties of the final product. This method is based on measuring the intensity of secondary X-ray radiation, which occurs when the sample is irradiated with primary X-rays.

X-ray structural analysis is used to determine the crystal structure and phase composition of cement. This method allows the identification of different crystalline phases, such as clinker minerals (alite, belite, aluminate and ferrite), which are formed during the firing of cement raw materials. With the help of X-ray structural analysis, it is possible to determine the quantitative composition of phases and identify possible impurities and inconsistencies in the cement structure.

Thus, the introduction of standard methods of X-ray research into the practice of cement production and quality control is a necessary step to ensure high quality of building materials and structures.

5.1. Equipment and materials

1. For X-ray studies, a high-resolution PANalytical Philips X'Pert PRO diffractometer was used: a parabolic Hegel mirror placed behind an X-ray tube with CuKα1 radiation length λ=1.54056 Å, followed by a four-crystal Bartels monochromator (4 ×Ge220) and a point detector with a triple analyzer crystal (3×Ge220). The divergence of the primary beam and the angular acceptance of the analyzer crystal used in front of the detector is $\Delta\alpha_{i,f}\approx$1-2 arcseconds.

2. Reference cement samples: samples with a known composition for equipment calibration.

3. Computer software: experimental X-ray data are processed using Match3 software.

4. Preparation of samples: equipment for grinding, mixing and pressing of samples.

5.2. Preparation of samples

1. Selection of samples: select broken concrete without coarse aggregate to be investigated.

2. Grinding: grind the samples to a powdery state to ensure uniformity.

3. Sifting: sift the powder through a sieve with a hole size of no more than 75 microns.

4. Pressing: press the powder in the form of tablets or applicate on a substrate for analysis.

5.3. Procedure steps:

1. Calibration of the device: use reference samples to calibrate the diffractometer.

2. Sample preparation: install the sample in the diffractometer holder.

3. Setting parameters: set the scaning parameters, such as X-ray tube voltage and current, starting angle.

4. Scaning: scan the sample obtaining a diffraction curve.

5. Analysis of the results: analyze the diffraction curve using the software, identify the phases and determine their quantitative composition.

Analysis of the results

Structural studies of the phase composition of cement and cement stone samples were carried out on the X'Pert PRO MRD diffractometer in a single-crystal scheme for $CuK_{\alpha 1}$ radiation. The initial samples were crushed and in the form of a finely dispersed powder were sifted through a sieve, the diameter of the cells of which was 75 µm.

Experimental X-ray data were analyzed using Match3 software using the Rietveld method.

Match3 is a software for analyzing crystal structures and calculating the corresponding X-ray or neutron patterns for polycrystalline samples. It is based on the idea of using specific crystallographic know-how for the intuitive generation of structural models.

Very often, the success of such software depends on the initial structure model. The user must effectively modify known crystal structures (change of translation and rotation of atoms or molecules, replacement, removal and embodiment of atoms or molecules, reduction of symmetry), or create new ones (in a relatively short time) only using crystallographic and crystallochemical knowledge. Therefore, Match3 provides support in the analysis of determining the parameters of the structure [11].

For the comparative analysis of the characteristics of the samples, phases typical for cement were chosen, which correspond to the following intensity maxima on the diffractogram (Fig. 5.1) [8]: for phase C_3A – at 2θ=33 degrees (lattice period d=2.70 Å); for the C_4AF phase (2θ=33.3 degrees) – d=2.64 Å, for the C_3S phase the repeatability of intensity maxima is characteristic – d=3.04 Å.

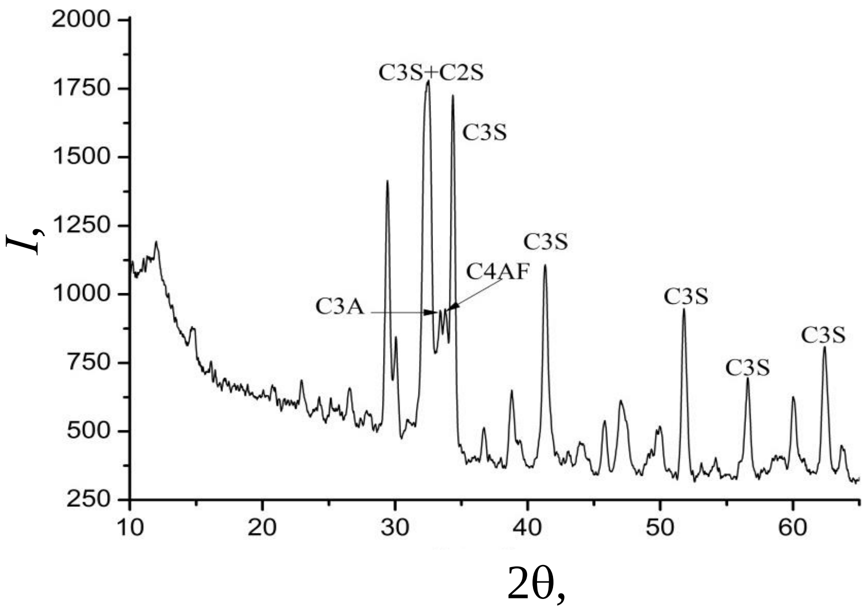

Fig. 5.1. Diffraction curve of the phase composition of cement containing various clinker minerals

For the β-C_2S phase, most of the intensity maxima overlap with the corresponding maxima of other clinker minerals, in particular the C_3S phase (at (2θ=33.3°)). For this mineral, a weak maximum at 2θ=33.3°, (d=2.89 Å) was chosen. To plot the calibration graphs, reference mixtures were prepared, the dispersion of which was ensured by sieving through a sieve with a mesh diameter of ~ 8 µm. The ratio of the main phases of clinker minerals in cement is given in Table 2.2 [12].

Table 5.1.

Quantitative ratios (in %) between the main phases of cement.

Clinker minerals	Chemical formula	Content, %
C_3S	Ca_3O_5Si	60,4
C_2S	Ca_2O_4Si	22
C_4FA	$Al_2Ca_4Fe_2O_{10}$	11,6
C_3A	$Al_2Ca_3O_6$	6

In general, it should be noted that this ratio of clinker minerals is within the normal range. The use of cement with a low C_3S content significantly complicates the production of high-strength concrete, in particular when using microsilica and metakaolin, since the effectiveness of these additives requires the presence of excessive $Ca(OH)_2$ portlandite in the hardening system, while systems with a low C_3S content are characterised by a reduced $Ca(OH)_2$ content [12].

The data of X-ray and spectral analysis show that a number of chemically active substances are formed in a series of samples with a strength of 120 MPa in the process of hydration of clinker minerals during concrete hardening (Fig. 5.2). These are, first of all, calcium oxide hydrate, calcium silicate hydrate and such structural gel models as Genite and Tobermorite. The results of the identification of the formed phases are given in Table 5.1.

The characteristic products of Portland cement hydration for samples in the diffraction curve of Fig. 5.1. are numbered and correspond to next compounds: Ettringite (1 - $Al_2Ca_6H_{66}O_{49.68}S_3$ - d/n=0,974; 0,563; 0,388; 0,278 nm); calcium hydrosilicates (4 - $Ca_3H_2O_{7.5}Si_{1.5}$ - d/n=0,278, 0,335, 0,181 nm); Genite (5 - $Ca_9H_{22}O_{32}Si_6$ - d/n=1,049; 0,262; 0,278 nm); Tobermorite (b - $Ca_2H_3O_{11}Si_3$ - layer thickness of 1.1 nm, d/n=0,308; 0,297; 0,351 nm).

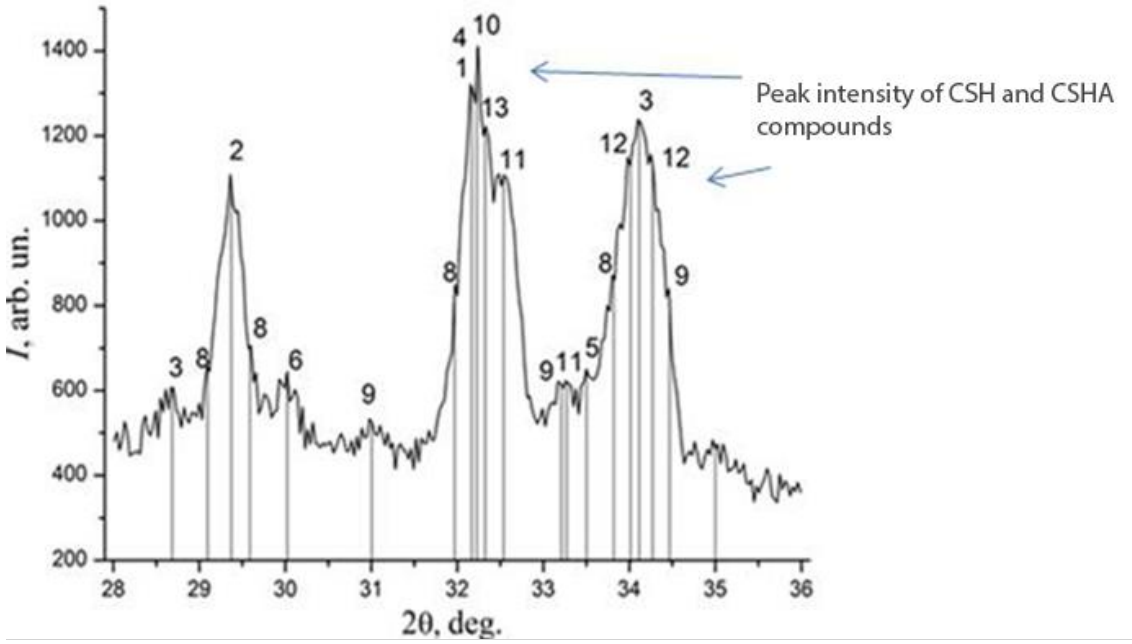

Fig.5.2. Fragment of the X-ray diffractogram

It is important that these maxima are located in the same angular positions as the intensity maxima for clinker minerals, in particular, for alite (C_3S) and belite (C_2S). This indicates their crucial role in the formation of the cement matrix.

Table 5.2.

List of compounds of the phase composition of hydration products (fig. 5.2).

№	Chemical formula	*d / n*	Назва сполуки
1	$Al_2Ca_6H_{66}O_{49.68}S_3$	0,974, 0,563, 0,388, 0,278,	Ettringite
2	$CaCO_3$	0,303, 0,191	Calcite
3	$Ca(OH)_2$	0,491, 0,262, 0,192	Portlandite
4	$Ca_3H_2O_{7.5}Si_{1.5}$	0,278, 0,335, 0,181	Hydrosilicate calcium
5	$Ca_9H_{22}O_{32}Si_6$	1,049, 0,262, 0,278	Genite
6	$Ca_2H_3O_{11}Si_3$	0,308, 0,297, 0,351	Tobermorite 1.1 nm
7	$Ca_{2.5}H_{11}O_{12.5}Si_3$	0,552, 0,310, 0,301	Tobermorite 1.4 nm
8	$Ca_5H_{10}O_{22}Si_6$	0,307, 0,301, 0,279	Clinotobermorite
9	$Ca_2H_2O_5Si$	0,287, 0,269, 0,260	Calcium silicate hydrate
10	$Ca_5H_2O_{10}Si_2$	0,303, 0,277, 0,256	Calcium silicate hydrate
11	$Al_2CaH_{10}O_{21}Si_6$	0,305, 0,275, 0,268	Calcium silicate hydroaluminates
12	$Al_2CaH_8O_{10}Si_{12}$	0,263, 0,262	Calcium silicate hydroaluminates
13	$Al_{3,5}Ca_3H_{9,7}O_{12}$	0,276, 0,309	CAH

According to the X-ray analysis, modification of the cement matrix with a complex of finely dispersed silica and aluminosilicate compounds at a certain ratio leads mainly to the formation of low-base calcium hydrosilicates and such C-S-H structural models as jenite (d/n: 1. 049; 0.262; 0.278) and tobermorite (d/n: 0.552; 0.310; 0.301; 0.308; 0.297; 0.351), which have a layered structure and are essentially nanomaterials. These phases were formed from the components $Ca(OH)_2$ and active silica at a Ca/Si ratio of 1.1-1.2 [12].

Laboratory work №6

Scanning electron microscopy of concrete

Introduction

Scanning electron microscopy (SEM) is one of the most powerful methods for studying the microstructure of materials. This technique allows obtaining images of the surface of samples with high resolution, which significantly exceeds the capabilities of optical microscopes. SEM is widely used in various fields of science and technology, including materials science, biology, nanotechnology, and others.

The principle of SEM operation

The basic principle of SEM is to use an electron beam that scans the surface of the sample. During scanning, electrons interact with surface atoms, causing different types of signals to be produced, such as secondary electrons, reflected electrons, and X-rays. These signals are used to form an image and obtain information about the composition and structure of the sample.

Key stages of SEM work:

Electron beam generation: Electrons are accelerated in a vacuum using an electron gun and shaped into a thin beam.

Scanning the sample: The electron beam scans the surface of the sample using a system of magnetic coils, which allows moving the beam in a given direction.

Interaction of electrons with the sample: During the interaction of electrons with atoms of the surface of the sample, secondary electrons and other signals are created.

Signal detection: Secondary electrons are collected by a detector that converts them into an electrical signal.

Image formation: The collected signals are processed by a computer to create an image of the surface of the sample.

SEM allows obtaining images with a resolution of several nanometers, which makes it an indispensable tool for studying materials at the micro- and nano-levels. In laboratory work with SEM, students will have the opportunity to study in detail the microstructure of concrete samples, determine their morphological features, identify defects and evaluate porosity. This will allow a deeper understanding of the properties of concrete and its behavior in various operating conditions.

6.1. Equipment and materials

1. Scanning electron microscopes Hitachi SU 70, Zeiss EXO 50;
2. Concrete samples of various types;
3. Vacuum unit;
4. Gold or palladium coating for samples (if necessary);
5. Clamps for samples;
6. A computer with software for image analysis, such as ImageJ, MATLAB

6.2. Preparation of samples

To obtain high-quality images in SEM, it is necessary to properly prepare the samples. Concrete samples must be clean and dry.

6.3. Imaging and analysis

The resulting images are analyzed to determine morphology, detect defects, and estimate porosity. Image analysis software allows you to obtain quantitative characteristics such as grain size, pore distribution, and other parameters.

6.4. Procedure steps:

Preparation of samples

1. Select concrete samples for research.
2. Clean the samples from dust and dirt using an ultrasonic bath or other methods.
3. Dry the samples in a drying cabinet.

6.5. SEM settings

1. Turn on the SEM and let it warm up.
2. Mount the sample in the holder and place it in the vacuum chamber of the microscope.
3. Pump out the air from the vacuum chamber to the required vacuum level.
4. Adjust the electron beam parameters (accelerating voltage, beam current) according to the sample type.

6.6. Receiving images

1. Perform an initial scan of the sample for orientation.

2. Select areas for detailed research.

3. Obtain high-quality images of selected areas by varying scan parameters to optimize image quality.

4. Save the obtained images for further analysis.

6.7. Image analysis

1. Use image analysis software to process the acquired data.

2. Determine the morphological features of the sample: grain size, shape of particles, presence of cracks and other defects.

3. Estimate sample porosity using image segmentation and pore counting methods.

6.8. Description of the study

Determination of the features of the effect of various modifiers and their complexes on the formation of hydrate phases and the microstructure of cement stone fractures was carried out using a «Zeiss» EVO-50 scanning electron microscope using a CCD detector that can process samples with a diameter of 25 mm at an analytical working distance of 8.5 mm thanks to the combination of a large degree of movement, inclined detectors and a conical objective lens (Fig. 6.1).

The elemental composition of the composites was determined using an X-ray analyzer Link-860, Oxford IncaEnergy 450.

Fig. 6.1. «Zeiss» EVO-50 electron microscope with CCD detector [13]

The analysis of the microstructure features of concrete chips was carried out using a scanning electron microscope (Hitachi SU 70) with a CCD detector. Elemental analysis of the objects was carried out using energy dispersive X-ray spectroscopy (EDX analysis).

Fig. 6.2 and Fig. 6.3 shows fragments of electron microscopy images, and Tables 6.1 and 6.2 show X-spectral analysis data in the areas of sample sections marked with numbers.

The list of elements and their percentage content indicates the presence of hydrosilicates and calcium aluminates, as well as calcium hydroxide, in the concrete matrix. It is characteristic that the content of the main components of the area bounded by lines 7 in Fig. 6.2 and 6.3 for samples №1 and №2 is practically the same. In local grains, the percentage content of the main elements also coincides, in particular, in grains 3 and 4 in Fig. 6.2 and 1, 2 and 3 in Fig. 6.3. At the same time, in intergranular zones 1 and 2 (Fig. 6.2), the carbon content is significantly (twice) lower and the calcium content is higher (twice) than in the corresponding zones 5 and 6 in Fig. 6.3. At the same time, the ratio of calcium to silicon is almost the same. However, in the same grain zones 5.6 in Fig. 6.2 and Fig. 6.3, the ratio of Ca/Si compounds is lower, for recipe №. 1 1.04-0.88, for recipe №2 0.77-0.76. This may indicate a greater amount of low basic calcium hydrosilicates.

The microstructure of the sections is significantly different in the electron raster images. For sample №2 in Fig. 6.3, it is more developed and compacted. The reason may be that the modified samples are characterized by a higher content of hydration products. Probably, in the process of hydration of clinker minerals during concrete hardening, a number of chemically active substances are formed, primarily calcium oxide hydrate and calcium silicate hydrate. It is likely that the metakaolin and microsilica in the concrete mixture create conditions for the transformation of unstable and soluble calcium hydroxide into strong crystalline calcium silicate hydrate (CSH). Therefore, the concrete structure is compacted and gives an increase in the strength index for sample №2.

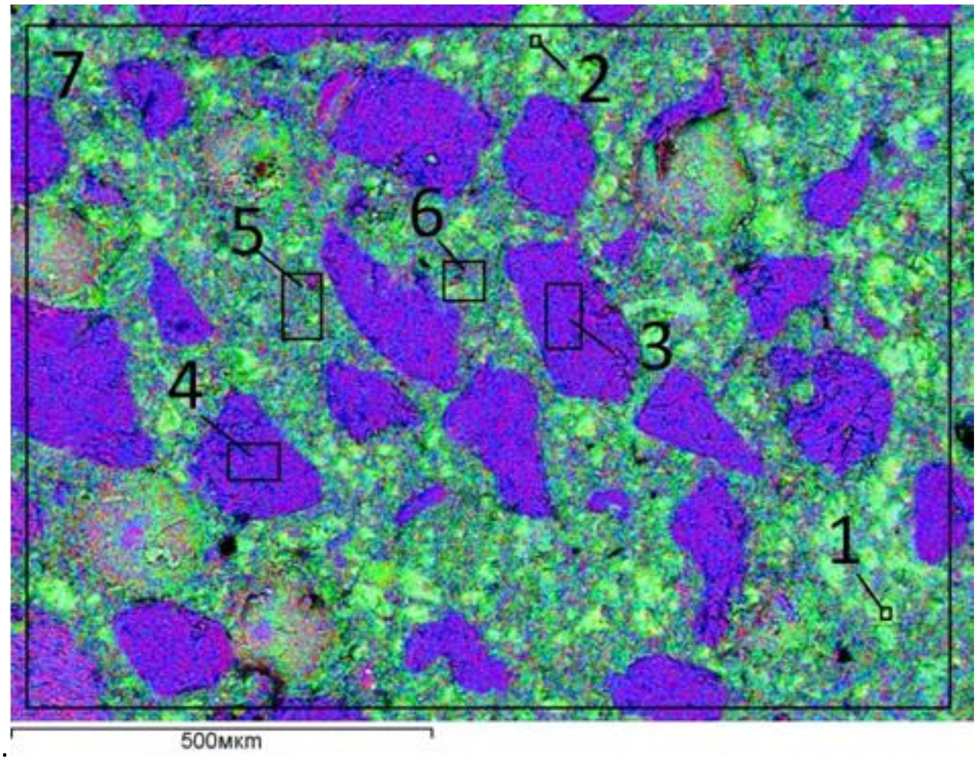

Fig. 6.2. Fragments of electronic images of the macro- and microstructure of the surface sections of the cement matrix of recipe №1

Table 6.1.

Spectral distribution of the main elements in the regions indicated by numbers of sections of the cement matrix of composition №1 (Fig. 6.2).

№	C	O	Mg	Al	Si	K	Fe	Ca
	%							
1	2.52	40.30	0.57	1.78	13.38	0.49	1.74	39.23
2	6.54	36.56	0.59	0.43	12.34	-	-	43.54
3	20.32	42.05	-	-	37.18	-	-	0.45
4	18.40	40.61	-	-	40.19	-	0.34	0.46
5	21.33	37.56	0.70	1.8	17.81	0.8	1.30	18.69
6	21.66	38.90	0.71	2.15	18.44	0.92	1.01	16.20
7	19.06	40.28	0.54	1.37	23.64	0.58	0.8	13.74

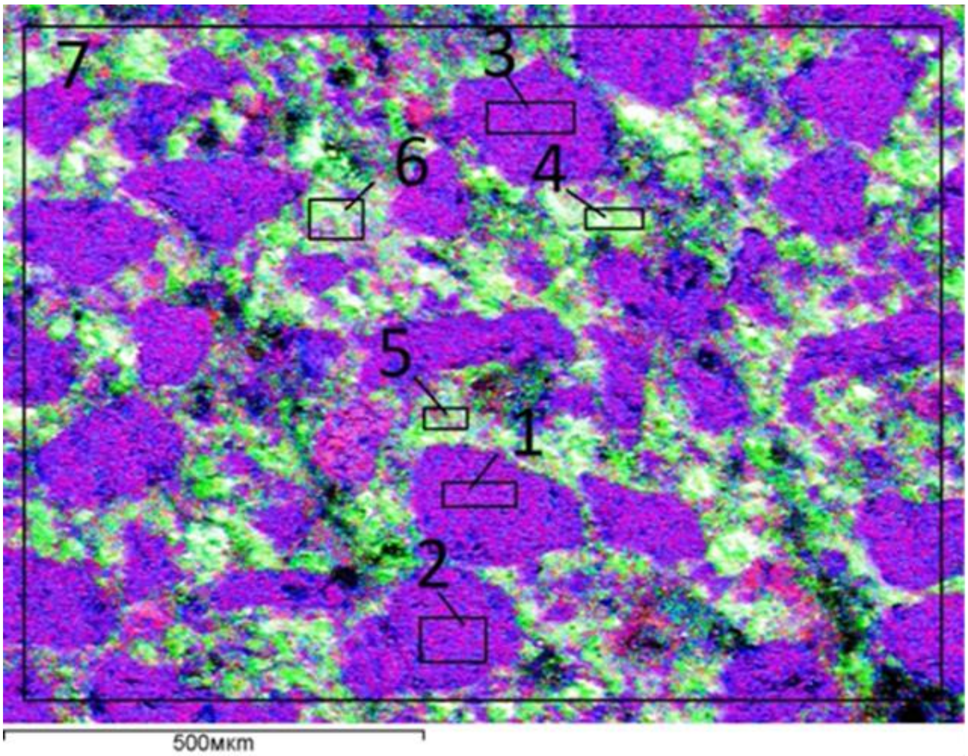

Fig. 6.3. Fragments of electronic images of the macro- and microstructure of the surface sections of the cement matrix of recipe №2

Table 6.2.

Spectral distribution of the main elements in the regions indicated by numbers of sections of the cement matrix of composition №2 (Fig. 6.3).

№	C	O	Mg	Al	Si	Fe	Ca
	%						
1	11.51	46.05	-	-	42.24	-	0.20
2	12.12	45.50	-	-	41.95	-	0.43
3	17.15	42.85	-	0.18	38.98	-	0.55
4	14.06	41.09	1.24	1.92	17.09	0.94	22.95
5	9.37	45.89	1.00	2.92	21.94	1.13	17.09
6	8.02	45.23	1.10	2.86	23.41	1.01	17.80
7	20.28	40.69	0.40	1.53	26.38	0.80	9.34

Optimal packing of fine aggregates is one of the key points in mixture development. Optimal (in Fig. 6.3) packaging forms a denser distribution of aggregate. As shown (Fig. 6.3), a large number of modifiers chemically interact with each other and with cement, thus forming a high-density composite with a low content of various types of pores.

Filling the pore structure with hydration products leads to a decrease in their volume, even a slight decrease in the pore volume (by 1-2%) is a consequence of an increase in the structural strength of the composite [14].

Results of scanning electron microscopy.

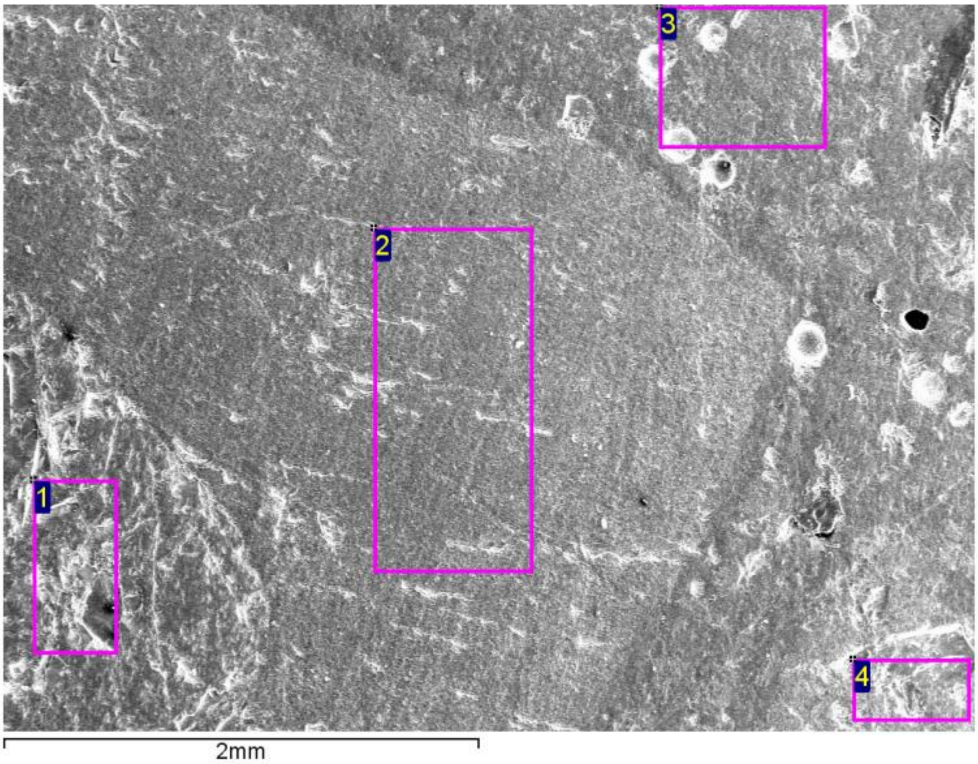

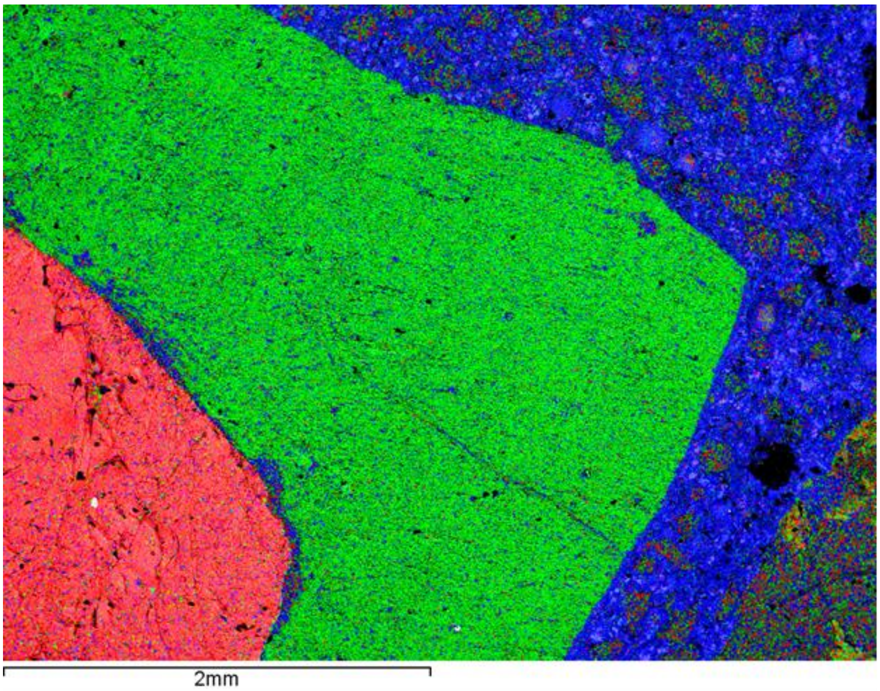

Fig. 6.4. SEM image of the boundary between aggregate and binder of the mixture №1 (red - Fe, green - Si, blue - Ca)

Table 6.3.

Spectral distribution of the main elements in the indicated areas of sections of the cement matrix composition №1 (Fig. 6.4).

Spectrum	in statics	C	O	Mg	Al	Si	K	Ca	Fe	total
1	Yes	10.78	37.57	4.00	8.70	16.26		0.92	21.77	100.00
2	Yes	15.81	39.68		7.72	27.51	8.39	0.90		100.00
3	Yes	21.60	39.86	0.60	1.15	24.39	0.59	11.10	0.71	100.00
4	Yes	12.55	45.71		0.58	40.17	0.54	0.44		100.00
Max		21.60	45.71	4.00	8.70	40.17	8.39	11.10	21.77	
Min		10.78	37.57	0.60	0.58	16.26	0.54	0.44	0.71	

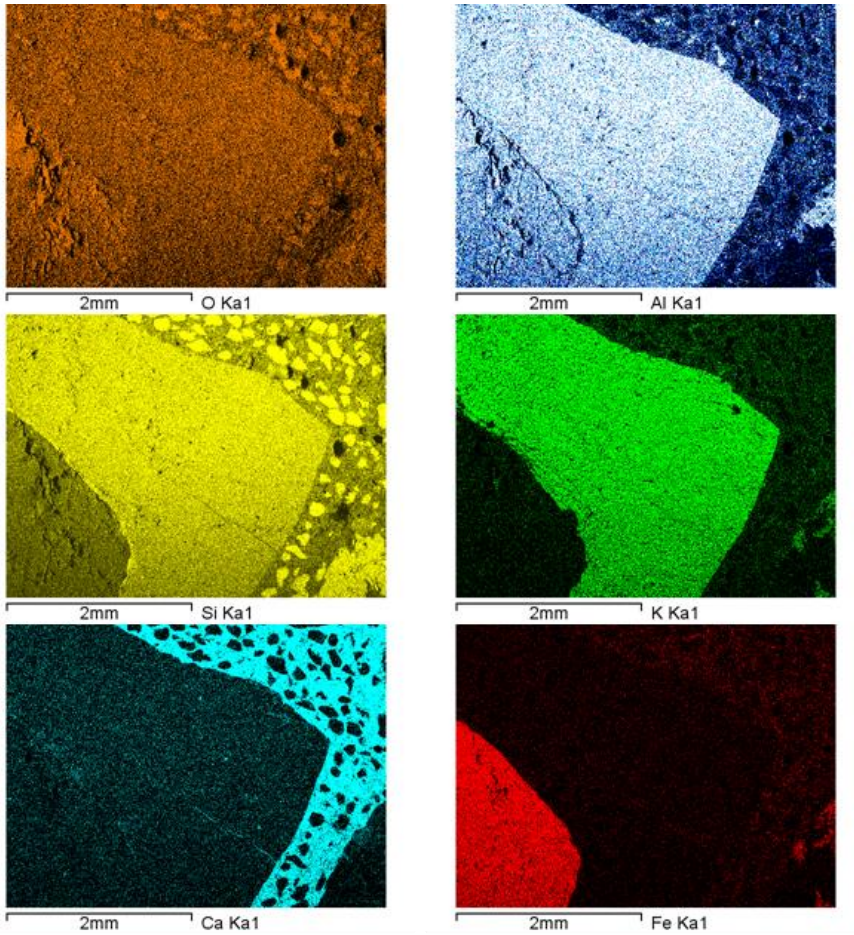

Fig. 6.5. Elemental maps of the distribution of compounds

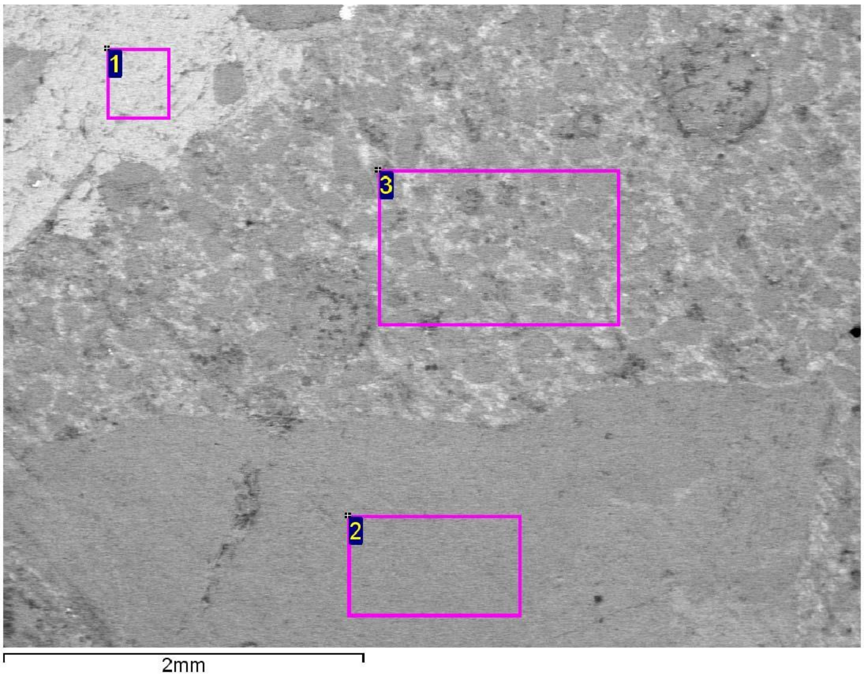

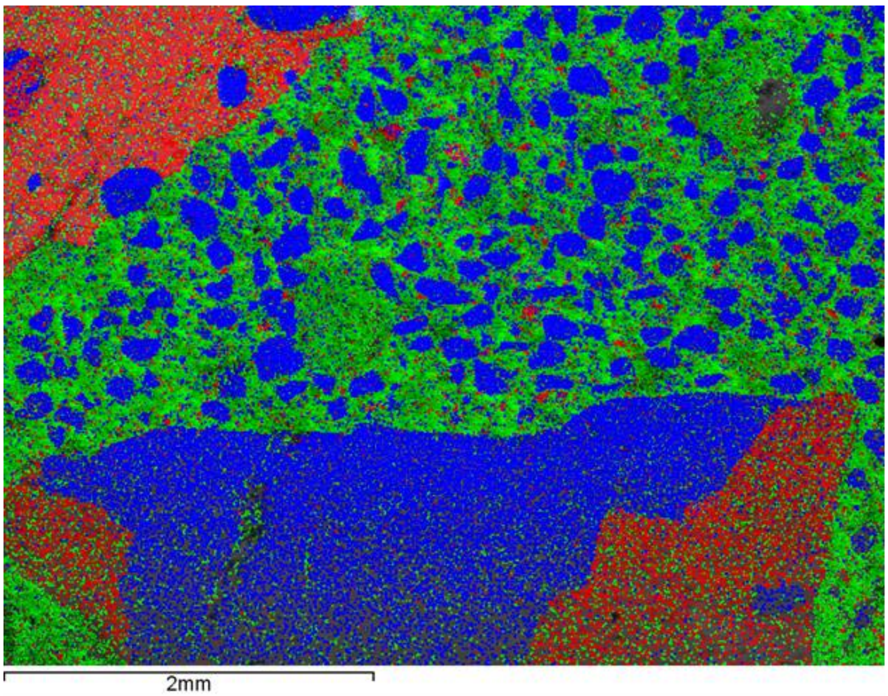

Fig. 6.6. The image of the boundary between aggregate and binder of the mixture №2 (red - Fe, green - Si, blue - Ca)

Table 6.4.

Spectral distribution of the main elements in the indicated areas of sections of the cement matrix composition №2 (Fig. 6.6).

Spectrum	in statics	C	O	Mg	Al	Si	K	Ca	Fe	total
1	Yes	14.11	37.04	3.89	8.66	16.54		0.89	18.87	100.00
2	Yes	16.43	43.50			39.60		0.47		100.00
3	Yes	20.49	40.89	0.51	1.50	25.53	0.52	9.84	0.72	100.00
Max		20.49	43.50	3.89	8.66	39.60	0.52	9.84	18.87	
Min		14.11	37.04	0.51	1.50	16.54	0.52	0.47	0.72	

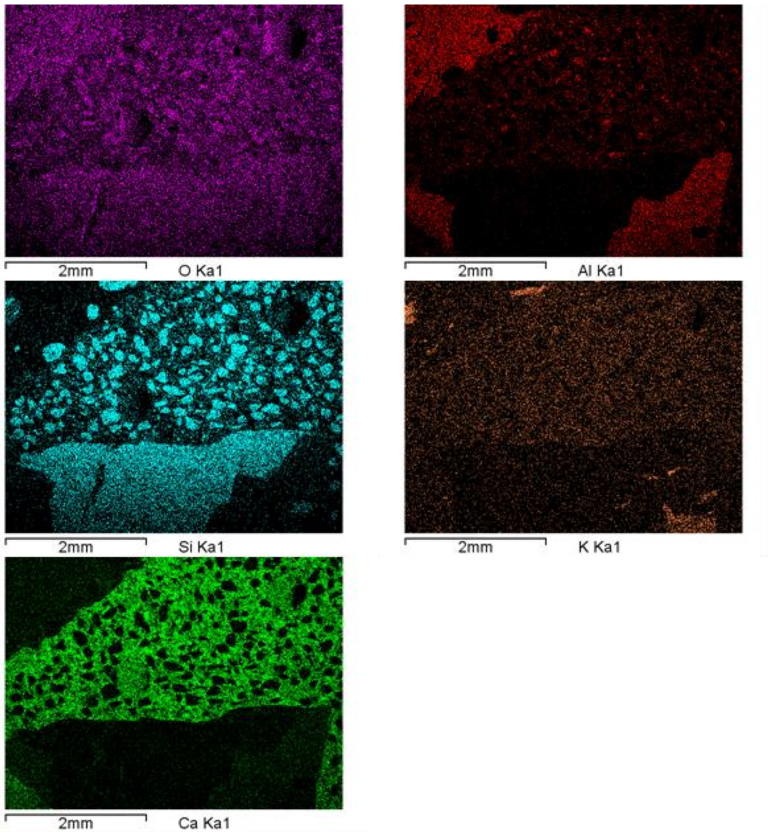

Рис. 6.7. Elemental maps of the distribution of compounds

References

1. EN 196-1:2005-05. Methods of testing cement. Part 1: Determination of strength;

2. Iken, Hans W.: Handbuch der Betonprüfung: Anleitungen u. Beispiele / Wolfgang Breit; Hans-Wilhelm Iken; Roman R. Lackner; Ulrich Wöhnl; Uwe P. Zimmer. 6. überarbeitete und erweiterte Auflage 2012 Düsseldorf: Verlag Bau+Technik, 2012;

3. EN 197-1:2011, IDT. Cement. Part 1. Composition, specifications and compliance criteria for ordinary cements;

4. EN 196-1:2007. Cement testing methods. Part 1. Determination of strength (EN 196-1:2005)

5. Patent UA 150717 URL: https://base.uipv.org/searchINV/search.php?action=viewdetails&IdClaim=281059

6. EN 206-1:2001-07. Concrete - Part 1: Specification, performance, production and conformity;

7. EN 12390-12:2020. Testing of hardened concrete. Part 3. Compressive strength of test samples;

8. DIN EN 12390-1. Testing of cement concrete. Part 1: Shape, dimensions and other requirements for samples and moulds;

9. EN 12390-2. Tests of cement concrete. Part 2. Production of samples and their hardening conditions for strength testing;

10. DIN EN 12390-3. Testing hardened concrete. Part 3. Compression test of samples;

11. B. Winkler, V. Milman, C.J. Pickard / Quantum mechanical study of Al/Si disorder in leucite and bicchulite, Mineral. Mag. 68 (2004) 819–824.

12. Sumariuk O.V., Romankevych V.F., Fodchuk I.M. / «Concrete composites of high structural strength and density, modified by a complex of finely dispersed additives based on nanosilica and metakaolin // Nanosystems, nanomaterials, nanotechnologies» 2018, №1 (16) p. 103-117;

13. R.K. Rastsvetaeva, N.B. Bolotina, A.E. Zadov, N.V. Chukanov / Crystal structure of fukalite dimorph Ca4(Si2O6)(CO3)(OH)2 from the Gumeshevsk deposit, the Urals, Dokl. Earth Sci. 405 (2005) 1347–1351;

14. O.V. Sumariuk, I.I. Gutsulyak, V.F. Romankevych V.V., Mykhailovych, Yu.T. Roman, I.M. Fodchuk. / The influence of the microstructure of concrete fractures on the strength of concrete

composites of high structural strength and density // Nanosystems, nanomaterials, nanotechnologies. – 2019. 17 №4, pp. 649 – 660;

15. J.F. Martirena, Robert L. Day, B. Middendorf, M. Gehrke / Lime-pozzolan binder as a very fine mineral admixture in concrete // (International Symposium on Ultra High Performance Concrete Kassel, Germany September 13-15, 2004);

16. K. Wille, A.E. Naaman, G.J. Parra-Montesinos / Ultra-High Performance Concrete with Compressive Strength Exceeding 150 MPa // ACI Materials Journal 108(1), 46 (2011).

Co-funded by the
Erasmus+ Programme
of the European Union

AMAZE

Erasmus+ Programme Key Action 2 Cooperation Partnerships for Higher Education (KA220-HED)
Agreement number 2023-1-RO01-KA220-HED-000155412
European Network for Additive Manufacturing in Industrial Design for Ukrainian Context – Acronym: AMAZE

e-Toolkit

CAD/CAM/CAE Design

Project Title	**European Network for Additive Manufacturing in Industrial Design for Ukrainian Context 2023-1-RO01-KA220-HED-000155412**
Output	**IO2 - AMAZE e-toolkit manual for digital learning in producing complex design industrial parts**
Module	**Module 3** **CAD/CAM/CAE design**
Date of Delivery	**June 2024**
Authors	**Igor FODCHUK, Mariana BORCHA, Nataliia VATAMANIUK, Volodymyr ROMANKEVYCH, Yurii SOBKO**
Version	**FINAL VARIANT, *14.06.2024***

This project has been funded with support from the Erasmus+ Programme Key Action 2 Cooperation Partnerships for Higher Education (KA220-HED). This publication [communication] reflects the views only of the authors, and the Commission cannot be held responsible for any use which may be made of the information contained therein.

Co-funded by the Erasmus+ Programme of the European Union

Contents

This project has been funded with support from the Erasmus+ Programme Key Action 2 Cooperation Partnerships for Higher Education (KA220-HED). This publication [communication] reflects the views only of the authors, and the Commission cannot be held responsible for any use which may be made of the information contained therein.

General information

These guidelines are aimed at learning Autodesk Revit at the level that allows to build a 3D model of a building and create basic architectural and construction drawings – plans, facades, sections [1, 4].

These guidelines can be used as supplementary documentation for practical training on following topics:

1. Description of the programme. Installation, interface, methods of work.
2. Setting up plan levels. Creating a grid of axes.
3. Description of walls, their characteristics.
4. Description of windows and doors, their properties. Create and configure types/styles.
5. Description of stairs and handrails, their properties. Custom shapes.
6. Description of floors and roofs. Building and editing.
7. Create a facade and section, flat and three-dimensional. Setting up the perspective view of the camera.
8. Visualisation – styles, materials and light sources.
9. Create and design Sheets. Transfer of Views (plans, facades, sections, 3D views) to sheets.
10. Create and configure text types and sizes.

This project has been funded with support from the Erasmus+ Programme Key Action 2 Cooperation Partnerships for Higher Education (KA220-HED). This publication [communication] reflects the views only of the authors, and the Commission cannot be held responsible for any use which may be made of the information contained therein.

1 Autodesk Revit interface

The program interface is largely similar to standard Autodesk programs such as AutoCAD, Inventor, 3D MAX [2, 5] (Fig. 1.).

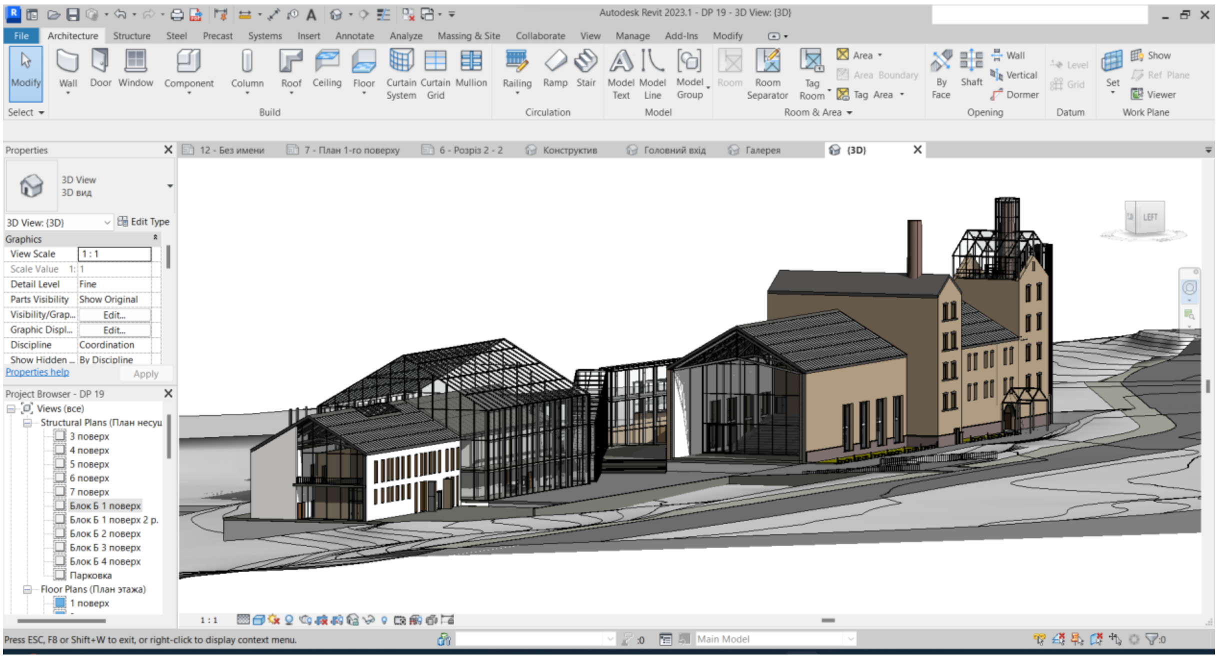

Fig. 1. Elements of the Revit interface [7]

1. Program menu – commands to open, save, print, etc.
2. Quick access panel (the content is customizable).
3. Info Center – file name, help, search.
4. Parameters panel - the content depends on the current command.
5. Select the TYPE (style) of the object (section in the «Properties» panel).
6. The Properties palette contains the basic settings of the current object.
7. Project Manager – switching between views: 3D model and flat drawings, design elements and documentation.

This project has been funded with support from the Erasmus+ Programme Key Action 2 Cooperation Partnerships for Higher Education (KA220-HED). This publication [communication] reflects the views only of the authors, and the Commission cannot be held responsible for any use which may be made of the information contained therein.

8. Status bar – hints and tips for operations.
9. View Control Panel – scale, detail, visualization, sun trajectory, shadows, view cropping, object isolation.
10. Drawing area – the main working area.
11. Toolbar – a set of tabs with groups of panels.
12. Toolbar tabs – standard and contextual (appear depending on the current create/edit command).
13. Windows with warnings about incompatibilities or errors.

View Control Bar

View Control Bar (Fig. 2.) is designed to configure the display of graphics in the current window – plan, facade, model [5]:

Fig. 2. View Control Bar

1. «Level of detail» – options «low», «medium», «high»;
2. «Visual style» – options «Framework», «Hide lines», «Shaded», «Fill», «Realistic», «Ray Traced»;
3. «Parameters/Sun trajectory» – for settings of the solar system broadcast (coordinates/date/time);
4. «Shadows» – display of falling shadows;
5. Show the Visualize dialog box (3D only);
6. «Crop view» – On/Off. Does not appear in perspective;
7. «Display of cropping area boundaries» – On/Off. For setting the boundaries of the View to be transferred to the Sheet;
8. «Lock 3D View» (3D only) – to prevent changing the viewpoint on the View;

This project has been funded with support from the Erasmus+ Programme Key Action 2 Cooperation Partnerships for Higher Education (KA220-HED). This publication [communication] reflects the views only of the authors, and the Commission cannot be held responsible for any use which may be made of the information contained therein.

9. «Show hidden elements» – to restore previously hidden objects on the View;
10. «Temporarily hide/isolate» – to make it easier to work with individual elements;
11. «Temporary View Properties» – temporary use of templates with settings for displaying objects on the View;
12. «Show/Hide Analytical Model» – to display on the screen the load-bearing elements in the form of an analytical model;
13. «Select a set of displacements» (3D only) – to display objects in the current view, to which the «move elements» command has been applied (conditional displacement relative to the real location).

Object Data structure

Objects in Revit have the following hierarchy [3] (Fig.3.).

1. *Category* – type of group of objects («windows», «doors», etc.). Typically used to describe general graphics properties.
2. *Family* – type of objects in a category group, defined dividing the set of used parameters.

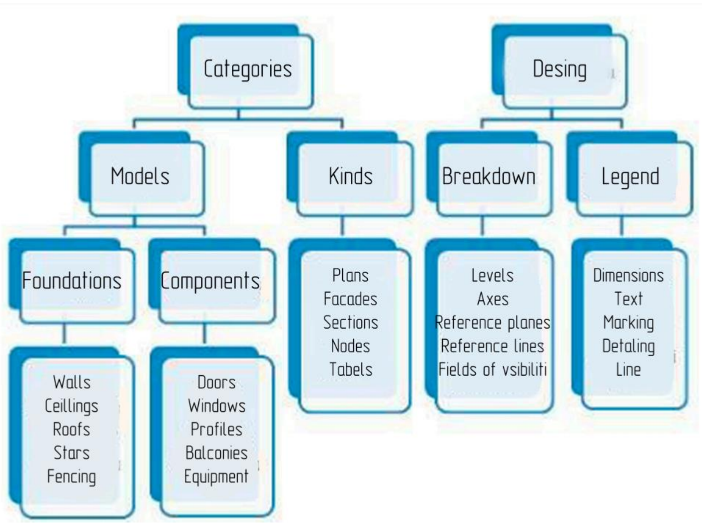

Fig. 3. Object Data structure

This project has been funded with support from the Erasmus+ Programme Key Action 2 Cooperation Partnerships for Higher Education (KA220-HED). This publication [communication] reflects the views only of the authors, and the Commission cannot be held responsible for any use which may be made of the information contained therein.

«Load Family» command (Insert tab, panel «Loading from Library»). Allows to load additional object descriptions into the project that are not included in the standard template.

3. *Types* – styles that define individual settings for parameters of elements of the same family.

The «Change Type» button in the «Properties» window allows you to go to mode for editing the parameters of the current object (wall, view, sheet...).

Work planes

The working plane is a virtual coordinate system in the plane in which drawing/editing commands are executed. It is automatically defined for each 'level' of the plan.

The reference plane is used as an auxiliary coordinate system, which is set manually (e.g. to work in the plane of a facade, section, wall surface or roof slope).

The «Reference Plane» command is active in Plan/Elevation views. Allows to specify with a segment the direction of a new «reference plane», orthogonal to the current view, its «working plane».

The «Set work plane» command is relevant when working in 3D views. Allows to switch to a reference plane either by a previously specified name or passing through the «Grid Axis...» or «Level...».

Show Work Plane command (tab «Architecture», «Work Plane» panel). Has On/Off states. Displaying the boundaries and internal lines of the «work plane» grid.

This project has been funded with support from the Erasmus+ Programme Key Action 2 Cooperation Partnerships for Higher Education (KA220-HED). This publication [communication] reflects the views only of the authors, and the Commission cannot be held responsible for any use which may be made of the information contained therein.

Drawing editing Modes

The «Binding Options» command allows to configure On/Off mode, automatic snaps, and step for tracked lengths/angles.

When creating or selecting Revit objects, temporary dimensions are tracked. They display both real dimensions (length, angle...) and in the form of indents from neighboring elements. Changes in size are carried out with a certain step specified in the program settings. The size snapping interval adjusts to the drawing dimensions in the views/screen and can be expanded by the user.

The following intervals are specified by default:

- size step for lengths – «1000 mm», «100 mm», «20 mm» and «5 mm»;
- dimension step for angular dimensions – «90°», «45°», «15°», «5°» and «1°».

If necessary, the values in the tracked dimensions can be entered from the keyboard.

Lines of the model

The model lines are individual segments – straight and arc, as a circle, ellipse or spline. All lines are created only in the current working plane (coordinate Z=0). They are mainly used as auxiliary tracking lines.

The «Model in Lines» command (Architecture tab, Model panel) loads the contextual tab «Change/Line Coordinates» with the Drawing and Line Styles panels.

The «Convert Lines» command is used to ensure that the selected «model lines» are only displayed in the current view.

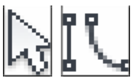

During the drawing/editing process, can specify a «line style» - thickened, thin, hidden...

This project has been funded with support from the Erasmus+ Programme Key Action 2 Cooperation Partnerships for Higher Education (KA220-HED). This publication [communication] reflects the views only of the authors, and the Commission cannot be held responsible for any use which may be made of the information contained therein.

When drawing lines in the «Parameters panel» you can specify: «Placement» plane (plan level), «Chain» (sequential drawing), «Offset» (from specified points), «Radius» (segment conjugations).

Colour, Weight, Line Type

The main elements of graphic design of drawing lines are their Colour, Weight (thickness) and Type (solid or set of strokes).

Areas, edges of objects can be shaded, filled with colour or gradient (transition from one colour to another), Material texture (in visualisation).

«Thin Lines» command controls the display of line weights on the screen.

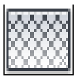

The «Fill patterns» command allows to create and/or edit a hatch type.

The «Material Characteristic Sets» command allows to set up physical characteristics of the material and visual (colour, texture, reflection, transparency...).

The «Line weights» command allows to set the correspondence between the used values of line weights in the programme and their thickness when printing (mm).

The «Line patterns» command allows to create and/or edit the type of lines – set the size and sequence of strokes.

This project has been funded with support from the Erasmus+ Programme Key Action 2 Cooperation Partnerships for Higher Education (KA220-HED). This publication [communication] reflects the views only of the authors, and the Commission cannot be held responsible for any use which may be made of the information contained therein.

Basic Editing Commands

In the process of working with «model lines» and objects, «basic» (standard for many programs) editing commands are widely used.

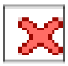

«Delete» command is equivalent to the Delete key for pre-selected objects.

«Move» command. After completing the selection of objects, two points are specified - the start and end points, with tracking of the direction (angle) and distance of transfer.

«Copy» command. In the «Parameter bar» sets the copying mode - On/Off. «Ortho» and «Multiple». As in the «Move» command, the start and end points are specified.

Additional commands «Copy» and «Paste with alignment to selected levels».

«Offset» command. Creates a «like» copy/transfer at a specified distance.

«Array» command. In the «Parameters panel» sets the array variant (linear/arc), number of elements, type of size indicated on the screen (between elements or total). The resulting group can be edited – the number of objects and sizes can be changed.

«Rotate» command. After selecting the items on the screen, you are required to specify the original (reference) angle and the new direction. In the «Parameter bar» can enable the «Copy» mode and request the point of the new «Center of rotation».

«Extend to Angle» command. Selects two linear elements that can form an angle.

This project has been funded with support from the Erasmus+ Programme Key Action 2 Cooperation Partnerships for Higher Education (KA220-HED). This publication [communication] reflects the views only of the authors, and the Commission cannot be held responsible for any use which may be made of the information contained therein.

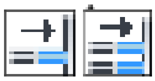

«Trim/Lengthen one/few elements» command.

After selecting the boundary lines to be trimmed (end the selection - Enter), the lines on the side that will remain are specified.

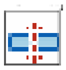

«Split element» command.

Allows to divide the element at the specified point into two parts.

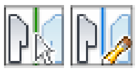

«Mirror-Select/Build Axis» commands.

In the first case, after finishing the selection of initial objects, the element that can serve as an axis is specified, in the second case, two points on the assumed symmetry axis are specified.

«Scale» command.

After selecting items, indicate with the cursor the point at the beginning and at the end of the «line», the change of size of which will be tracked, then one may enter/specify a new length.

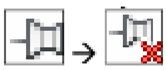

The «Attach» and «Unattach» commands.

A «pinned» object is not available for editing and changing the «properties».

This project has been funded with support from the Erasmus+ Programme Key Action 2 Cooperation Partnerships for Higher Education (KA220-HED). This publication [communication] reflects the views only of the authors, and the Commission cannot be held responsible for any use which may be made of the information contained therein.

2 Views

Viewport – a limited space, a window that displays elements of a drawing/model from a specified viewpoint, level of detail, and scale of design elements.

Revit views are the analogue of Autocad viewports. Unlike in Autocad, all work is initially performed on Views. «Project Manager» groups viewports according to their purpose - Plans, Facades, Sections, 3D views.

The «Default 3D view» and «Camera» commands activate the «3D views section» in the Project Manager and create an isometric or perspective view.

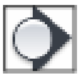

The «Section» command activates the «Sections (Node number)» section in the Project Manager and creates a view along the section line.

The «Facade» and «Level» commands allow to create additional views in the «Facades (Building Facade)», «Floor Plans» and «Ceiling Plans» sections.

The «Copy view» command allows to create additional copies of the view for drawing design.

This project has been funded with support from the Erasmus+ Programme Key Action 2 Cooperation Partnerships for Higher Education (KA220-HED). This publication [communication] reflects the views only of the authors, and the Commission cannot be held responsible for any use which may be made of the information contained therein.

3 Level

Level – an object used to set the floor elevation. It is available on facade views. When creating a level, the corresponding plan, ceiling and construction views are automatically created.

Floor plans are considered to be the main type of architectural and construction drawings. «Levels» allow you to specify heights for floor plan views and for spatial referencing of objects (Fig. 4.).

By default, the «Architectural» template has two «Levels» - at «0.000» and «4000» and their corresponding Plan/Ceiling Views. It is possible to create/change the level height mark on the facade views.

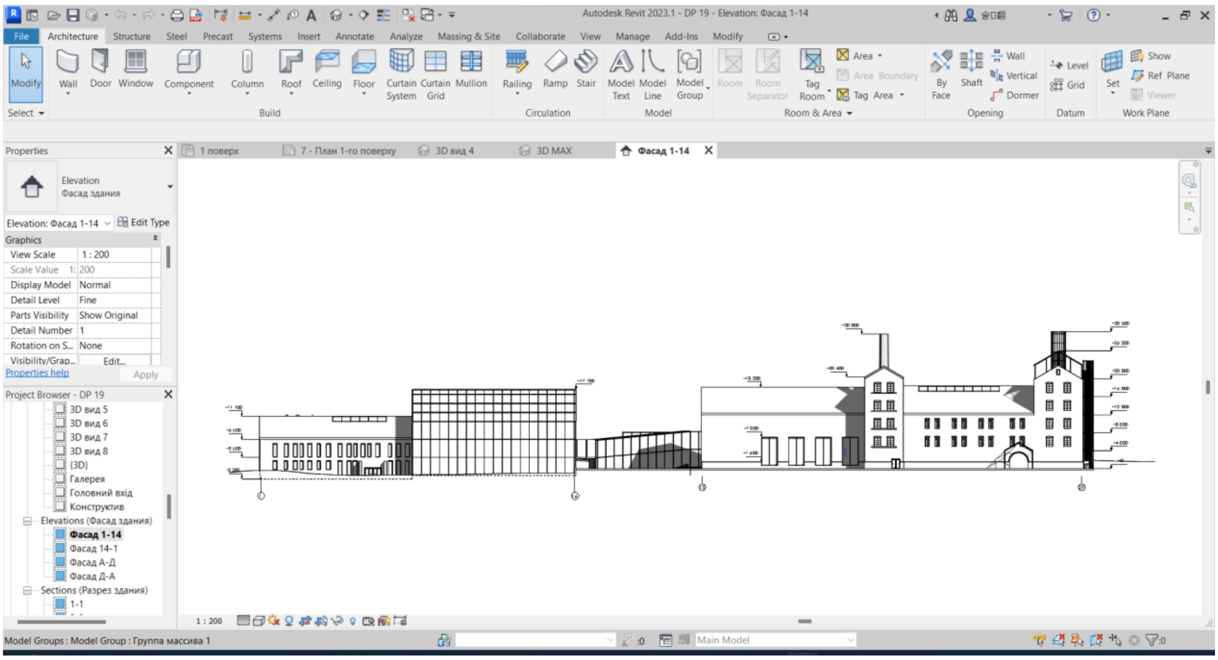

Fig. 4. Levels on the Facades tab [7]

This project has been funded with support from the Erasmus+ Programme Key Action 2 Cooperation Partnerships for Higher Education (KA220-HED). This publication [communication] reflects the views only of the authors, and the Commission cannot be held responsible for any use which may be made of the information contained therein.

4 Axes

Axes – in drawings are labelled «centre» lines used to anchor (centre, edge or offset) the structures of a building (foundations, walls, columns). Usually a rectangular grid of axes is used, but a radial grid is also possible, as well as individual «randomly» orientated or «broken» lines (Fig. 5.).

Axes marks - graphic design of an axis line by a circle with text in the centre.

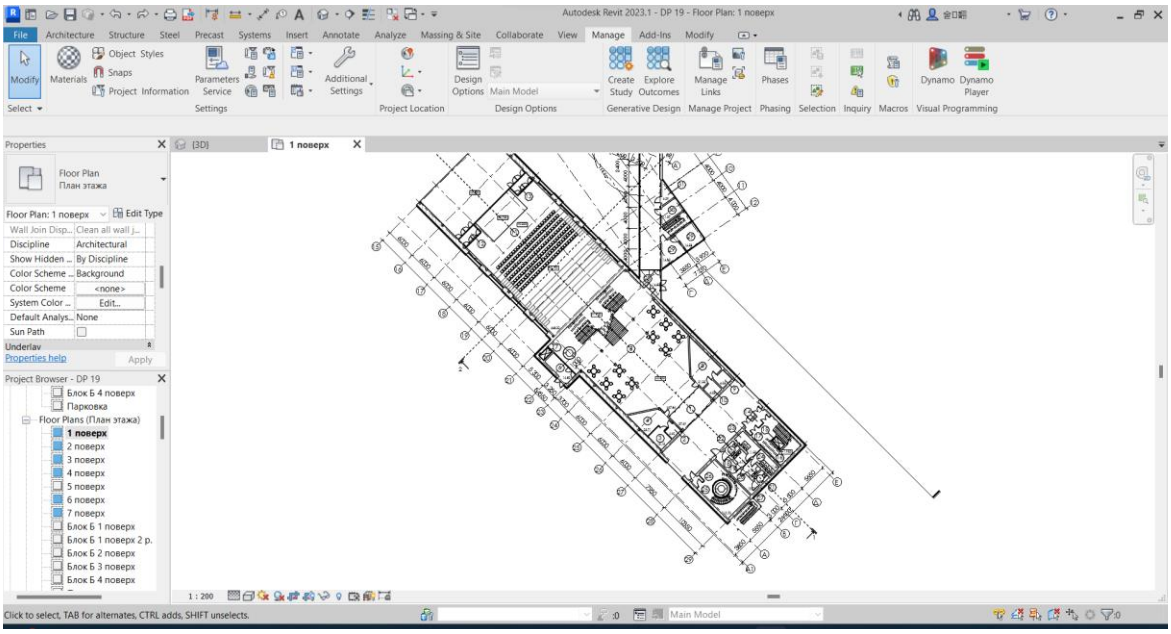

Fig. 5. Axes, columns and dimensions on the plan [7]

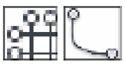

Command Grid. The axis line can consist of one or more segments, straight or arc-shaped. The size of the axis mark depends on the view scale. It is possible to rename the axis in the «Properties» window.

The control fields/nodes allow you to switch marker display on/off, to build an endmark, to extend and to align centrelines.

This project has been funded with support from the Erasmus+ Programme Key Action 2 Cooperation Partnerships for Higher Education (KA220-HED). This publication [communication] reflects the views only of the authors, and the Commission cannot be held responsible for any use which may be made of the information contained therein.

5 Architectural constructions

Construction is one of the main tectonic and expressive means of architecture. These are systems for cutting the walls of a building into separate elements – large panels or large blocks, shapes, sizes and patterns of filling openings, translucent fences – geometric surfaces of multi-span roofs, etc.

Architectural constructions are a comprehensive characterization of the structural solution of a building and its parts by material, products, structure, constituting a particular part of the building, means of protection of cutting actions, construction technology, taking into account all physical and technical factors [8].

5.1 Walls

A wall is usually a vertical supporting or enclosing structure that separates the boundaries of a room (Fig. 6.) [8].

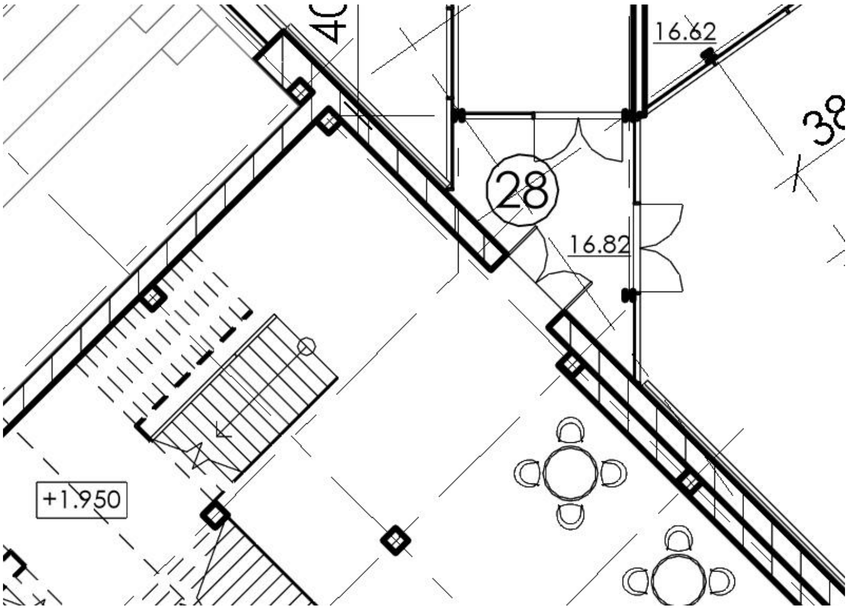

Fig. 6. Part of the drawing of the plan with walls [7]

This project has been funded with support from the Erasmus+ Programme Key Action 2 Cooperation Partnerships for Higher Education (KA220-HED). This publication [communication] reflects the views only of the authors, and the Commission cannot be held responsible for any use which may be made of the information contained therein.

Revit uses two types of walls (and commands for them) – «Wall: partition» and «Wall: load-bearing». Any type of walls and their combinations can be used for architectural and construction drawings and 3D models, as a common set of families and their types/styles is used, and the «load-bearing structures» parameter can always be On/Off in «Properties». The main difference is the additional commands for reinforcing load-bearing walls.

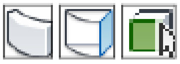

The «Wall - Partition/Bearing» command. Allows using standard drawing commands to build straight or curved wall segments.

During construction/editing it is required to control the following values in the «Parameter bar» and/or in «Properties».

- «Level»/ «Base dependence» - specifies the level from which the construction is performed. By default - the level of the current plan.
- Construction direction, up or down ('Parameter bar'). By default it can be «Depth» (down). It is recommended to set «Height» (up). Switching the values will recalculate the offsets in the «Properties» window.
- «Top dependency» - usually set as «Not attached», but it is possible to be attached to a higher level, with an offset from it.
- «Not Attached Height» - for walls with heights that are not referenced to the elevation of the above lying «level». It is recommended to specify the full height of the wall in the structure, rather than repeating its construction at each floor.
- «Offset from below» (from the construction level) - usually used to model the «basement» section of walls for 3D.
- «Reference line» - by «Wall centreline» or «Finish surface: External/Internal» (external boundaries).

This project has been funded with support from the Erasmus+ Programme Key Action 2 Cooperation Partnerships for Higher Education (KA220-HED). This publication [communication] reflects the views only of the authors, and the Commission cannot be held responsible for any use which may be made of the information contained therein.

By default, the «Architectural» template offers to use a set of walls of three types of families.

- «Basic» - the main type of walls used, monolithic or multilayer (in thickness).
- «Stained glass» - curtain walls. Mainly used for modelling exterior glazing of facades and storefronts. Can also be used for modelling windows with non-standard aperture shape and binding grid.
- «Composite» - multi-layered (in height). Represents a set of types of «base» walls located on top of each other.

By default, the walls have a rectangular profile (facade), which can be changed if necessary.

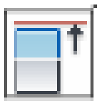

If there are elements in the model that limit the walls from top/bottom (roof, terrain, floor slab), the command «Join Top/Base» is used.

The «Wall Profile» command allows to manually edit the geometry of the outer contour.

5.2 *Columns, struts, beams*

Column - a vertical support working in compression.

Strut - a building element connecting two nodes of a frame, truss, etc. It is located on the diagonal of a closed contour and provides structural rigidity.

Beam - a horizontal or inclined beam working mainly in bending [8].

This project has been funded with support from the Erasmus+ Programme Key Action 2 Cooperation Partnerships for Higher Education (KA220-HED). This publication [communication] reflects the views only of the authors, and the Commission cannot be held responsible for any use which may be made of the information contained therein.

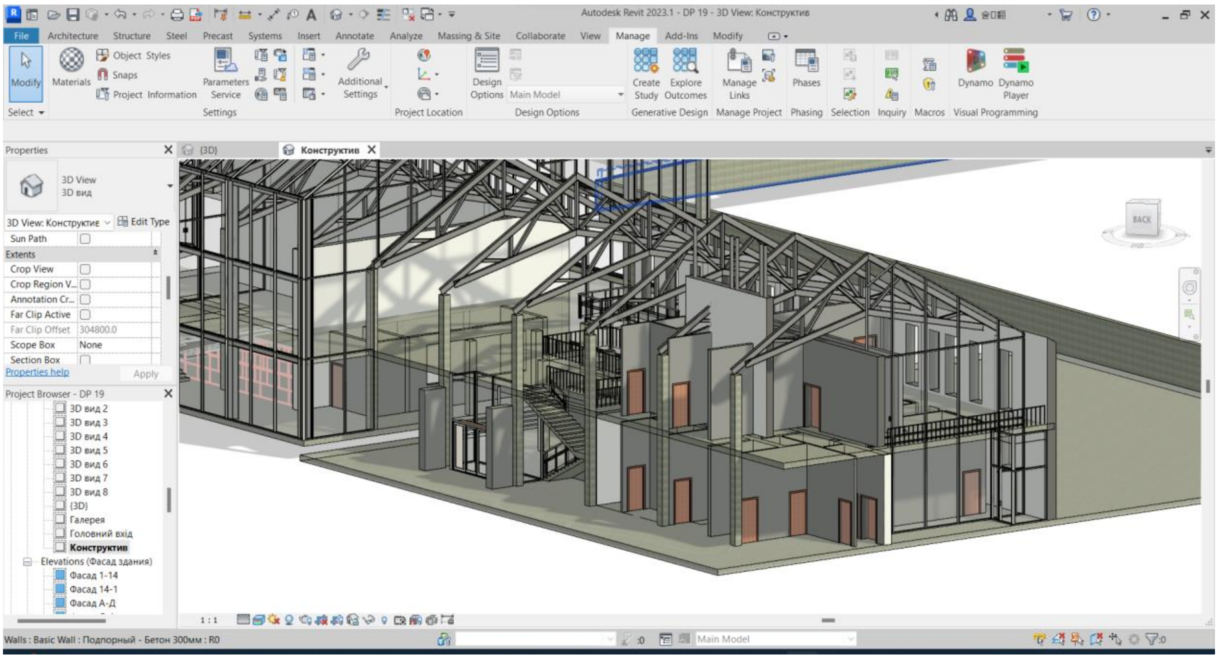

Fig. 7. Design of structural elements [7]

In the Revit interface, on the «Architectural» tab, only one type of linear load-bearing (and architectural) structure is available – «Column». To access the «Beam» and «Slope» and the structures based on them («Truss» and «Beam System»), it is necessary to go to the «Construction» tab (Fig. 7.).

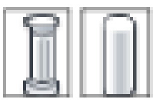

Command Column. «Supporting» or «Architectural».

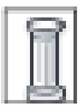

«Architectural» is the default «rectangular section column». Always inserted vertically. The insertion point is specified.

This project has been funded with support from the Erasmus+ Programme Key Action 2 Cooperation Partnerships for Higher Education (KA220-HED). This publication [communication] reflects the views only of the authors, and the Commission cannot be held responsible for any use which may be made of the information contained therein.

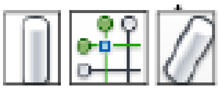

«Supporting». The column can be either vertical or inclined. «Vertical» columns can be automatically arranged according to the intersection points of the centrelines. When inserting an «Inclined» column, the start and end points are specified (in the plan view), and in the «Parameters panel» – the plan «levels» and offsets from them.

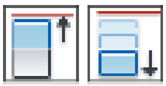

Columns, like walls, can use the Join/Disconnect Top/Base commands.

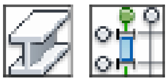

Beam commands. Beams can be automatically built/placed along axis grid lines (if there are columns previously placed along the same grid). Unlike «columns» and «struts», the shape of a «beam» can be defined not only as a rectilinear segment, but also as an arc or spline curve.

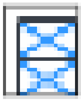

Scatter commands. When the command is activated in the «Parameter bar», the levels of the start and end anchorages and their offsets are specified.

The «Truss» command allows to insert into the model structure in the form of a truss. If necessary, the shape of the upper/lower belt and the structure of the internal connections can be quickly changed.

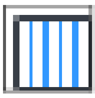

The «Beam system» command allows to build a structure in the form of parallel beams inside a given contour.

This project has been funded with support from the Erasmus+ Programme Key Action 2 Cooperation Partnerships for Higher Education (KA220-HED). This publication [communication] reflects the views only of the authors, and the Commission cannot be held responsible for any use which may be made of the information contained therein.

5.3 Doors, windows

Window is a structural element of a building, forming a glazed opening in the wall, which serves for the entry of light into the room and ventilation. It consists of the elements of a frame, bindings and glazing. It may have platbands, sill and cornice constructions, lining of wall jambs/sides in the opening.

Roof skylight – basically a hermetically sealed «window» in the gable/floor plane, designed for light access and ventilation.

Door – an opening in a wall for entering and leaving a room, fitted with sashes.

Doorway – an opening in walls/partitions/floors not filled as in windows/doors.

In Revit, windows and doors are rigidly tied to walls. The wall thickness offset can only be set in the window type settings. The door leaf is rigidly bound to the outer boundary of the wall at the family description level.

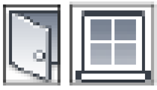

«Door/Window» commands. In the «Properties» window, select the family and type describing the shape and dimensions, specify «bottom bar height». Use tracking dimensions for exact placement when inserting/editing. Use the control arrows to specify the outside of the wall for the selected object. For doors, also specify the hinge side/opening direction (clockwise or anti-clockwise).

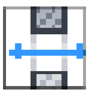

The «In wall» command. By default, only the rectangular shape of the 'opening' can be set in the wall. In «Properties» sets «Base dependence» (floor plan level), «height», offset «bottom» or «top».

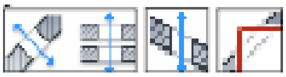

The commands «Edge», «Shaft», «Vertical» allow to build apertures in floor, ceiling or roof slabs.

This project has been funded with support from the Erasmus+ Programme Key Action 2 Cooperation Partnerships for Higher Education (KA220-HED). This publication [communication] reflects the views only of the authors, and the Commission cannot be held responsible for any use which may be made of the information contained therein.

5.4 Staircases

Stairs – a functional and structural element providing vertical connections for pedestrians.

Ramp – a gentle sloping platform (slope, ramp) connecting two horizontal surfaces of different heights, usually designed for wheeled vehicles.

A staircase in Revit is one of the most complex types of construction. It can be «assembled» both from individual components (span, platform) and built from a sketch.

Staircase command. When building stairs in the «Parameters panel» specifies «anchoring» (centre or edge) and «current width of the rung». In the «Properties» window the stair height (lower and upper «level», offsets) and the number of steps are set. The dimensions of the stair structures, stair height restrictions are set in the description of the type/style.

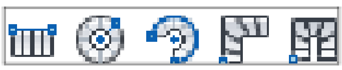

The main component of the staircase is the «Span». The shape of the span can be «Straight», «Spiral», etc.

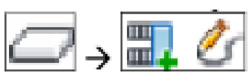

Additional component «Ramp». Used in multi-span staircases.

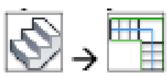

The «Stairs - By sketch» command. Allows to build the whole staircase by sketch.

This project has been funded with support from the Erasmus+ Programme Key Action 2 Cooperation Partnerships for Higher Education (KA220-HED). This publication [communication] reflects the views only of the authors, and the Commission cannot be held responsible for any use which may be made of the information contained therein.

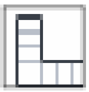

«Border» – construction of separate contour lines of «left» and «right» edge of the march;

«Stair tread» – construction of step lines connecting the opposite edges/borders of the march;

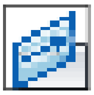

«Direction of the march» - drawing a line along which will pass the arrow indicating the «direction» of the march ascent;

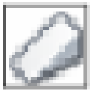

The ramp command. Unlike a staircase, it has restrictions on the slope and length of the «march» (more sloping) specified in the style/type.

Usually the staircase on a porch/terrace has a side «barrier» that fills the gap under the rung/platform. There are two main ways to form such a «partition».

Railings are railings for stairs, balconies, terraces. They are usually about one metre high. As a rule, they consist of posts, longitudinal supporting structures, balusters and handrail between them.

The command «Railing. Trajectory sketch». The railing will be built on the current plan level.

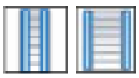

The command «Railing - Place on base». Allows to restore the guardrail on the stairs.

This project has been funded with support from the Erasmus+ Programme Key Action 2 Cooperation Partnerships for Higher Education (KA220-HED). This publication [communication] reflects the views only of the authors, and the Commission cannot be held responsible for any use which may be made of the information contained therein.

5.5 Overlap

Overlap – structural elements that divide the interior space of a building into floors and serve to absorb load and transfer it to walls or individual supports.

Ceiling – usually the lower surface of the overlap or covering of a building, limiting the room from above, may be supplemented with ‘suspended’ structural and finishing elements.

Second light (in architecture) – a room with completely or partially missing ceiling overlaps on one or several floors.

Revit uses two types of overlaps (and their commands) – «Overlap: Architectural» and «Overlap: Load-bearing». For architectural drawings (plans, sections) and 3D models, either option is suitable, as the same set of types/styles is used, and the «load-bearing structures» parameter can always be switched On/Off in Properties. The main difference is the additional commands for load-bearing plates associated with reinforcement.

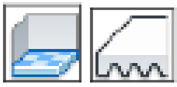

The command «Overlap: architectural/substantial». The floor sketch is built on the plan view. In the «Properties» of the floor/ceiling overlap slabs can specify type, plan level and offset from it.

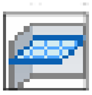

«Ceiling» command. The ceiling is displayed in «ceiling plans» and 3D views.

A slope line/arrow can be specified for floor/ceiling slabs for the entire surface.

5.6 Roof

Roof – the upper structure of a building that protects it from rain, snow and sun.

Slope – specified in degrees or the ratio of the difference in height of two points to the distance between them. Describes the angle of slope of a gable.

This project has been funded with support from the Erasmus+ Programme Key Action 2 Cooperation Partnerships for Higher Education (KA220-HED). This publication [communication] reflects the views only of the authors, and the Commission cannot be held responsible for any use which may be made of the information contained therein.

Co-funded by the Erasmus+ Programme of the European Union

Pediment – the absence of a slope on the specified side of the roof. The shape is given/limited by the side slopes. The space under the roof on the gable side is usually filled/limited by a wall. *Overhang* – a roof slope projecting outwards beyond the wall boundaries.

Gutter – a channel for collecting and draining water.

Mansard roof – a roof with gable slopes of broken shape, providing for the interior of the side and upper enclosure (partial or complete replacement of walls and ceiling overlaps). It is intended to provide maximum volume for interior spaces under the roof.

The roof in Revit is an architectural element. Its main purpose is to show the shape/thickness of the slopes and to serve as a boundary for trimming walls. If a diagram/model of beams and rafters is required, it is created manually, from individual linear structures – columns, beamsand struts or groups of them – trusses and beam systems.

Three commands are mainly used to build a roof.

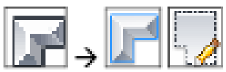

Roof contour command. It is used in roofs with a constant slope. The thickness of the slope is postponed from the specified level upwards.

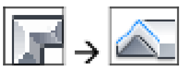

The extrude roof command. It is mainly used for modelling slopes with variable slopes.

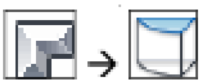

The roof by edge command. Allows to build roof slope along the edge of the forming element.

This project has been funded with support from the Erasmus+ Programme Key Action 2 Cooperation Partnerships for Higher Education (KA220-HED). This publication [communication] reflects the views only of the authors, and the Commission cannot be held responsible for any use which may be made of the information contained therein.

6 Visualisation

Visualisation – a method of presenting information in the form of an optical image. In architecture – graphical representation of the designed building and its surrounding area.

Visual styles – settings for displaying elements, lighting and shadows.

Ray tracing – technology of building an image of three-dimensional models, in which the reverse trajectory of ray propagation (from the screen to the source – reflection effect) is tracked.

Visual styles are used to quickly present the model on the screen in different graphics styles (Fig. 8., 9.). They are set in the View Control Panel.

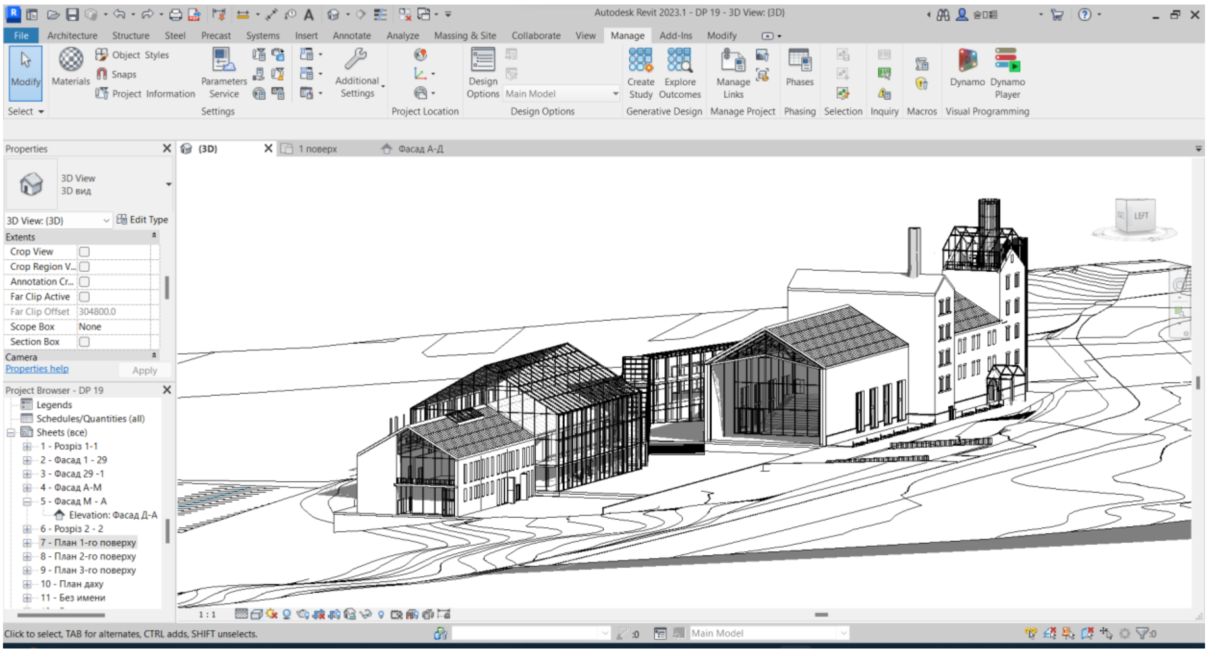

Fig. 8. Hidden line style [7]

This project has been funded with support from the Erasmus+ Programme Key Action 2 Cooperation Partnerships for Higher Education (KA220-HED). This publication [communication] reflects the views only of the authors, and the Commission cannot be held responsible for any use which may be made of the information contained therein.

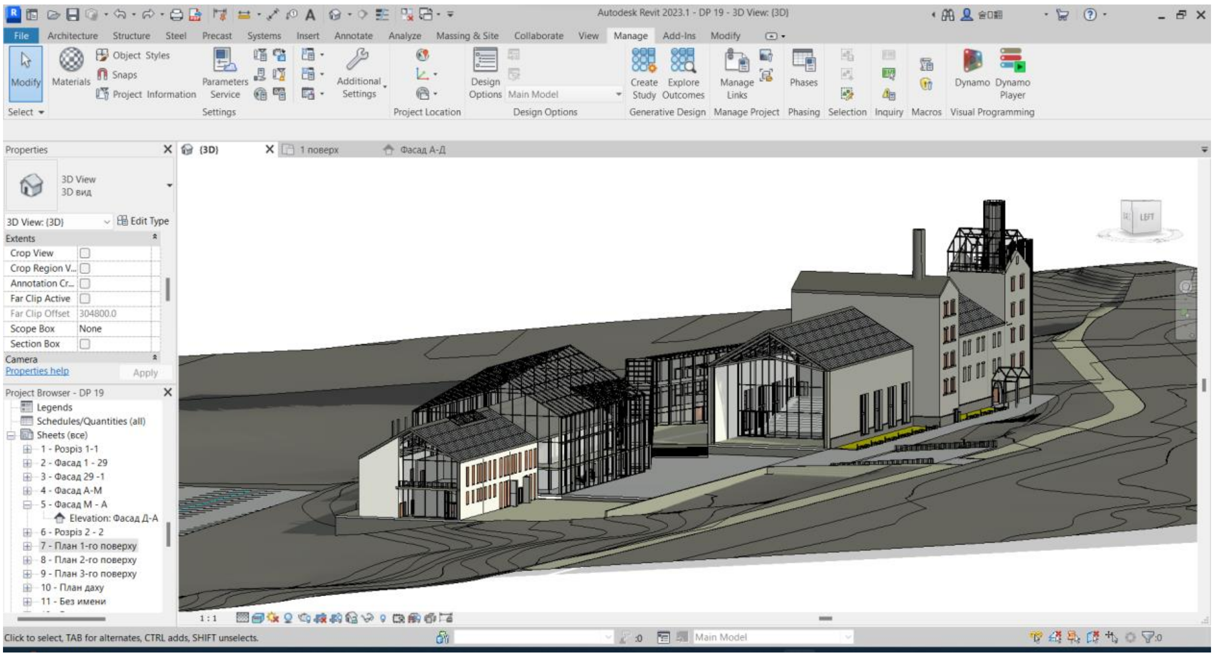

Fig. 9. Realistic style [7]

Frame. Models with all edges and lines.

Hidden line. All edges and lines, except those that are hidden, are displayed. The ‘transparency’ of the objects material is taken into account.

Tinted. Conditional lighting with a standard light source. Materials are displayed in a common colour, without texture mapping. The transparency of the material is taken into account.

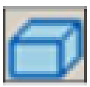

Fill. Uniformly fill objects. Materials are displayed in a common colour, without drawing texture. The transparency of the material is taken into account.

This project has been funded with support from the Erasmus+ Programme Key Action 2 Cooperation Partnerships for Higher Education (KA220-HED). This publication [communication] reflects the views only of the authors, and the Commission cannot be held responsible for any use which may be made of the information contained therein.

Realistic. Conditional lighting with standard light source. Material texture display. Material transparency is taken into account.

Ray tracing. The most realistic (and resource-intensive) visual style. More accurate visualisation of transparency and lighting. If material settings allow, objects can reflect each other.

Materials

Paint command. Allows to apply the library material for visualisation to a separate, specified facet of the object (Fig. 10.).

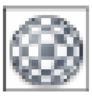

The «Materials» command. Opens a window with a standard library of materials. Allows to create new materials using bitmap images for colour and texture settings, reflection, transparency, self-glow, extrusion and other effects.

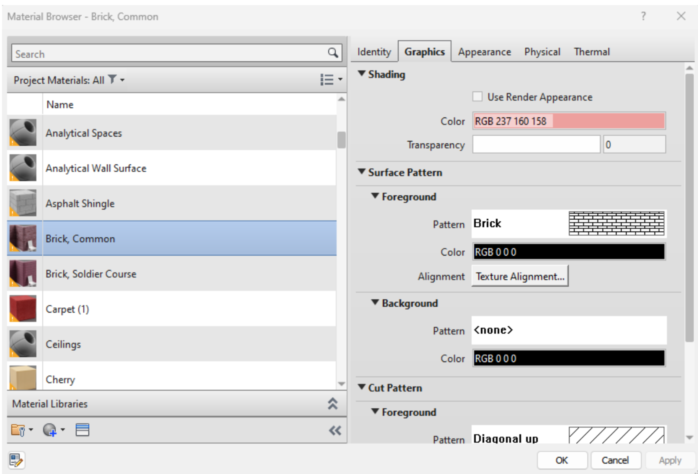

Fig. 10. Materials [7]

This project has been funded with support from the Erasmus+ Programme Key Action 2 Cooperation Partnerships for Higher Education (KA220-HED). This publication [communication] reflects the views only of the authors, and the Commission cannot be held responsible for any use which may be made of the information contained therein.

Light sources

By default, the standard light source (for the visual styles tinted, realistic and trace) is located «top, right» (relative to the screen). If necessary, it is possible to switch on solar lighting and arrange various variants of artificial light sources – point, linear, area.

The «Graphics display parameters» command. Allows setting the independent remote light source (sun) in the current view.

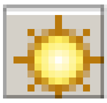

«Sun Trajectory».Allows using the ‘sun trajectory’ tool on the screen to fine-tune the sunlight depending on the time of year/day.

In Revit it is necessary to prepare for visualisation from the very beginning of work on the project. In the process of model creation and object settings it is required to select the «material» of construction taking into account the visualisation, to divide the surfaces of walls, roofs, floors and other elements into areas with different materials, to adjust natural lighting and to arrange artificial light sources (Fig. 13.).

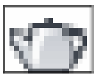

Visualisation command. Available only in 3D views. Performs «rendering» (toning) of the 3D model according to the materials and light sources used (Fig. 11., 12.).

This project has been funded with support from the Erasmus+ Programme Key Action 2 Cooperation Partnerships for Higher Education (KA220-HED). This publication [communication] reflects the views only of the authors, and the Commission cannot be held responsible for any use which may be made of the information contained therein.

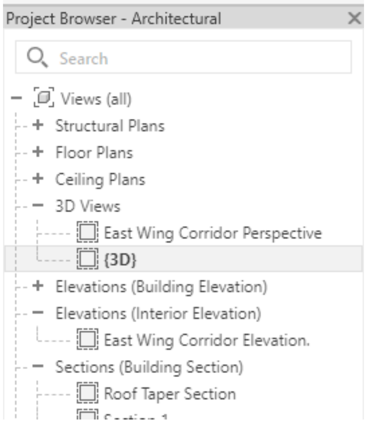

Fig. 11. 3D views in the project manager

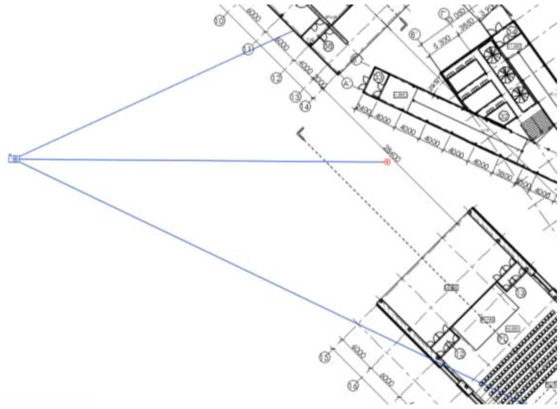

Fig.12. Installing a camera on a floor plan

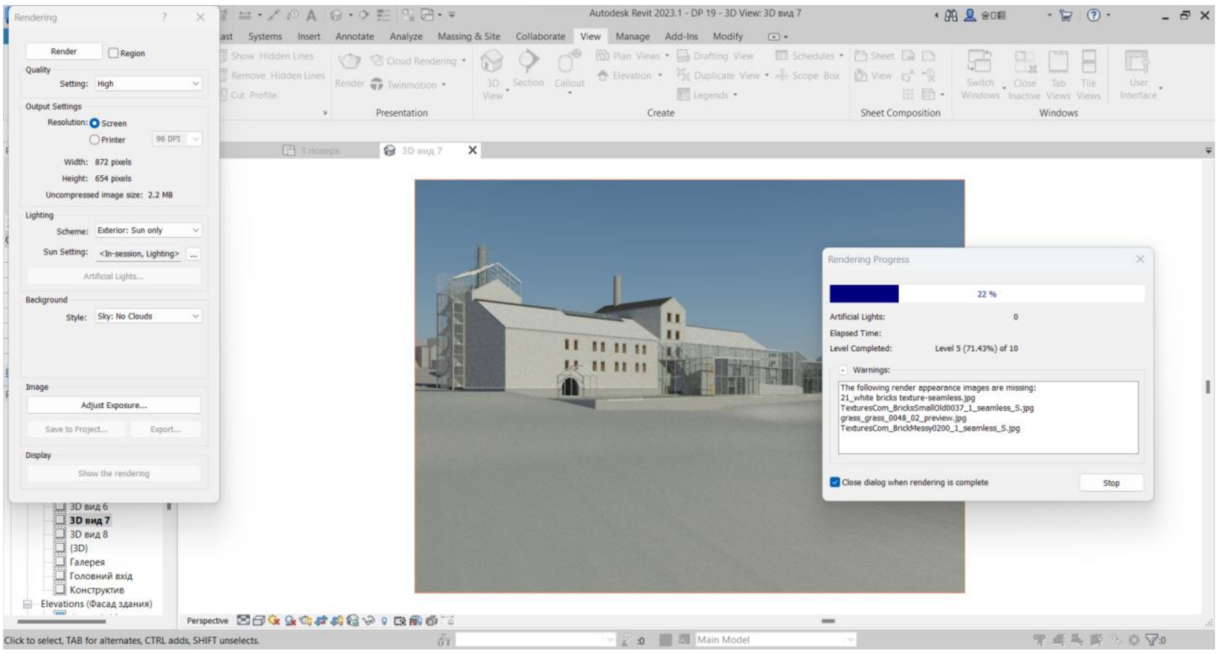

Fig. 13. The rendering process in Autodesk Revit [7]

This project has been funded with support from the Erasmus+ Programme Key Action 2 Cooperation Partnerships for Higher Education (KA220-HED). This publication [communication] reflects the views only of the authors, and the Commission cannot be held responsible for any use which may be made of the information contained therein.

7 Fasade, section

Facade – the exterior, front face of a building, and a drawing of the orthogonal projection of the building onto a vertical plane. The default options are «East», «West», «North» and «South» (Fig. 14.).

Section – visual dissection of an object by one or more planes. In architecture it is used for conventional representation of the configuration of architectural details, internal spaces on the drawing and characterizes the shape (Fig. 15.).

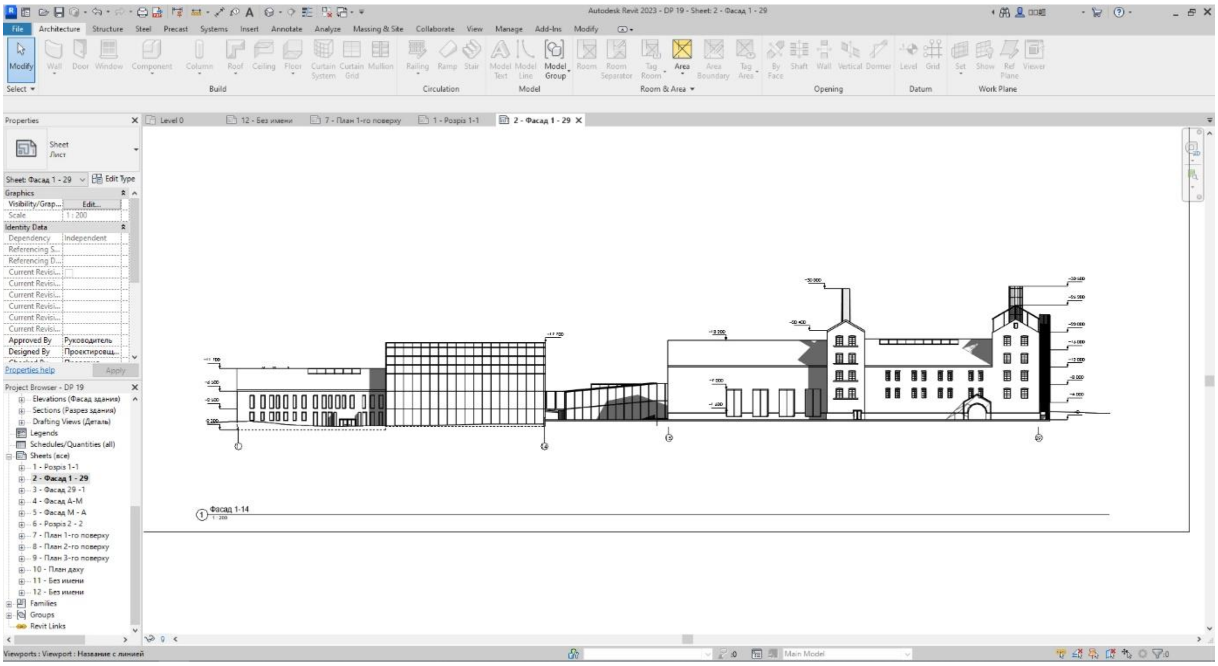

Fig. 14. Facade in Autodesk Revit [7]

This project has been funded with support from the Erasmus+ Programme Key Action 2 Cooperation Partnerships for Higher Education (KA220-HED). This publication [communication] reflects the views only of the authors, and the Commission cannot be held responsible for any use which may be made of the information contained therein.

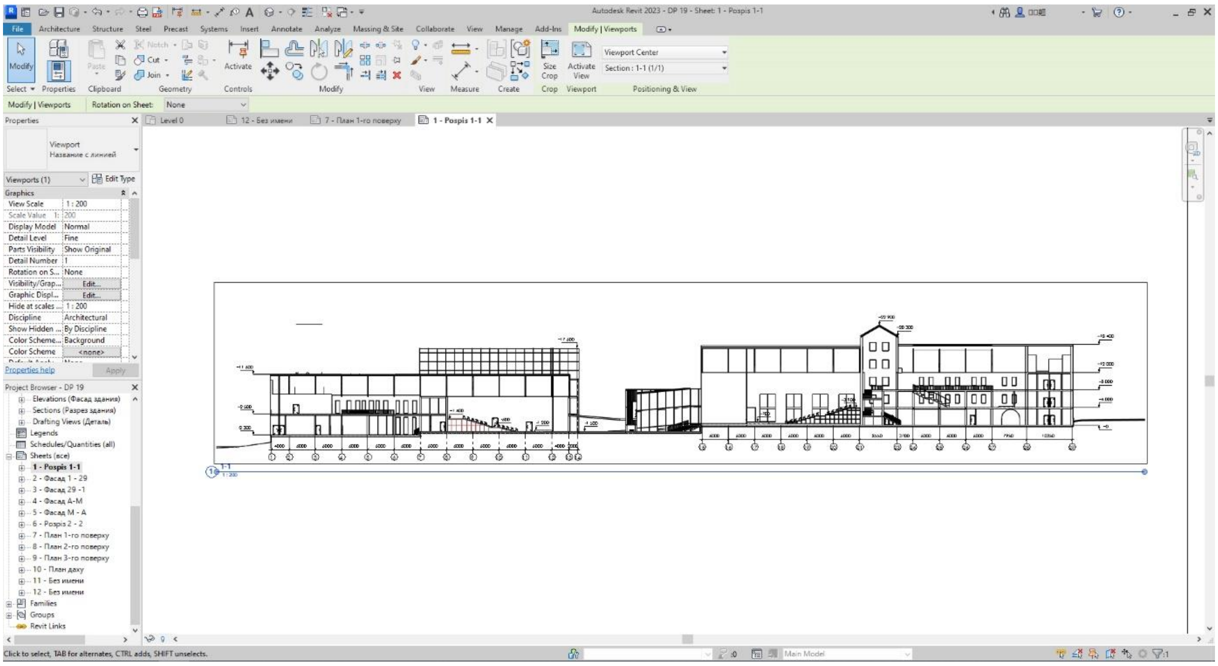

Fig. 15. Section in Autodesk Revit [7]

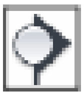

Cut command. The cut line is drawn on the plan view. If the cut line does not cross the structure (passes outside), the resulting view is similar to the facade.

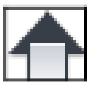

Facade command. Builds an additional facade marker on the plan view. Creates a new view in the «Project Manager» in the «Facades» section.

This project has been funded with support from the Erasmus+ Programme Key Action 2 Cooperation Partnerships for Higher Education (KA220-HED). This publication [communication] reflects the views only of the authors, and the Commission cannot be held responsible for any use which may be made of the information contained therein.

8 Text

Text in Revit is used as an independent object in the design of drawings and sheets, as well as part of dimensional elements, stamps, marks, explications, and notations (Fig. 16.).

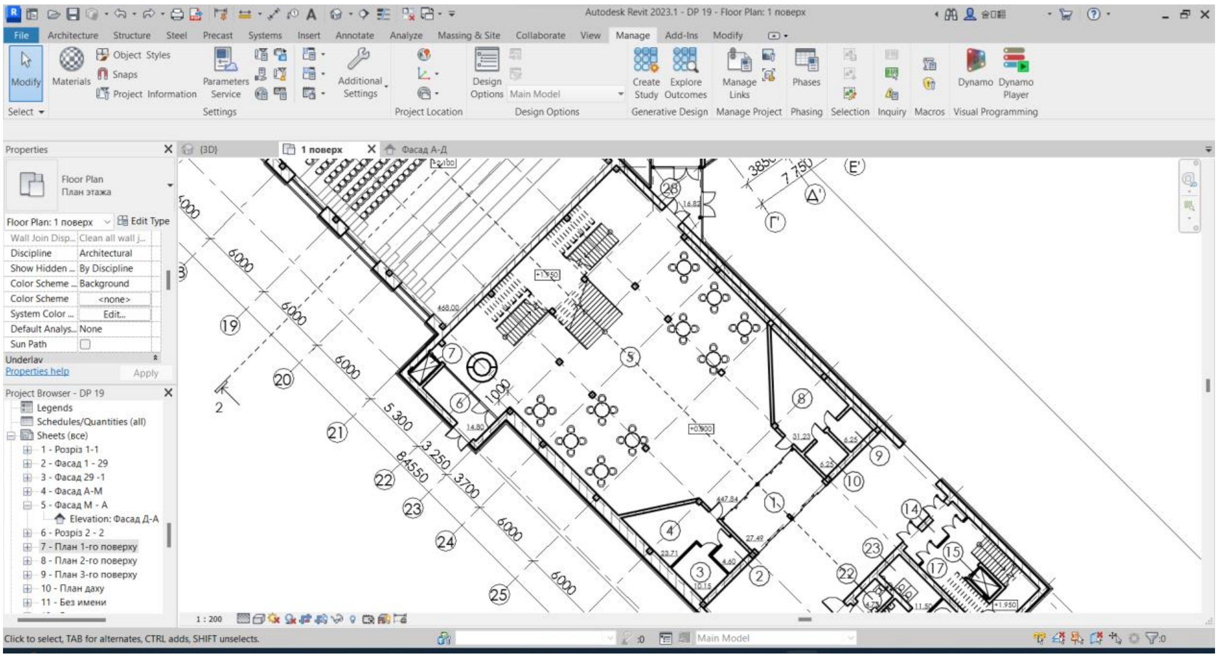

Fig. 16. Part of the ground floor plan with specification [7]

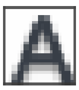

Text command. Specify an entry point or width limits (with a frame). In the first case, the text has no line length restrictions, in the second case, it automatically moves the word beyond the boundary to a new line.

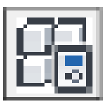

Parameters such as font, height, character proportions are set by the text type/style.

This project has been funded with support from the Erasmus+ Programme Key Action 2 Cooperation Partnerships for Higher Education (KA220-HED). This publication [communication] reflects the views only of the authors, and the Commission cannot be held responsible for any use which may be made of the information contained therein.

9 Dimensions

Dimensions are the elements that define dimensions and distances in project views. There are two types of dimensions in Revit: temporary and permanent.

Temporary dimensions are created automatically when components are placed. They track object dimensions and indents. They are displayed while the object is being built or when the object is selected. They can be converted to permanent dimensions.

Permanent dimensions are created for drawing design.

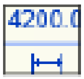

The size in the drawing can be obtained by converting the temporary «tracking size» (click the size icon below the text with the cursor) or by calling the corresponding command.

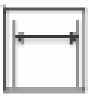

«Linear» – always parallel to either the horizontal or vertical axis of the current view. Placed between two or more points.

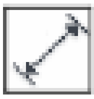

«Parallel» is a basic dimension on drawings. It is attached to the faces of objects. It is drawn parallel to the specified points, object boundaries like wall or doorway.

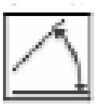

«Angle». It is required to specify two lines that form an angle. For walls in the «Parameters panel» you can select the anchoring – axis or boundaries.

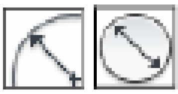

«Radial» and «Diameter». It is required to specify an arc or circle – a line of a model, a contour, a wall. «Radius» and «Diameter» use different arrow options.

This project has been funded with support from the Erasmus+ Programme Key Action 2 Cooperation Partnerships for Higher Education (KA220-HED). This publication [communication] reflects the views only of the authors, and the Commission cannot be held responsible for any use which may be made of the information contained therein.

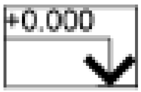

«Height mark». Used on facade/section views.

Basic parameters of the graphic:

- «Emphasis type» – set «Line»;
- «Serif» – set «Diagonal, 3mm» (for linear types of size) or «Blackened arrow, 30 degrees» (for radiuses, diameters, angles);
- «Weight of serif lines» – it is recommended to set «1»;
- «Dimensional/auxiliary line extensions» – it is recommended to set «1.5 mm»;
- Control of the auxiliary (dependent) line – select the option «Indent from element» (from the anchor point/boundary) or «From dimension line» (to set a uniform size of the dependent lines). In the next line set their values to «1.5-3 mm».

This project has been funded with support from the Erasmus+ Programme Key Action 2 Cooperation Partnerships for Higher Education (KA220-HED). This publication [communication] reflects the views only of the authors, and the Commission cannot be held responsible for any use which may be made of the information contained therein.

10 Sheets

Paper size is the standardized size of a sheet of paper. The international standard for paper sizes, ISO 216, is based on the metric system of measures.

Stamp – the design of a sheet of paper in the form of a frame and tables describing the drawing.

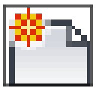

The «Sheet» command (View tab, Sheet Composition panel) or the «New sheet...» command (Fig. 17., 18.).

When preparing drawings for printing, created and designed views (plans, facades, sections, 3D) are «transferred» to Sheets:

1) switch to the Sheet created in the «Project Manager»;

2) select «Add View...» in the «context menu» of the Sheet or «drag and drop» the required View from the «Project Manager».

The size of the View window transferred to the Sheet depends on its scale (except for perspective) and trim borders. The shape and size of the trim borders can be adjusted both before and after the transfer to the Sheet (Fig. 19., 20.).

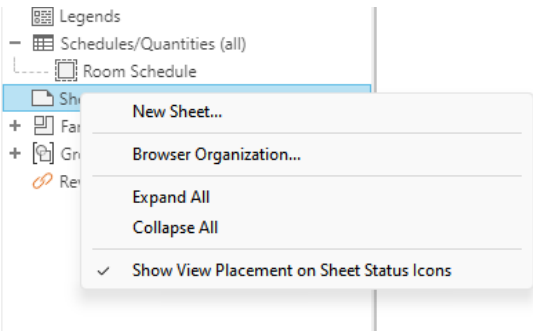

Fig. 17. Sheets tab

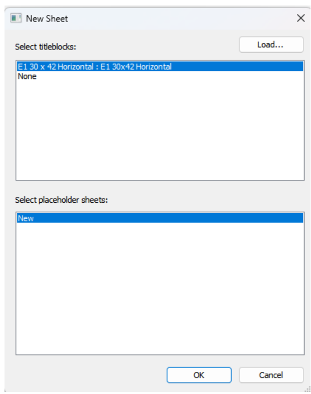

Fig.18. The window for creating a new sheet

This project has been funded with support from the Erasmus+ Programme Key Action 2 Cooperation Partnerships for Higher Education (KA220-HED). This publication [communication] reflects the views only of the authors, and the Commission cannot be held responsible for any use which may be made of the information contained therein.

Fig. 19. A blank sheet

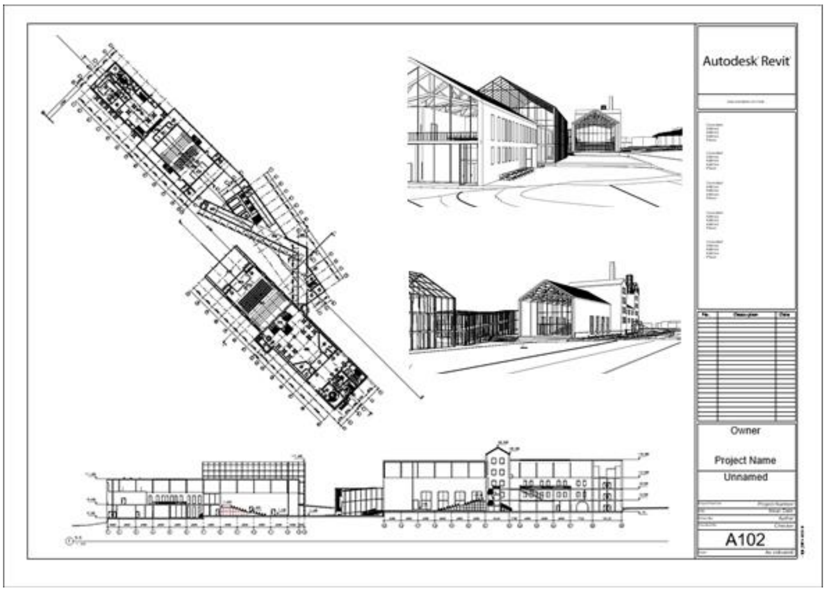

Fig. 20. Completed sheet

This project has been funded with support from the Erasmus+ Programme Key Action 2 Cooperation Partnerships for Higher Education (KA220-HED). This publication [communication] reflects the views only of the authors, and the Commission cannot be held responsible for any use which may be made of the information contained therein.

11 Task

The purpose of the design task is to design an individual residential building. In the process of designing, the student must complete the project of a manor house as an expressive three-dimensional composition and a comfortable living environment, taking into account the requirements for the organisation of living space.

The main tasks of the design exercise are as follows:

- development of a residential building of a manor type, based on the requirements of the design task;
- taking into account the requirements of compositional balance, structural stability and functional feasibility when designing an object;
- study of building codes and regulations used in the design of low-rise residential buildings.

The project should provide for:

- development of the space-planning structure of a residential building taking into account a certain composition of premises, the author's concept, considerations of convenience, regulatory requirements for insolation, lighting, fire evacuation;
- selection of an appropriate structural system to ensure the stability of the building, reduce material consumption and heat loss during its operation;
- placement of the main and auxiliary buildings and organisation of the territory, taking into account the current planning and regulatory requirements.

It is planned to build a two- or three-storey building with a height of floor height of at least 2.8 m (preferably 3.0 - 3.6 m), with a technical underground (if necessary, a basement) and an attic (in case of a pitched roof).

The underground (1.9 - 2.50 metres high) is intended for technical rooms (water supply network entry point) and for the passage of utilities (heating, water supply and sewerage

This project has been funded with support from the Erasmus+ Programme Key Action 2 Cooperation Partnerships for Higher Education (KA220-HED). This publication [communication] reflects the views only of the authors, and the Commission cannot be held responsible for any use which may be made of the information contained therein.

networks). The basement (with a height not lower than the above-ground floors) can be designed to accommodate rooms with a recreational function, as well as utility rooms and storerooms. The attic is designed to protect the premises from overheating and overcooling. It is permissible to arrange an attic floor with residential premises.

Vestibules with a depth of at least 1.4 m should be provided at all external entrances to the building. The floor level of the premises at the entrance to the building should be at least 0.15 m higher than the sidewalk level in front of the entrance.

Entrance stairs should be duplicated by ramps for the movement of children and wheelchairs. The width of the internal staircase should be at least 0.9 m, and its maximum slope should be 1:1.25.

The living area of the house consists of a daytime area and a quiet rest area. The daytime area includes a living room, study, kitchen, dining room (or kitchen-dining room), and some recreational facilities; the quiet rest area includes bedrooms, which should be isolated from the active area, rooms for storing personal belongings (dressing rooms) and individual sanitary facilities adjacent to the bedrooms.

When designing a building on two or three levels, the active recreation area, as a rule, is located on the ground floor. It is not allowed to design of pass-through rooms (the exception is the dining room, which may border the kitchen on one side and the living room on the other).

Auxiliary rooms are intended for cooking, washing, storage of food, personal and household items and clothing. The auxiliary premises include: kitchen pantries, utility pantries, sanitary facilities, wardrobe, laundry room, mezzanine and built-in wardrobes, boiler room. It is advisable to design a utility entrance to the house from the utility area and the kitchen.

Sanitary facilities and bathrooms can be separate and combined (depending on their number and location). They should be designed on all floors of a residential building. The

This project has been funded with support from the Erasmus+ Programme Key Action 2 Cooperation Partnerships for Higher Education (KA220-HED). This publication [communication] reflects the views only of the authors, and the Commission cannot be held responsible for any use which may be made of the information contained therein.

location of sanitary facilities above living rooms is not allowed. These rooms are allowed to be located above the kitchen with the use of common engineering communications.

Internal staircases can be with one or two flights and/or with winders. The width of the flight is at least 0.9 m. It is desirable that the stairs are illuminated with natural (daylight) light.

Next, the project drawings are developed. The project includes the following drawings:

- situational plan of the design site location M1:500;
- general plan of the site M1:200;
- floor plans showing elements of engineering equipment and furniture M1:100, M1:50;
- facades: main, side, or courtyard M 1:50, M 1:100;
- section M 1:100, M 1:50;
- axonometry or perspective (building with its surroundings).

Note: It is possible to use ideas and sketches for designing a building from already finished student works.

This project has been funded with support from the Erasmus+ Programme Key Action 2 Cooperation Partnerships for Higher Education (KA220-HED). This publication [communication] reflects the views only of the authors, and the Commission cannot be held responsible for any use which may be made of the information contained therein.

12 References

1. Revit [Electronic resource] // General information. Access mode: https://ru.wikipedia.org/wiki/Revit;
2. Autodesk Knowledge Network [Electronic resource] // Information about Revit. Access mode: https://knowledge.autodesk.com/ru/support/revit- products/getting-started/caas/CloudHelp/cloudhelp/2018/RUS/Revit- GetStarted/files/GUID-D8835F8E-1330-4DBC-8A55-AF5941056C58-htm.html;
3. Autodesk Revit [Electronic resource] // Revit Architecture. Architectural design. Access mode: http://icad/software/item/autodesk_revit/;
4. Autodesk [Electronic resource] // Software for building information modelling. Access mode: https://www.autodesk.ru/products/revit/features;
5. Autodesk Knowledge Network [Electronic resource] // Parts of the User Interface. Access mode: https://knowledge.autodesk.com/support/revit-products/getting-started/caas/CloudHelp/cloudhelp/2019/ENU/Revit-GetStarted/files/GUID-7793667D-5657-4382-9BEC-F7CB6AC8F53E-htm.html;
6. Autodesk [Electronic resource] Architectural design and construction of buildings. Access mode: https://www.autodesk.ru/products/revit-family/case-studies/architectural-design;
7. VOLGUSHEV O., TOVBYCH V., VATAMANIUK N. Architectural and planning features of the renovation of industrial buildings on the example of the Brewery in Chernivtsi. ChNU, Chernivtsi;
8. MIZYAK M. «Architectural structures»: Study guide. Kharkiv: KHNAMG, 2008. 198 p.

This project has been funded with support from the Erasmus+ Programme Key Action 2 Cooperation Partnerships for Higher Education (KA220-HED). This publication [communication] reflects the views only of the authors, and the Commission cannot be held responsible for any use which may be made of the information contained therein.

Co-funded by the
European Union

AMAZE

Erasmus+ Programme Key Action 2 Cooperation Partnerships
for Higher Education (KA220-HED)
Agreement number 2023-1-RO01-KA220-HED-000155412
European Network for Additive Manufacturing in Industrial Design for Ukrainian Context

Toolkit

Reverse Engineering

Project Title	**Agreement number 2023-1-RO01-KA220-HED-000155412** ***European Network for Additive Manufacturing in Industrial Design for Ukrainian Context***
Output	**IO2 - AMAZE e-toolkit manual for digital learning in producing complex design industrial parts**
Module	**Toolkit** **Reverse Engineering**
Date of Delivery	**June 2024**
Authors	**Natalia WIERZBICKA, Remigiusz ŁABUDZKI, Adam PATALAS, Paweł ZAWADZKI**
Version	**FINAL VARIANT, *14.06.2024***

Co-funded by the European Union

Contents

1 Introduction

Reverse engineering in the context of product manufacturing involves analyzing an existing product to understand its design, functionality, and components. This process can provide valuable insights for various applications in product development and manufacturing. Here's a detailed description of how reverse engineering applies to product manufacturing:

a) **Product Analysis and Improvement**
- *Understanding Competitors*: manufacturers can reverse-engineer competitor products to analyze their strengths and weaknesses, allowing them to identify potential improvements or innovative features.
- *Quality Enhancement*: by dissecting a product, manufacturers can identify areas for improvement in terms of materials, design, and functionality. This can lead to the creation of higher-quality, more efficient products.

b) **Cost Reduction**
- *Material Selection*: reverse engineering can help manufacturers identify better or more cost-effective materials that can be used in production without compromising quality.
- *Streamlining Production*: analyzing how an existing product is made can provide insights into simplifying manufacturing processes, which can lower labor and material costs.

c) **Intellectual Property and Innovation**
- *Patent Analysis*: by reverse engineering, companies can gain insights into patented technologies. This understanding can guide them in avoiding infringement and developing their own novel solutions.
- *Inspiring New Designs*: generating ideas from existing products can inspire innovation and the development of new features or entirely new products.

d) **Legacy Products and Support**
- *Replacement Parts*: for older products or machines that are no longer in production, reverse engineering can be an essential method for creating replacement parts that are no longer available on the market.
- *Upgrades and Modifications*: engineers can analyze legacy systems or machinery to devise modern upgrades that enhance performance or adapt the product to new requirements.

e) **Quality Control and Testing**
- *Benchmarking Standards*: by reverse engineering products, companies can establish benchmarks for quality and performance, helping them maintain high standards in their manufacturing processes.
- *Testing Against Specifications*: it allows for validating that a reverse-engineered product meets specified design requirements and industry standards.

f) **Sustainability and Recycling**
- *Material Recovery*: reverse engineering can aid in understanding how to disassemble products for easier recycling and recovery of materials.
- *Eco-friendly Design*: insights gained through reverse engineering can lead to the redesign of products using more sustainable materials and methods.

g) **Rapid Prototyping**
- *Speeding Up Prototyping*: reverse engineering can significantly shorten the product development cycle by providing an existing model on which to base new designs. 3D scanning and CAD modeling can quickly generate prototypes based on reverse-engineered data.

Reverse engineering in product manufacturing involves analyzing a product to understand its design, architecture, and functionality. It allows manufacturers to recreate and improve existing products, ensure compatibility, or develop new products based on existing ones. Here are several common techniques used in reverse engineering:

- Physical Disassembly:

The most straightforward method, involving taking apart the product to study its components, materials, and assembly processes.

- 3D Scanning:

Using laser scanners or structured light scanners to capture detailed 3D models of products. These scans help in analyzing geometry and dimensions accurately.

- Computer-Aided Design (CAD) Reconstruction:

After scanning or measuring, CAD software can be used to create a digital model of the product. This is especially useful for capturing complex shapes and geometries.

- Material Analysis:

Testing and analyzing materials used in the product helps in understanding their properties, sourcing alternatives, or ensuring compliance with standards.

- Functional Analysis:

Assessing how the product functions through testing and observation. This may involve evaluating performance, durability, and user interaction.

- Electrical Analysis:

For electronic products, circuit design analysis can be performed to understand the layout and functioning of electronic components.

- Software Analysis:

For products that incorporate software, reverse engineering techniques such as code decompilation or static/dynamic analysis help understand the software’s functionality.

- Prototyping:

Creating prototypes based on the reverse-engineered data allows for testing and validation of the new design or modifications.

- Metrology:

Utilizing measurement techniques to obtain precise dimensions and tolerances of components, ensuring accuracy in replication.

Each technique can be utilized individually or in combination, depending on the complexity of the product and the objectives of the reverse engineering process. Reverse engineering plays a crucial role in product development, competitive analysis, and innovation within manufacturing industries (Fig. 1) [1].

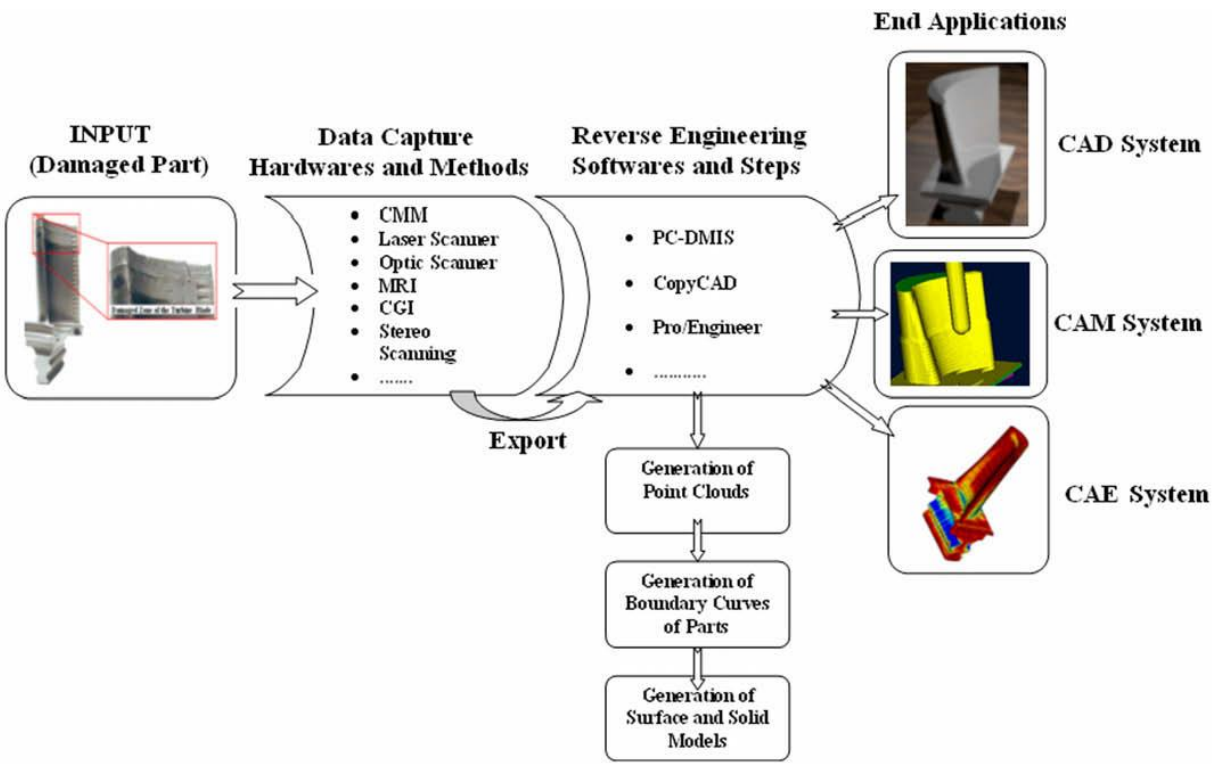

Fig. 1. The whole process of RE should be computer aided [1]

2. Reverse Engineering techniques

2.1 CMM Scanning

Optical scanning is a critical technique used in reverse engineering to create digital representations of physical objects. This process typically involves using advanced imaging technology to capture the geometry, shape, and sometimes even the color or texture of an object. Here's a detailed breakdown of how optical scanning contributes to reverse engineering:

Key Elements of Optical Scanning in Reverse Engineering:

Scanning Technology:
3D Laser Scanners: These devices use laser beams to capture the precise dimensions of an object. They work by measuring the time it takes for a laser to bounce back from the surface, generating thousands or millions of data points that form a point cloud representation of the object.
Structured Light Scanners: These employ a series of projected light patterns to capture geometry. The deformations in the projected patterns are analyzed to reconstruct the object's surface.
Photogrammetry: This technique uses multiple photographs taken from different angles to create a 3D model. Software analyzes the overlapping images to derive spatial coordinates.

Data Capture:
Point Cloud Generation: The scanning process results in a point cloud, which is a large collection of data points defined by their X, Y, and Z coordinates. This serves as the raw data for further processing.
Resolution and Accuracy: The quality of the scanner affects the resolution (detail captured) and accuracy (closeness to true dimensions) of the point cloud. Higher resolution scanners provide better fidelity for intricate parts.

Data Processing:
Mesh Creation: After capturing the point cloud, specialized software is used to convert this data into a 3D mesh. This involves connecting the dots to create a continuous surface that represents the scanned object.

Surface Texture and Color Mapping:
If the scanner captures color information, textures can be applied to the 3D model, making it more realistic and useful for visualization or analysis.
Reverse Engineering Applications:

Design Modification:
Engineers and designers can analyze the geometry of existing products and use the data to create improvements or modifications.
CAD Model Creation: The processed data can be translated into CAD (Computer-Aided Design) models, allowing for further development, simulation, and manufacturing.

Quality Control and Inspection:

Optical scanning can be used to compare current products against original specifications, identifying deviations and ensuring quality standards.

Benefits:
Speed: Optical scanning enables quick and efficient capturing of complex geometries compared to manual measurement techniques.
Non-destructive: The process is typically non-invasive, allowing the original object to remain intact.
Versatility: It can be applied to a wide range of materials and object sizes, from small mechanical components to large industrial parts or architectural structures.

Challenges:
Data Management: The large volumes of data generated can require substantial processing power and sophisticated software to manage and interpret.

Accuracy Limitations: While modern scanners are highly accurate, factors such as surface reflectivity, environmental conditions, and setup can affect data quality.

In summary, optical scanning plays a significant role in the reverse engineering workflow, facilitating the transformation of physical objects into digital models that can be analyzed, modified, and reproduced with precision. This technology finds applications across various industries, from manufacturing and automotive to healthcare and cultural heritage preservation.

As illustrated in Fig. 1, application of 3D scanning in RE process involves three main steps: (1) scanning, (2) point processing, and (3) application specific geometric model development. These steps shown in the figure illustrate the different phases the engineer takes the object from physical state to a point cloud and transforms it into a CAD model. The scanning phase consist of choosing scanning techniques, preparing the part, and performing the actual scanning. The output is a point cloud. This is usually a file consisting of the (x, y, z) coordinates often complimented by a black/white intensity or a colour for each measurement point [2]. 3D scanning devices are divided into two categories: (1) contact and (2) non-contact scanners. Contact devices use probes that follow the physical surface, similar to CMM method. The accuracy of contact devices is good, though they can be slow because points are registered sequentially at the probe. Another problem is that contact pressure is used, meaning soft materials cannot accurately be measured [3]. Non-contact scanners such as lasers and optics, computer vision, photogrammetry, light detection and ranging (LiDAR), and imaged based techniques [8], on the other hand, capture geometry without physical contact. These devices can capture large amounts of data in short time, though they suffer several issues including poor accuracy compared with contact devices [3,4]. The challenge with non-contact scanners is when scanning surfaces parallel to laser axis. Since light is used in scanning, non-contact devices have problems with shiny surfaces, resulting in a need for temporary coating. Although these problems limit the use of non-contact scanners to cases where speed and magnitude of

data capture is more important than accuracy, the technological developments in the area are constantly improving [3]. Geng et al. [4] proposed a hybrid method where non-contact methods are used for path planning for CMMs, yielding a combination of high speed and high accuracy.
The point processing phase consists of importing the raw point cloud data, reducing the noise, and reducing the number of points using filter algorithms. The point cloud data can be merged in cases when the whole part is captured in multiple scans. Different software providers have different solutions for merging files. The application specific geometric model development phase is the most complex activity in RE [3]. The main reason is the need for advanced surface fitting algorithms to generate accurate surfaces. Since most CAD software are not designed for the large amount of data in point clouds, separate software is needed for the complex and heavily researched process of transforming point clouds into surfaces that can be used in CAD software [4].

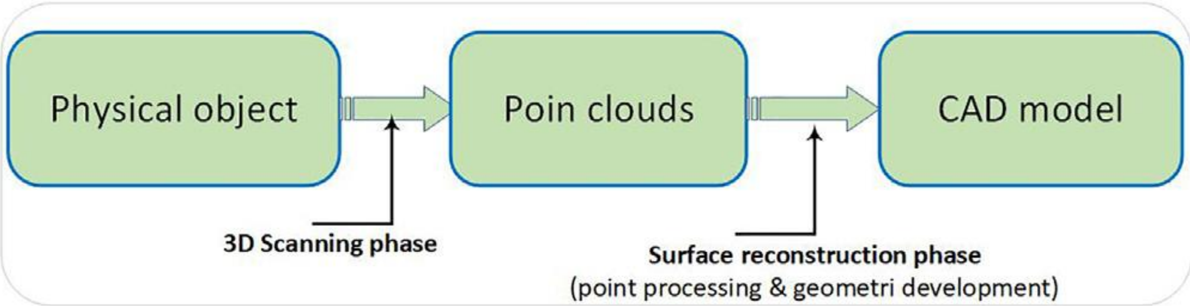

Fig. 2. Generic RE process using 3D scanning technology [5]

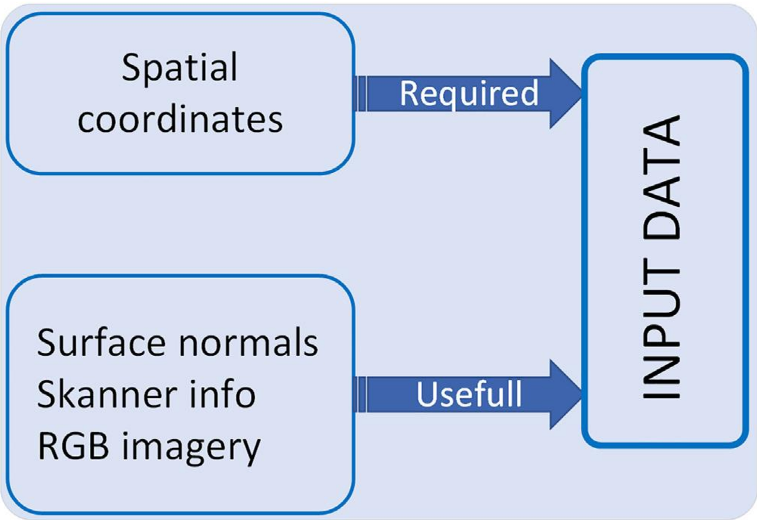

Fig. 3. Input Data for Surface Reconstruction [5]

This section presents the methodology and results from the physical experiment on a 3D printed metal cylinder with complex internal geometry, which was reverse engineered using a handheld non-contact 3D laser scanner. A smaller test of product quality control using a CMM was also conducted and is presented (fig. 3).

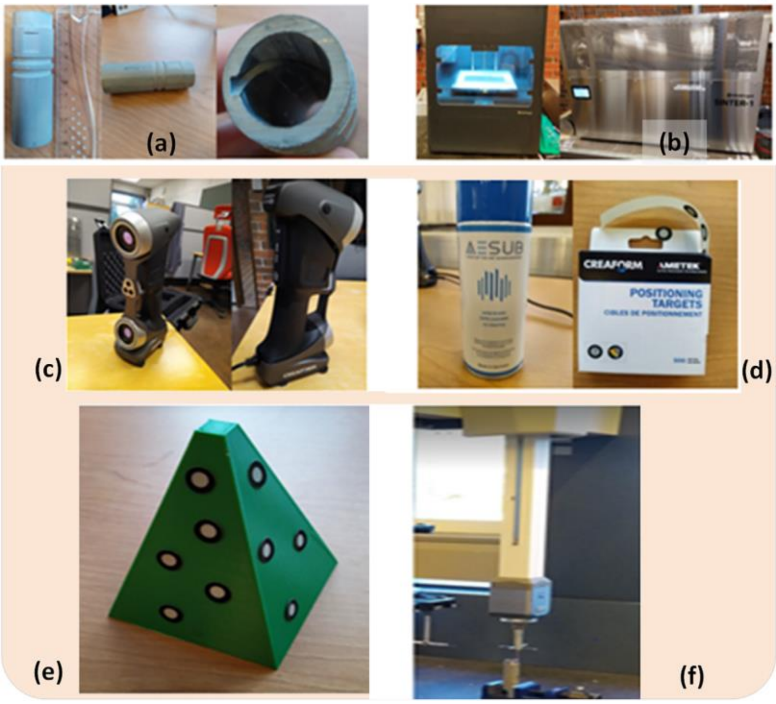

Fig. 4. Equipment used in the experiment (a) Test objects for RE, (b)Metal X 3D printer with sintering facility, (c) Handheld 3D scanner, (d) Coating spray and positioning target, (e) Plastic support pyramid and (f) CMM probe [5]

The goal of the experiment is to study the possibilities that 3D scanning technology can provide in RE process and product quality control purposes. Fig. 4 shows the equipment used in the experiment. In addition, software tools such as VX Scan and Model, and Autodesk Inventor were used. The components, shown in Fig. 5(a) were modelled in Autodesk Inventor and transferred to STL file format for 3D printing and sintering (Fig. 5(b)). To imitate RE of a degraded part having rough surface due to corrosion and wear, as well as to avoid the effects of shiny surfaces, the test sample was covered in a white coating spray (Fig. 5). Position markers were then placed on the surface of the component and the pattern of the markers are used to recognize the spatial location of each scanning point as the scanner is moved around. While scanning, it is observed that the scanner could not properly capture the geometry even though the test sample was covered in coating spray and position targets. A plastic pyramid covered with position markers was therefore used as a base for the scanner to find some known geometry to initiate the scanning process. This enabled the scanner to find the component properly. The component was first scanned as shown in Fig. 5 (R) before it was turned 180^{o} and scanned again.

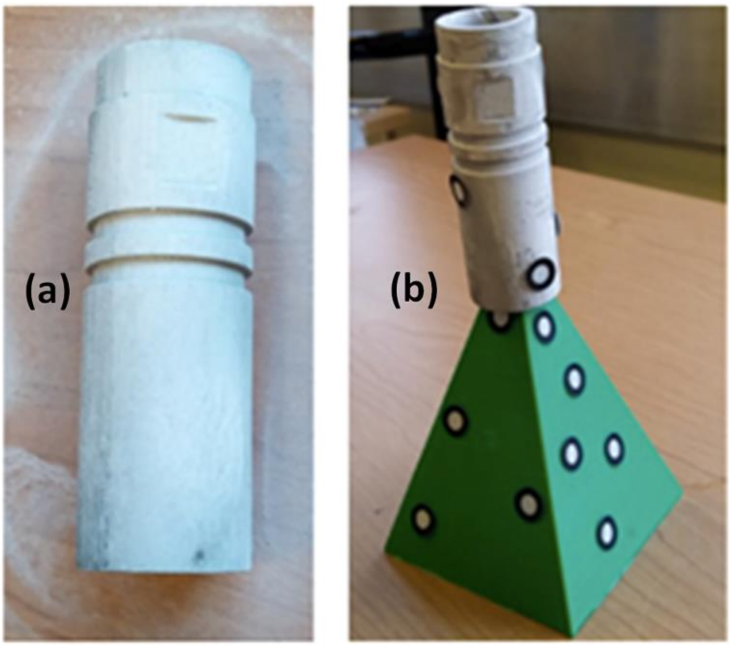

Fig. 5. Component (a) with coating, and (b) scan setup on support pyramid [5]

Once the physical scanning was completed, the scanned data was transferred into VX Model data and merged into one point cloud using a ‘‘best-fit” algorithm for matching points and geometry and some manual adjustments. The point cloud was then optimized and transformed into surfaces using different surface modelling techniques before being transformed into CAD model format in Inventor. After the process of merging, optimizing, surface reconstruction, and CAD modelling in Inventor the product QC with a contact device (CMM) was done by measuring the roundness of the cylinder at its thickest radius (Fig. 7, main view 20 mm from the right edge). The CMM was used to make QC by measuring along a predetermined path and to determine the roundness deviation from the CAD model. The results are presented in Fig. 6, where the nominal value is presented as the black circles and the two red circles are the given design tolerances (±0.05 mm). The results show that the roundness exceeds the tolerances at most measurement points and additional surface treatment would be needed in a real-life production process. The maximum deviation measured was 0.214 mm.

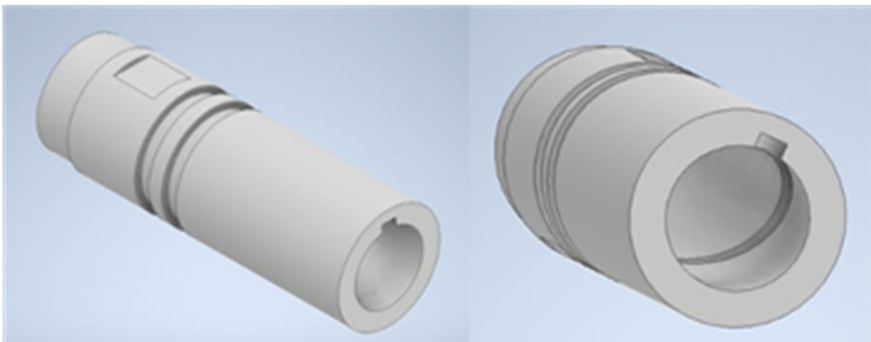

Fig. 6. 3D model of the original design of test object [5]

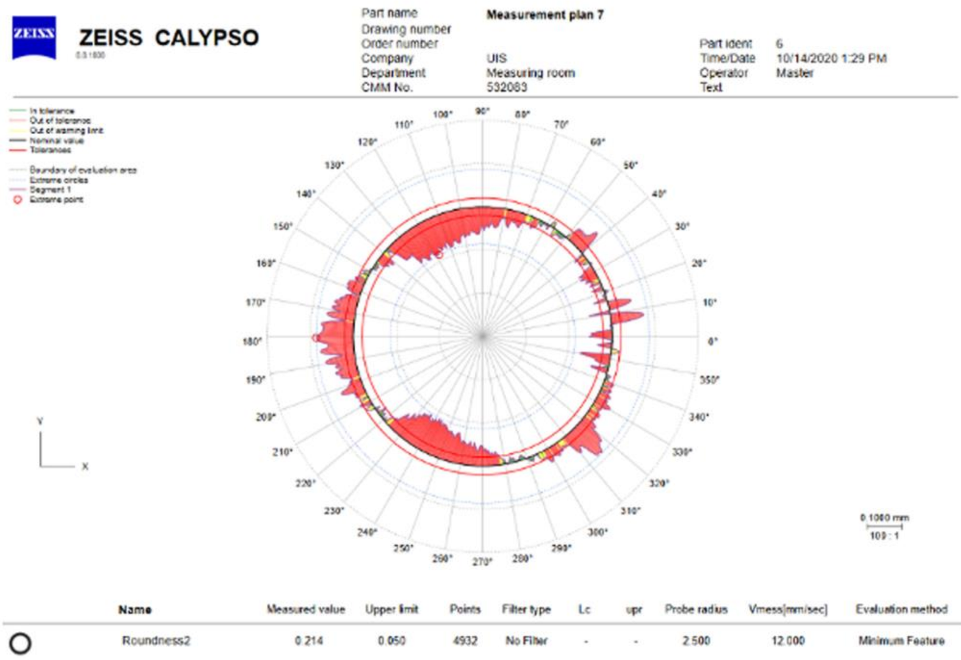

Fig. 7. Roundness measurement results from CMM [5]

The output of the physical scanning was saved as two raw point cloud files, one from each side of the test object. These are shown side by side in Fig. 8. The raw files contain unwanted information like i.e., the pyramid and table geometry. The original point clouds also included features like holes, spikes, noise, and outliers.

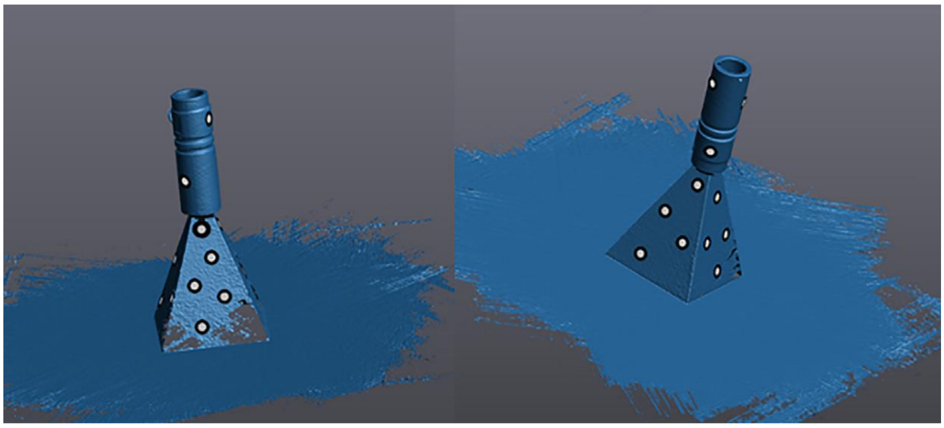

Fig. 8. Raw point clouds of the scanned sample [5]

The pyramid and floor points were then removed by removing all points located below a defined plane (Fig. 9). Large outliers were also removed manually by selecting points within a specified rectangle. Upon removing the unwanted points of the two separate scans of the component, i.e. point clouds captured from both sides, it is observed that both scans have missing data on different locations. However, scanning the component from two opposite direction (rotated 180^o) is that the missing data in one scan will be complimented by the other.

Some of the visually observed missing data visible in Fig. 10(a - c), where the 1–2 cm internal scan range is also shown. The next part of the process was to align the separate scans to each other, and this was done by manually translating and rotating the scans to approximately fit and then using the ''best-fit'' tool in VX model. This fits the scans to each other by shared geometry within a set tolerance of 1 mm (Fig. 10(d) – (f)). As can be observed from these figures, some of the missing data shown in Fig. 10(c) were filled. The file was then converted into a mesh of triangles with vertices on each point.

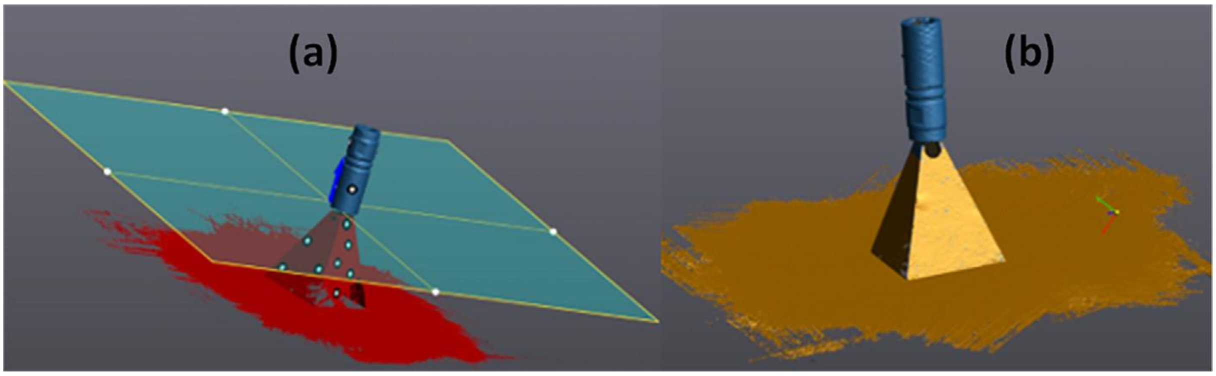

Fig. 9. Removing irrelevant point clouds by cutting plane (a) and removing outliers by manual selection (b) [5]

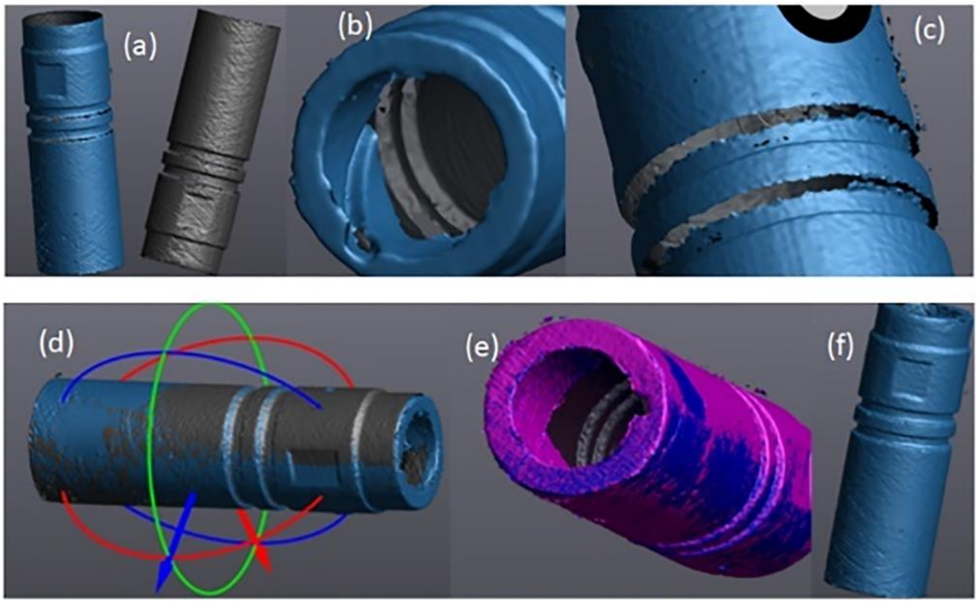

Fig. 10. Results of scanned object (a) Separate Scans, (b) Internal Scan, (c) Scanned surface with missing data, (d) manual aligned scanned model, (e) ''Best-fit'' model and (f) Merged scan [5]

Some point cloud optimization steps were done before starting the surface reconstruction steps (Fig. 11). First, the ''clean-mesh'' algorithm was applied, removing isolated patches, spikes, small holes, and singular vertices. Then, holes were filled using the ''fill hole'' algorithm by selecting edges of holes and the proper level of curvature by trial and error. Fig. 10(b) illustrates the process of the hole filling. The final process was the surface reconstruction phase, which was done using two ways: (1) by creating primitives based on optimal fit to points, and (2) by creating NURBS surfaces that more accurately render the surface with its corresponding roughness. The primitives-based method uses the mesh to find best-fit cylinders, planes, triangles, etc.

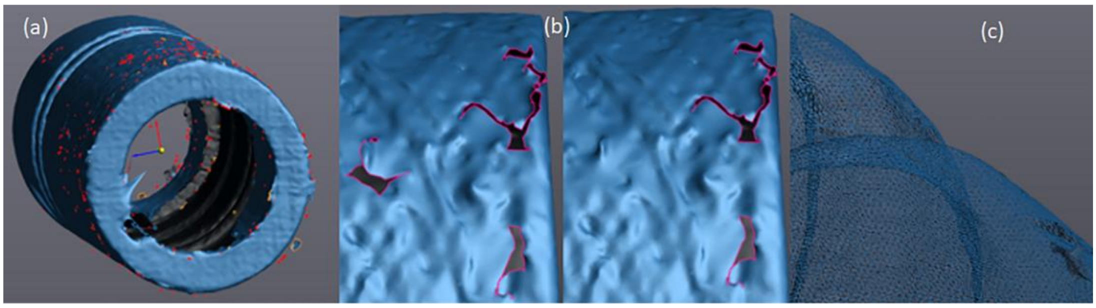

Fig. 11. Pre-surface construction of scanned object (a) «Clean-mesh», (b) Holes before and after fill, and (c) Mesh of triangles [5]

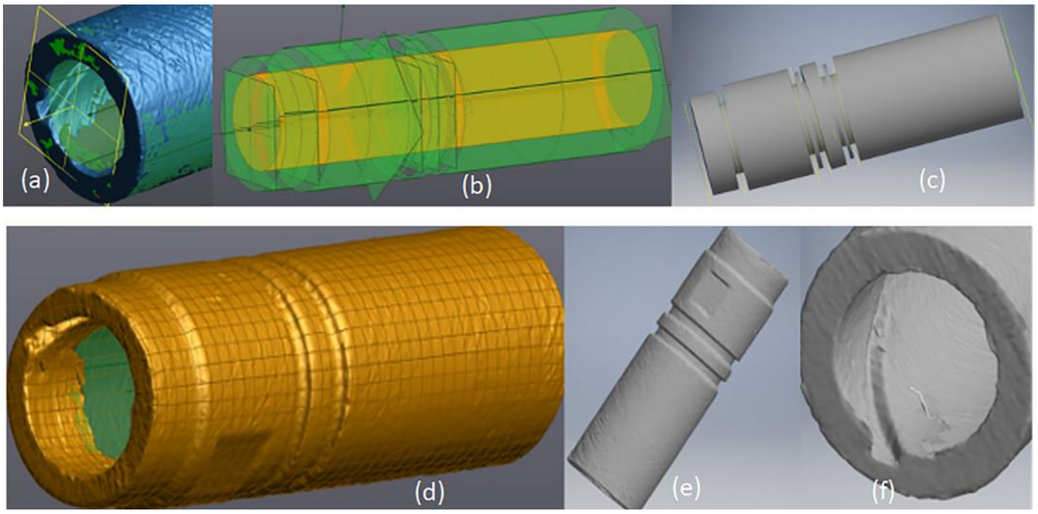

Fig. 12. Surface reconstruction phase (a) Extraction of primitives, (b) View of primitives, (c) Primitives as solids, (d) NURBS surface, (e) Surface in CAD environment, and (f) Internal surface of the model [5]

Fig. 12(a – c) shows the fitting of the primitives, the primitives themselves, and the solids exported to the CAD software. In the CAD environment, the solid cylinders were extended to go from plane to plane, the inside cylinder was used to extrude the hollow section, and the internal geometry was made using the ‘‘coil” function. The NURBS surface method, on the other hand, takes the mesh and transforms it to NURBS surfaces as shown in Fig. 12(d -f). The surface was then exported to Inventor as a surface model. The surface model itself only has 1– 2 cm of internal geometry on each side, due to the limited scan range.

2.2 Optical Scanning

The purpose of reverse engineering is to manufacture another object based on a physic and existing object for which 3D CAD is not available. The first we need digital version of object. Because our car’s volume button has free formed surfaces we decided to use optical 3D scanning technology to obtain the point cloud of existing object. With the help of point cloud we can developed 3D CAD model which will be used for manufacturing of button pair. We used for manufacturing of pair of buttons machine for selective laser sintering Formiga P 100.
The scanner converts the physical object into point cloud. This kind of reverse engineering can be used to make digital 3D record of the objects, for security copies, shows it in presentations to the competitors about how it works, identify potential patent infringement [9]. In our case, we will take advantage of a plastic object. More specifically a plastic button of which we will manufacture both sides, right side and left side form polyamide PA2200 [9,10,11]. This button is used for turning up the volume of a car’s radio. It has surfaces which have to be perfectly copied because it is the most important part of the button. Behind this surface there are three cylinders and a square which will be used to fix the button on the car's steering wheel.
Clearly our case is a case about reverse engineering applied to objects. We are going to scan a physical object which has a complicated geometry and some surfaces. Our piece is small and therefore we need to use the lens with the size 350 x 280 x 280 mm. The lens permits to get a better mesh with more points [9]. The button has to be provided with encoded points which are situated strategically for ensuring a correct mesh. Fig. 2.1 shows button from front and back side and there are also encoded points.

Fig. 2.1. Button front and back side with encoded points [17]

For scanning the whole button we have to rotate few times to get every views of the button. Because the button is black the light is reflected, and we cannot get the right point cloud. This is the reason why we have to paint the piece with a developer spray which paints the button in white, so the button is prepared to be scanned. ATOS Core – Optical 3D Scanner ATOS Core is the specialist for the three-dimensional measurement of small components up to 500 millimeters in size. The sensor forms the basis for a diverse range of measuring tasks – from simple 3D scanning to fully automated measurement and inspection processes (Fig. 2.2). The scan has to be done in a dark space, it helps to accomplish a more accurate point cloud, and also it is good to avoid damages on the mesh. After some scans and picking the best one, we have to orientate the mesh with the software. Fig. 2.3 shows mesh after scanning.

Fig. 2.2 Optical 3D Scanner ATOS Core

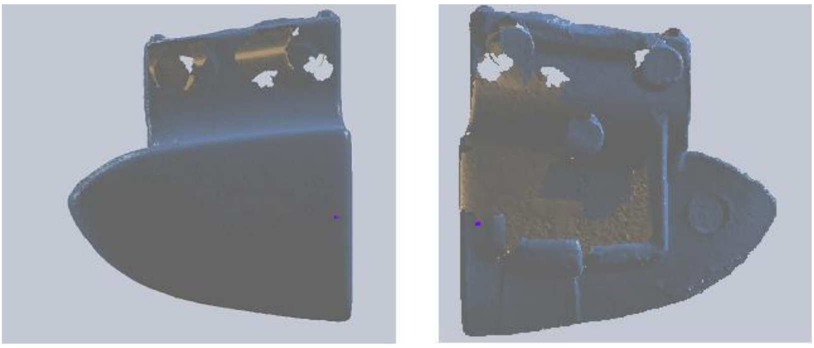

Fig. 2.3. Mesh after scanning [17]

The mesh is not perfect (Fig. 2.3) it contains some holes and some damages on the surfaces. But SolidWorks has a feature which helps to repair the mesh. It consists in filling the holes and to join the damages to the parts. At the end, the mesh looks much better than before and it is really an approximated version of the real button. We can see some holes and some areas that are not filled (Fig. 2.3). The feature called mesh wizard is capable of repairing this mesh. On the picture (Fig. 2.4) we see the mesh perfectly repaired.

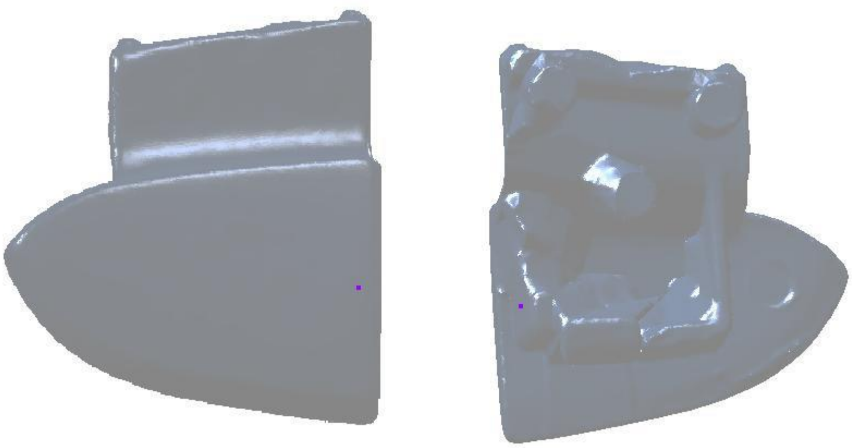

Fig. 2.4. Repaired mesh [17]

We have to take care of this part because it is the most important surface. For doing this surface we were use the feature called surface wizard. This feature helps us to create the surfaces automatically (Fig. 2.5), but we have to take care and check if the mesh is drawn correct. Also we can check if the sensitivity is correct because it depends on the sensitivity if it can be more accurate. Anyway, we can draw the surface manually by painting the mesh there where we want a surface, also we can paint manually if the painted part does not adjust correctly [14,15].

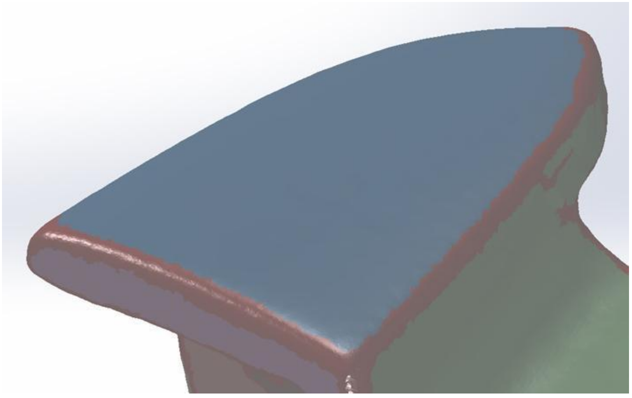

Fig. 2.5. Mesh painted automatically [17]

Three surfaces have to be created and adjusted perfectly (Fig. 2.5). The order of the procedure does not matter, because after this we are going to cut and extend the surfaces. Final result of cutting of excess of surfaces is shown on figure (Fig. 2.6).

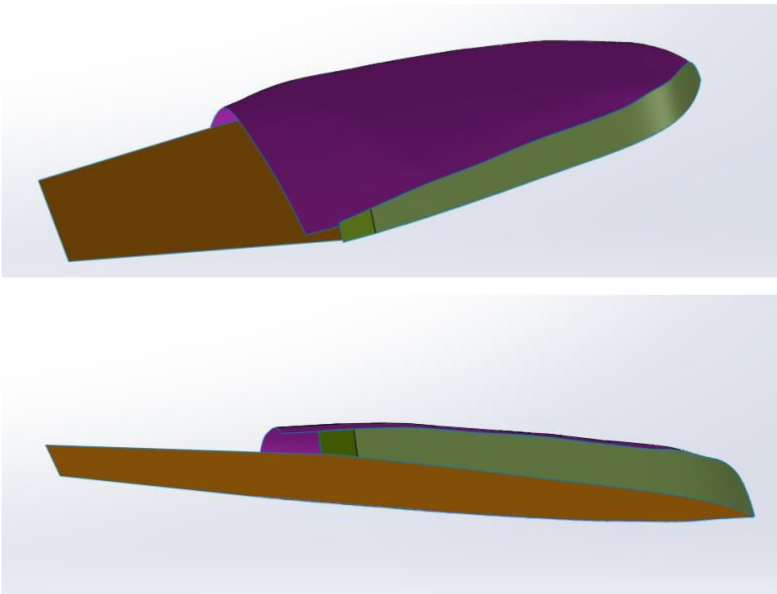

Fig. 2.6. Created surfaces and excess cutted away [17]

For creating these surfaces, we will follow the similar process as before. With the feature surface wizard we are going to do the reference surface. In this case it will be planar surface. To avoid the problems we are going to draw the first surface (reference surface) and other surfaces will be refers to this surface. The other surfaces can be created by just creating a plane perpendicular to the reference surface and selecting, with the option coincidence, the part of the mesh where we want to create a plane. Considering this last rule we draw a line in the sketch and we extrude it, in direction of reference surface (Fig. 2.7).

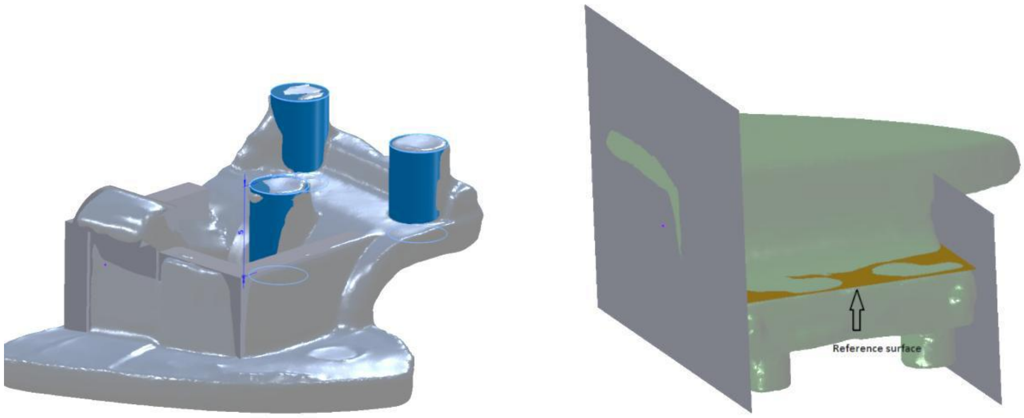

Fig. 2.7. Created surfaces, reference surface and cylinders [17]

With the feature combined we joined the parts. When the cylinder and square have the right geometry it is time to combine everything. Finally we have a single solid (Fig. 2.8). If everything is correct and there are no offsets or two surfaces at the same place, we are able to do a fillet on the specified edges. Finally we have our button and it looks like the real button (Fig. 2.8), we can compare with the mesh in SolidWorks.

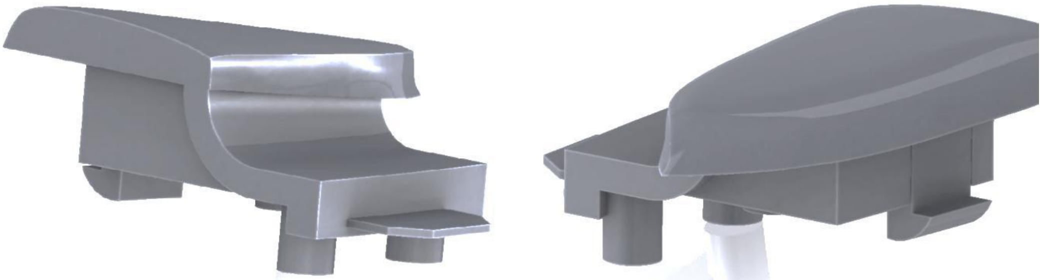

Fig. 2.8. 3D Cad model done [17]

The extension of the file is .SLDPRT, for working as a mesh we save this file with the extension .STL. We open the file with the software Netfabb studio basic which will helps us to orientate and define the position and also, to define the layers of the mesh. The first thing that we have to do is to add both parts "buttonleft.stl" and "buttonright.stl". These parts have to be orientated and positioned correctly. After that, we defined the slices the default option is a slice each 0.015 mm, for the button this is correct. The height to start is 0 mm and the height to finish 12.711 mm. The slices will be created and with the control of the simulation we can observe how the piece will be created.
The machine of selective laser sintering is compact, cost-efficient and a highly productive system for the additive manufacturing of plastic parts. It is ideal to manufacture small series production. It can manufacture piece with complex geometry. The maximum height that it can manufacture is 330 mm.
Technical data of FORMIGA P 100. FORMIGA P 100 Effective building volume 200 mm x 250 mm x 330 mm Building speed (depending on material) up to 24 mm/h Layer thickness (depending on material) 0.1 mm Laser type CO2, 30 W Scan speed during building up to 5 m/s Power supply 16 A Power

consumption 2 kW Compressed air supply 10 m3/h Dimensions (W x D x H) System incl. powder containers and touch screen 1320 mm x 1067 mm x 2204 mm Weight approx. 600 kg Unpacking and sieving station (optional) 1200 mm x 700 mm x 1500 mm Data preparation PC Current Windows operating system Software EOS RP Tools (optional); Desktop PSW CAD interface STL (optional: converter to all common formats).

Fig. 2.9. FORMIGA P 100 [16]

This machine is capable of manufacturing pieces with a complex geometry. To build plastic pieces it uses STL files with three-dimensional geometries. The basic principle is based on the sintering of the plastic powder using a CO2 laser. The laser sintering process is, basically, heating the plastic powder above the melting point (184°C) by exposure with the laser beam. The heater has an important job which is to maintain a homogenous temperature in the workspace. This is very important because if in the process the temperature is not equal around the platform the piece can be deformed and the machine can have serious problems. After melting the plastic powder and making the geometry of a layer, it is refrigerated by nitrogen. The shrinkage of the solid when is melted is compensated by appropriate scaling. The last process is repeated layer by layer to form the final solid.

To manufacture the button, previously drawn by "SolidWorks", orientated, positioned and the slices defined by "Netfab studio basic", it is time to use the selective laser sintering machine Formiga P100. This machine is provided with the software "EOS PSW" which is used to define the position and the quantity of the pieces that we want to manufacture in the platform, to define the parameters of the machine and to simulate the process which the machine will follow.

The principal screen of the software "EOS PSW" is the view of the work platform. We added a pair of buttons and situate the buttons in the middle of the screen and then we can see a preview of the platform (Fig. 2.10). This principal screen has important tools which help us to get information about the work that we have to do.

The principal screen of the software "EOS PSW" is the view of the work platform. We added a pair of buttons and situate the buttons in the middle of the screen and then we can see a preview of the platform (Fig. 2.10). This principal screen has important tools which help us to get information about the work that we have to do.

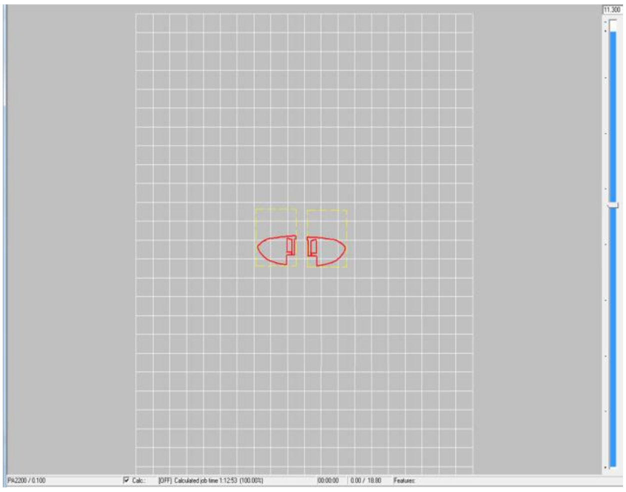

Fig. 2.10. Workspace [17]

The machine is capable of taking advantage of almost all workspace, so we try to fill of the workspace with buttons to get more production (Fig. 2.11). It is really good for the production because it only elevates the production time slightly and in this case we can obtain 21 couples of buttons. In our case, for one couple of buttons the estimated job time is 1:12:53 and for 21 couple of buttons is 1:25:50, proving that the time is just a little bit increased. Also, it is important to define the position of the button 0.5 mm upper from the platform, otherwise it could be stuck with the platform.

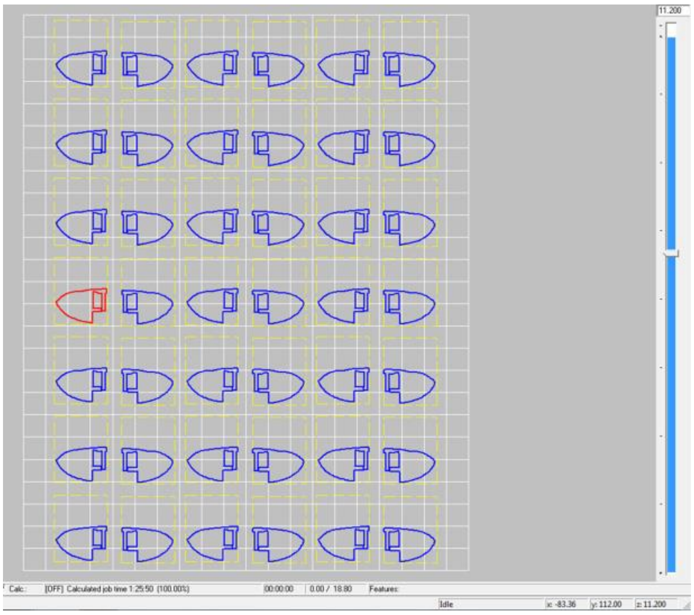

Fig. 2.11. Platform full of pieces [17]

The machine to clean the pieces (Fig. 2.12) has two hoses, the small one ejects air, and the big one sands. The big one is used to clean the piece in general and the small one for cleaning the small holes or edges (Fig. 2.13). It is important to take special care with the hoses of sands, because if a part of the piece is exposed for a long time to the hoses of sands it could be damaged.

Fig. 2.12. Cleaning machine [17]

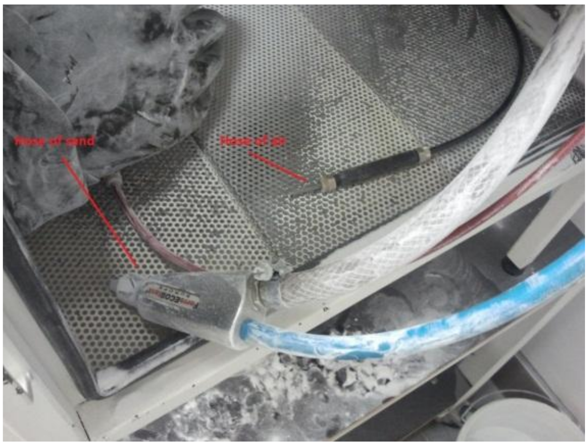

Fig. 2.13. Hoses [17]

And finally we get one couple of buttons with both sides (Fig. 2.14). Right side can be compared with the first button from which we obtained the data and check if the button is quite similar to be accepted.

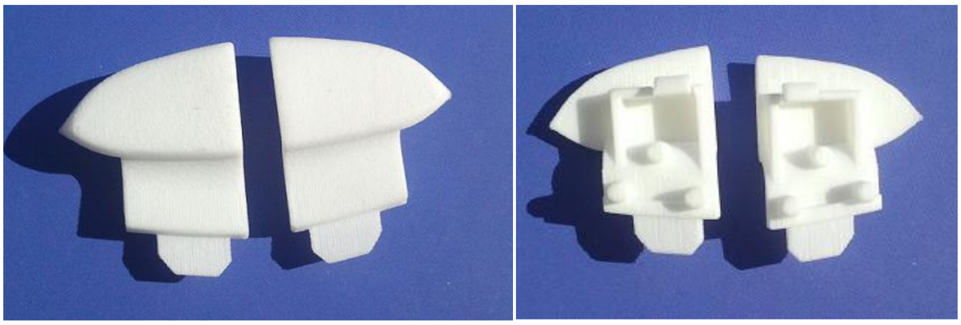

Fig. 2.14. Front and rear buttons manufactured [17]

The case studied has permitted us to discover how the reverse engineering can be useful for manufacturing already existing pieces. In this paper we showed how a 3D scanner works and its applications in the reverse engineering field. We showed how to get data from the objects with the scanner. Also, with different software we could repair the mesh, orientate it and define the position of the mesh. Thanks to the complex form of the button we showed how to create a solid by SolidWorks, drawing the different surfaces and solids. In our case we did not have the left side of the button and thanks to the creation of the solid we could make the mirror part and reverse engineering permitted to us to manufacture this part. Reverse engineering is one of the best forms to manufacture prototypes or short productions. The selective laser sintering machine permits an easy and cheap manufacturing of pieces.

3. Application of reverse engineering to the production of biomedical engineering products

Reverse engineering is pivotal in medical life sciences, providing significant advantages such as reduced time and costs, along with enhanced product accuracy. Modern medical production systems integrate advanced measurement techniques to precisely capture human anatomy, sophisticated software for CAD model design, cutting-edge fabrication technologies, and innovative materials for improved manufacturing outcomes. In fields like orthopedics, dentistry, and reconstructive surgery, reverse engineering enables detailed imaging, modeling, and replication of a patient's bone structure, allowing surgeons to meticulously plan and evaluate procedures before actual implementation.

3.1 Reverse engineering in prosthetic application

Reverse engineering has become increasingly significant in orthopedic applications, revolutionizing the way medical professionals approach treatment and surgical planning. By using advanced imaging techniques like CT scans and MRIs, reverse engineering allows for the precise capture of a patient's bone structure and anatomy. This data is then used to create detailed 3D models through Computer-Aided Design (CAD) software.

In orthopedics, these 3D models are instrumental in developing custom implants and prosthetics that perfectly match the patient's unique anatomical features. For instance, in joint replacement surgeries, reverse engineering ensures that implants are tailored to fit the patient, leading to better outcomes and faster recovery times. Additionally, surgeons can use these models to simulate and plan complex procedures in advance, minimizing risks and improving the precision of the surgery.

The application of reverse engineering in orthopedics not only enhances the accuracy and effectiveness of treatments but also significantly reduces the time and cost involved in developing and implementing medical solutions. It is a powerful tool that supports personalized medicine, where treatments are specifically designed for individual patients, leading to improved overall patient care and satisfaction.

Filip Górski and colleagues, in their article "Development and Testing of an Individualized Sensorized 3D Printed Upper Limb Bicycle Prosthesis for Adult Patients" present the design and evaluation of a personalized prosthetic device tailored for an adult patient, specifically for activities such as bicycle riding. The prosthesis was developed using 3D scanning, semi-automated design with the AutoMedPrint system, and low-cost Fused Deposition Modelling (FDM) technology for 3D printing. It features integrated force and movement sensors and was subjected to rigorous testing across various dynamic scenarios to assess functionality, mitigate potential risks, and refine the design prior to activating the end effector. The article comprehensively details the design, production, and testing processes, showcasing the successful implementation and identifying areas for mechanical and electrical improvements [18].

The design process began with the development of an intelligent, modular model for an upper limb prosthesis. This cohesive device consists of multiple interconnected components. Anthropometric and configuration data are imported directly from an external Excel file, allowing the automated generation of anatomically matched prosthesis components and various configurations. The model supports the quick production of personalized prostheses, including a compressive-release socket (CRS), a forearm with an elbow joint, and a C-shaped end effector with a Cardan joint at the wrist (Fig. 3.1.) [18].

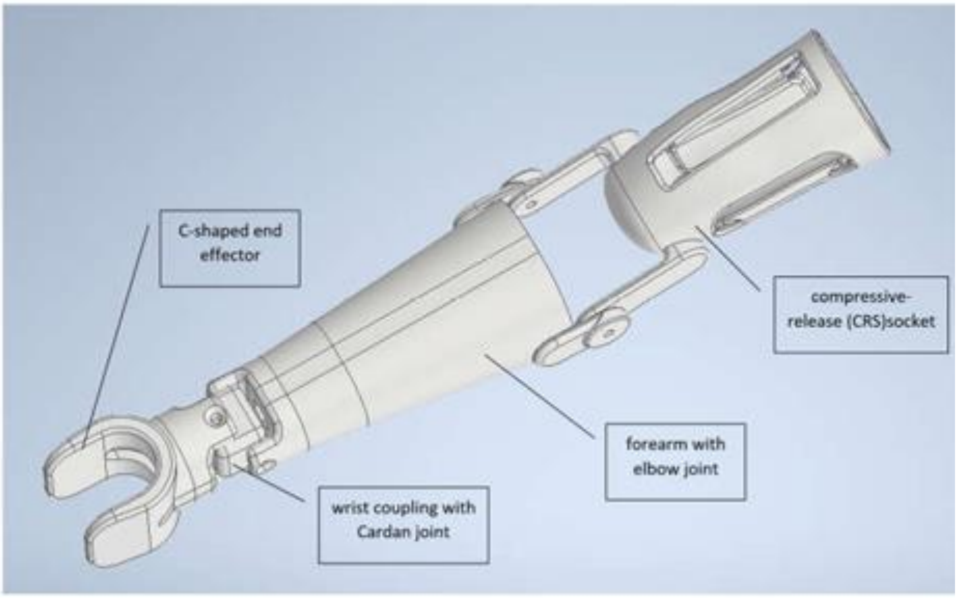

Fig. 3.1. Basic variant of an intelligent CAD model created in Autodesk Inventor [18]

The prosthesis model was customized for a 40-year-old male patient born without a right forearm or functioning elbow joint. Both upper limbs were 3D scanned, and the data were processed using the AutoMedPrint system's hardware and software capabilities (Fig. 3.2.) [18].

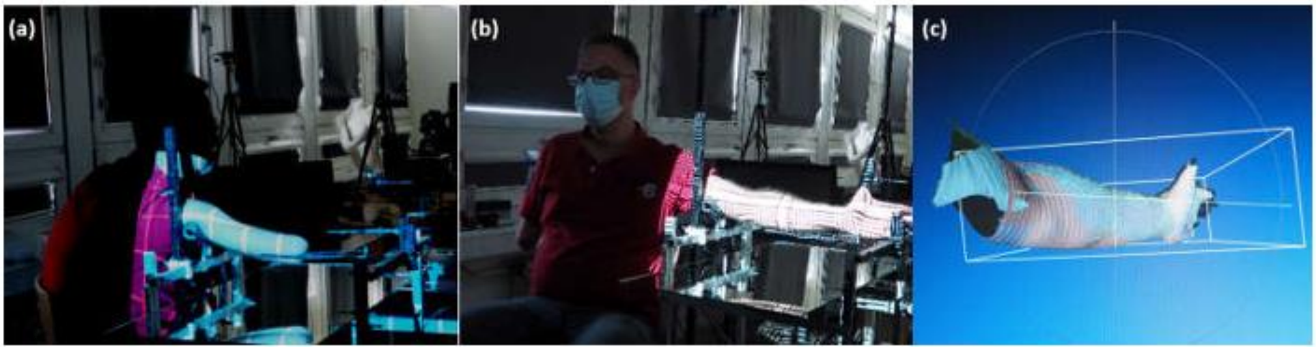

Fig. 3.2. 3D scanning of patient: (a) stump; (b) healthy arm; and (c) mesh data during processing [18]

The initial prosthesis was manufactured and tested by the patient. After minor strength-related adjustments, the prototype was successfully tested during bicycle riding, and the patient received the prosthesis (Fig. 3.3.) [18].

Fig.3.3. Tests of initial, mechanical version of the prosthesis: (a) laboratory tests and (b) usability tests [18]

The research continued with the integration of a mechatronic component into the system, enhancing its functionality by enabling interaction with electronic and mechanical elements. This addition aimed to improve the system's responsiveness and adaptability in practical applications. Following the integration, a series of tests were conducted to assess the mechanical properties of the modified system, including its durability, flexibility, and overall performance under various conditions. The results of these tests provided valuable insights into the effectiveness of the mechatronic enhancements and their potential for further development in similar applications.

3.2 Reverse engineering in hand therapy

The paper "Development and Studies of VR-Assisted Hand Therapy Using a Customized Biomechatronic 3D-Printed Orthosis," authored by Filip Górski and colleagues, explores the creation, testing, and use of a wrist–hand orthosis for hand therapy in a teenage patient with congenital paresis. The team enhanced a standard 3D-printed orthosis with sensors, transforming it into a motion controller for virtual reality (VR). Due to the patient’s wrist and hand impairments, standard VR controllers were not an option, so the orthosis was adapted by integrating custom electronics and motion trackers. A VR game, developed in collaboration with physiotherapists, replaced traditional VR inputs with those from the customized orthosis. This game was then tested on patients and evaluated by an expert to determine its effectiveness and identify areas for further improvement in the orthosis design [19].

To realize the concept of the customized wrist orthosis, the AutoMedPrint system was employed. AutoMedPrint is an advanced platform for the rapid, automated design of 3D-printable orthopedic and prosthetic devices, with a focus on wrist–hand orthoses and upper limb prostheses. The prototype system features a mechanized 3D scanning station equipped with automated algorithms for scan processing and data extraction, as well as intelligent CAD models for orthopedic products. The system has received numerous accolades, including being named the Polish Product of the Future in 2022 [19].

Fig. 3.4. shows the AutoMedPrint prototype, while Fig. 3.5. illustrates the system's operational methodology. Additionally, virtual reality technology played a significant role in the system's development and the products it generates [19].

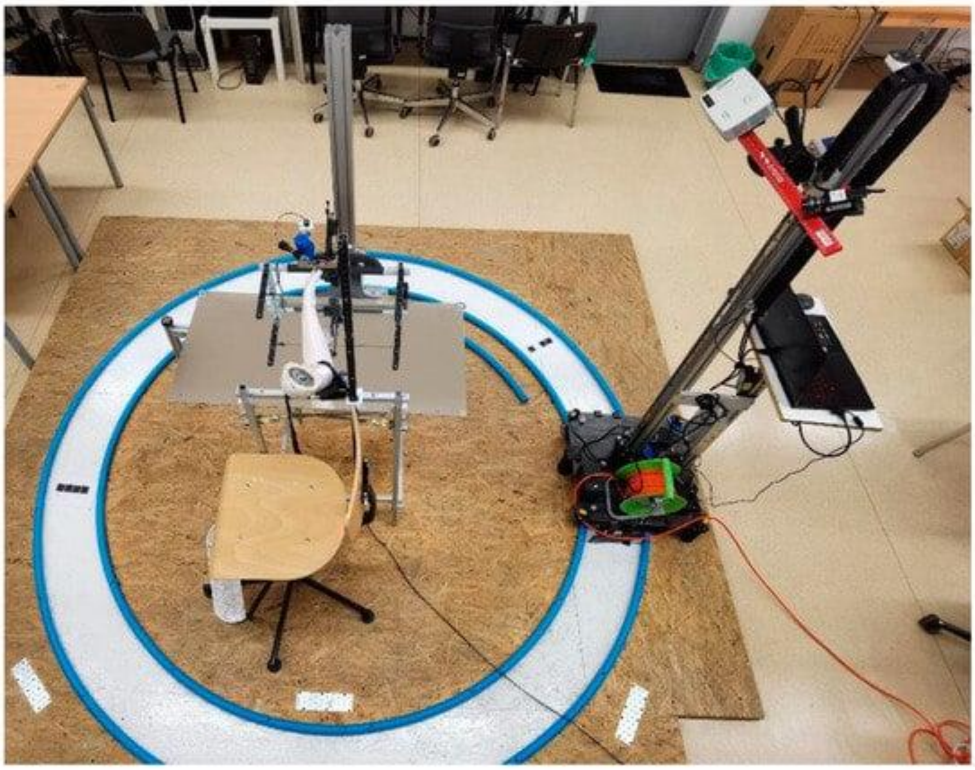

Fig.3.4. Prototype of AutoMedPrint system (scanning rig) [19]

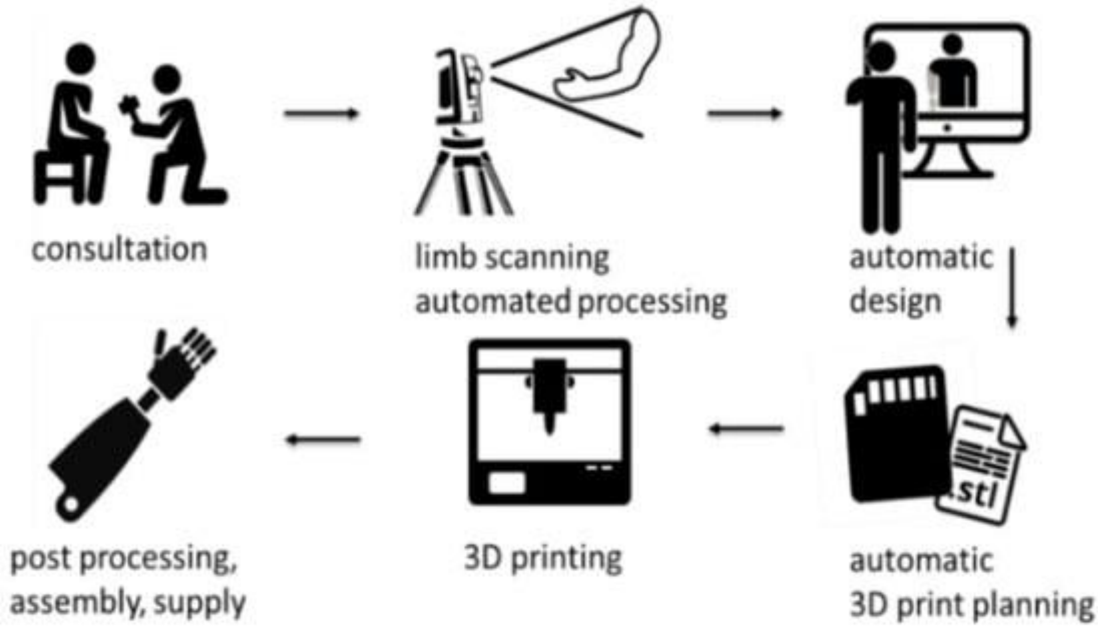

Fig.3.5. Workflow of the AutoMedPrint system [19]

The research presented in this paper was inspired by a 13-year-old boy with congenital paresis, a condition causing partial or complete muscle weakness present at birth due to developmental anomalies or nervous system injuries. This condition limits movement and function in affected areas, making early diagnosis and intervention crucial for improving mobility and quality of life [19].

The patient has restricted mobility in various upper limb joints: limited extension, abduction, and external rotation in the shoulder; minimal flexion in the elbow; and constrained pronation in the distal radioulnar joint with no radial or ulnar movement. Additionally, the wrist joint shows no active extension of the distal radiocarpal joint, impacting daily activities and requiring specialized rehabilitation [19].

The therapeutic orthosis design was based on 3D anatomical scans of the patient's arms. The healthy left arm was scanned in a neutral position using the David SLS-3 scanner, while the right arm was scanned in a comfortable position using the EinScan Pro 3D scanner. The scanned meshes were then digitally merged, with the healthy left arm mirrored and scaled to fit the right forearm (Fig. 3.6.) [19].

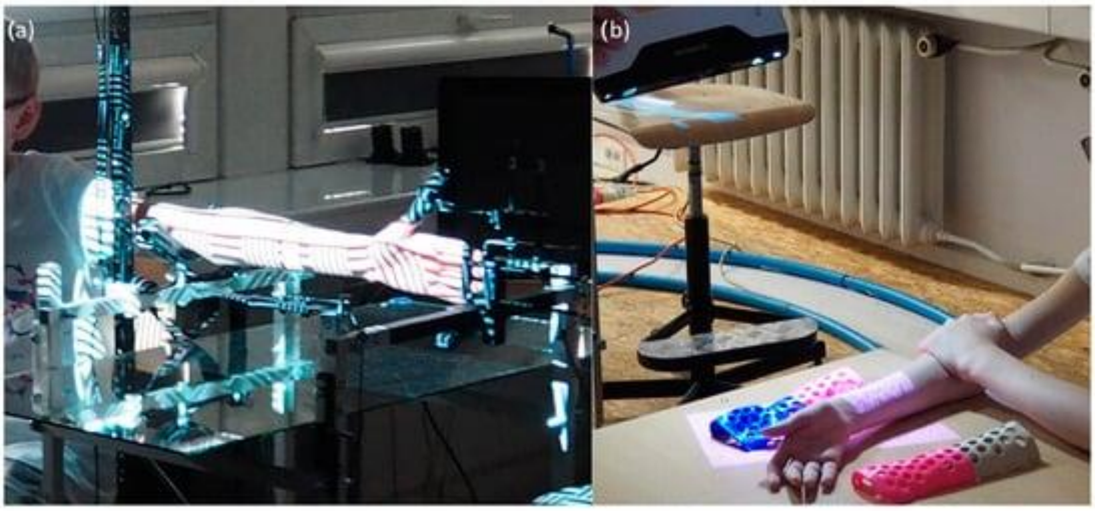

Fig.3.6. Scanning of the patient, (a) left arm—mechanized rig, (b) right arm—manual scan [19]

For the resulting hand model, data extraction was performed using automated MeshLab and MS Excel macros from the AutoMedPrint system. A design table in MS Excel was created, detailing 11 planes of the arm with 16 points per plane. The orthosis design included a 3 mm offset for lining and a default thickness of 4 mm for durability, with additional cutouts for daily activities and exercises [19].

The orthosis was manufactured using FlashForge Creator Pro 3D printers with FFF (FDM) technology, printed with PLA material at a layer thickness of 0.25 mm and 30% infill, taking approximately 4 hours per part. Post-processing included grinding and lining the interior with foam. The patient used the orthosis for 9 months, showing slight improvement in movement and muscle development. Due to growth, a new orthosis was made after re-scanning the patient. The orthoses are shown in Fig. 3.7. a,b and the case was detailed in previous studies by the authors [19].

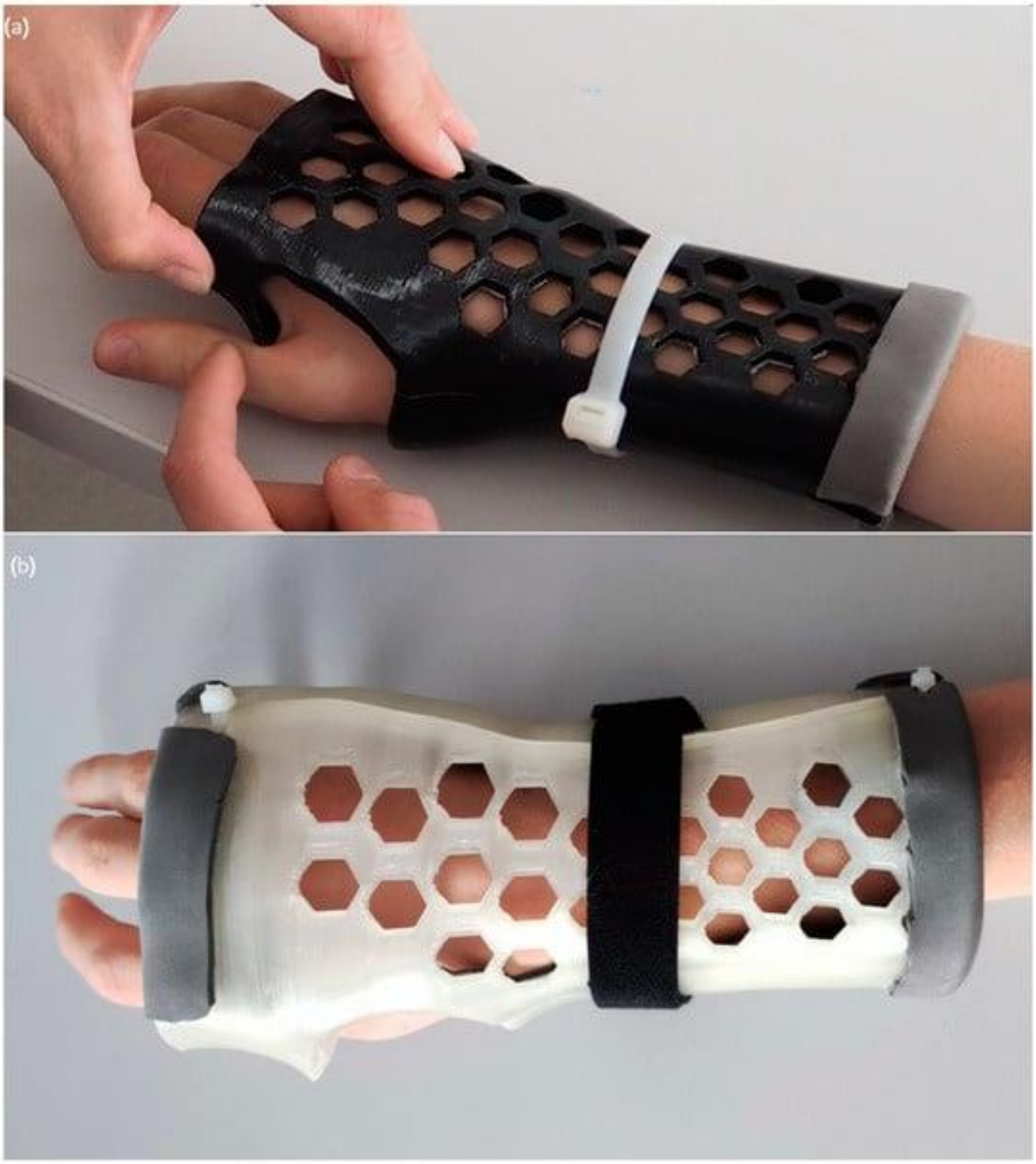

Fig.3.7. Customized therapeutic orthosis: (a) first version, and (b) second version (10 months later) [19]

The orthosis was largely successful, enhancing the patient's functionality. To make therapy more engaging, gamification in virtual reality was introduced. To facilitate prototype development, another orthosis was made for one of the system's creators. The design and printing process was repeated for this new orthosis, as shown in Fig. 3.8., using the same parameters and materials. This orthosis was then used for further development of the electronics and VR application, detailed in the following sections [19].

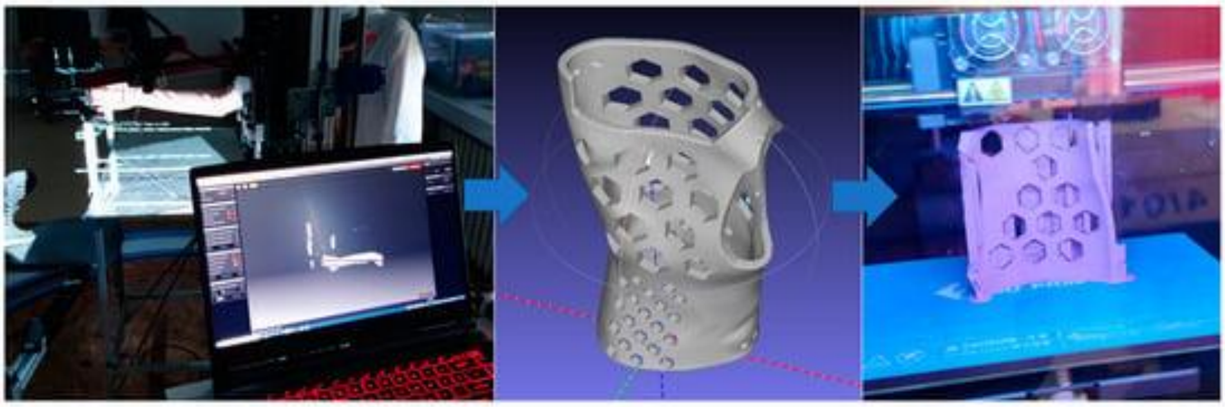

Fig.3.8. Customized therapeutic orthosis design and production for the purpose of VR system prototyping [19]

The study introduced a specialized application designed to support physical therapy exercises within a virtual reality (VR) environment. By leveraging the immersive and interactive nature of VR, the application allows patients to engage in tailored rehabilitation exercises more effectively. The virtual setting not only enhances patient motivation by making exercises more engaging and visually stimulating but also provides real-time feedback on movements, ensuring proper form and technique during therapy sessions. Additionally, the application offers customizable exercise routines that can be adapted to individual patient needs, making it a versatile tool for various stages of rehabilitation. This innovative approach accelerates the recovery process by combining traditional rehabilitation with the advanced capabilities of virtual reality technology, allowing patients to make faster and more consistent progress.

4. Conclusions

Reverse engineering refers to the process of analyzing and replicating an object, artifact, or software that lacks adequate documentation to uncover its design, materials, specifications, or functions. This method involves thoroughly examining a system or component to gain insight into its structural and functional elements. The process often begins with capturing precise digital measurements of the component, typically using optical scanners (non-contact methods) or coordinate measuring machines (CMMs, contact methods). These measurements result in point cloud data, which are then used to create a detailed 3D model through CAD/CAM/CAE or similar software.

Reverse engineering is especially useful when design modifications are necessary for a product that no longer has its original CAD model available. Additionally, it plays a vital role in inspecting and analyzing complex geometries for wear and tear, where manual inspection would be challenging, labor-intensive, and costly. The process also supports competitive benchmarking, providing companies with valuable insights into their competitors' design strategies, materials, and manufacturing processes.

In the medical field, reverse engineering has proven to be indispensable. It enables the creation of highly accurate simulations of medical implants and prosthetics before they are introduced into the human body. By testing and optimizing designs digitally, medical professionals can save both time and costs, while potentially improving patient outcomes. For instance, reverse engineering can be used to craft custom implants that fit individual patients' anatomy perfectly, thus improving success rates in surgical procedures.

The overarching goal of reverse engineering is to reduce lead times and shorten manufacturing cycles by speeding up the product development process. In a fast-paced, competitive market, where innovation is key, businesses are increasingly adopting reverse engineering techniques to refine their products and gain a competitive edge. This approach accelerates the prototyping and testing phases, allowing for quicker market introduction of new or improved products.

However, while reverse engineering offers numerous advantages, there is still room for improvement in terms of efficiency and precision. The algorithms used in reverse engineering need continuous refinement to minimize inaccuracies and ensure higher fidelity in the final 3D models. Enhanced precision will lead to better results and open new avenues for applying reverse engineering in fields such as aerospace, automotive, and healthcare.

By continually advancing reverse engineering methods, industries can produce higher-quality products, reduce errors in design, and improve innovation timelines, ensuring that reverse engineering will play an increasingly critical role in the future of manufacturing and technology development.

4. *References*

1. Eyup Bagci, Reverse engineering applications for recovery of broken or worn parts and re-manufacturing: Three case studies. Advances in Engineering Software 40 (2009) 407–418.
2. E. Lindskog, J. Berglund, J. Vallhagen, B. Johansson, Procedia CIRP 44 (2016) 126–131.
3. V. Raja, Introduction to Reverse Engineering, In: Reverse Eng., V. Raja and J. K. Fernandes, Eds., London, Springer, (2007), 1-9.
4. Z. Geng, B. Bidanda, Review of reverse engineering systems - current state of the art, Virtual Phys. Prototyping 12 (2) (2017) 161–172.
5. Robin H. Helle, Hirpa G. Lemu, A case study on use of 3D scanning for reverse engineering and quality control. Materials Today: Proceedings 45 (2021) 5255–5262.
6. L. Li, N. Schemenauer, X. Peng, Y. Zeng, P. Gu, A reverse engineering system for rapid manufacturing of complex objects, Robotics and Computer-Integrated Manufacturing. 18, 1, (2002) 53-67.
7. T. Várady, R. R. Martin, J. Cox, Reverse engineering of geometric models, Computer-Aided Design. 29, 4 (1997) 255-268.
8. Brajlih, T., Tasic, T., Drstvensek I., Valentan B., Pogacar, V., Balic, J., Acko, B.: Possibilities of using three-dimensional optical scanning in complex geometrical inspection. Strojniski vestnik - Journal of Mechanical Engineering, vol. 57, 11, (2011) 826-833.
9. Lokesh, K., Jain, P.K.: Selection of rapid prototyping technology. Advanced production Engineering & Management, vol. 5, 2 (2010), 75-84
10. Yasa, E., Kruth, J.: Aplication of laser re-melting on selective laser melting parts. Advanced production Engineering & Management, vol. 6, 4 (2011), 259-270.

11. Technological documentation for EOS Formiga P100 machine, Munchen Germany: EOS, 2008.
12. Technological documentation for ATOS GOM II optical scanner, Braunschweig, Germany: GOM, 2007.
13. 3D Scanning Gallery for Industry Applications: [Internet]. 3D Solutions.Avaliable at: http://www.3d3solutions.com/resources/ [22.5.2013]
14. Characteristics Polyamide:[Internet]. Moldkar. Avaliable at: http://moldkar.com/materials.pdf [22.5.2013]
15. EOS Series. Avaliable at: http://www.bibus.hu/fileadmin/product_data/eos/documents/ eos_series_formiga_p_100_catalogue_en.pdf [22.5.2013]
16. FORMIGA P110-laser sintering 3D printer for rapid prototyping-EOS: [Internet]. EOS Manufacturing solutions Avaliable at: http://www.eos.info/systems_solutions/plastic/ systems_equipment/formiga_p_110 [22.5.2013]
17. Matej Paulic* , Tomaz Irgolic,Joze Balic, Franc Cus, Andrej Cupar, Tomaz Brajlih, Igor Drstvensek, Reverse Engineering of Parts with Optical Scanning and Additive Manufacturing. Procedia Engineering 69 (2014) 795 – 803.
18. Górski, F.; Rybarczyk, D.; Wichniarek, R.; Wierzbicka, N.; Kuczko, W.; ˙ Zukowska, M.; Regulski, R.; Pacurar, R.; Comsa, D.-S.; Baila, D.-I.; et al. Development and Testing of an Individualized Sensorised 3D Printed Upper Limb Bicycle Prosthesis for Adult Patients. Appl. Sci. 2023, 13, 12918.
19. Górski, F.; Grohs, A.; Kuczko, W.; Zukowska, M.; ˙ Wichniarek, R.; Siwiec, S.; Bˇailˇa, D.-I.; Zelenay, M.; Pˇacurar, R.; Sanfilippo, F. Development and Studies of VR-Assisted Hand Therapy Using a Customized Biomechatronic 3D Printed Orthosis. Electronics 2024, 13, 79.

Co-funded by the
European Union

AMAZE

Erasmus+ Programme Key Action 2 Cooperation Partnerships
for Higher Education (KA220-HED)
Agreement number 2023-1-RO01-KA220-HED-000155412
European Network for Additive Manufacturing in Industrial Design for Ukrainian Context

e-Toolkit
Computer Programming

Project Title	**European Network for Additive Manufacturing in Industrial Design for Ukrainian Context** **2023-1-RO01-KA220-HED-000155412**
Output	**IO2 - AMAZE e-toolkit manual for digital learning in producing complex design industrial parts**
Module	**Module 5** **Computer Programming**
Date of Delivery	**June 2024**
Authors	**Beatriz Gloria BONILLA GARCÍA, César Arcadio BONILLA GARCÍA, Sergio VIZCAINO**
Version	**FINAL VARIANT, *14.06.2024***

Co-funded by the European Union

AMAZE

Contents

.

1 Additive Manufacturing

Additive manufacturing, also known as 3D printing, has revolutionized the production of objects and components across various industries. A fundamental aspect of this technology is the programming and code that control 3D printers. In this context, various programming languages and software are used to design models, generate print paths, and optimize the manufacturing process. Below is an extensive exploration of how programming integrates into additive manufacturing, with practical examples illustrating key principles and techniques.

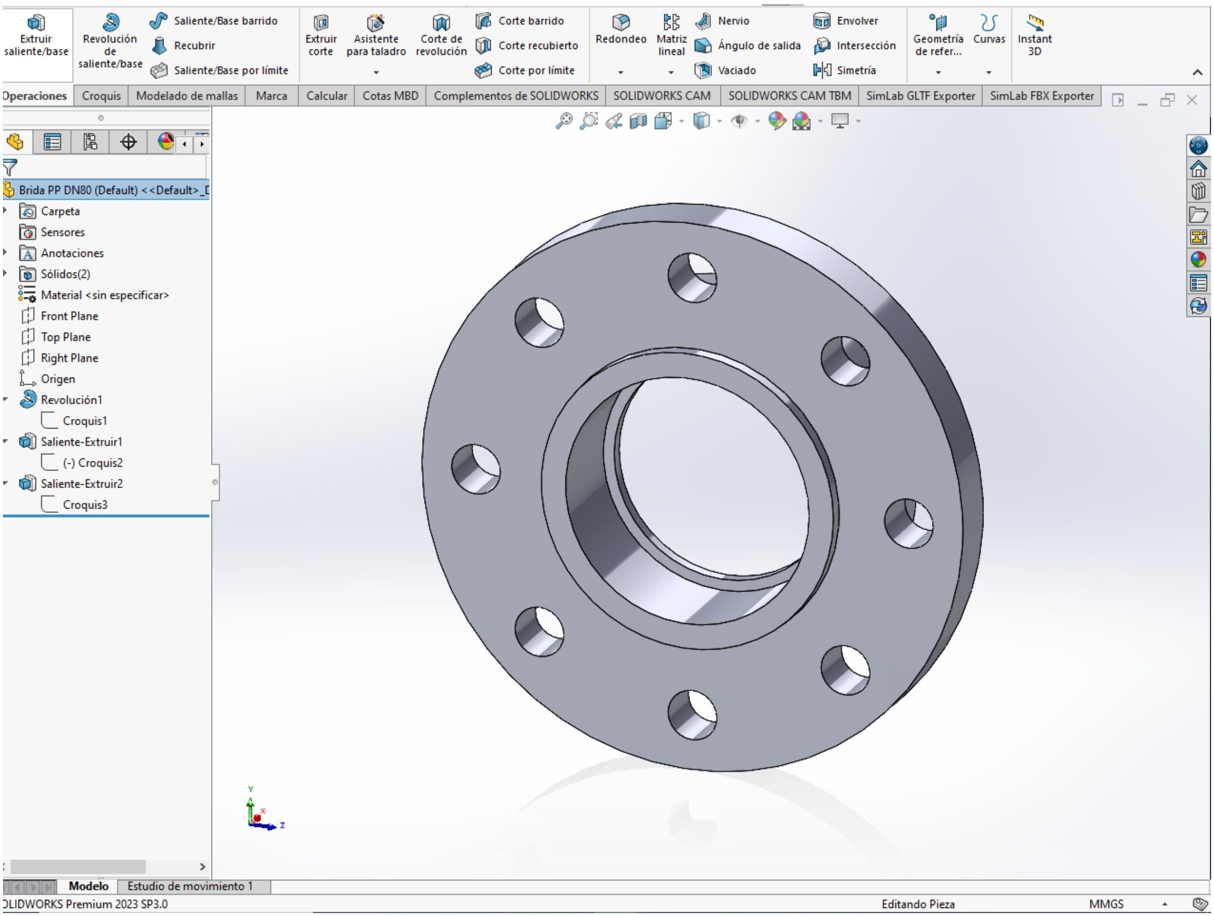

1.1 Basic Concepts of Additive Manufacturing and Programming

Additive manufacturing is based on the principle of building objects layer by layer from a digital model. The process begins with computer-aided design (CAD), which is translated into a format understandable by the 3D printer, typically an STL (Standard Tessellation Language) file. This file is then converted into specific instructions for the printer through a process called "slicing."

Programming Languages Used

1. G-Code: The most common programming language for 3D printers is G-Code. This language controls the movement of the printer, the temperatures of the nozzles and print beds, and other crucial parameters. Each line of G-Code represents a specific instruction, such as moving the nozzle to a certain position or extruding a specific amount of material.

2. Python: Often used to develop scripts that automate and optimize different aspects of the printing process. Python is particularly useful in creating custom tools for pre-processing and post-processing STL files.

3. JavaScript: Used in web applications and cloud-based 3D printing environments. Tools like OctoPrint, which allow remote control of 3D printers, are written in Python but also make extensive use of JavaScript for the user interface.

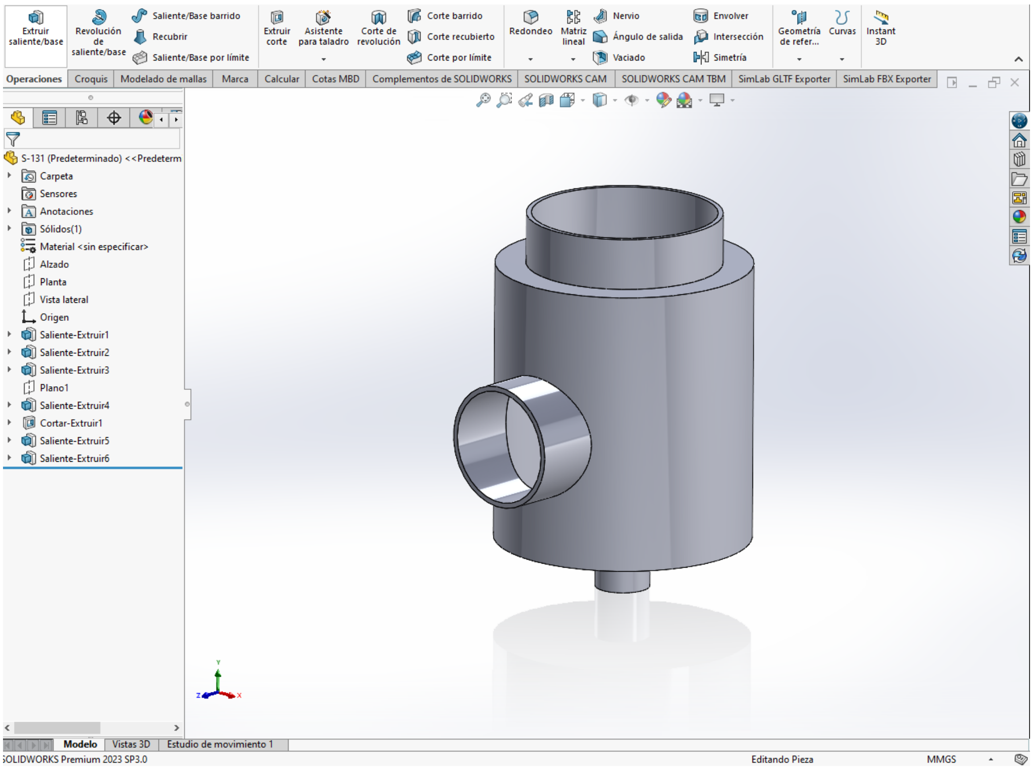

1.2 Practical Example: Generating G-Code with Python

Imagine we want to write a Python script that generates G-Code for a simple cube. The goal is to understand how a three-dimensional object is translated into step-by-step printing instructions.

```python

```
def generate_gcode_cube(size, layer_height, extrusion_width):
    gcode = []

    # Initialization
    gcode.append("G21 ; set units to millimeters")
    gcode.append("G90 ; use absolute coordinates")
    gcode.append("M82 ; use absolute distances for extrusion")

    # Printing parameters
    gcode.append("M104 S200 ; set extruder temperature to 200")
    gcode.append("M140 S60 ; set bed temperature to 60")
    gcode.append("G28 ; home all axes")
    gcode.append("G1 Z5 F5000 ; lift nozzle")
    gcode.append("G92 E0 ; reset extrusion distance")

    # Wait for heating
    gcode.append("M109 S200 ; wait for extruder temperature")
    gcode.append("M190 S60 ; wait for bed temperature")

    # Print cube
    num_layers = int(size / layer_height)
    for layer in range(num_layers):
        z_height = layer * layer_height
        gcode.append(f"; Layer {layer}")
        gcode.append(f"G1 Z{z_height:.2f} F1000 ; move to layer height")

        for _ in range(4):
```

```
        gcode.append(f"G1 X{size} Y0 F1500 ; move to X{size} Y0")
        gcode.append(f"G1 X{size} Y{size} ; move to X{size} Y{size}")
        gcode.append(f"G1 X0 Y{size} ; move to X0 Y{size}")
        gcode.append(f"G1 X0 Y0 ; move to X0 Y0")
        gcode.append(f"G92 E0 ; reset extrusion distance")
        gcode.append(f"G1 E{extrusion_width:.4f} F300 ; extrude material")

    # Finalization
    gcode.append("G28 ; home all axes")
    gcode.append("M104 S0 ; turn off extruder")
    gcode.append("M140 S0 ; turn off bed")
    gcode.append("M84 ; disable motors")

    return "\n".join(gcode)

# Generate G-Code for a 20 mm cube with 0.2 mm layers and 1.0 mm extrusion width
gcode = generate_gcode_cube(20, 0.2, 1.0)
with open("cube.gcode", "w") as file:
    file.write(gcode)
```

1.3 Slicing Software and Path Generation

Slicing software is crucial for additive manufacturing as it converts the 3D model into layers and generates the necessary G-Code for printing. Some of the most used programs include:

1. Cura: An open-source software developed by Ultimaker. Cura allows users to adjust numerous printing parameters and visualize the generated print paths.

2. PrusaSlicer: Another open-source software offering advanced features for optimizing prints, including support for multiple materials and customized support configurations.

3. Simplify3D: A commercial software known for its flexibility and advanced path generation capabilities. Simplify3D allows detailed control over every aspect of the slicing process.

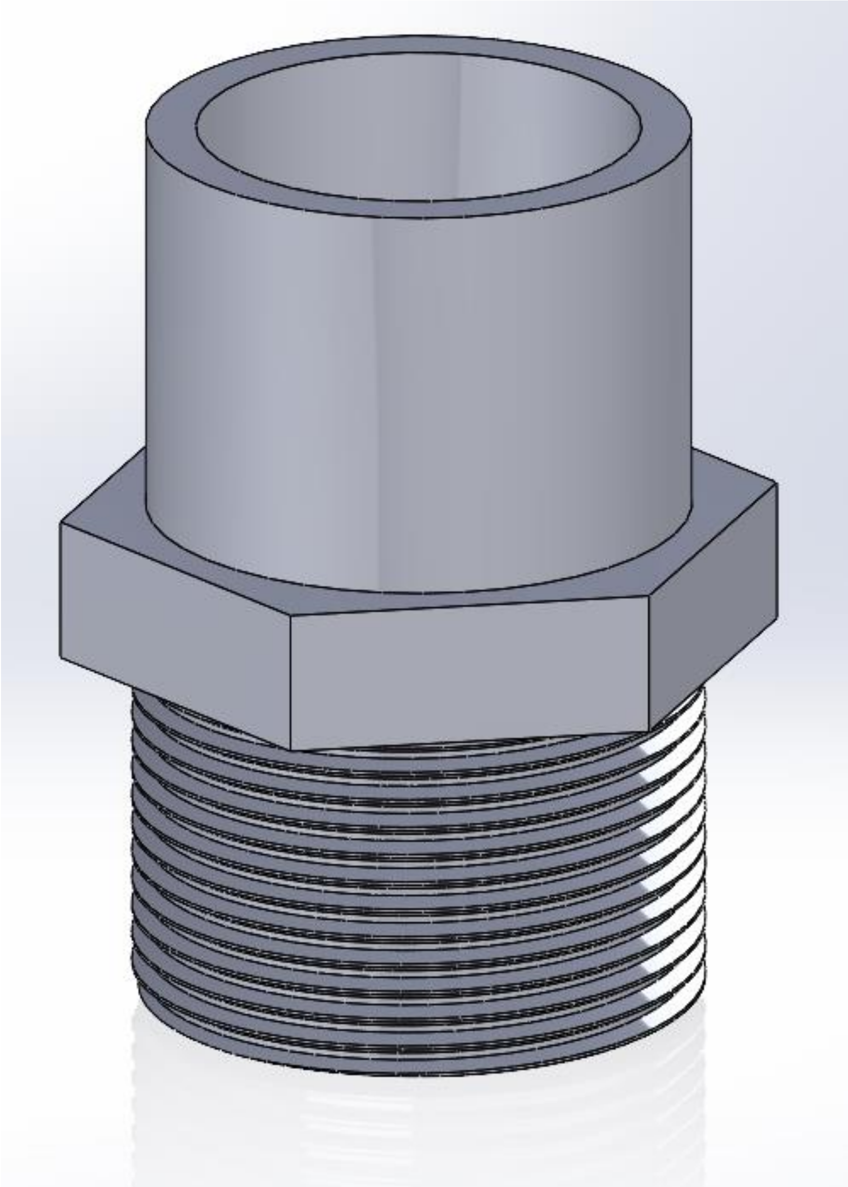

1.4 Practical Example: Configuring Cura for Optimal Printing

Properly configuring slicing software is essential for achieving high-quality prints. Below is an example of how to adjust printing parameters in Cura for a complex object:

1. Layer Height Adjustment:
   - Parameter: Layer Height

- Description: Controls the thickness of each layer. A lower value results in higher resolution but longer print times.
- Example: For a detailed print, set the layer height to 0.1 mm.

2. Infill Density:
- Parameter: Infill Density
- Description: Determines the amount of material inside the object. A higher percentage increases strength.
- Example: Set infill density to 20% for a balance between strength and print time.

3. Print Speed:
- Parameter: Print Speed
- Description: Defines the speed at which the nozzle moves. Lower speeds generally result in better quality.
- Example: Set print speed to 50 mm/s for high-quality printing.

1.5 Optimization and Automation of the Printing Process

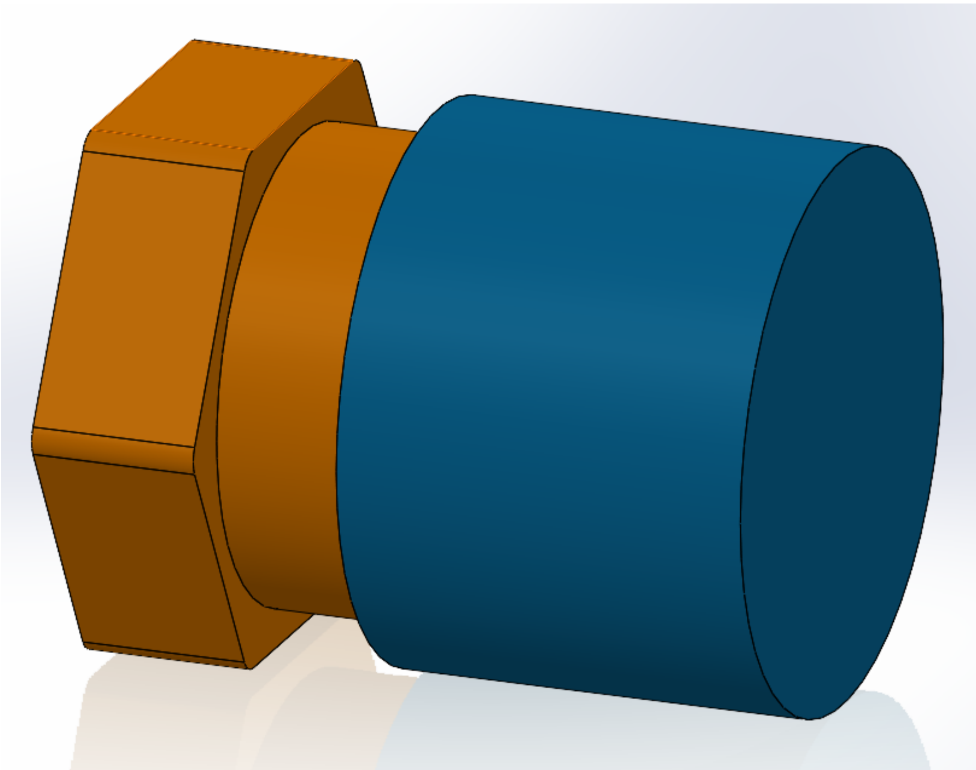

Programming enables not only the creation of efficient print paths but also the automation of various stages of the additive manufacturing process. For example, with custom scripts, users can automate the generation of supports, optimize part orientations, and set up multiple printers for mass production.

1.6 Practical Example: Automation with OctoPrint and Python

OctoPrint is a powerful tool that allows remote control of 3D printers. Below is an example of how to use Python to automate common tasks using the OctoPrint API:

```python
import requests

# OctoPrint API configuration
octoprint_url = "http://localhost:5000"
api_key = "YOUR_API_KEY"

# Function to upload a G-Code file
def upload_gcode(file_path):
    with open(file_path, "rb") as file:
        files = {'file': file}
        response = requests.post(f"{octoprint_url}/api/files/local", files=files, headers={"X-Api-Key": api_key})
        return response.json()

# Function to start a print
def start_print(file_name):
    payload = {"command": "select", "print": True}
    response = requests.post(f"{octoprint_url}/api/files/local/{file_name}", json=payload, headers={"X-Api-Key": api_key})
    return response.json()

# Upload and start printing
file_path = "path/to/your/gcode/file.gcode"
upload_response = upload_gcode(file_path)
```

file_name = upload_response['files'][0]['name']

start_print(file_name)
```

### 1.7. Challenges and Considerations in Programming for Additive Manufacturing

While programming for additive manufacturing offers many advantages, it also presents significant challenges. Error management, precise printer calibration, and material optimization are just a few of the issues that need to be addressed.

1. Error Management: It is crucial to implement mechanisms to detect and correct errors in real-time during printing. This may include using sensors and machine vision algorithms to monitor the printing process.

2. Calibration and Maintenance: The accuracy of 3D printers depends on proper calibration. Automated scripts can help perform regular calibrations and necessary adjustments to maintain print quality.

3. Material Optimization: Programming can also optimize material usage, ensuring minimal waste while maintaining structural integrity and quality.

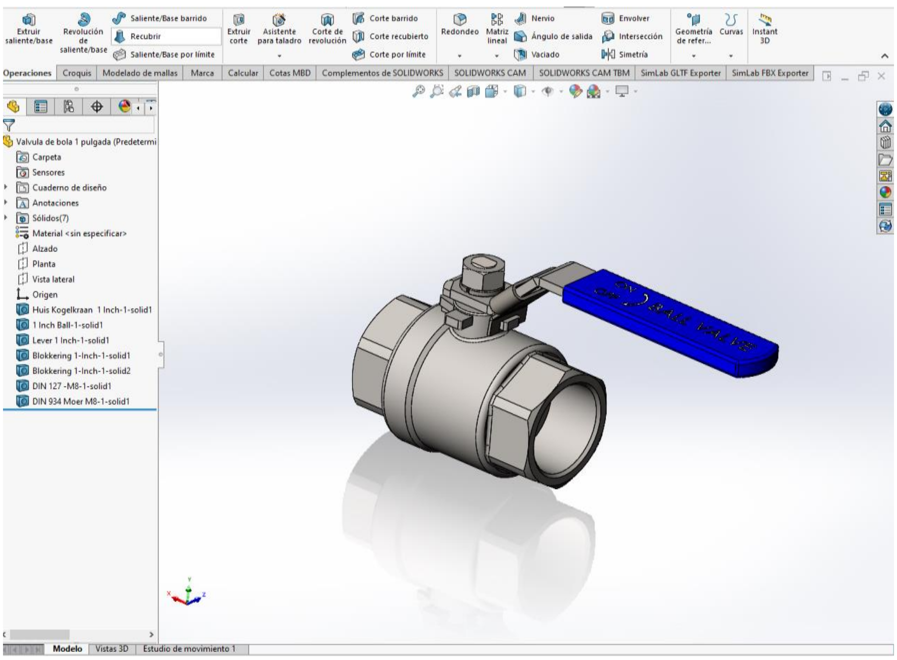
```

2. Examples step by step

2.1 Exercise 1: Designing and Coding a 3D Object

Objective: Create a simple 3D object using code.

Required Tools: OpenSCAD (free CAD software based on code).

Step-by-Step:

- Installing OpenSCAD:

Download and install OpenSCAD from www.openscad.org.

- Introduction to OpenSCAD Code:

OpenSCAD uses a specific programming language to design 3D objects.
Basic example of code for a cube:

```
// Code for a 20x20x20 mm cube
cube([20, 20, 20]);
```

- Creating a More Complex Shape:

Combining geometric primitives (cube and cylinder):

```
// Code for a cube with an embedded cylinder
difference() {
 cube([30, 30, 30]);
 translate([15, 15, -10])
 cylinder(h=50, r=10);
}
```

- Generating the STL File:

Save the design as an STL file that can be used by most 3D printers.

File -> Export -> Export as STL

2.2 Exercise 2: Parametric Design Automation

Objective: create a parametric object that can be adjusted through variables.

Required Tools: OpensSCAD

Step-by-step:

- Defining parameters:

Use variables to define the dimensions of an object:

```
// Defining parameters
base_length = 50;
base_width = 30;
base_height = 10;
hole_diameter = 5;
```

- Using Parameters in the Design:

Create an object that can be easily adjusted by changing the values of the vairables:

```
// Code for a parametric object
difference() {
  cube([base_length, base_width, base_height]);
  translate([base_length/2, base_width/2, -1])
  cylinder(h=base_height+2, r=hole_diameter/2);
}
```

3. Conclusions

Programming is crucial in additive manufacturing, impacting everything from generating G-Code to automating complex printing processes. By using various programming languages and tools, developers can optimize print quality, reduce errors, and enhance overall efficiency. Key benefits include:

Optimizing Print Quality: Custom scripts adjust printing parameters dynamically for high precision and reduced defects.

Reducing Errors: Automated systems detect and correct issues in real-time, minimizing waste and ensuring quality.

Enhancing Efficiency: Sophisticated workflows manage multiple prints, optimize material usage, and streamline processes.

Practical examples, such as using OpenSCAD for parametric modeling and Python for automating slicing, highlight the importance of coding skills in modern manufacturing. As 3D printing technology evolves, programming becomes increasingly valuable, driving innovation and new applications in the field.

4. References

Books

1. “Additive Manufacturing Technologies: Rapid Prototyping to Direct Digital Manufacturing" by Ian Gibson, David W. Rosen and Brent Stucker

2. “Programming 3D Applications with HTML5 and WebGL" by Tony Parisi

3. “Additive Manufacturing: Design, Methods, and Processes" by Steinar Westhrin Killi

Publications

1. "Additive Manufacturing: A Review" in Journal of Manufacturing Science and Engineering

2. "Process Planning for Additive Manufacturing of Functionally Graded Materials" in Procedia CIRP

3. "CAD and Additive Manufacturing" in Materials & Design

Web

1. Additive Manufacturing Research Group Loughborough University

2. 3D Printing Industry

3. All3DP

4. GitHub

Applications in Enterprise Dynamics – 10.3 version

Enterprise Dynamics software teach the students, the basic skills to create their own simulation model and interpret the results. The software has 5 windows:

- *A menu bar*: among others for opening and saving files.
- *The library*: The library includes all atoms a user can place into a model. Each atom has a certain function. By combining the right atoms, it is possible to re-create ('model') a business process in Enterprise Dynamics.
- *The model layout window*: this is where the model is being built.
- *The run control*: use this to reset and start the model and to regulate its execution speed.
- *The clock displays* the simulated time already elapsed during the simulation (not the real time!).

The main menu is to be found in the menu bar, which is subdivided as follows:
File - Make, open or save files, to set preferences and to control standard functions such as printing.
Display - Open viewer and layout windows to display models and to open the library windows with modeling objects.
Simulate - Open a Run Control or Clock window. Design and perform an experiment.
Results - To generate reports and graphics of a single simulation run or evaluate results of an experiment.
Tools - Contains tools such as the 4DScript interact and Autofit to fit a distribution to given data.
Help - Open the documentation, the Example Wizard as well as to find company and versioninformation. Developer Tools useful for developer to create libraries an attribute function
In the Library, exist the Basic Modeling that contain 1-Product, 2-Source, 3-Queue, 4-Server, 5-Sink, 6-Node, 7-Container.

Application 1 – Modelling and simulation of a manufacturing process with 2 machine-buildings.
For the first application, it used 1-product, 2-Source, 3-Queue, 4-Sever and 5-Sink. The process was repeated for the second line. In the model layout, it must realize the arches between atoms, and then we can start the simulation using Run Control, using green triangle. The clock starts to measure the time of simulation, as in Figure 1.
In Figure 2 is presented the command 3D Viewer of the manufacturing process simulation for the 2 machine-buildings.
In Figure 3 is shown the command 3D Builder of the manufacturing process simulation for the 2 machine-buildings.

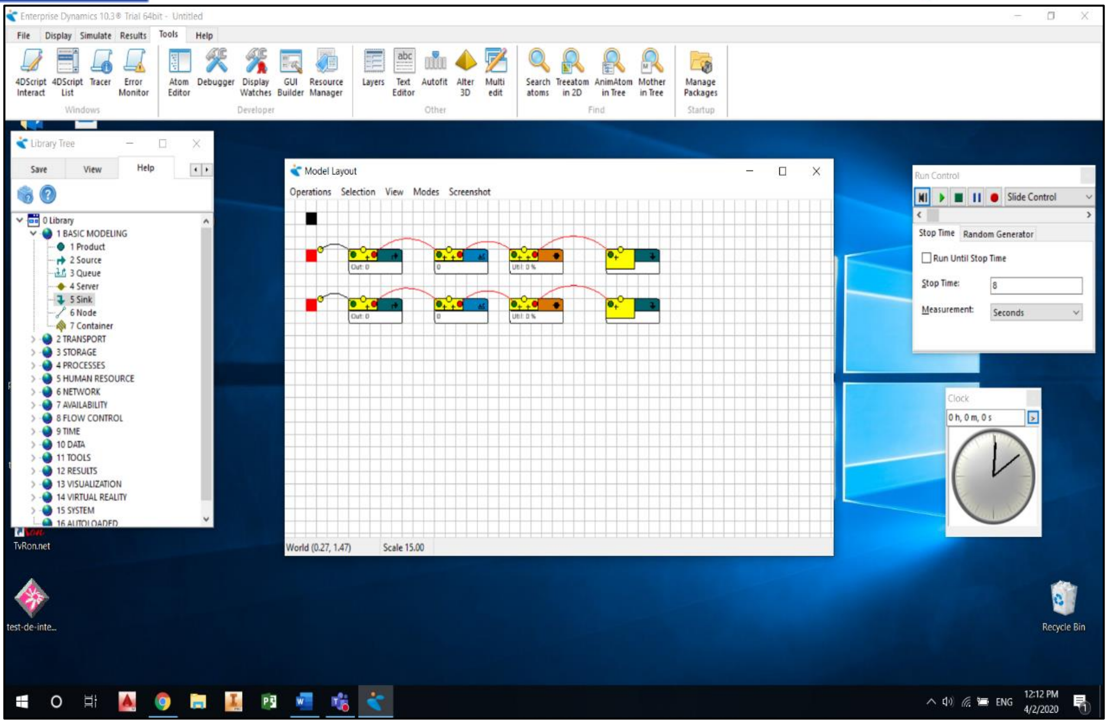

Figure 1. Modelling and simulation of a manufacturing process with 2 machine-buildings

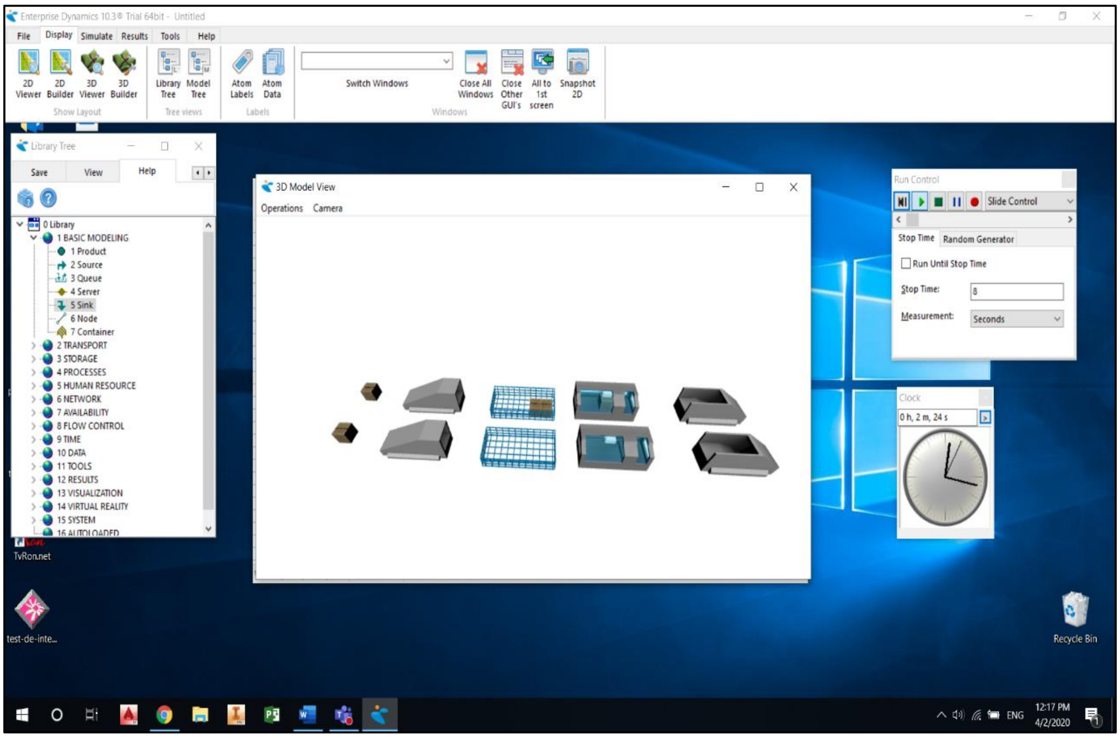

Figure 2. 3D Viewer of the manufacturing process simulation for the 2 machine-buildings

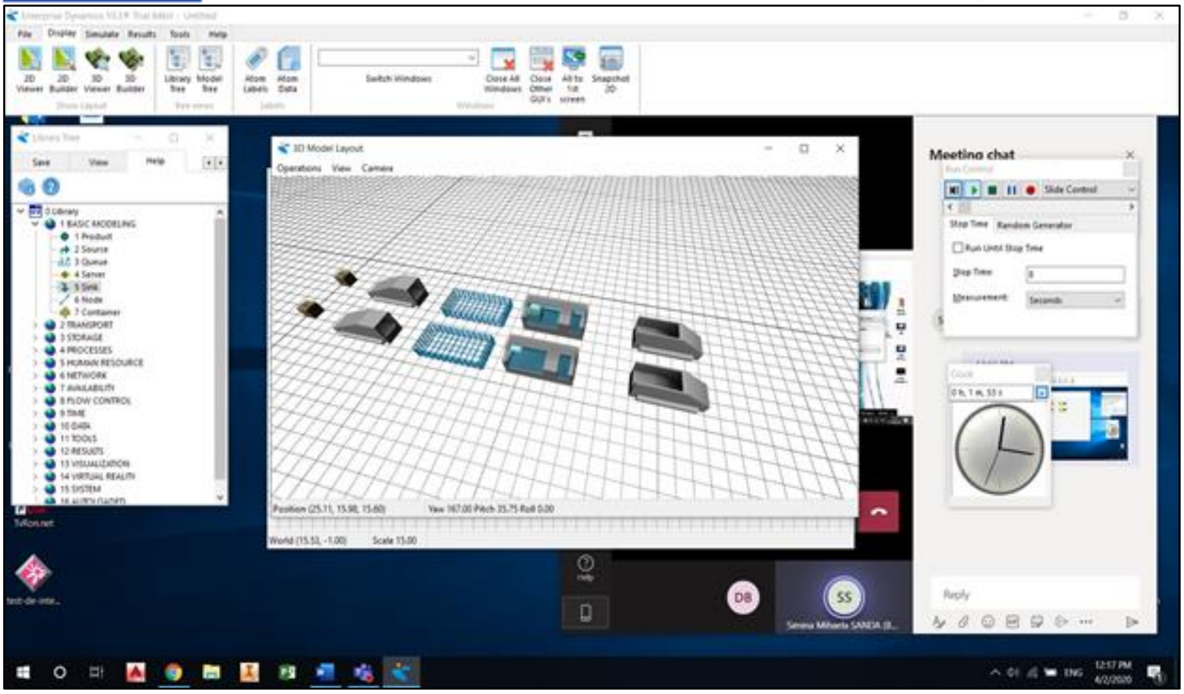

Figure 3. 3D Builder of the manufacturing process simulation for the 2 machine-buildings

Application 2 - Modelling and simulation of a manufacturing process with 3 machine-buildings.
In Figure 4 is presented the modelling and simulation of a manufacturing process with 3 machine-buildings. In this case it used the command Arrival List, when exist 5 products, having the quantity, as in Figure 5.

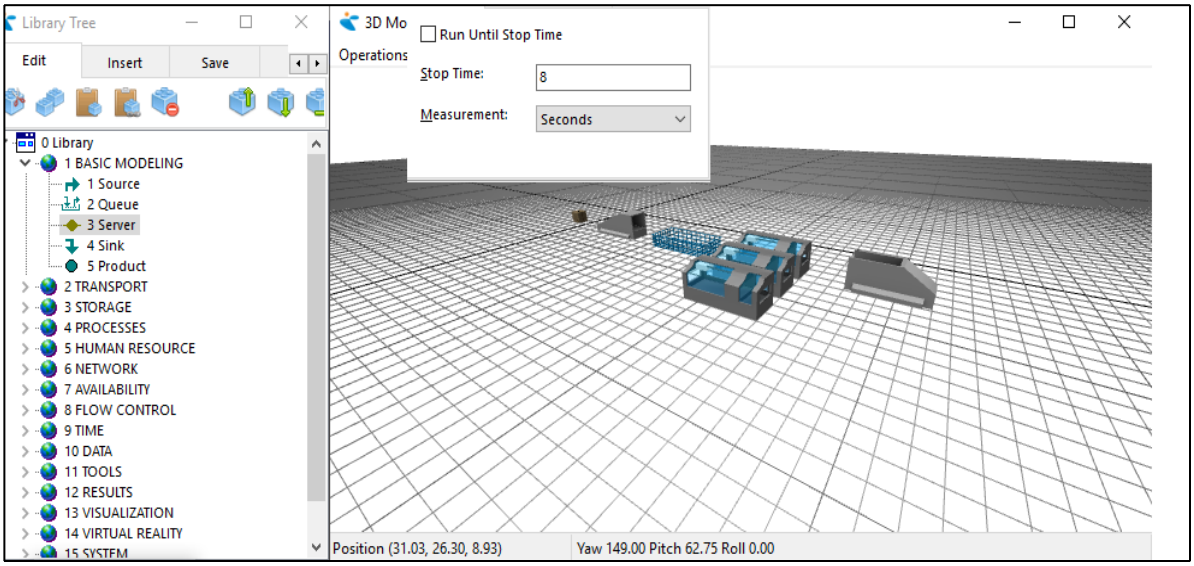

Figure 4. Modelling and simulation of a manufacturing process with 3 machine-buildings

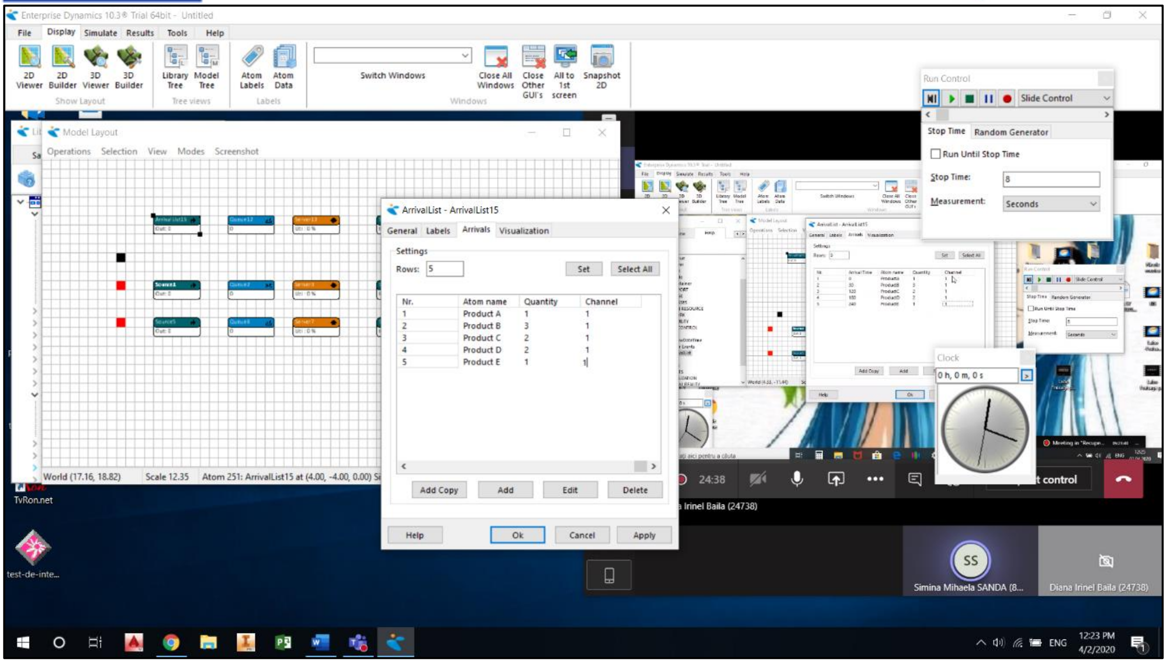

Figure 5. Arrival List, when exist 5 products, having the quantity

For the transport of the products between the machine-buildings, can be used form 2-Transport: 1-conveyors, 2-floorbound, 3-elevation, 4-robots, 5-cranes. In this case, it was used 2-floorbound, and the submenu 2-advanced transporter, as in Figure 6.

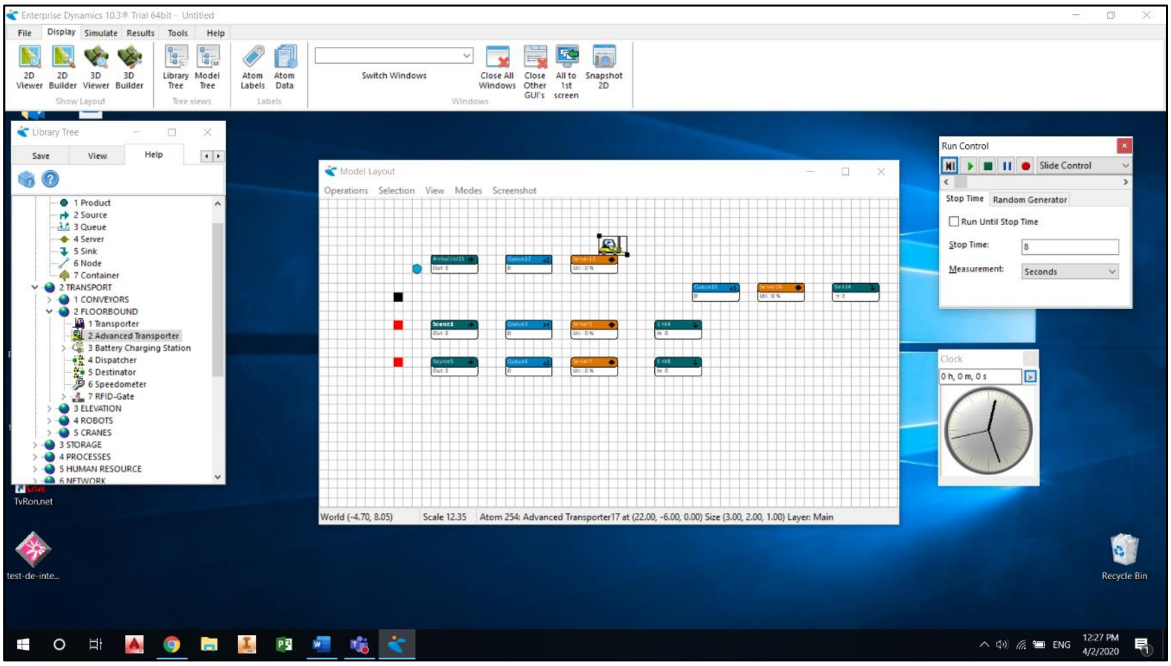

Figure 6. Advanced transporter used for the transport simulation of the products between 2 machine-buildings.

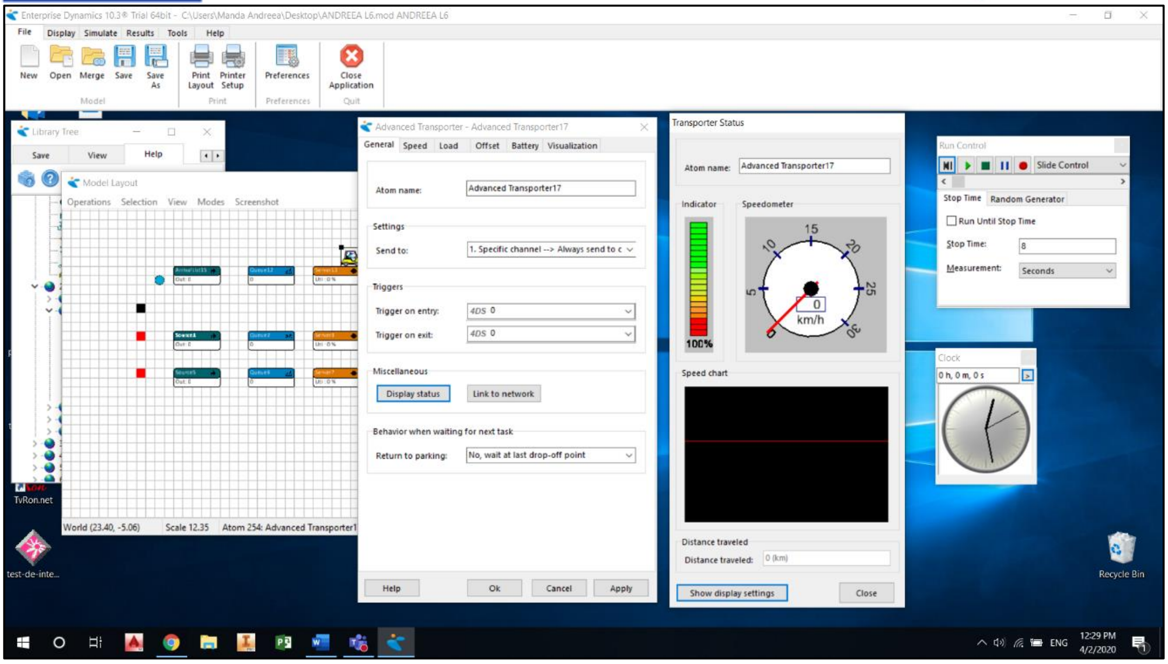

Figure 7. Transporter status with speedometer and distance traveled for Advanced Transporter

In Figure 7 can be see the Transporter status, consisting in speedometer and distance traveled. In Figure 8, it is shown the simulation, using 3D Viewer.

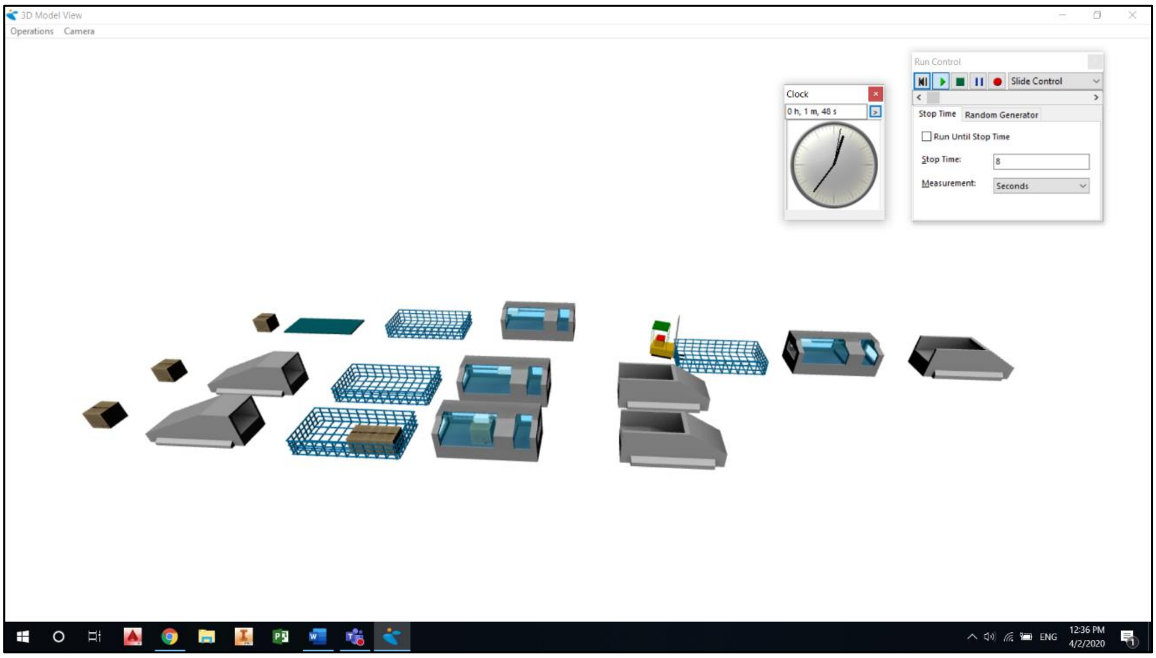

Figure 8. Modelling and simulation a manufacturing process with 4 machine-buildings, using 3D Viewer

In Figure 9, can be shown the modelling and simulation of manufacturing process with 4 machine-buildings, using 3D Builder.

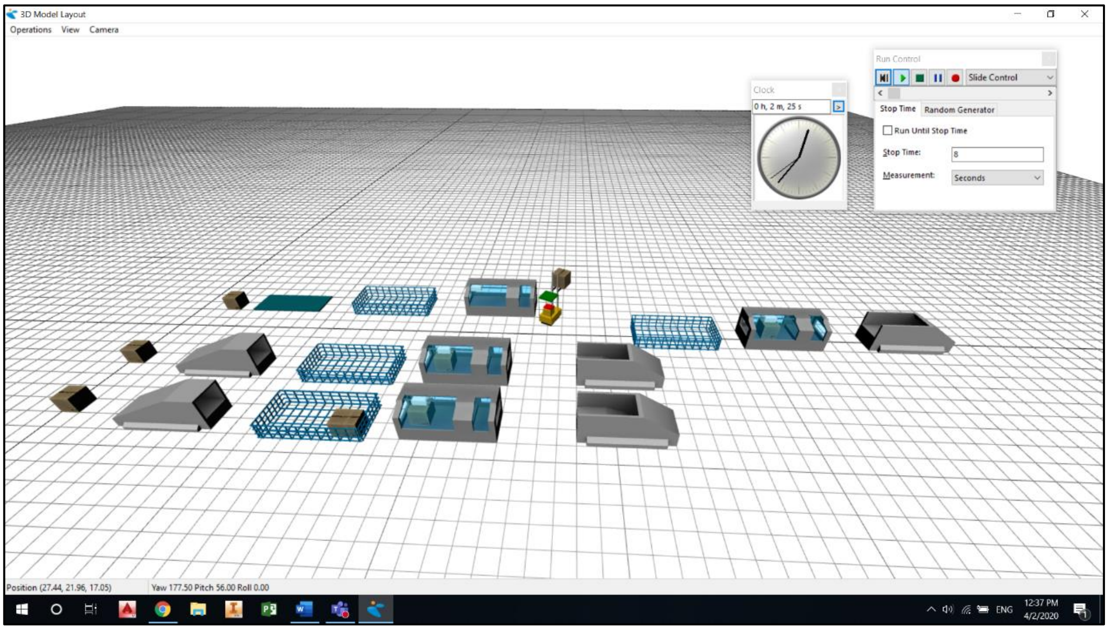

Figure 9. Modelling and simulation of manufacturing process with 4 machine-buildings, using 3D Builder

In the menu Library Tree, exist the submenu 12-Results, and the submenu 1-Status with: 1-Statusindicator, 2-StatusMonitor, 3-StatusHistogram, 4-StatusMonitorStockedBar. For the Gantt diagram can be used the submenu 2-Gantt. In this application, it will be used to see the status of the machine-building, 2-StatusMonitor as in Figure 10.

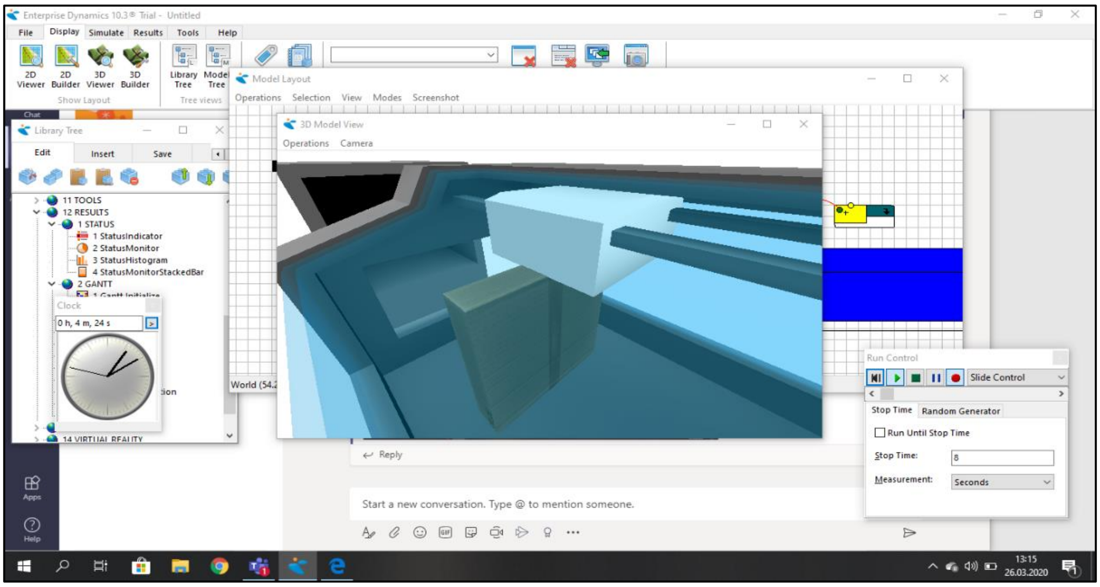

Figure 10. The status of the machine-building, using the menu 12-Results, and the submenu 2-StatusMonitor

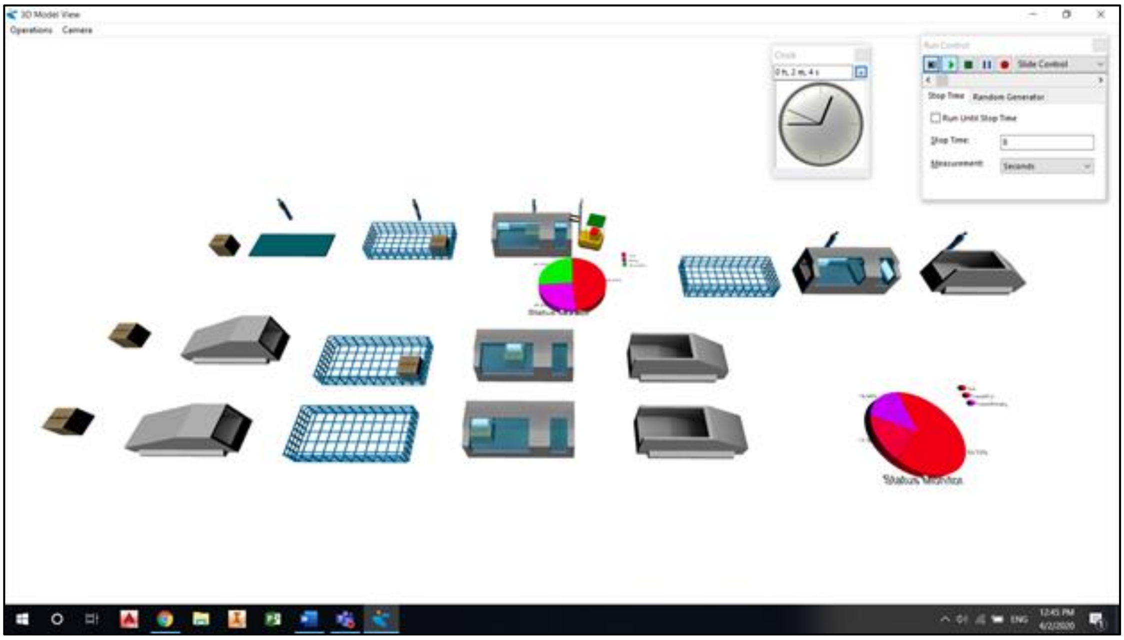

Figure 11. Modelling and simulation of manufacturing process with 4 machine-buildings, visualizing the status monitor, using 3D Viewer

In Figure 11 is remarked the modelling and simulation of manufacturing process with 4 machine-buildings, visualizing the status monitor, using 3D Viewer, and in Figure 12, using 3D Builder.

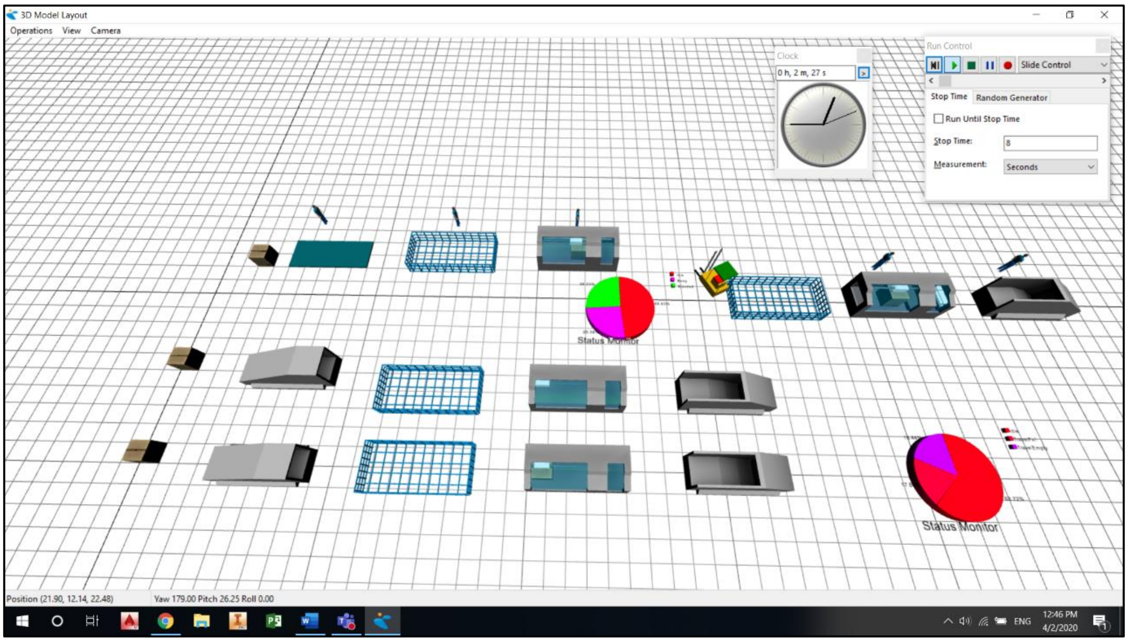

Figure 12. Modelling and simulation of manufacturing process with 4 machine-buildings, visualizing the status monitor, using 3D Builder

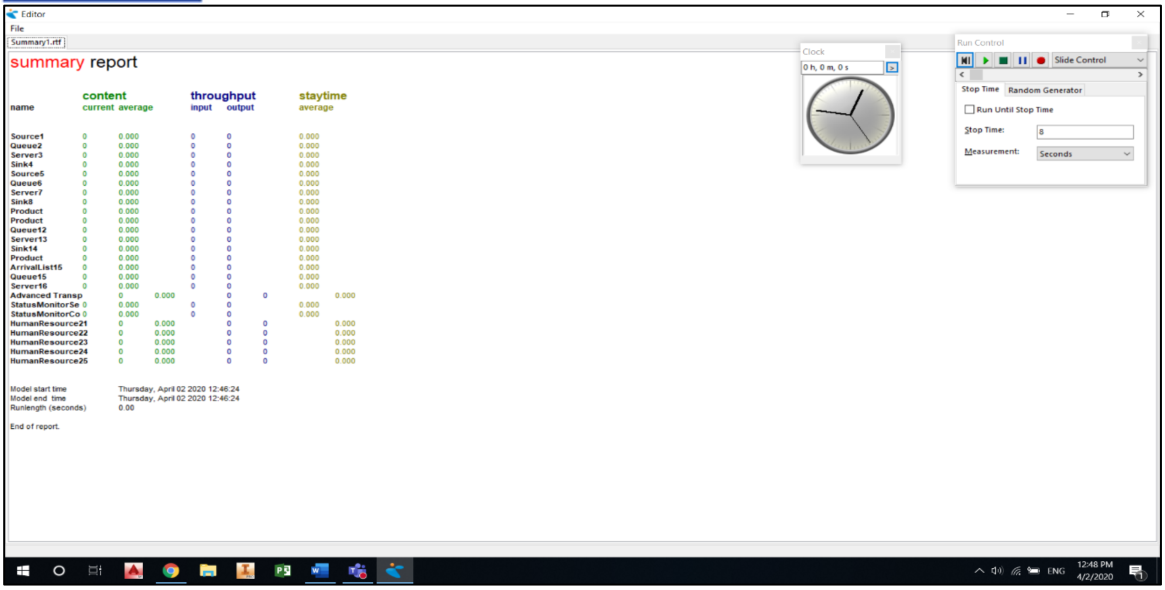

Figure 13. Summary report for the application 2 concerning the modelling and simulation of manufacturing process with 4 machine-buildings

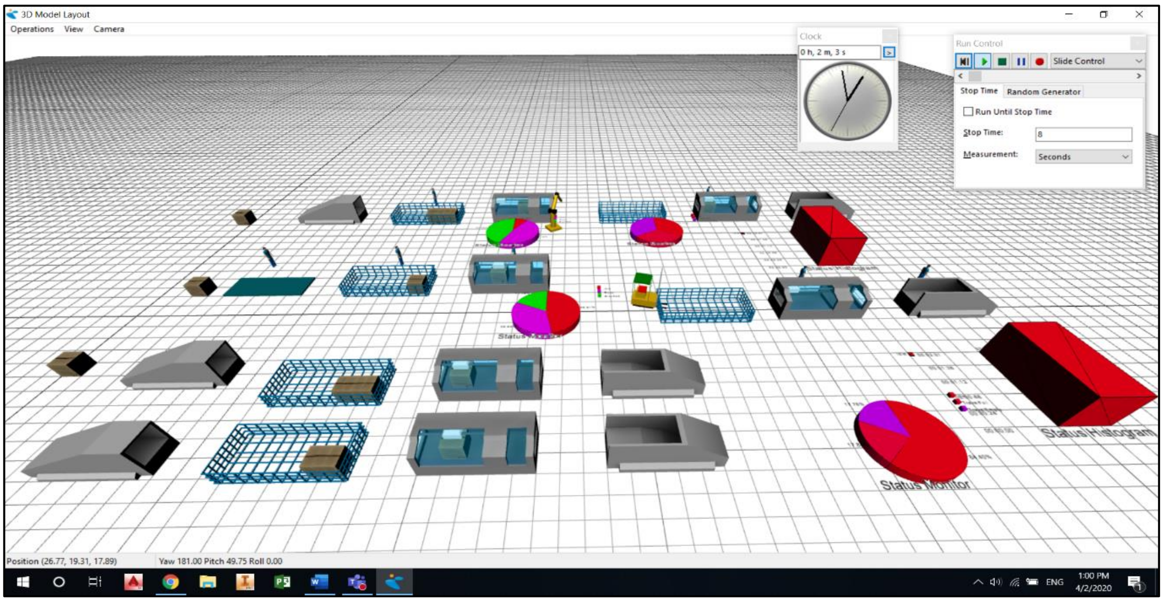

Figure 14. The status of the machine-building, using the menu 12-Results, and the submenu 2-StatusHistogram

In Figure 13 is presented the summary report for application 2 concerning the modelling and simulation of manufacturing process with 4 machine-buildings. In Figure 14 is shown the status of the machine-building, using the menu 12-Results, and the submenu 2-StatusHistogram.

References: [1] Enterprise Dynamics Tutorial - file:///C:/Users/Admin/Downloads/Enterprise%20Dynamics%20Tutorial%20(1).pdf

Co-funded by the European Union

AMAZE

Erasmus+ Programme Key Action 2 Cooperation Partnerships for Higher Education (KA220-HED)
Agreement number 2023-1-RO01-KA220-HED-000155412
European Network for Additive Manufacturing in Industrial Design for Ukrainian Context

e-Toolkit
Sensors and Electronics

Project Title	**European Network for Additive Manufacturing in Industrial Design for Ukrainian Context** **2023-1-RO01-KA220-HED-000155412**
Output	**IO2 - AMAZE e-toolkit manual for digital learning in producing complex design industrial parts**
Module	**Module 6** **Sensors and Electronics**
Date of Delivery	**June 2024**
Authors	**Diana BĂILĂ, Andrei DUMITRESCU, Nicolae IONESCU**
Version	**FINAL VARIANT, *14.06.2024***

Co-funded by the European Union

AMAZE

Contents

1. *Hybrid 3D Printing of soft electronics*

Hybrid 3D printing is a new innovative technology to manufacture soft electronics by combining direct ink writing of conductive and dielectric elastomeric materials with automated pick-and-place of surface mount electronic components within an integrated additive manufacturing platform. Using this approach, insulating matrix and conductive electrode inks are directly printed in specific layouts.

Then, the passive and active electrical components are integrated to manufacture the desired electronic circuitry by using an empty nozzle (in vacuum-on mode) to pick up individual components, introduce them onto the substrate, and then deposit them (in vacuum-off mode) in the desired location, as in Figure 1. Then, the interconnection of components are via printed conductive traces to yield soft electronic devices that can be used for application in wearable electronics, soft robotics, and biomedical devices.

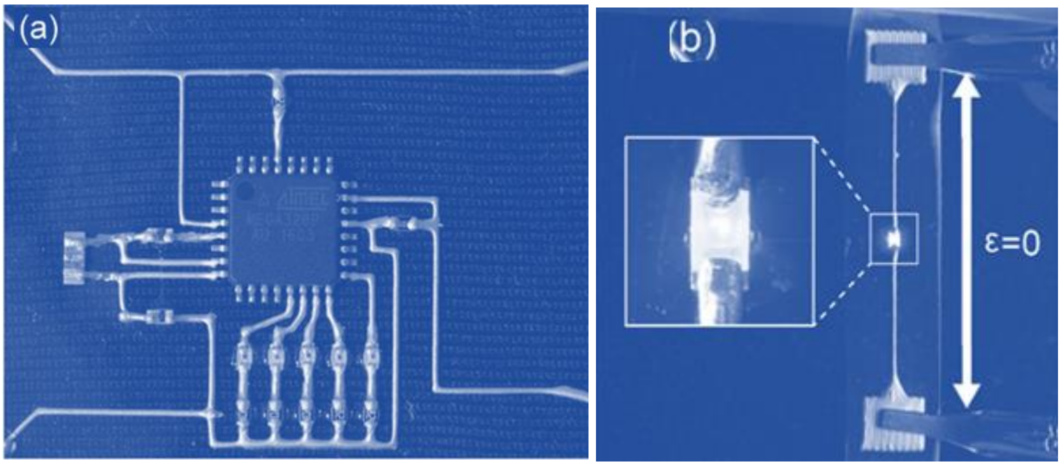

Fig.1. a) Image of microcontroller circuit fabricated by hybrid 3D printing, in which surface mount electrical components are interconnected with printed AgTPU electrodes onto an underlying TPU matrix. b) Image of hybrid 3D printed LED device; the inset shows interface of surface mount LED with the AgTPU electrodes.

Over the past decade, additive manufacturing has seen significant advancements, leading to an increase in the production of affordable hybrid 3D printers. These 3D hybrid printers are equipped with interchangeable heads, allowing for various processes such as 3D printing, CNC cutting, laser engraving, or deposition of pasty materials.

In this study, a prototype of a hybrid 3D printer DIY (Do It Yourself) was developed, and was equipped with g-code software necessary for 3D printing process and for CNC cutting.

The materials used for construction for this hybrid 3D printer were very cheap and accessible and some of electronic components are reused and recovered from old equipment and the functional 3D hybrid printer obtained can be a model for sustainability of products.

The research aimed to create a 3D hybrid printer prototype, incorporating recycled and recovery of stepper motors and different electronics components from old equipment, enabling sustainable of product development. Hybrid 3D printers are multifunctional printers that will replace traditional 3D printers in the future or min-CNC and will be finding in most households, because of their varied functionality. A hybrid 3D printer ZMorph is presented in figure 1. [1-10]

Fig. 2. Interchangeable heads of 3D Hybrid Printer

Hybrid 3D printers are equipped with several interchangeable heads: as simple 3D print head, 3D dual head, CNC head, laser engraving head and ceramic material deposition head, as in the Figure 2.

Fused Deposition Modeling technology (FDM) uses a variety of filament-like materials of PLA, ABS, nylon, etc. [2] The mechanical strength of the manufactured parts is very good, often existing 3D printers that are sold with 3D printed components in their composition. [3] Hybrid 3D printers used this technology for printing 3D parts.

The mechanical strength of the 3D printed parts is very good, often existing 3D printers that are sold with 3D printed components in their composition.

The hybrid prototype 3D printer made in this research also has in its composition, 3D printed parts, 3D printed directly on itself, like the red brackets of the printed table and the head CNC components.

FDM technology is based on the materialization of a CAD product by adding successive layers. The object is saved in the stl. file to be used by 3D printer software. This technology permits the building supports necessary for the 3D printed parts. [1-10]

The prototypes obtained by FDM technology, do not require any additional post-processing treatments and can be used immediately, presenting a high-quality surface.

The Additive Manufacturing technology helps identify any problems that may arise in the design and conception. [1-10]

ZMorph printer can print layers up to 50 microns. ZMorph 3D hybrid printer is equipped with five interchangeable heads allowing printing, milling, drilling and engraving materials widely. The manufacturing dimensions of ZMorph printer are 300x235x165 mm. The manufactured materials of this printer are very different from PLA, ABS, special filaments wood, etc. The software used of this printer is Voxelizer. The price of a hybrid 3D printer is quite high, around 4000 euros. This research tries to realize a low cost hybrid 3D printer, around 500 euros, that will be using for didactic and researches experiments. [1-10]

2. *Electronic components used for the manufacture of 3D hybrid printer, type DIY (do it yourself)*

The experimental research consists of manufacturing a hybrid 3D printers DIY (do it yourself), low cost, using readily available cheap materials and tools.

Fig 3. Structure design of 3D printer. Fig 4. Cutting and drilling of the plates

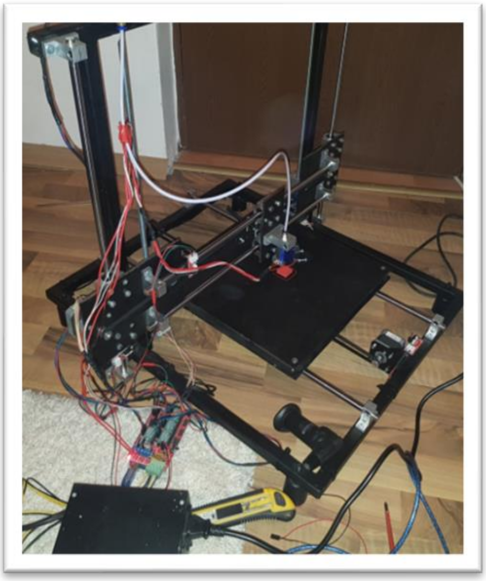

Fig 5. Assembly and welding of 3D printer parts.

For the design steps, it was considered the sizing of structural elements depending on the size of standard components used (clamps catching SK10, SK16, bearings SC10UU, linear guide Ø10, motors NEMA17) in construction of 3D printer structure, which will be manufactured in welded rectangular profile 20x20 mm, as follows in figure 3 below. Cutting and drilling of the plates are presented in Figure 4.

Then, it was realized the cutting and drilling plates of PTFE material which will form the printing table, it has been the attaching of the stirrups and linear guides, to the fixing table and uncoupling the bed springs and adjustable thumbscrew to facilitate leveling, as in Figure 5.

It made cutting boards and were positioned linear bearings. NEMA17 motors were attached and completed the construction.

Concerning the electrical connections, it has realized different connections between controller and stepper motors. In order to achieve electrical control network used: a development board - Arduino MEGA 2560, a 1.4 Ramps SHIELD module, 5 Drivers 4988, as in Fig.6.

Fig 6. Arduino MEGA 2560 board.

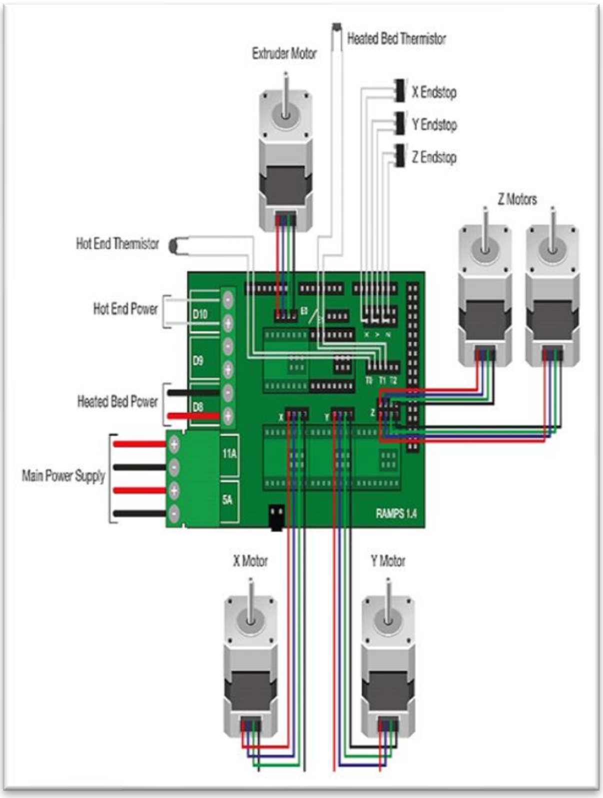

Fig 7. Electrical installation scheme.

The electrical installation scheme is shown in Figure 7. It used a power supply PC PSU 12V 14.6 and an endstop with mechanical feeler as in figure 8 and figure 9.

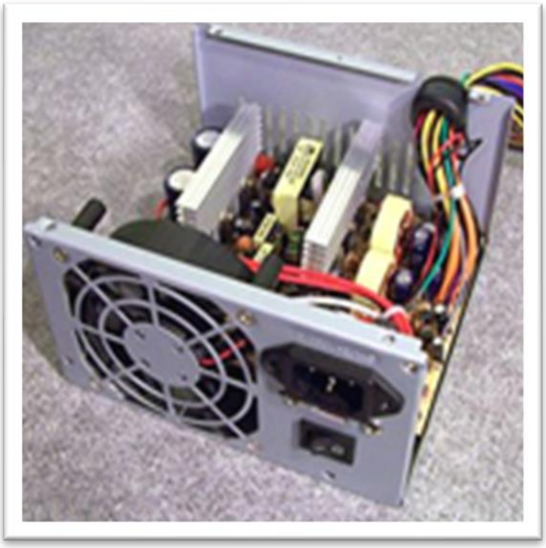

Fig 8. Power supply PC PSU 12V 14.6.

Fig 9. Endstop with mechanical feeler.

The single-pole stepping motors with 4 phases have been converted into 2 phases by eliminating " the mid-point" of the coils A and B (MA:MB), as in figure 10.

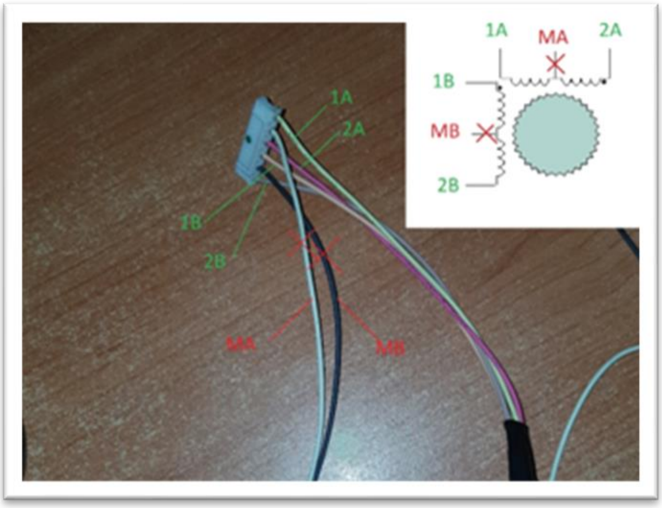

Fig 10. Stepping motors.

For 3D printer operation was performed scheduling and optimization software. Implementation of physical parameters of the printer was done using Marlin1.1 code as in figure 11, uploaded on the development board Arduino MEGA 2560. [1-10]

```
/**
 * Default Axis Steps Per Unit (steps/mm)
 * Override with M92
 *                                      X, Y, Z, E0 [, E1[, E2[, E3[, E4]]]]
 */
#define DEFAULT_AXIS_STEPS_PER_UNIT   { 80, 100, 1600, 94.3 }

/**                                Fulie z20    Fulie z16    Surub P2    Extruder MK8
 * Default Max Feed Rate (mm/s)
 * Override with M203
 *                                      X, Y, Z, E0 [, E1[, E2[, E3[, E4]]]]
 */
#define DEFAULT_MAX_FEEDRATE          { 300, 300, 5, 25 }

/**
 * Default Max Acceleration (change/s) change = mm/s
 * (Maximum start speed for accelerated moves)
 * Override with M201
 *                                      X, Y, Z, E0 [, E1[, E2[, E3[, E4]]]]
 */
#define DEFAULT_MAX_ACCELERATION      { 2500, 2500, 2500, 10000 }

/**
 * Default Acceleration (change/s) change = mm/s
 * Override with M204
```

Fig 11. Marlin1.1 code used for 3D hybrid printer prototype.

```
#define TEMP_SENSOR_0 1
#define TEMP_SENSOR_1 0
#define TEMP_SENSOR_2 0
#define TEMP_SENSOR_3 0
#define TEMP_SENSOR_4 0
#define TEMP_SENSOR_BED 1
#define TEMP_SENSOR_CHAMBER 0
```

Fig 12**.** Thermistor type used (100K).

With its aid were set issues, as thermistor type used (100K) in figure 12:
- Port for the connection;
- Extruders number;
- Existence heated bed;
-Thermistor type used (100K);
-Maximum axes travel;
-Required number of steps per mm (the pitch of the threads);
-Point0 (homing point);
-Size table printed, as in figure 13;
-Maximum acceleration, as in figure 14;
-Maximum voltage motors.

```
#define X_HOME_DIR -1
#define Y_HOME_DIR -1
#define Z_HOME_DIR -1

// @section machine

// The size of the print bed
#define X_BED_SIZE 260
#define Y_BED_SIZE 260
// Travel limits (mm) after homing, corresponding to endstop positions.
#define X_MIN_POS 0
#define Y_MIN_POS 0
#define Z_MIN_POS 0
#define X_MAX_POS 260
#define Y_MAX_POS 260
#define Z_MAX_POS 280
```

Fig 13. Size table printed programming.

```
#define DEFAULT_ACCELERATION          2500    // X, Y, Z and E acceleration for printing moves
#define DEFAULT_RETRACT_ACCELERATION  3000    // E acceleration for retracts
#define DEFAULT_TRAVEL_ACCELERATION   2500    // X, Y, Z acceleration for travel (non printing) moves
```

Fig 14. Maximum acceleration programming.

G-code can be obtained using various programs using models in a "Stl" as: Slic3r and its extension Pronterface or Simplify 3D, both programs also providing a good calibration printing parameters (printing speed, infill, thickness the outer walls, the height of the layers, the width of the filament, temperature) shown in figure 15. In figure 16 are presented the physical 3D parts obtained by 3D printing using the 3D hybrid printer prototype.

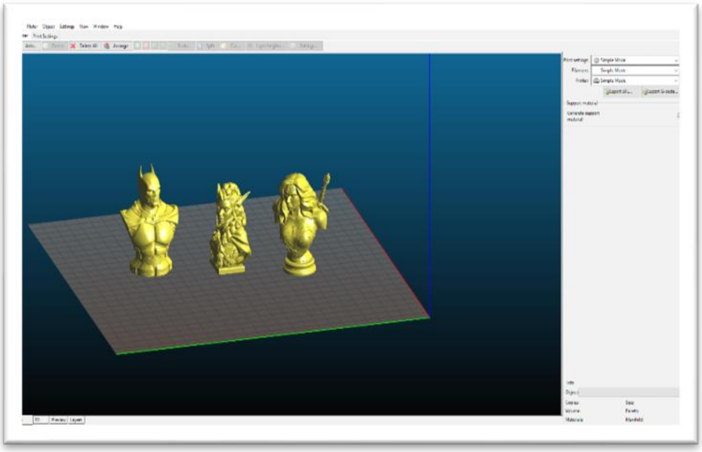

Fig 15. Slic3r program used to create g-code's.

Fig 16. Physical 3D printed parts.

In figure 17 are shown the components of the hybrid 3D printer. In figure 18 are presented the exchangeable CNC tool head, some components of them are manufacture by 3D printing. In figure 19 is presented the CNC drilling on the 3D hybrid printer, using the CNC head. [1-10]

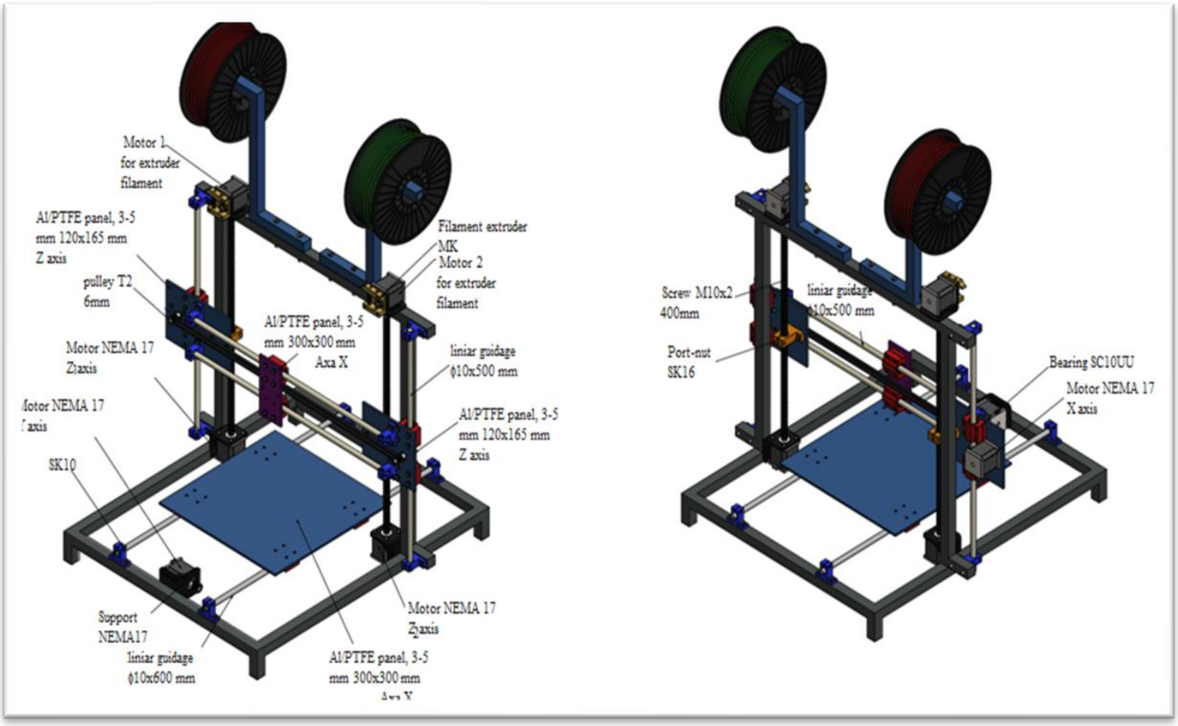

Fig 17. Components of hybrid 3D printer.

Fig 18. CNC head of 3D hybrid printer.

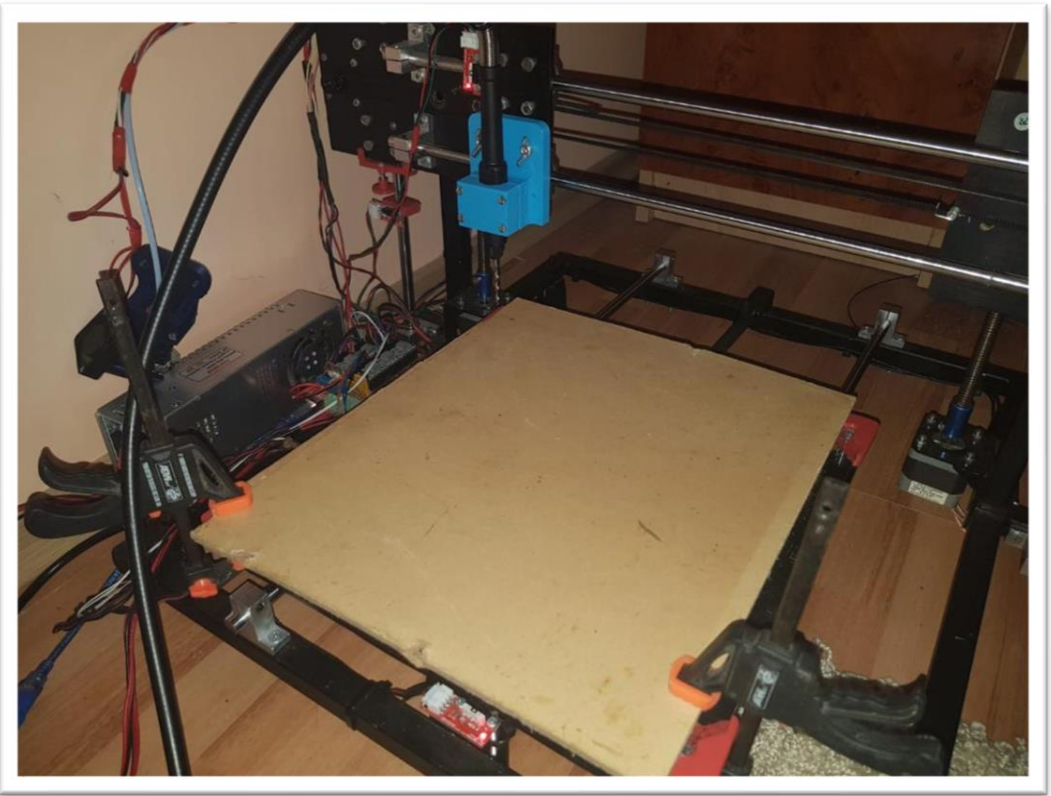

Fig 19. CNC drilling on the 3D hybrid printer.

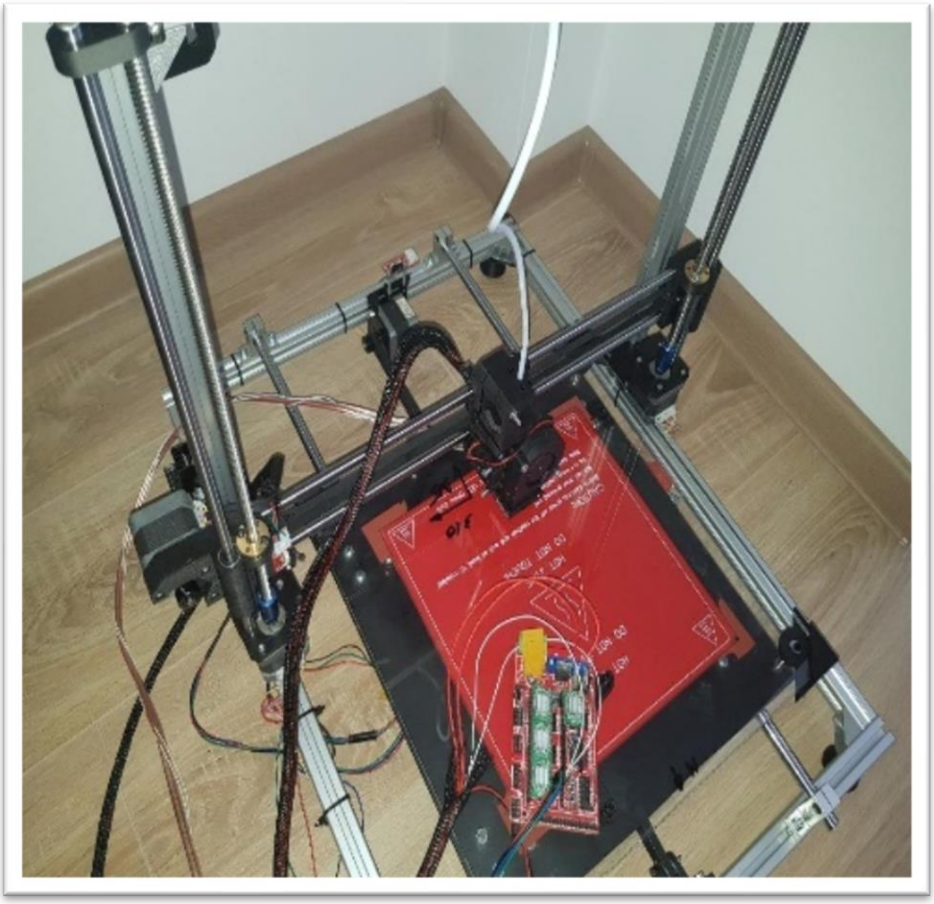

Fig 20. FDM extruder on the 3D hybrid printer

The practical realization of a hybrid 3D printers DIY (do it yourself) using existing tools and inexpensive materials in any household was presented in this research.
Some of the elements used in hybrid 3D printer were recycled from old electronic equipment; this may lead to the sustainable development of the product.

Hybrid prototype 3D printer made in this research has been done on a low budget and is equipped with simple 3D print head (figure 20) and CNC head. The software used to perform the G-code has been Simplify 3D. The innovative part of this research was the electronics used, the programming and optimization software. The dimensions of pieces manufactured by this 3D hybrid printer are 300x300x200 mm, having a very well precision of 0.2 mm. [1-10]

3. *Electronic Components*

3.1 Power source

At present, mostly (lead–acid) batteries are used as a power source. Many different types of batteries can be used as a power source for robots. They range from lead–acid batteries, which are safe and have relatively long shelf lives but are rather heavy compared to silver–cadmium batteries which are much smaller in volume and are currently much more expensive. Designing a battery-powered robot needs to take into account factors such as safety, cycle lifetime, and weight. Generators, often some type of internal combustion engine, can also be used. However, such designs are often mechanically complex and need fuel, require heat dissipation, and are relatively heavy. A tether connecting the robot to a power supply would remove the power supply from the robot entirely. This has the advantage of saving weight and space by moving all power generation and storage components elsewhere. However, this design does come with the drawback of constantly having a cable connected to the robot, which can be difficult to manage. Potential power sources could be:

-pneumatic (compressed gases)

-solar power (using the sun's energy and converting it into electrical power)

-hydraulics (liquids)

-flywheel energy storage

-organic garbage (through anaerobic digestion)

-nuclear

3.2. Actuation

Actuators are the "muscles" of a robot, the parts which convert stored energy into movement. By far the most popular actuators are electric motors that rotate a wheel or gear, and linear actuators that control industrial robots in factories. There are some recent advances in alternative types of actuators, powered by electricity, chemicals, or compressed air.

Figure 21. Electronic components manufactured by 3D Printing [6]

Electric motors

The vast majority of robots use electric motors, often brushed and brushless DC motors in portable robots or AC motors in industrial robots and CNC machines. These motors are often preferred in systems with lighter loads, and where the predominant form of motion is rotational.

Linear actuators

Various types of linear actuators move in and out instead of by spinning, and often have quicker direction changes, particularly when very large forces are needed such as with industrial robotics. They are typically powered by compressed and oxidized air (pneumatic actuator) or an oil (hydraulic actuator) Linear actuators can also be powered by electricity which usually consists of a motor and a leadscrew. Another common type is a mechanical linear actuator that is turned by hand, such as a rack and pinion on a car.

Series elastic actuators

Series elastic actuation (SEA) relies on the idea of introducing intentional elasticity between the motor actuator and the load for robust force control. Due to the resultant lower reflected inertia, series elastic actuation improves safety when a robot interacts with the environment (e.g., humans or workpieces) or during collisions. Furthermore, it also provides energy efficiency and shock absorption (mechanical filtering) while reducing excessive wear on the transmission and other mechanical components. This approach has successfully been employed in various robots, particularly advanced manufacturing robots and walking humanoid robots.

The controller design of a series elastic actuator is most often performed within the passivity framework as it ensures the safety of interaction with unstructured environments. Despite its remarkable stability and robustness, this framework suffers from the stringent limitations imposed on the controller which may trade-off performance. The reader is referred to the following survey which summarizes the common controller architectures for SEA along with the corresponding *sufficient* passivity conditions. One recent study has derived the *necessary and sufficient* passivity conditions for one of the most common impedance control architectures, namely velocity-sourced SEA. This work is of particular importance as it drives the non-conservative passivity bounds in an SEA scheme for the first time which allows a larger selection of control gains.

Piezo motors

Recent alternatives to DC motors are piezo motors or ultrasonic motors. These work on a fundamentally different principle, whereby tiny piezoceramic elements, vibrating many thousands of times per second, cause linear or rotary motion. There are different mechanisms of operation; one type uses the vibration of the piezo elements to step the motor in a circle or a straight line. Another type uses the piezo elements to cause a nut to vibrate or to drive a screw. The advantages of these motors are nanometer resolution, speed, and available force for their size. These motors are already available commercially and being used on some robots.

Elastic nanotubes

Elastic nanotubes are a promising artificial muscle technology in early-stage experimental development. The absence of defects in carbon nanotubes enables these filaments to deform elastically by several percent, with energy storage levels of perhaps 10 J/cm^3 for metal nanotubes. Human biceps could be replaced with an 8 mm diameter wire of this material. Such compact "muscle" might allow future robots to outrun and outjump humans.

Sensing

Sensors allow robots to receive information about a certain measurement of the environment, or internal components. This is essential for robots to perform their tasks, and act upon any changes in the environment to calculate the appropriate response. They are used for various forms of measurements, to give the robots warnings about safety or malfunctions, and to provide real-time information about the task it is performing.

3.3. Electronic components used in robotics and prosthetics

Prostheses are complex systems whose main role is to replace a limb of a living being that, for various reasons, has been amputated or is a congenital malformation. Interdisciplinary teams made up of doctors and various specialists/engineers with skills in product development, additive manufacturing, electronics, IT, etc. are needed for the manufacture, assembly and maintenance of prostheses, which, in some cases, are considered special bionic arms (Fig. 22).

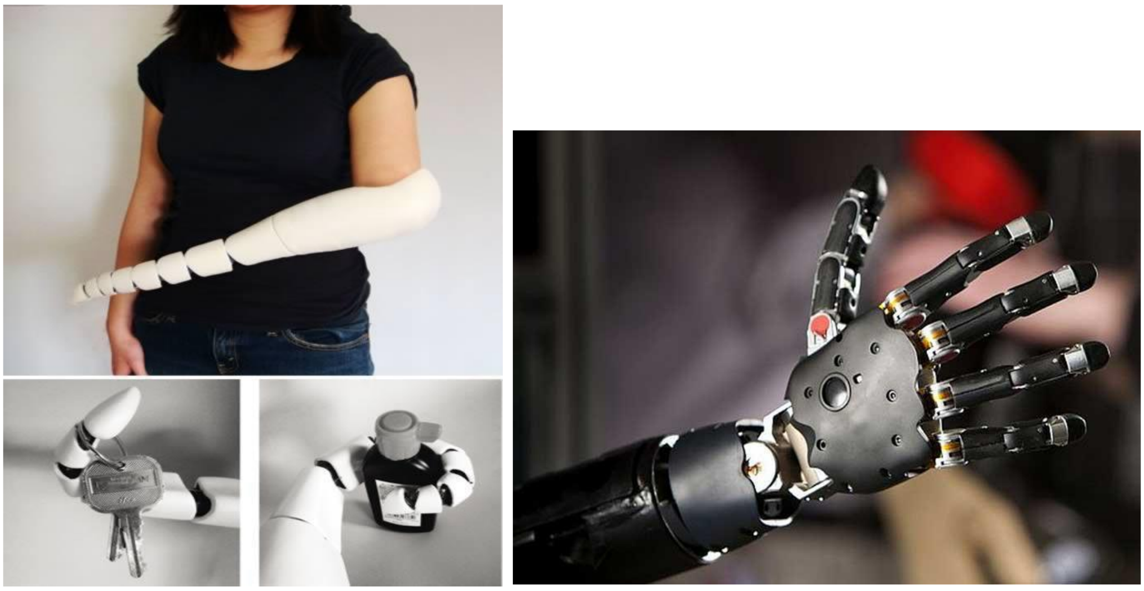

Figure 22. Special bionic arm (Gorski, 2022) [11,12,13]

The whole team must approach the development of the prosthesis product according to the concrete situation of the patient, following a series of steps such as the evaluation of the medical situation, scanning the limb, prescribing all the characteristics of the prosthesis, manufacturing using additive manufacturing, attaching the prosthesis to the patient, monitoring the functioning of the prosthesis, etc.

In the classic approach, the prosthesis manufacturing process begins with the creation of a mold of the limb that requires prosthesis. Depending on the specific situation, the prosthesis is made of various materials such as, for example, thermoplastic materials with low density and high resistance. Also, advanced materials such as carbon fibers, titanium and its alloys, Kevlar, etc., can be used, which ensure high strength, durability and low mass, but with the disadvantage of increasing the cost of manufacturing the prosthesis. Prostheses that have

additional functions and have characteristics very close to those of a natural limb, require advanced electronic systems, sensors, transducers and other specific mechatronic elements.
In specialized literature, there is no unitary classification of prostheses. For example, lower limb prostheses are named and classified according to the degree of amputation and/or after surgeons who developed various prosthetic procedures [¿?]:

- Prostheses that are assembled above the knee - Transfemoral Prostheses;
- Prostheses that are assembled below the knee – Transtibial Prostheses;
- Prostheses for Syme's amputation;
- Knee prostheses;
- Hip prostheses;
- Prostheses for Hemi-pelvictomy;
- Prostheses for partial leg amputation: Pirogoff, Talo-Navicular and Calcaneo-cuboid (Chopart), Tarso-metatarsal (Lisfranc), Trans-metatarsal, Metatarsal-phalangeal, Ray amputations, toe amputations;
- Prostheses for Van Nes rotationplasty".
- Prosthetics on wheels that are widely used in the rehabilitation of injured domestic animals (dogs, cats, pigs, rabbits, etc.).

Raw materials and materials used in making prostheses
Considering the large number of requirements that prostheses must satisfy the most important materials for their manufacture are considered to be the following:

- Plastic materials: Polyethylene, Polypropylene, Acrylics, Polyurethanes;
- Wood;
- Metals with low density: Titanium, Aluminium;
- Composite materials: Carbon fiber reinforced polymers.

1.2.1. Designing and making the attachment part of the prosthesis with the anatomical limb

Making the attachment part with the affected limb is done in several stages, starting with taking over the anatomical shape of the patient with a precision high enough for a good assembly with the prosthesis. This takeover is carried out, with or without taking into account any padding, through several methods, the most important of which are the making of molds (with plaster or other materials), scanning the surface with or without contact followed by computerized processing of data etc. Creating the 3D model of the patient's damaged limb is a very important step that requires specialized software programs.

According to Gorski (Ggorski, 2022), the process of making a prosthesis or orthosis has six stages as shown in figure 23.

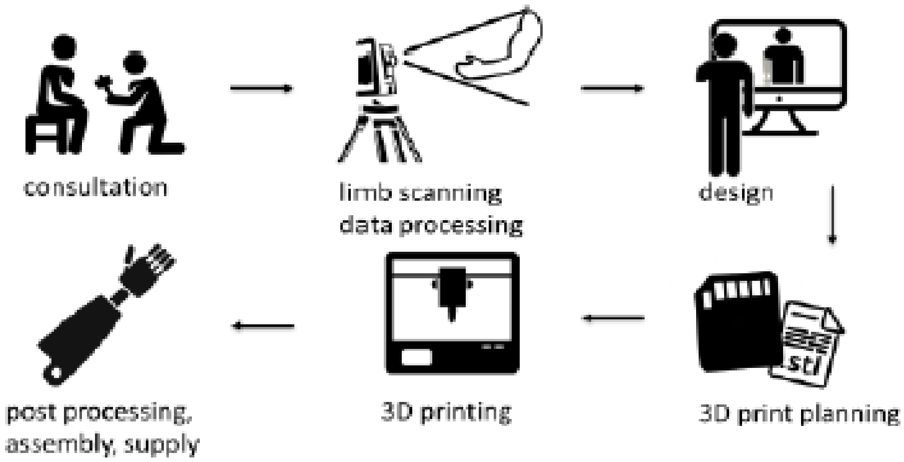

Figure 23. The process of making the orthosis/prosthesis (Gorski, 2022a) [11,12,13]

Also, in specialized literature (Gorski, 2022), three types of processes for making a prosthesis/orthosis are addressed: traditional process, modern process and automated process (fig. 24).

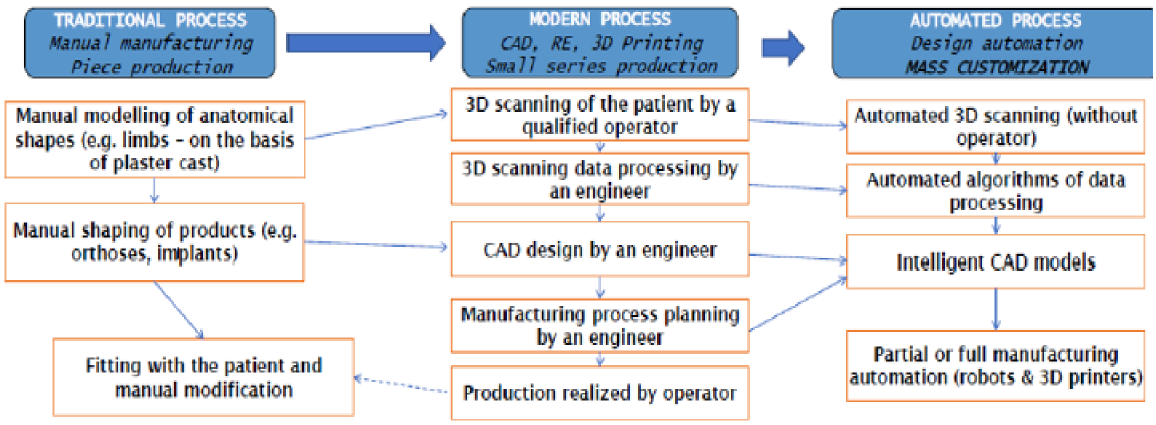

Figure 24. Comparative analysis between Traditional Process, Modern Process and Automated Process for the manufacture of custom prostheses and orthoses (Gorski, 2022a) [11,12,13]

4. *Economic development of 3D hybrid printers on the market*

Concerning the design stage, it was considered the sizing of structural elements depending on the size of standard components used (clamps catching SK10, SK16, bearings SC10UU, linear guide Ø10, motors NEMA17) in construction of 3D printer structure, being manufactured in welded rectangular profile 20x20 mm. It was realized the cutting and drilling plates of PTFE material which will form the printing table, it has been the attaching of the stirrups and linear guides, to the fixing table and uncoupling the bed springs and adjustable thumbscrew to facilitate leveling. It made cutting boards and were positioned linear bearings and NEMA17 motors were attached and completed the construction. [1-7]

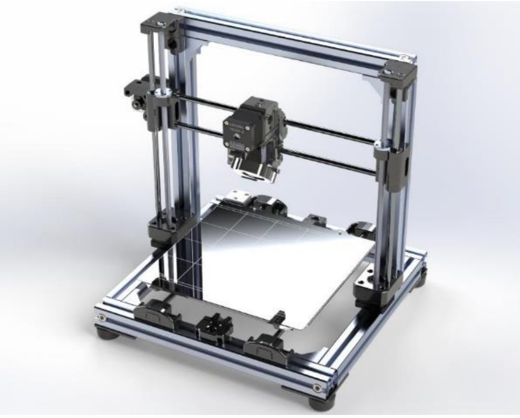

Fig 25. Model of 3D Printer - FDM

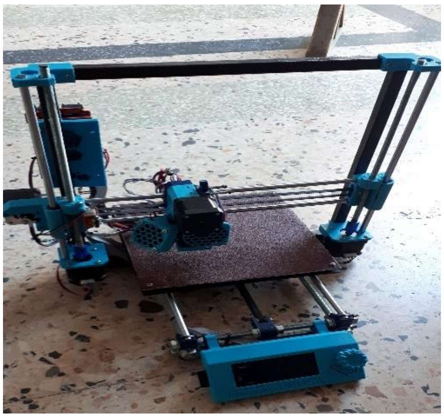

Fig 26. Manufacture of 3D hybrid printer with interchangeable 3D Printing head

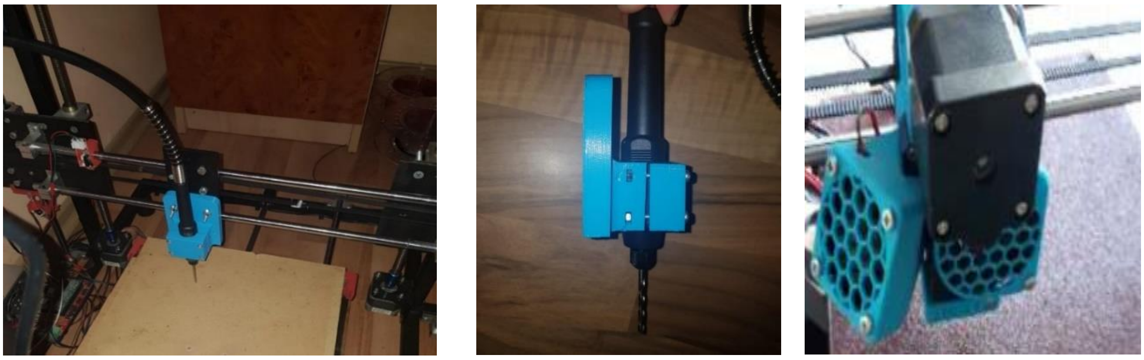

a) b) c)

Fig 27. a) Manufacture of 3D hybrid printer with interchangeable head; b) CNC head; c) extruder

In the figure 25 is shown a model of 3D Printer that used FDM technology and in the figure 26 is presented the 3D hybrid printer manaufacture with interchangeable 3D Printing head, an extruder for 3D printing and heat table. In the figure 27a) it is presented manufacture with the interchangeable CNC head and in figure 27b) it is presented the CNC head prepared for drilling process. The figure 27c present the extruder head of 3D printer. [1-7]

In the table 1 are presented the costs of the components for the manufacture of the hybrid 3d printer. The total cost for manufacturing a 3D hybrid printer (do it yourself) with two heads interchangeable arrives at 2467,13 Ron (approx.514 Euro).

Table 1. The costs of the components of the hybrid 3d printer

Nb.	**Component**	**Unit Price [Ron]**	**Pieces**	**Total costs (Ron)**
1	Extruded aluminium profile	5.5	40	220
2	Nema 17 TIP 42HD4027-02	69.99	5	349.95
3	RamBO	49.99	1	49.99
4	Arduino 2560 R3	59.99	1	59.99
5	DRV 8855	20	3	60
6	A4988	15	1	15
7	Extruder MK8	55	1	55
8	Teflon 4/2	25	1	25
9	Pulley M4	20	2	40
10	Belt tensioner	15	2	30
11	Belt T2	14	4	56
12	Guides Φ8	3.6	32	115.2
13	Bearing 8	14	8	112
14	Guides Φ10	4	12	48
15	Bearing housing 10	21	4	84
16	Corner 20x40	9	4	36
17	Plate L	12	2	24
18	Channel nut T Easy drop	1.7	50	85
19	Square nut M5 T5	0.2	40	8
20	Screws M5X8	0.4	40	16
21	Screws M5X12	0.6	30	18
22	Sk10	20	4	80
23	Wired hotbed	72	1	72
24	Bowden block	20	1	20
25	Thermocouple 12v	24	1	24
26	Teflon M6 2x3	8	1	8
27	Wired thermistor	22	2	44
28	Insert M6	9	1	9
29	Removable coupling M6	12	2	24
30	Hotbed support Y	40	1	40

31	Glass 300x300 mm	15	1	15
32	Kevlar part	12	3	36
33	Nema 17 support	12	2	24
34	Filament PETG/PLA	85	2	170
35	Cable 0,75	2	4	8
36	Source 30A12v	110	1	110
37	Power cable	6	1	6
38	Fan 40x40x2	12	2	24
39	Trapezoidal screw T8X375	38	2	76
40	Blower 50x50	14	1	14
41	LCD+ cables	76	1	76
42	Endstop	10	3	30
43	Coupler 5x8	12	2	24
44	Nut T8x2	9	2	18
45	Screws M3x25	0,2	40	8
Total price				2467,13 (514 Eur)

Concerning the electrical connections, it has realized different connections between controller and stepper motors. In order to achieve electrical control network were used: a development board - Arduino MEGA 2560, a 1.4 Ramps SHIELD module, 5 Drivers 4988. Concerning the electrical installation, it was used a power supply PC PSU 12V 14.6 and an endstop with mechanical feeler. The software used for the implementation of physical parameters of the printer was Marlin1.1 code, uploaded on the development board Arduino Mega 2560. Slic3r and its extension Pronterface or Simplify 3D, both programs also provide good calibration printing parameters (printing speed, infill, thickness the outer walls, the height of the layers, the width of the filament, temperature). [1-13]

Comparing the cost of 3D hybrid printer (do it yourself) with two interchangeable heads with other 3D hybrid printers existing on the market, as in the figure 28, can remark a a considerable difference in costs, achieving a considerable economy by making your own printer. In addition, at any time your own printer can be improved, as needed, with the latest types of print heads on the market.

.

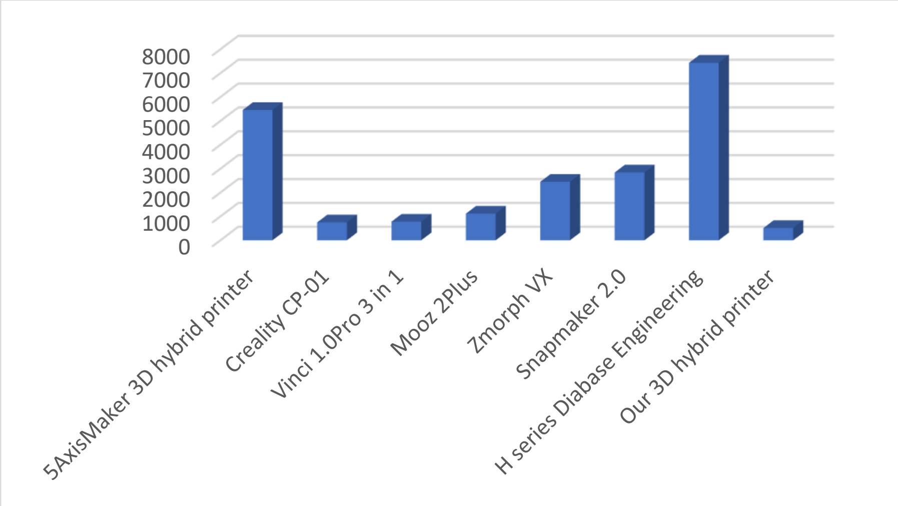

Fig 28. Comparative prices for 3D hybrid printers

Conclusions

The advantages of 3D hybrid printers manufacture using chips materials and reusing some electrical components from older equipment is the smaller price of this, that allow to realize a sustainable product. The hybrid printer fabricated in this research was realized with a small budget, being equipped with a simple 3D print head and a CNC head, the software used to perform the g-code has been Simplify 3D.

In the last ten years, the Romanian additive manufacturing industry was realized a real revolution grace of the sophisticate materials and new performing equipment and in this research the innovative part was the electronics used, the programming and the optimization software.

In the future will attend an exponential sales growth of 3D hybrid printers in medicine, aerospace, automotive, tooling, electronics, jewelry and other.

References:

1- D.I. Băilă, S. Tonoiu, M.C. Ștefan, I. Sapadin Experimental researches concerning the manufacture of multitool 3D printer, type DIY (do it yourself), IOP Conference Series: Materials Science and Engineering, 682(1), 2019 -DOI: 10.1088/1757-899X/682/1/012016
2-https://zmorph3d.com/frontpage
3-https://www.instructables.com/id/A-low-cost-3D-printer-with-basic-tools/
4-Marlin Firmware- http://marlinfw.org/
5-https://en.wikipedia.org/wiki/Prosthesis

6-https://en.wikipedia.org/wiki/Robotics#Actuation
7-https://en.wikipedia.org/wiki/Sensor
8-https://en.wikipedia.org/wiki/Actuator
9- Paternò, L., Dhokia, V., Menciassi, A. *et al.* A personalised prosthetic liner with embedded sensor technology: a case study. *BioMed Eng OnLine* **19**, 71 (2020). https://doi.org/10.1186/s12938-020-00814-y
10- Băilă D, Tonoiu S, The costs concerning the manufacturing of hybrid 3D printer, 40th IBIMA Seville 2022.
11- Górski Filip, *Computer Aided Design of 3D printed patient-specific devices*, Emerald Summer School, University of Agder, Norway, September, 2022
12 – Păcurar, R., Górski, F., Sanfilippo, F., Băilă, D., Zelenay, M., Comșa, D., Sabău, E., Labudzki, R., Gallia, M., Savu, T., Ionescu, N., Ulmeanu, M., Jugravu, B., Enache, V., Zaharia, C., Radu, I., Źukowska, M., Rybarczyk J., Rybarczyk D., Regulski, R., Wierzbicka, N., Wichniarek, R., Kuczko, W. EMERALD Ebook for developing of biomimetic mechatronic systems – ISBN 978-973-53-3157-3, Ed. Risoprint Cluj-Napoca, 2023
13- Păcurar, R., Górski, F., Sanfilippo, F., Băilă, D., Rabara, B., Økter, M, Comșa, D., Sabău, E., Źukowska, M., Rybarczyk, D., Wierzbicka, N., Wichniarek, R., Kuczko, W., Regulski, R., EMERALD e-toolkit for teaching purposes, basic knowledge about realizing biomimetic mechatronic systems – ISBN 978-973-53-3048-4, Ed. Risoprint Cluj-Napoca, 2023

Co-funded by the European Union

AMAZE

Erasmus+ Programme Key Action 2 Cooperation Partnerships for Higher Education (KA220-HED)
Agreement number 2023-1-RO01-KA220-HED-000155412
European Network for Additive Manufacturing in Industrial Design for Ukrainian Context

e-Toolkit
Virtual Reality / Augmented Reality

Project Title	**European Network for Additive Manufacturing in Industrial Design for Ukrainian Context** **2023-1-RO01-KA220-HED-000155412**
Output	**IO2 - AMAZE e-toolkit manual for digital learning in producing complex design industrial parts**
Module	**Module 7** **Virtual Reality / Augmented Reality**
Date of Delivery	**June 2024**
Authors	**Beatriz Gloria BONILLA GARCÍA, César Arcadio BONILLA GARCÍA, Sergio VIZCAINO**
Version	**FINAL VARIANT, *14.06.2024***

Contents

1 Programming in Virtual Reality

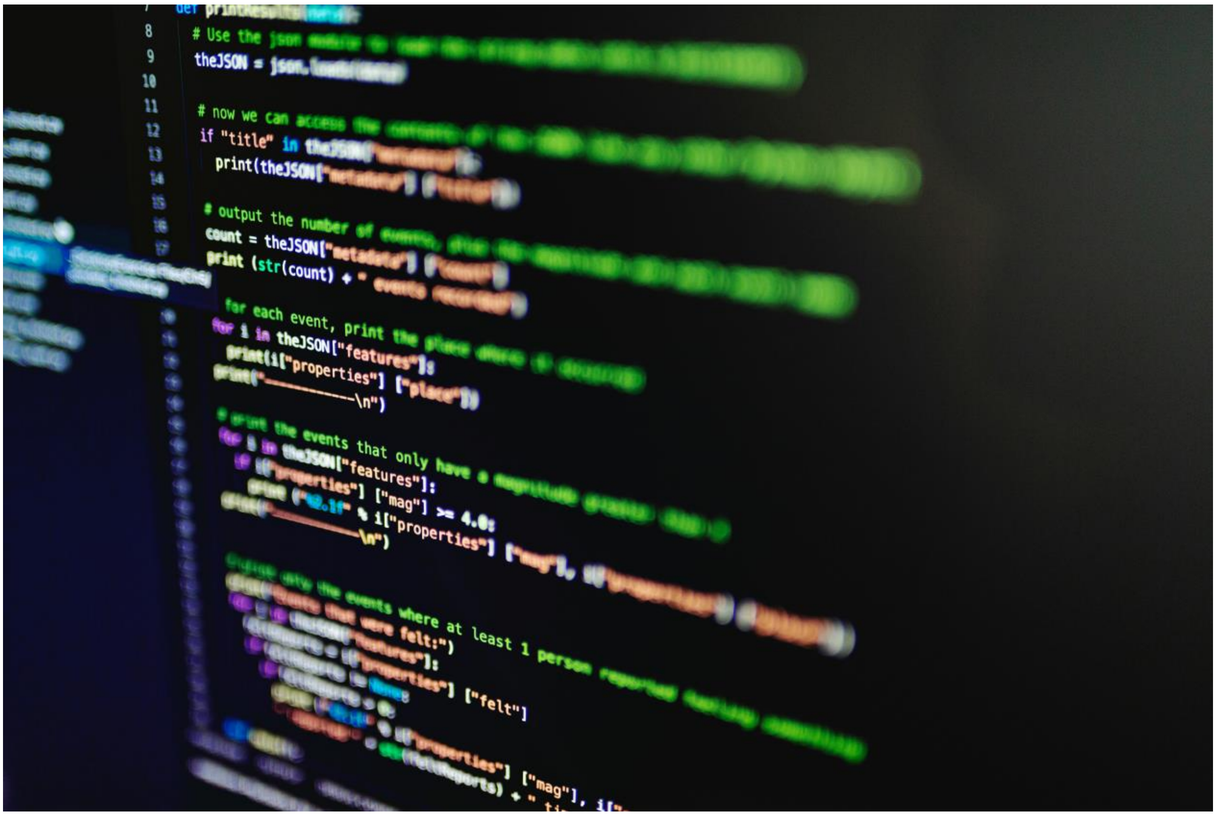

Programming code in the development of virtual reality (VR) applications is a complex and multifaceted discipline that involves a combination of skills in design, computer science, and creativity. Developing VR applications requires a deep understanding of computer science principles and graphic design, as well as proficiency in programming languages such as C#, C++, and Python. One of the most commonly used engines for creating VR applications is Unity, which allows developers to write scripts in C# to control the logic and behavior of objects in a virtual environment. Another popular engine is Unreal Engine, which uses the C++ programming language and offers a visual scripting system called Blueprint, making development easier for those who prefer a more visual approach.

The programming process for VR involves several crucial steps. First, developers must create a three-dimensional model of the environment and the objects that compose it. This can include anything from landscapes and buildings to characters and vehicles. These models are then imported into the game engine, where developers write scripts to define how the objects interact with each other and with the user. This can include implementing realistic physics, collision detection, and specific behaviors such as movements or reactions to certain events. Additionally, VR programming must consider performance optimization, as virtual environments are often very demanding in terms of computational resources.

Another critical aspect of VR application programming is implementing user interaction. This involves the use of input devices such as motion controllers, haptic gloves, and VR headsets, which must be programmed to respond accurately and smoothly to the user's actions. Developers must ensure that these interactions are intuitive and natural to provide an immersive and enjoyable experience. It is also essential to integrate spatial audio, allowing sounds to come from different directions, enhancing the sense of presence in the virtual environment.

Furthermore, VR programming does not stop at creating interactive content. Developers must also consider aspects such as accessibility, usability, and user experience, ensuring that applications are easy to use and accessible to people with various abilities. This can involve creating intuitive user interfaces and implementing customization options to cater to different needs and preferences.

In summary, programming in the development of virtual reality applications is a dynamic field that requires a combination of technical and creative skills. It involves creating 3D models, scripting for interaction and behavior, performance optimization, and designing immersive and accessible user experiences. With the continuous advancement of VR technology, developers face constant challenges and opportunities to innovate and improve the way we interact with virtual worlds.

1.1 Example

More detailed example including code developed for a virtual reality (VR) application for the additive manufacturing industry. Let's focus on the visualization and control of a virtual 3D printer from the VR user's perspective.

Step 1: Setting up the development environment

Software installation:

Download and install Unity from the official website.
Download and import the Oculus SDK into your Unity project.

Project creation:

Open Unity and create a new 3D project.
Defines an initial scene where the 3D printer and other elements of the environment will be located.

Step 2: Design of the virtual environment

3D printer modeling: use 3D modeling software such as Blender or Autodesk Maya to create the 3D printer model.

Import the model into Unity and place it in the scene.

Environment design:

Create a virtual environment that represents the 3D printer's work area. Includes a work table, tools and other relevant objects.
Add lighting and visual effects to improve the user experience.

Step 3: Implementation of user interaction

Virtual user interface:

Design a virtual user interface using the Unity UI system. Create buttons to control 3D printer functions, such as start, pause, and cancel printing.
Adds visual indicators to show printer status and the progression of the printing process.

User Controls:

Use the Oculus SDK to implement interaction with Oculus Touch controllers.

Assign actions to controller buttons and joysticks to interact with the user interface and objects in the environment.

CODE

```
using UnityEngine;
public class PrinterController : MonoBehaviour
{
  public GameObject printerObject;
  private Printer printer;
  private void Start()
  {
    printer = printerObject.GetComponent<Printer>();
  }
  public void StartPrinting()
  {
    printer.StartPrinting();
  }
  public void PausePrinting()
  {
    printer.PausePrinting();
  }
  public void CancelPrinting()
  {
    printer.CancelPrinting();
  }
}
```

Step 4: Integration with the 3D printer

Print simulation:

Create a C# script to simulate the printing process. This script could generate print layers progressively and update the 3D model of the printed part accordingly.

Uses Unity coroutines to control the timing and progression of the printing process.

CODE

csharp

Copy code

```
using UnityEngine;
using System.Collections;
public class Printer : MonoBehaviour
{
   public GameObject printedObject;
   public float layerHeight = 0.1f;
   public float printSpeed = 1f;
   private Coroutine printingCoroutine;
   public void StartPrinting()
   {
      printingCoroutine = StartCoroutine(PrintCoroutine());
   }
   public void PausePrinting()
   {
      if (printingCoroutine != null)
      {
         StopCoroutine(printingCoroutine);
      }
   }
   public void CancelPrinting()
   {
      if (printingCoroutine != null)
```

```
    {
        StopCoroutine(printingCoroutine);
        Destroy(printedObject); // Delete printed object
    }
}
private IEnumerator PrintCoroutine()
{
    while (printedObject.transform.localScale.y < 10) // Example of maximum print height
    {
        yield return new WaitForSeconds(printSpeed);
        // Generate new print layer
        GameObject newLayer = GameObject.CreatePrimitive(PrimitiveType.Cube);
        newLayer.transform.position = new Vector3(printedObject.transform.position.x, printedObject.transform.position.y + printedObject.transform.localScale.y, printedObject.transform.position.z);
        newLayer.transform.localScale = new Vector3(printedObject.transform.localScale.x, layerHeight, printedObject.transform.localScale.z);
        newLayer.GetComponent<Renderer>().material.color = Color.blue;
        newLayer.transform.parent = printedObject.transform;
```

Step 5: Testing and Refinements

Functionality tests:

Test the app on a compatible VR device to make sure all features and controls work correctly.
Make adjustments as necessary to improve the user experience and fix potential errors.

Performance Optimization:

Optimizes the app to ensure smooth and fluid performance on VR devices.
Reduce graphical load and optimize scripts to improve overall application performance.

Step 6: Deployment

Compilation and packaging:

Build your app for the target platform, such as Oculus Rift or Oculus Quest.

Packages the application along with all the resources necessary for its distribution.

Distribution and feedback:

Distribute the app to end users through the appropriate app stores.

Collect comments and feedback from users to identify areas for improvement and make future updates.

This is a more detailed example that includes code developed for a VR application for the additive manufacturing industry. Remember that each project may have specific requirements, so be sure to adapt this example to your particular needs.

1.2 Main coding commands

- **Printer:** This is a script attached to the object that represents the virtual 3D printer in the Unity scene.
- **printedObject:** A reference to the object that represents the printed object in the Unity scene. It is assigned from the Unity editor.
- **layerHeight:** The height of each print layer.
- **printSpeed:** The printing speed, which determines the time between each layer.
- **printingCoroutine:** A reference to the coroutine that controls the printing process.
- **StartPrinting():** This method starts the printing process by creating a new coroutine.
- **PausePrinting():** This method stops printing by pausing the current coroutine.
- **CancelPrinting():** This method cancels printing by stopping the coroutine and destroying the printed object.
- **PrintCoroutine():** This coroutine simulates the printing process. Generates new print layers with a time interval until the printed object reaches a predefined maximum height.

2 Programming in Augmented Reality

Programming code in the development of augmented reality (AR) applications is a dynamic field that combines skills in programming, interaction design, and real-time data processing to overlay digital information onto the physical world. This process begins with choosing an appropriate platform, such as Apple's ARKit, Google's ARCore, or frameworks like Vuforia, which provide specific tools and libraries for AR application development. Common programming languages in this field include Swift and Objective-C for iOS, Java and Kotlin for Android, and C# when using the Unity engine.

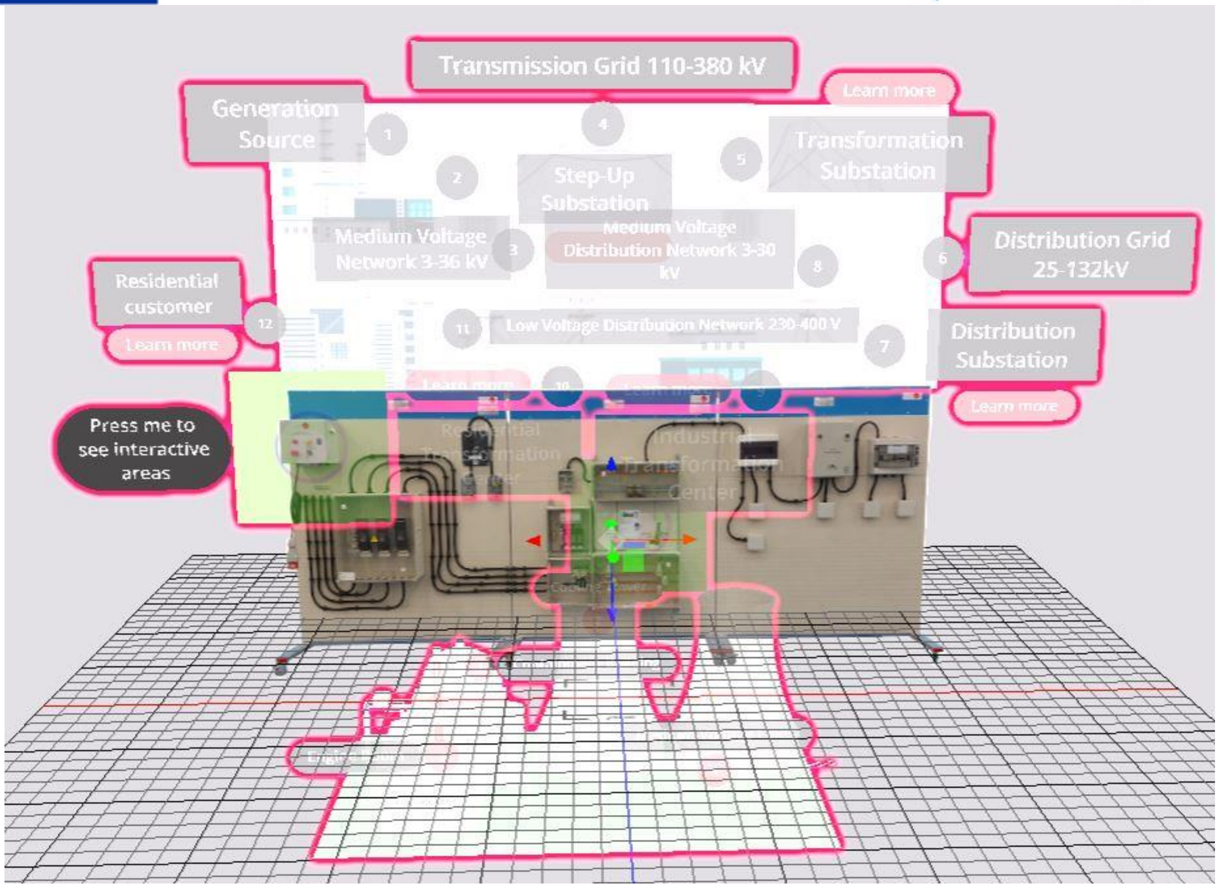

Onirix is a platform designed to simplify the development and implementation of augmented reality (AR) applications in an accessible way, without requiring advanced programming knowledge. Its main features include an intuitive web-based visual editor, multiplatform support for iOS and Android, and advanced algorithms for image recognition and tracking, as well as spatial mapping and simultaneous localization (SLAM). Additionally, it offers APIs and SDKs to integrate AR capabilities into existing mobile applications and analytical tools to track and improve the performance of AR experiences.

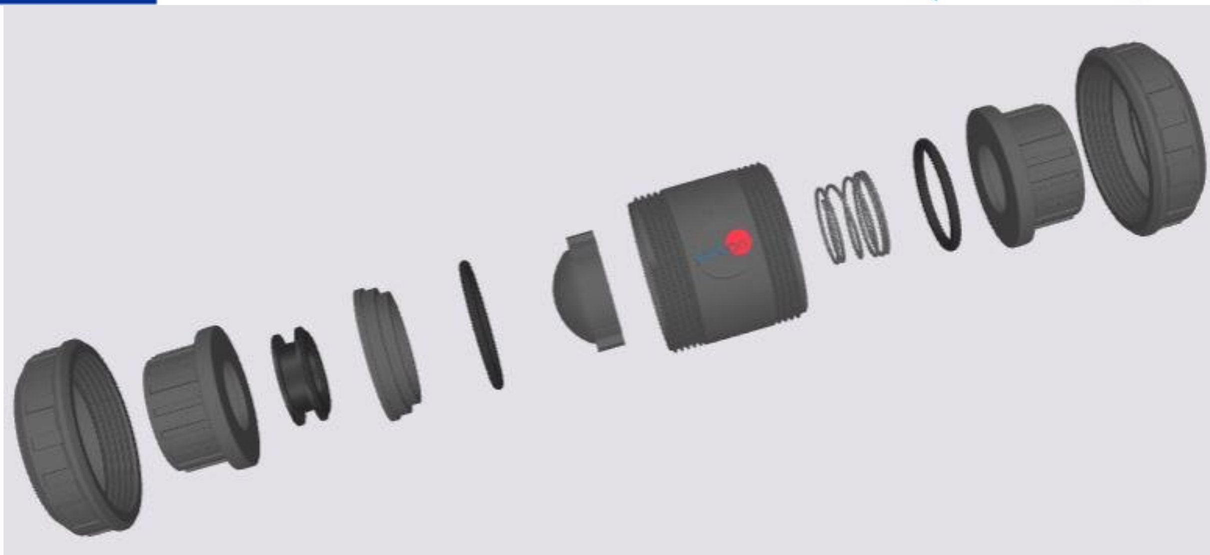

Onirix is scalable and allows for collaboration on AR projects, facilitating teamwork. The applications of Onirix span marketing and advertising, education and training, tourism and culture, and retail and e-commerce. Brands can create interactive experiences for advertising campaigns, educational institutions can develop immersive learning tools, museums can offer interactive tours, and stores can allow customers to visualize products in their environment before purchasing. In summary, Onirix simplifies the creation and distribution of AR experiences, making it an attractive option for developers and businesses.

One of the initial stages in developing an AR application is environment recognition, which involves detecting and mapping the physical space. This is achieved through computer vision algorithms and simultaneous localization and mapping (SLAM) techniques. These algorithms analyze images captured by the device's camera to identify surfaces, objects, and key features of the environment, allowing digital elements to be precisely anchored in the physical space. This process requires meticulous programming to ensure accurate and efficient mapping, minimizing latency and optimizing performance.

```
JS

const overlay = document.querySelector("#overlay");
const logo = document.createElement("img");
logo.setAttribute("id", "my-custom-logo");
logo.setAttribute("src", "https://assets.ipzmarketing.com/data/90d7a3a4ac699d3145e3
overlay.appendChild(logo);



var language = navigator.language || navigator.userLanguage;

if (language == 'es-ES') {
document.getElementById("my_custom_div").innerHTML =
        `Mueve el dispositivo hasta que aparezca el cuadrado blanco y pulsa +`

document.getElementById("ox-progress-loading-text").innerText =
  "Cargando experiencia...";

} else {
    document.getElementById("my_custom_div").innerHTML =
        `Move the device until the white square appears and press +`

    document.getElementById("ox-progress-loading-text").innerText =
  "Loading experience...";
}
```

Another crucial aspect is user interaction with augmented elements. Developers must write code that allows for intuitive and natural interaction, leveraging gestures, movements, and screen touches. This can include manipulating 3D objects, triggering animations, and executing commands based on user input. Designing these interactions requires not only programming skills but also a deep understanding of ergonomics and user experience to ensure the application is easy and enjoyable to use.

Additionally, AR application programming must address the integration of relevant and contextualized digital content. This involves using APIs to obtain real-time data, such as geospatial information, weather data, or domain-specific databases. Developers must write code that not only retrieves this information but also presents it in a coherent and useful manner for the user, enhancing the AR experience with precise and updated data.

CSS

```css
/*Logo y color*/
#webar-powered-img {
  display: none;
}

#overlay {
  background-color: #007cb0 !important;
}

#my-custom-logo {
  position: absolute;
  width: 220px;
  bottom: 200px;
  left: calc(50% - 100px);
}

#watermark-logo {
    position: fixed;
    bottom: 50px;
    left: 50px;
    opacity: 0.5;
    width: 100px;
    height: auto;
}



/*Barra de carga*/
#ox-progress-bar-container {
  background-color: #ec0e2d !important;
}

#ox-progress-bar {
  background-color: #02587d !important;
}

#ox-progress-loading-text {
  color: #7e1120 !important;
}

#ox-progress-percentage-text {
  color: #7e1120 !important;
}

/*Recuadro de instrucciones*/
.container {
  position: relative;
  height: 100vh;
}
```

Performance optimization is another significant challenge in AR application development. Developers must ensure their code is efficient and that the application can run smoothly on a variety of devices with different hardware capabilities. This can involve optimizing graphics, efficiently managing memory, and minimizing power consumption to extend the device's battery life.

HTML

```html
<img id="watermark-logo" src="https://assets.ipzmarketing.com/data/90d7a3a4ac699d314
  <div class="container">
    <div class="transparent-box">
      <div id="my_custom_div"></div>
        </div>
  </div>

```

In summary, programming in the development of augmented reality applications is a comprehensive discipline that requires a combination of technical skills in programming, interaction design, and performance optimization. From environment recognition and user interaction to digital content integration and resource optimization, each aspect of AR development involves unique challenges that must be addressed with precision and creativity. With the continuous advancement of AR technology, developers have the opportunity to create innovative experiences that transform the way we interact with the world around us.

2.1 Example

Detailed code example for an augmented reality (AR) application that allows you to view and control a virtual 3D printer. We will use Unity with Vuforia as an AR development platform.

Step 1: Setting up the development environment

1. Software installation:
   - Download and install Unity from the official website.
   - Install Vuforia from the Unity Asset Store.

2. Project creation:
   - Open Unity and create a new 3D project.
   - Import the Vuforia package to your project.

Step 2: Design of the virtual environment

1. 3D printer modeling:
   - Use 3D modeling software such as Blender or Autodesk Maya to create the 3D printer model.
   - Import the model into Unity and place it in the scene.

2. Environment design:
   - Create a virtual environment that represents the work area of the 3D printer. Includes a work table, tools and other relevant objects.
   - Add lighting and visual effects to improve the user experience.

Step 3: Implementing User Interaction

1. Virtual user interface:
   - Design a virtual user interface that is overlaid on the mobile device screen or augmented reality glasses. You can use the Unity UI system to create buttons and panels.
   - Adds buttons to control 3D printer functions, such as start, pause and cancel printing.

2. User Controls:
   - Uses Vuforia to detect user gestures, such as taps and swipes, on the device screen.

Step 4: Integration with the 3D printer

1. Print simulation:
   - Use Unity scripts to simulate the printing process. For example, you can use coroutines to progressively generate print layers.

```csharp

using UnityEngine;

using System.Collections;

public class Printer : MonoBehaviour

```
{
   public GameObject printedObject;
   public float layerHeight = 0.1f;
   public float printSpeed = 1f;
   private Coroutine printingCoroutine;
   public void StartPrinting()
   {
      printingCoroutine = StartCoroutine(PrintCoroutine());
   }
   public void PausePrinting()
   {
      if (printingCoroutine != null)
      {
         StopCoroutine(printingCoroutine);
      }
   }
   public void CancelPrinting()
   {
      if (printingCoroutine != null)
      {
         StopCoroutine(printingCoroutine);
         Destroy(printedObject); // Delete printed object
      }
   }
   private IEnumerator PrintCoroutine()
   {
      while (printedObject.transform.localScale.y < 10) // Example of maximum print height
      {
         yield return new WaitForSeconds(printSpeed);
```

```
        // Generar nueva capa de impresión

        GameObject newLayer = GameObject.CreatePrimitive(PrimitiveType.Cube);

        newLayer.transform.position = new Vector3(printedObject.transform.position.x,
printedObject.transform.position.y + printedObject.transform.localScale.y,
printedObject.transform.position.z);

        newLayer.transform.localScale = new Vector3(printedObject.transform.localScale.x,
layerHeight, printedObject.transform.localScale.z);

        newLayer.GetComponent<Renderer>().material.color = Color.blue;

        newLayer.transform.parent = printedObject.transform;

      }

   }

}
```

Step 5: Testing and Refinements

1. Functionality tests:
   - Test the app on a mobile device or AR glasses to make sure all features and controls work correctly.
   - Make adjustments as necessary to improve the user experience and fix potential errors.

Step 6: Deployment

1. Compilation and packaging:
   - Compile the app for the target platform, such as iOS or Android.
   - Package the application along with all the resources necessary for its distribution.

2. Distribution and feedback:
   - Distribute the application through the corresponding application stores.
   - Collect comments and feedback from users to identify areas for improvement and make future updates.

This is a basic example to start developing an augmented reality application for the additive manufacturing industry. You can expand and improve this code according to your specific needs.

2.2 Main coding commands

•**Printer:** This is a script attached to the object that represents the virtual 3D printer in the Unity scene.

•**printedObject:** A reference to the object that represents the printed object in the Unity scene. This object must be previously assigned in the Unity editor.

•**layerHeight:** The height of each print layer.

•**printSpeed:** The print speed, which determines the time between each layer.

•**printingCoroutine:** A reference to the coroutine that controls the printing process.

•**StartPrinting():** This method starts the printing process by creating a new coroutine.

•**PausePrinting():** This method stops printing by pausing the current coroutine.

•**CancelPrinting():** This method cancels printing by stopping the coroutine and destroying the printed object.

•**PrintCoroutine():** This coroutine simulates the printing process. It iterates until the printed object reaches a certain maximum height, generating print layers at regular time intervals.

3 Conclusions

Coding for augmented reality (AR) and virtual reality (VR) is a dynamic and rapidly evolving field that demands advanced, multidisciplinary programming skills. One of the main conclusions in this area is the need for a deep understanding of programming languages like C#, C++, and JavaScript, which are fundamental for developing applications on popular platforms like Unity and Unreal Engine. These development environments provide specific tools and libraries that facilitate the creation of immersive and highly interactive experiences.
A critical aspect of AR and VR programming is performance optimization. Developers must write efficient code to ensure applications can handle large volumes of graphical data in real-time without causing noticeable latency, which is essential to maintain immersion and avoid issues like motion sickness. This involves advanced memory management techniques, optimized rendering algorithms, and the utilization of parallel processing and GPUs.
Programming for AR and VR also requires an innovative approach to user interface (UI) and user experience (UX) design. Unlike traditional 2D applications, developers must create three-dimensional interfaces that are intuitive and natural. This involves implementing gesture and voice controls, as well as integrating motion sensors and eye-tracking to enhance user interactivity and immersion.

Additionally, developers need to be familiar with AR and VR-specific APIs and SDKs, such as ARKit and ARCore for mobile devices, and OpenXR for cross-platform applications. These tools provide access to advanced features like spatial mapping, surface detection, and interaction with virtual objects in the real world.

Another significant challenge is real-time data management and manipulation. AR and VR environments often require the capture and processing of sensory data in real-time, which involves implementing complex image and signal processing algorithms. Artificial intelligence and machine learning play a crucial role in this context, improving the accuracy and adaptability of applications to various environments and user behaviors.

In summary, programming for AR and VR is a highly specialized discipline that combines advanced technical skills with creativity and a deep understanding of human-computer interaction. Developers must be prepared to tackle complex challenges and stay updated with the latest technological advancements to create immersive and transformative experiences.

4 References

Books

1. "Unity in Action: Multiplatform Game Development in C# with Unity 5"
   - Autor: Joe Hocking

2. "Learning Virtual Reality: Developing Immersive Experiences and Applications for Desktop, Web, and Mobile"
   - Autor: Tony Parisi

3. "Augmented Reality: Principles and Practice"
   - Autores: Dieter Schmalstieg, Tobias Hollerer

4. "Programming 3D Applications with HTML5 and WebGL: 3D Animation and Visualization for Web Pages"
   - Autor: Tony Parisi

Web

1. Unity Documentation
   - Unity Technologies
   - Performance Optimization

2. Unreal Engine Documentation
   - Epic Games
   - Unreal Engine Documentation

3. ARKit Overview
   - Apple Inc.
   - *ARKit Overview*

4. ARCore Overview
   - Google Developers
   - ARCore Overview

5. Mixed Reality Design Guidelines
- Microsoft
- Mixed Reality Design Guidelines

6. Virtual Reality: UX Issues and Design Solutions
- Nielsen Norman Group

7. A Survey of Augmented Reality
- Ronald T. Azuma
- Presence: Teleoperators and Virtual Environments

8. A Survey of Augmented Reality
- Mark Billinghurst, Adrian Clark, Gun Lee
- Foundations and Trends® in Human–Computer Interaction

9. Onirix Documentation
- Onirix
- Onirix Developer Documentation